From gene structure to neuronal circuits:

Genetic rescue of CB1 receptor function in cortical glutamatergic networks

Dissertation

zur Erlangung des Grades

"Doktor der Naturwissenschaften"

am Fachbereich Biologie

der Johannes Gutenberg-Universität

in Mainz

Sabine Rühle

geb. am 13.01.1983 in Bad Neustadt an der Saale

Mainz, 2012

Dekan:

1. Berichterstatter:

2. Berichterstatter:

Tag der mündlichen Prüfung: 14.06.2012

Table of contents

1 Summary / Zusammenfassung

1.1 Summary

A main topic of current neurobiological research is to establish causal relationships between genes, molecules and functions. Several studies using knock-out and pharmacological approaches showed the *necessary* role of the cannabinoid type 1 (CB1) receptor in a plethora of cellular neuronal functions and behaviors. However, caused by technological limitations, the *sufficient* role of the CB1 receptor in the same processes has not been established yet. To further understand the mechanisms underlying these processes, a novel mouse line for cell type-specific rescue from CB1 receptor deficiency (Stop-CB1) was generated. To this end, a loxP-flanked stop cassette was introduced into the CB1 receptor gene locus in order to repress CB1 receptor expression throughout the entire body, including the brain. By crossing this mouse line with a mouse line ubiquitously expressing Cre recombinase (Ella-Cre), complete and functional reactivation of CB1 receptor expression by excision of the stop cassette was demonstrated by histological, electrophysiological and behavioral analyses. To further address the role of intact CB1 receptor signaling in specific neuronal subpopulations, the Stop-CB1 line was crossed with a mouse line (Nex-Cre) expressing Cre recombinase selectively in cortical glutamatergic neurons and, thus, endogenous levels of CB1 receptor were reactivated cell-type specifically. Rescue of CB1 receptor expression in cortical glutamatergic neurons was sufficient to restore the alterations of global CB1 receptor deletion in food intake and was largely sufficient to restore normal levels of neuroprotection and innate anxiety. In contrast, rescue of the CB1 receptor on cortical glutamatergic neurons modified the time course of depolarization-induced suppression of excitation (DSE) in the amygdala and promoted sustained freezing behavior in auditory fear conditioning. These data revealed that the limited amount of CB1 receptor expressed in cortical glutamatergic neurons plays a key and sufficient role to modulate specific neuronal functions.

The great majority of the studies investigating the role of the CB1 receptor to advance the knowledge for treatment of human pathologies have been carried out in mice. However, the molecular structure of the mouse *Cnr1* gene coding for the CB1 receptor had been poorly characterized. In this thesis, the mouse *Cnr1* gene was found to be more complex than previously described. It contains 7 exons separated by 6 introns and has two additional retained introns in the coding exon (exon 7). The *Cnr1* gene produces several transcript variants in hippocampus, caudate putamen and cerebellum with different 5' UTR exon assemblies. Splicing of the retained introns in the coding exon generates two novel splice variants with shortened N-termini that have different signaling efficiencies. These findings on the exon-intron structure of the mouse *Cnr1* gene add to a better understanding of regulatory processes and allelic variations contributing to pathological phenotypes observed in the rodent model.

1.2 Zusammenfassung

Eine der wichtigsten Aufgaben der aktuellen neurobiologischen Forschung besteht darin, kausale Zusammenhänge zwischen Genen, Molekülen und Funktionen herzustellen. Die *notwendige* Rolle des Cannabinoid Typ 1 (CB1) Rezeptors wurde in etlichen Studien mit „Knock-out"-Mäusen und pharmakologischen Ansätzen gezeigt. Ob der CB1 Rezeptor in denselben Vorgängen jedoch auch eine *hinreichende* Rolle spielt, wurde aufgrund von technologischen Limitierungen noch nicht ermittelt. Um die zugrunde liegenden Mechanismen dieser Vorgänge besser entschlüsseln zu können, wurde eine neuartige Mauslinie zur zelltypspezifischen Rekonstruktion des CB1 Rezeptors im Hintergrund einer CB1 Rezeptor Defizienz (Stop-CB1) generiert. Dazu wurde eine von loxP-Seiten flankierte Stop-Kassette in den Genlokus des CB1 Rezeptors eingebracht, um die Expression des CB1 Rezeptors im kompletten Körper inklusive des Gehirns zu unterdrücken. Durch das Kreuzen dieser Mauslinie mit einer Mauslinie mit ubiquitärer Expression der Cre Rekombinase (Ella-Cre), wurde die Stop-Kassette ausgeschnitten. Dass die daraus resultierende Reaktivierung der CB1 Rezeptor Expression vollständig und funktional ist, wurde mithilfe von histologischen, elektrophysiologischen und Verhaltens-Analysen bewiesen. Um zu untersuchen, welche Rolle eine intakte CB1 Rezeptor Signalwirkung in bestimmten Untergruppen von Neuronen spielt, wurde die Stop-CB1 Mauslinie mit einer Mauslinie verpaart, die Cre Rekombinase selektiv in glutamatergen Neuronen des Cortex exprimiert (Nex-Cre). Dadurch wurde der CB1 Rezeptor speziell in diesen Neuronen auf endogenem Niveau re-exprimiert. Die Rekonstruktion des CB1 Rezeptors in glutamatergen Neuronen des Cortex war hinreichend, um die durch kompletten Verlust des CB1 Rezeptors hervorgerufenen Veränderungen der Nahrungsaufnahme wiederherzustellen. Des Weiteren war die Rekonstruktion des CB1 Rezeptors auf diesen Neuronen fast hinreichend, um normale neuroprotektive Eigenschaften und normales Angstverhaltens wiederherzustellen. Im Gegensatz dazu wurde durch Rekonstruktion des CB1 Rezeptors in glutamatergen Neuronen des Cortex der zeitliche Ablauf der depolarisationsinduzierten Unterdrückung der Erregung („DSE") in der Amygdala abgeändert. Einhergehend damit wurde das verlängerte Erstarren als Reaktion auf ein Furcht-konditioniertes Tonsignal gefördert. Diese Daten zeigen, dass der CB1 Rezeptor in glutamatergen Neuronen im Cortex trotz seiner geringen Menge eine Schlüsselrolle spielt und hinreichend ist um bestimmte neuronale Funktionen zu modulieren.

Die große Mehrheit der Studien mit dem Ziel, die Bedeutung des CB1 Rezeptors zu erforschen, wurde mit Mäusen durchgeführt. Das aus diesen Studien gewonnen Wissen soll dazu dienen, Behandlungsmöglichkeiten für humane Pathologien zu entwickeln. Die molekulare Struktur des Maus *Cnr1* Gens, das für den CB1 Rezeptor kodiert, war bisher jedoch nur schlecht charakterisiert. Die Ergebnisse der vorliegenden Arbeit zeigen, dass das Maus *Cnr1* Gen komplexer ist, als es bisher beschrieben wurde. Es besteht aus 7 Exons, die von 6 Introns getrennt werden, und hat zwei weitere „retained" Introns (Introns die beibehalten werden können) im Protein-kodierenden Exon (Exon 7).

Das *Cnr1* Gen produziert verschiedene Transkriptvarianten in Hippocampus, Caudate Putamen und Cerebellum mit unterschiedlicher Zusammensetzung der 5‘ nicht-translatierten Region. Spleißen der „retained“ Introns aus dem kodierenden Exon führt zu zwei bisher unbekannten Spleißvarianten mit kürzeren N-Termini und veränderten Signaltransduktionseigenschaften. Diese Erkenntnisse über die Exon-Intron-Struktur des Maus *Cnr1* Gens tragen zum verbesserten Verständnis der im Mausmodell beobachteten pathologischen Phänotypen bei, da sie nun besser mit regulatorischen Prozesse und Variationen des Allels verknüpft werden können.

2 Introduction – a general overview of the cannabinoid system

The plant *Cannabis sativa* is one of the oldest medicinal herbs and has been used since thousands of years for its therapeutic and mood-altering properties. In 1964, Δ^9-tetrahydrocannabinol (Δ^9-THC) was identified as the major psychoactive component of *Cannabis* (Gaoni & Mechoulam, 1964). It was not until the early 1990s when the receptors for Δ^9-THC were identified in animal tissues. The cannabinoid type 1 (CB1) receptor was cloned and characterized in 1990 (Matsuda *et al.*, 1990) and was found to be largely expressed in the central nervous system (CNS). The second cannabinoid receptor (CB2) was identified three years later and was found to be mainly present in the immune system (Munro *et al.*, 1993). The CB1 receptor is the most abundant G-protein coupled receptor (GPCR) in the brain and is mainly found at the presynaptic terminals of different types of neurons in the CNS. Two fatty acid derivates, N-arachidonoyl ethanolamide (anandamide, AEA) (Devane *et al.*, 1992) and 2-arachidonoyl glycerol (2-AG) (Mechoulam *et al.*, 1995) are the major endogenous ligands (called endocannabinoids) for the cannabinoid receptors. Endocannabinoids modulate synaptic efficacy and neural activity by retrograde signaling. This chapter gives a short overview on the molecular basis of the endocannabinoid system (ECS) and the plethora of functions it exhibits.

2.1 Distribution of the CB1 receptor in the CNS

The CB1 receptor is mostly found in neurons, but additionally to its well characterized distribution on neuronal plasma membranes, it is also present in glia cells (reviewed in Stella, 2010) and was recently also identified on membranes of neuronal mitochondria (Bénard *et al.*, 2012). Within the scope of this work, the following chapter is focused on CB1 receptor distribution on neuronal plasma membranes.

The CB1 receptor is found in several brain regions, including neocortex, hippocampus, nucleus accumbens, basal ganglia, hypothalamus, amygdala, and cerebellum (Herkenham *et al.*, 1991). The expression level of the CB1 receptor does not reflect the functional significance, as it was shown that very low levels of CB1 receptor expression underlie very important functions in specific regions or cell types (Marsicano & Kuner, 2008). As the CB1 receptor is preferentially targeted to presynaptic sites, the distribution of CB1 receptor mRNA and protein do not necessarily overlap (Figure 2.1). Axonal projections can be located very far from the cell body, for example the strongest CB1 receptor immunoreactivity and agonist binding is found along the striatonigral and striatopallidal pathways as

well as in substantia nigra pars reticulata and the globus pallidus, in both of which CB1 mRNA is reported not to be expressed (Mátyás *et al.*, 2006). Thus, it is important to take the detection system used into consideration when looking at the expression pattern of the CB1 receptor. Two distinct patterns of CB1 receptor expression are found, i.e. uniform and non-uniform distribution, which depend on the brain region the receptor is expressed in. A uniform CB1 receptor mRNA expression is found in striatum, thalamus, hypothalamus, cerebellum and lower brain stem, whereas in cortical areas, a non-uniform expression pattern is detected representing different expression levels of CB1 mRNA in different cell types (Marsicano & Lutz, 1999). In cerebral cortex, hippocampus and amygdala, high expression levels of CB1 receptor mRNA are found in inhibitory interneurons, whereas much lower expression levels are found in excitatory neurons (Marsicano & Lutz, 1999). The very important functional consequences arising from the expression on these different neuronal subpopulations are discussed in Chapter 2.5.

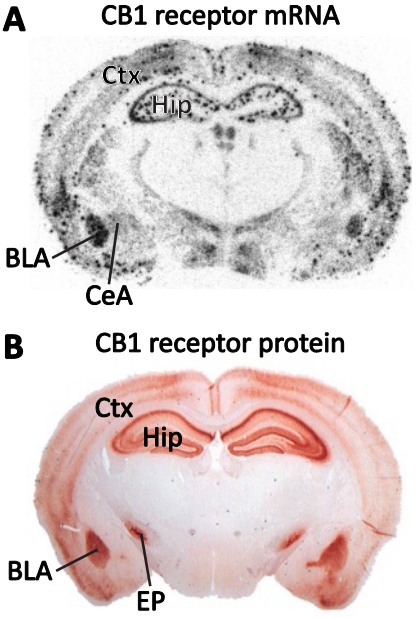

Figure 2.1: CB1 receptor is highly expressed throughout the brain.
Micrographs of coronal sections show **(A)** the expression of CB1 receptor mRNA as detected by *in situ* hybridization with a specific riboprobe for the CB1 receptor (performed by Krisztina Monory, Lutz group), and **(B)** the distribution of CB1 receptor protein as detected by immune-histochemistry with an antibody against the CB1 receptor (performed by Martin Häring, Lutz group). BLA, basolateral amygdala; Ctx, cortex; CeA, central nucleus of the amygdala; EP, entopeduncular nucleus; Hip, hippocampus.

In the following, a more detailed description of CB1 receptor neuroanatomy is given for the hippocampal and amygdaloidal formations, as the modulatory role of CB1 receptor in these regions is one focus of this work.

In the hippocampus, the interneurons expressing high levels of CB1 mRNA coexpress glutamic acid decarboxylase 65k (GAD65) and cholecystokinin (CCK) (Marsicano & Lutz, 1999). At protein level, the CB1 receptor is localized on axon terminals of CCK-positive basket cells surrounding pyramidal neurons (Katona *et al.*, 1999). Lower levels of CB1 receptor mRNA are found in calbindin- and calretinin-positive interneurons, but not in parvalbumin-positive basket cells (Marsicano & Lutz, 1999). The presence of the CB1 receptor on glutamatergic neurons in the hippocampus has been intensely debated. Although CB1 receptor mRNA was detected on CA1 and CA3 pyramidal neurons

(Marsicano & Lutz, 1999), several studies did not detect any CB1 receptor immunoreactivity in these neurons (Freund *et al.*, 2003; Marsicano & Kuner, 2008). Better detection methods and the use of genetically modified animals revealed that CB1 receptor protein is indeed also expressed on glutamatergic neurons, including hippocampal and cortical pyramidal cells and mossy cells in the dentate gyrus, but at much lower levels (Kawamura *et al.*, 2006; Domenici *et al.*, 2006; Monory *et al.*, 2006). Mossy cells seem to contain the highest level of CB1 receptor immunoreactivity amongst the excitatory hippocampal neurons (Kawamura *et al.*, 2006; Monory *et al.*, 2006). Despite its lower expression level, CB1 receptor on glutamatergic hippocampal neurons was shown to exhibit very important functions (see 2.6.2).

The amygdala is composed of several subnuclei, and the CB1 receptor is expressed differentially in the different parts. It can be subdivided into the cortical-derived basolateral amygdala (BLA) comprised of glutamatergic principal projection neurons and γ-aminobutyric acid (GABA)ergic local interneurons, and a striatal-derived component including the central and medial nuclei comprising medium spiny-like GABAergic neurons (Swanson & Petrovich, 1998; Pape & Paré, 2010). In the BLA, CB1 receptor mRNA is expressed in CCK-positive and calbindin-positive interneurons (Marsicano & Lutz, 1999). CB1 immunoreactivity is detected in large CCK-positive interneurons, but not in small CCK-positive ones (McDonald & Mascagni, 2001; Katona *et al.*, 2001). Also on calretinin-positive (around 30%) and a few parvalbumin-positive interneurons, low levels of CB1 receptor mRNA are detected (Marsicano & Lutz, 1999). Furthermore, 38% of CB1 receptor-expressing neurons within the BLA co-express corticotrophin releasing hormone receptor type 1 (CRHR1) mRNA (Hermann & Lutz, 2005). In pyramidal neurons in the BLA, CB1 receptor mRNA is expressed at low levels (Mailleux & Vanderhaeghen, 1992), and CB1 receptor immunoreactivity is only detectable in perikarya of pyramidal neurons after colchicine treatment (McDonald & Mascagni, 2001). In the central part of the amygdala, CB1 receptor mRNA is expressed in low levels, but expression differences within the subregions have remained unclear (Hermann & Lutz, 2005; Chhatwal *et al.*, 2005). For CB1 receptor immunoreactivity, a mesh-like pattern is observed mostly in medioventral parts of the central amygdala, with denser networks in the medial than in the lateral part (Kamprath *et al.*, 2011).

2.2 Endocannabinoids

The CB1 receptor can be activated by exogenously applied cannabinoids as well as endogenous lipid ligands. The best characterized endocannabinoids, AEA and 2-AG, are synthesized in an activity-dependent manner. AEA is synthesized by action of the phospholipase D from N-arachidonoyl phosphatidyl ethanolamine (NAPE) (Figure 2.2). By transferring the arachidonate group from a phospholipid to phosphatidyl ethanolamine, NAPE is replenished (Piomelli, 2003). For the synthesis

of 2-AG, phospholipase C (PLC) hydrolyzes phosphatidylinositol and produces diacylglycerol (DAG). DAG lipase then hydrolyses DAG to the monoacylglycerol 2-AG (Piomelli, 2003). The concentration of 2-AG in the brain is about 200 fold higher than AEA, suggesting its involvement in housekeeping functions (Stella *et al.*, 1997).

After activity-dependent synthesis at the post-synapse, AEA and 2-AG are released in the synaptic cleft, acting as retrograde messengers at presynaptically located CB1 receptor (Kreitzer & Regehr, 2002; Alger, 2002). Both release and reuptake of endocannabinoids seem to be facilitated by a membrane transport process (Fowler & Jacobsson, 2002). Recently, a catalytically silent variant of fatty acid amide hydrolase (FAAH), named FAAH1 like AEA transporter (FLAT), was identified as a putative AEA transporter (Fu *et al.*, 2012). For 2-AG, the reuptake mechanism is still unknown.

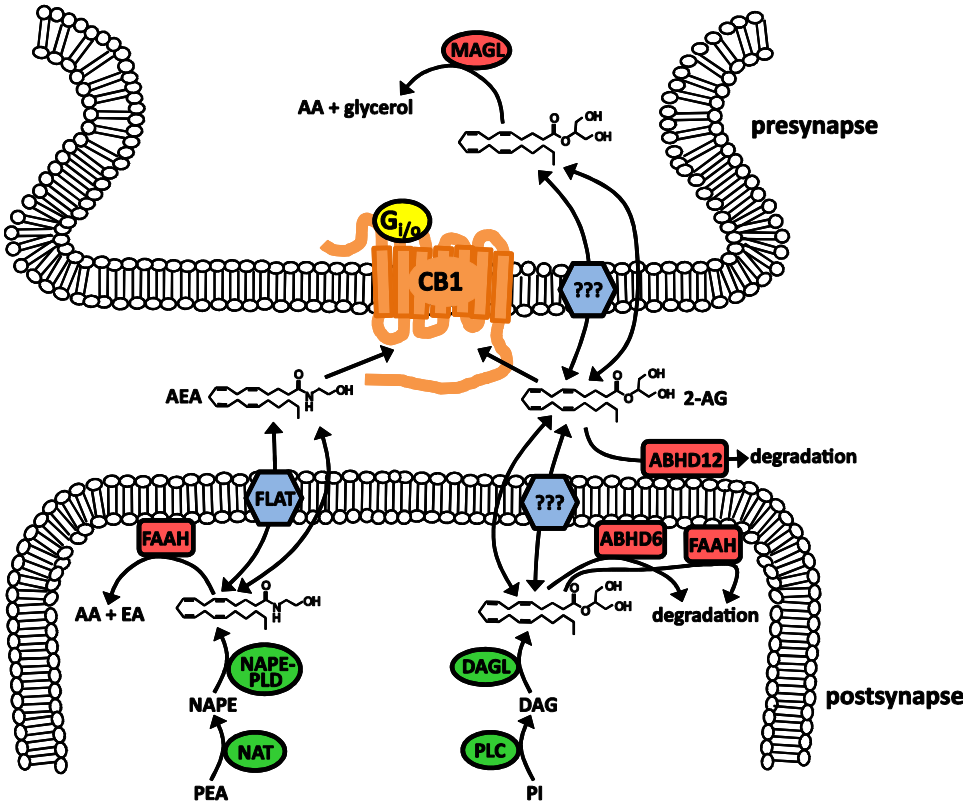

Figure 2.2: Schematic representation of the synthesis, release, reuptake and degradation of endocannabinoids. AEA and 2-AG are synthesized in the postsynaptic neuron from which they are released. They travel retrogradely over the synaptic cleft and activate presynaptic CB1 receptor. AEA is mainly degraded by FAAH in the postsynapse, while the main 2-AG degrading enzyme MAGL is found in the presynapse. 2-AG, 2-arachidonoyl glycerol; AA, arachidonic acid; ABHD6/12, α-β-hydrolase domain 6/12; AEA, anandamide; EA, ethanolamine; DAG, diacyl glycerol; DAGL, DAG lipase; FAAH, fatty acid amide hydrolase; FLAT, FAAH1 like AEA transporter, MAGL, monoacylglyceride lipase; NAPE, *N*-arachidonoyl phosphatidyl ethanolamine; NAPE-PLD, NAPE-specific phospholipase D, NAT, *N*-acyltransferase; PEA, phosphatidyl ethanolamine; PI, phosphatidyl inositol; PLC, phospholipase C.

In the presynapse and postsynapse, endocannabinoids are enzymatically hydrolyzed. AEA is primarily hydrolyzed to arachidonic acid by the postsynaptic, membrane bound enzyme FAAH (Cravatt *et al.*, 1996; Gulyas *et al.*, 2004). Accumulation of 2-AG is controlled by the primarily soluble,

presynaptic monoglyceride lipase (MAGL) (Dinh *et al.*, 2002) and, to a much lesser extent, by the membrane bound postsynaptic α-β-hydrolase domain 6 (ABHD6) (Blankman *et al.*, 2007; Marrs *et al.*, 2010), the luminal oriented hydrolase ABHD12 (Blankman *et al.*, 2007) and FAAH (Di Marzo & Maccarrone, 2008). Also cytochrome p450 enzymes and cyclooxygenase 2 (COX-2) were shown to oxidize both AEA and 2-AG (Kozak *et al.*, 2004).

The differential compartmentalization of the endocannabinoid degrading machinery could be one reason for the differential effects mediated by AEA and 2-AG *in vivo* via the CB1 receptor. Whereas blocking AEA hydrolysis was shown to reduce pain, depression and anxiety, but have no effect on locomotion and body temperature (Calignano *et al.*, 1998; Kathuria *et al.*, 2003; Gobbi *et al.*, 2005; Long *et al.*, 2009), blocking 2-AG degradation was shown to reduce body temperature, locomotion and, like AEA, pain (Long *et al.*, 2009; Alger & Kim, 2011). The fine-tuned actions of the different endocannabinoids accounting for these differential effects still need to be established.

2.3 CB1 receptor signaling

Activation of the CB1 receptor causes several effects through multiple intracellular signaling pathways. The seven-transmembrane domain receptor predominantly mediates signal transduction by the $G_{i/o}$ subfamily of G proteins. Activation of the CB1 receptor inhibits cyclic adenosine monophosphate (cAMP) production via inhibition of adenylyl cyclase (AC), leading to downregulation of protein kinase A (PKA) signaling (Childers & Deadwyler, 1996) (Figure 2.3). CB1 receptor activation also inhibits several classes of ion channels in a cAMP-dependent or -independent manner. The CB1 receptor was reported to enhance the activation of the voltage-dependent A-type potassium channel (Deadwyler *et al.*, 1995) and the inwardly rectifying potassium channels (Mackie *et al.*, 1995), and to inhibit the activity of N- and P/Q-type voltage-dependent calcium channels (Twitchell *et al.*, 1997) and D- and M-type potassium channels (Mu *et al.*, 1999). Furthermore, CB1 receptor activation leads to phosphorylation of the p42/p44 mitogen-activated protein kinase (MAPK) (Bouaboula *et al.*, 1995) and leading to expression of the immediate early genes c-fos, zif268 and brain-derived neurotrophic factor (BDNF) (Derkinderen *et al.*, 2003). Stimulation of the CB1 receptor also induces the activation of several kinases including focal adhesion kinase (FAK) (Derkinderen *et al.*, 1996), c-Jun N-terminal kinase (JNK) (Rueda *et al.*, 2000), p38 MAPK (Derkinderen *et al.*, 2001), and protein kinase B/Akt (PKB) via phosphatidyl inositol-3-kinase (PI3-K) (Gómez del Pulgar *et al.*, 2000; Galve-Roperh *et al.*, 2002). Apart from the numerous kinases, protein phosphatase 3 (calcineurin) was also shown to be activated by CB1 receptor (Cannich *et al.*, 2004). It is important to keep in mind that these signaling pathways were described in different cellular systems and do not necessarily occur in the same cell types.

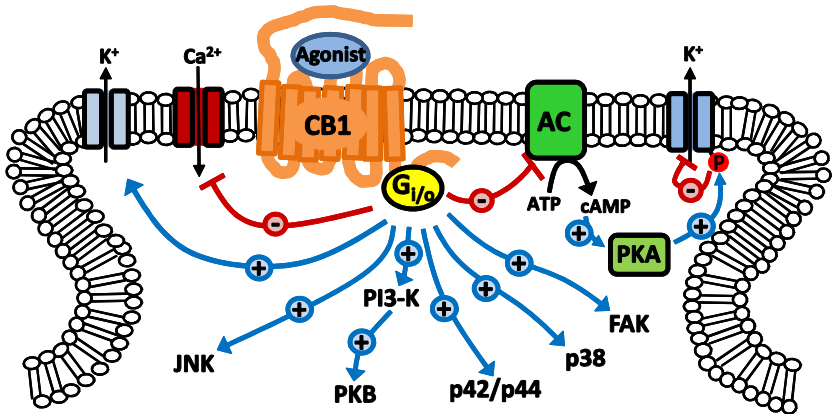

Figure 2.3: Schematic representation of the signal transduction pathways mediated by the activation of CB1 receptor. For detailed description of the signaling pathways, see text. AC, adenylyl cyclase; FAK, focal adhesion kinase; JNK, c-Jun N-terminal kinase; p38, p42/42, mitogen activated protein kinases; PI3-K, phosphatidyl inositol-3-kinase; PKA, protein kinase A; PKB, protein kinase B.

Numerous studies demonstrated that the activation of CB1 receptor inhibits the release of various neurotransmitter (reviewed in Kano *et al.*, 2009), including glutamate (Lévénés *et al.*, 1998), GABA (Szabo *et al.*, 1998), glycine (Jennings *et al.*, 2001), acetylcholine (Gifford & Ashby, 1996), norepinephrine (Ishac *et al.*, 1996), dopamine (Cadogan *et al.*, 1997), serotonin (Nakazi *et al.*, 2000) and CCK (Beinfeld & Connolly, 2001).

2.4 Endocannabinoid-mediated synaptic plasticity

Endocannabinoids are released from postsynaptic neurons and induce transient or persistent suppression of transmitter release, leading to short-term and long-term synaptic plasticity, respectively.

The release of endocannabinoids leading to short-term depression (eCB-STD) can be induced by different stimulation protocols, i.e. postsynaptic depolarization, activation of postsynaptic G_q-coupled receptors and combined G_q-coupled receptor activation with depolarization (Hashimotodani *et al.*, 2007). Depolarization-induced suppression of transmitter release was shown to be present at inhibitory synapses, named depolarization-induced suppression of inhibition (DSI) (Ohno-Shosaku *et al.*, 2001; Wilson & Nicoll, 2001), and at excitatory synapses, named depolarization-induced suppression of excitation (DSE) (Kreitzer & Regehr, 2001). The strong depolarization of the postsynaptic neuron activates voltage-gated Ca^{2+} channels, causes elevation of Ca^{2+} concentration and thus triggers biosynthesis of endocannabinoids (reviewed in Kano *et al.*, 2009). The second form of eCB-STD is driven by activation of G_q-coupled receptors on the postsynapse. Strong activation of several receptors including group I metabotropic glutamate receptor (Maejima *et al.*, 2001), muscarinic acetylcholine receptor (Kim *et al.*, 2002), CCK receptor (Foldy *et al.*, 2007) and orexin receptor (Haj-Dahmane & Shen, 2005) stimulates endocannabinoid release. The release depends on PLC, suggesting that 2-AG is likely to function as the retrograde messenger (Hashimotodani *et al.*, 2005; Maejima *et al.*, 2005). The third form of eCB-STD is induced

by a combination of mild Ca^{2+} elevation and mild receptor activation, but the amount of endocannabinoids released is much higher than the simple sum of the amounts produced by individual stimuli, suggesting a synergistic effect (Ohno-Shosaku *et al.*, 2002*a*).

Endocannabinoids are also involved in long-term synaptic plasticity. Release of endocannabinoids during DSI was shown to facilitate induction of long-term potentiation (LTP) in the hippocampus (Carlson *et al.*, 2002). In several brain regions, stimulation resulting in LTP of excitatory synapses simultaneously caused long-term depression (LTD) at neighboring inhibitory synapses (Marsicano *et al.*, 2002; Chevaleyre & Castillo, 2003; Azad *et al.*, 2004). This process called long-term depression of inhibition (dubbed iLTD in the amygdala (Marsicano *et al.*, 2002) and LTD-I in the hippocampus (Chevaleyre & Castillo, 2003)) is mediated by endocannabinoids. By the persistent reduction of GABAergic transmission, LTD of inhibition can enhance excitatory synaptic transmission. Similarly, CB1 receptor-dependent LTD of excitation was described in cortico-striatal synapses (Gerdeman *et al.*, 2002; Robbe *et al.*, 2002).

2.5 The ECS as a bimodal regulator[1]

CB1 receptor activation as well as pharmacological or genetic interference with the molecular machinery of the ECS are often reported to exhibit biphasic responses (e.g. Lafenêtre *et al.*, 2007, 2009; Rubino *et al.*, 2008*b*; Bellocchio *et al.*, 2010; Häring *et al.*, 2011). Several characteristics of the ECS might contribute to the biphasic effects.

2.5.1 CB1 receptor on glutamatergic and GABAergic neurons

As discussed above, the CB1 receptor is located on different neuronal subpopulations, including glutamatergic and GABAergic neurons (see 2.1). Activation of the CB1 receptor by endocannabinoids leads to a reduction of neurotransmitter release by a retrograde mechanism (Wilson & Nicoll, 2002; and see 2.4). Mediated by CB1 receptor activation, the CB1 receptor agonists Δ^9-THC and WIN55,212-2 were shown to inhibit GABA release (Laaris *et al.*, 2010). In addition, CB1 receptor-mediated inhibition of glutamate release was also demonstrated in rats (Hoffman *et al.*, 2010) and mice (Kawamura *et al.*, 2006). Depending on whether the experimental conditions predominantly modulate excitatory or inhibitory transmission (i.e. glutamatergic or GABAergic), the effect of the absence of CB1 receptor signaling will lead to different behavioral outcomes. Notably, the great majority of CB1 receptor is located on GABAergic neurons in the brain. However, the discrete location of CB1 receptor on glutamatergic neurons enables cannabinoids to exert important functions (Monory *et al.*, 2006).

[1] The following chapter has been modified from Ruehle et *al.* (2012).

2.5.2 ECS basal functionality (tonic *vs.* phasic activation)

In addition to the distinct abundance of CB1 receptor on GABAergic and glutamatergic neurons, it is of central interest to define the basal activity of CB1 receptor on both neuronal subpopulations. This property of the CB1 receptor will determine to which extent it can be additionally activated by a rise in endocannabinoid levels depending on the basal activation that is present under normal circumstances. Recent studies have shown a difference in basal activity between CB1 receptor localized on GABAergic and glutamatergic populations (Slanina & Schweitzer, 2005; Roberto *et al.*, 2010). CB1 receptor antagonists, such as AM251 and SR141716, were shown to increase inhibitory transmission in the central nucleus of the amygdala (CeA), suggesting a tonic activation of CB1 receptor on GABAergic neurons under basal conditions (Roberto *et al.*, 2010). This effect was regulated by the postsynaptic neuron in response to elevated Ca^{2+} levels. Moreover, blockade of CB1 receptor moderately but significantly augmented excitatory neurotransmission, indicating a tonic activity of the ECS also on this system (Slanina & Schweitzer, 2005). In this study, 2-AG was proposed as the endocannabinoid responsible for the tonic inhibition of excitatory neurotransmission, and the interaction with the inhibitory network was excluded using $GABA_A$ and $GABA_B$ receptor antagonists. Nevertheless, increases of glutamate release induced by AM251 were never higher than 110% of the tonic release (Slanina & Schweitzer, 2005), whereas augmentation of GABAergic release after treatment with the same CB1 receptor antagonist reached levels of 130-140% (Roberto *et al.*, 2010). Hence, the tonic inhibition mediated by CB1 receptor is much more relevant on GABAergic synapses than on glutamatergic synapses. Consequently, CB1 receptor on GABAergic terminals are thought to be a general suppressor of GABA release (predominantly relevant in tonic activation), while CB1 receptor on glutamatergic terminals has a different physiological role and is responsible for the on-demand inhibition only after excessive glutamate release (predominantly relevant in phasic activation) (Katona & Freund, 2008).

2.5.3 Neuronal subpopulations classified by CB1 receptor agonist sensitivities

Keeping in mind the relevance of the differences between GABAergic and glutamatergic neurons in terms of CB1 receptor basal activity and its abundance, there is another fundamental aspect to consider; the relation between CB1 receptor localization and sensitivity to CB1 receptor agonists. The term sensitivity refers to the capacity of the CB1 receptor to be activated by a CB1 receptor agonist and consequently to mediate DSI or DSE. In fact, DSI and DSE are not equally executed, as excitatory transmission was estimated to be about 30-fold less sensitive to cannabinoids than inhibitory transmission (Ohno-Shosaku *et al.*, 2002*b*). Accordingly, biochemical experiments

using blockers of enzymes implicated in synthesis and degradation of 2-AG and AEA confirm that the more abundant 2-AG is the most probable endocannabinoid implicated in DSE (Hashimotodani *et al.*, 2007). These studies also suggest the existence of three different types of synapses classified by their sensitivity to the CB1 receptor agonist WIN55,212-2. Whereas excitatory synapses are homogeneous and have a moderate sensitivity, inhibitory synapses are dichotomized into two distinct populations, one with a high sensitivity and one that is not sensitive to WIN55,212-2. Recent experiments demonstrated that inhibitory synapses that are sensitive to cannabinoid-induced DSI can even be further subdivided into two different groups. The group with higher sensitivity is formed by perisomatically projecting basket cells (BC), while the dendritically projecting Schaffer-collateral associated cells (SCA) belong to the group with lower sensitivity to WIN55,212-2 (Lee *et al.*, 2010). Given the different neuroanatomical features of these two different neuronal subtypes, the action of a different endocannabinoid ligand cannot be excluded, due to the fact that the 2-AG synthesizing molecular pathways are located in dendritic spines (Katona *et al.*, 2006), and consequently, SCA synapses should have a higher sensitivity than BC synapses, which is certainly not the case. Nevertheless, it is worth mentioning that the relative density of CB1 receptor on GABAergic and glutamatergic neurons is not a reliable indicator *per se* of their respective strengths in regulating neurotransmitter release. As a matter of fact, the presence of presynaptic functional differences downstream of CB1 receptor, involving coupling to G proteins and/or Ca^{2+} channels, was shown to be different between GABAergic and glutamatergic neurons. A recent study revealed that the capacity to recruit G proteins is higer for CB1 receptor located on glutamatergic terminals than on GABAergic terminals (Steindel *et al.*, 2008), suggesting a compensatory effect to the lower abundance of CB1 receptor on glutamatergic terminals.

2.5.4 Promiscuity of endocannabinoids

In addition to the differential expression, basal activation and sensitivity of CB1 receptor on glutamatergic and GABAergic synapses, the promiscuity frequently reported for endocannabinoids may contribute to the biphasic properties of cannabinoid signaling.

The implication of receptors different from CB1 receptor was proposed to explain certain aspects of the behavior after cannabinoid exposure. For example, 2-AG-mediated suppression of inhibitory transmission was not blocked by the CB1 receptor antagonist LY320135, but with the CB2 receptor antagonist AM630 (Morgan *et al.*, 2009), revealing an interesting role for the CB2 receptor in (endo)cannabinoid signaling and, consequently, a possible influence of the ECS on behavior via CB2 receptor activation. Furthermore, AEA can also activate transient receptor potential vanilloid type 1 (TRPV1) channel and thus can trigger LTD in the dentate gyrus (Chavez *et al.*, 2010; Puente *et al.*, 2011). AEA was shown to exhibit biphasic properties, acting for example in a low dose as an

anxiolytic agent on CB1 receptor and in a higher dose as an anxiogenic agent on TRPV1 channel (Rubino *et al.*, 2008*a*). Recently, 2-AG was also shown to be promiscuous, as it potentiates $GABA_A$ receptors at low concentrations of GABA (Sigel *et al.*, 2011).

For investigations of the modulatory role of the CB1 receptor, all these factors complicating the interpretations need to be carefully considered.

2.6 Physiological role of the ECS

In the brain, the ECS is involved in the regulation of a large variety of functions (for review, see Kano *et al.*, 2009). In this thesis, the role of CB1 receptor function in a subset of these physiological functions was analyzed, namely feeding behavior, neuroprotection, anxiety and extinction of fear memories. This chapter gives an overview of the role of the ECS in these physiological processes and behaviors.

2.6.1 Endocannabinoid-mediated control of food intake

By processing information on availability and palatability of food and by integrating information on type and amount of recently consumed nutrients from the gastrointestinal tract, energy expenditure from various organs and energy storage from adipose tissue, a complex neuronal network regulates food intake (Morton *et al.*, 2006). Endocannabinoid signaling was shown to stimulate orexigenic pathways by acting in hypothalamic areas, which control food intake and energy balance and by modulating cortico-limbic pathways, which control the motivational and pleasurable effects of eating (Di Marzo & Matias, 2005; Quarta *et al.*, 2011). In the hypothalamus, the effects of endocannabinoids and of CB1 receptor agonist and antagonist on food intake are mediated by complex interactions of several neuronal circuits in the arcuate nucleus, the paraventricular nucleus and the lateral hypothalamus with several anorectic and orexigenic mediators (reviewed in Bermudez-Silva *et al.*, 2012). The ECS-mediated modulation of the rewarding properties involves a series of synaptically interconnected circuits linking the prefrontal cortex (PFC), the amygdala, the ventral tegmental area, the nucleus accumbens and the ventral pallidum and includes interactions with the mesolimbic dopaminergic and the opioid system (Bermudez-Silva *et al.*, 2012). In addition to their high abundance in the nervous system, endocannabinoids and the CB1 receptor are also present in peripheral cells and tissues controlling energy homeostasis, including gut, liver, adipose tissue, skeletal muscle and pancreas (Matias & Di Marzo, 2007). This peripheral expression of CB1 receptor was shown to be a very important modulator of satiety and energy expenditure (Quarta *et al.*, 2010, 2011). Within the scope of this work, this chapter is focused on endocannabinoid-modulated control of acute food intake in the CNS.

The ECS is activated after stressful or harmful conditions to restore the homeostasis in the brain (Hill *et al.*, 2010). Short periods of food deprivation activate the ECS by increased levels of AEA and 2-AG in the limbic forebrain and, to a lesser extent, of 2-AG in the hypothalamus (Kirkham *et al.*, 2002), in order to regulate the levels of orexigenic and anorexigenic mediators and induce food intake (Matias & Di Marzo, 2007). Genetic deletion or pharmacological blockade of the CB1 receptor abolished the observed increase in food intake after a short period of fasting (Di Marzo *et al.*, 2001). By the use of mouse lines with specific deletions of the CB1 receptor from cortical glutamatergic neurons or GABAergic neurons, Bellocchio *et al.* (2010) have shown a bimodal role of the CB1 receptor in the regulation of food intake after short food deprivation: CB1 receptor-dependent acute inhibition of cortical glutamatergic transmission contributes to fasting-induced hyperphagia, whereas inhibition of inhibitory GABAergic transmission in the ventral striatum mediates the fasting-induced hypophagic effect of endogenous CB1 receptor signaling. The same results were found when prefed animals were exposed to palatable food (Bellocchio *et al.*, 2010). Furthermore, the authors also showed that agonist-induced activation of CB1 receptor in either glutamatergic (low doses) or GABAergic neurons (high doses) accounts for the biphasic action of Δ^9-THC with low doses being hyperphagic and high doses being hypophagic (see 2.5).

2.6.2 Neuroprotective properties of the ECS

A strict excitation-inhibition balance is necessary for appropriate neuronal functionality. Excessive excitatory activity or hypersynchronous neuronal activity in the brain leads to neuronal damage and cell death and can induce epileptiform seizures, leading to long-lasting changes of network activity and the development of a hyperexcitable state (Ben-Ari & Cossart, 2000; McCormick & Contreras, 2001). The mechanisms underlying temporal lobe epilepsy can be investigated by the use of animal models of epilepsy.

Status epilepticus, a continuous or repetitive seizure activity for at least 30 min without regaining consciousness, can be modeled in rodents by injection of the muscarinic acetylcholine receptor agonist pilocarpine. After half an hour, the status epilepticus is terminated by injection of the $GABA_A$ receptor positive allosteric modulator diazepam. Pilocarpine-induced status epilepticus is followed by a latent period and later by a state of hyperexcitability and the appearance of spontaneous recurrent seizures (Curia *et al.*, 2008). In the acute phase of epilepsy, a significant downregulation of the CB1 receptor was described (Falenski *et al.*, 2009; Karlócai *et al.*, 2011). The effect of CB1 receptor level reduction was analyzed using CB1 receptor knock-out mice, which displayed an increased seizure severity and a higher mortality rate in the acute phase (Karlócai *et al.*, 2011). In the chronic phase, an upregulation of the CB1 receptor was described (Wallace *et al.*, 2003; Bhaskaran & Smith, 2010*a*). An increased CB1 receptor expression in the molecular layer excitatory

neurons in the reorganized dentate gyrus was found together with a CB1 receptor-mediated reduction of miniature excitatory post-synaptic current frequency (Bhaskaran & Smith, 2010*a*). Selective analysis of the expression pattern of the CB1 receptor on hippocampal GABAergic axon terminals showed also a sprouting of fibers of CB1 receptor-expressing interneurons and/or the elevation of the level of CB1 receptor (Maglóczky *et al.*, 2010). Another recent study also revealed an increase of CB1 receptor levels in both asymmetric and symmetric synapses (Karlócai *et al.*, 2011), suggesting an increased number of CB1 receptor-positive mossy cell axons and subcortical fibers as well as a sprouting of the surviving CB1 receptor-positive interneurons, leading to an increased density or CB1 receptor-positive inhibitory fibers. Taken together, the decrease of the CB1 receptor during the acute seizure phase may lead to an elevation of glutamate release and the subsequent development of recurrent seizures. The increase of the CB1 receptor in the chronic phase may serve as a neuroprotective mechanism by decreasing the excitability and synchronization by reducing glutamate and GABA release (Karlócai *et al.*, 2011). Interestingly, a significantly increased expression of TRPV1 channel was observed after pilocarpine-induced temporal lobe epilepsy. TRPV1 channel can be activated by the endocannabinoid AEA (see 2.5.4) and can thus contribute to enhanced excitatory circuit activity in the synaptically reorganized dentate gyrus of mice with temporal lobe epilepsy (Bhaskaran & Smith, 2010*b*).

The acute phase of seizures can also be modeled with kainic acid (KA)-induced seizures. Injection of KA leads to excessive excitatory transmission in the brain, inducing acute epileptiform seizures (Ben-Ari & Cossart, 2000). CB1 receptor-deficient mice showed a higher susceptibility for KA-induced epileptiform seizures, showing that CB1 receptor exhibits neuroprotective properties (Marsicano *et al.*, 2003). Upon KA-induced seizures, increased production of AEA (Marsicano *et al.*, 2003) and 2-AG (Wettschureck *et al.*, 2006) in the hippocampus activates cannabinoid receptors and induces protective intracellular signaling cascades (Marsicano *et al.*, 2003). Phosphorylation of p42 and p44 MAPKs and transcription of the c-fos, zif268 and BDNF genes was shown to be reduced in mice lacking CB1 receptor on all forebrain principal neurons (Marsicano *et al.*, 2003). The distinct temporal profile of endocannabinoid release after seizure induction is crucial, as only a transient increase of endocannabinoids provided protection against KA-induced seizures, whereas increase of endocannabinoid levels before the excitotoxic event did not reduce seizure severity (Marsicano *et al.*, 2003; Monory & Lutz, 2008). As the CB1 receptor is expressed on both GABAergic and glutamatergic neurons in the hippocampus, the generation of mouse lines with subtype-specific CB1 receptor-deficiencies (Marsicano *et al.*, 2003; Monory *et al.*, 2006) provided insight into the role of the CB1 receptor in neuroprotection. Mice with cortical glutamatergic neuron-specific deletion of the CB1 receptor displayed a higher susceptibility to KA-induced seizures, whereas mice with deletion of the CB1 receptor from GABAergic neurons showed the same response as wild-type littermates

(Marsicano *et al.*, 2003; Monory *et al.*, 2006). Furthermore, adeno-associated virus (AAV)-mediated overexpression of the CB1 receptor in pyramidal neurons of the hippocampus was shown to protect against seizure-induced excitotoxicity (Guggenhuber *et al.*, 2010). These data prove that CB1 receptor expressed on excitatory glutamatergic axon terminals is responsible for the anti-convulsant effect.

2.6.3 The ECS in anxiety and fear memory[2]

Negative emotions, such as anxiety and fear, alert the organism to potentially dangerous or harmful stimuli, and can hence promote survival. However, when anxiety and fear responses are disproportional in intensity, chronic, irreversible and/or not associated with any actual risk, they can impair physical and psychological functions. Such overreactions may be symptomatic of anxiety-related neuropsychiatric disorders, such as generalized anxiety, phobia and post-traumatic stress disorder (Graham *et al.*, 2011). Recent studies have provided new insights into the molecular basis of the modulatory role of the ECS in anxiety (here defined as innate fear) and its involvement in different phases of fear learning (here defined as acquired fear).

2.6.3.1 Anxiety

In various anxiety paradigms, such as the Vogel conflict test, light/dark box and elevated plus maze, CB1 receptor agonists, antagonists and other drugs interfering with the molecular machinery of the ECS were reported to induce biphasic effects, with lower doses being anxiolytic and higher doses being anxiogenic (Viveros *et al.*, 2005; Lafenêtre *et al.*, 2007). The similarity and reproducibility between these models where different components of the anxiety state can be measured, suggests a strong involvement of the ECS in anxiety. Nevertheless, experimental conditions, species differences and previous experiences of subjects among other parameters also affect the animals' reaction. Several studies using CB1 receptor knock-out mice reported anxiogenic responses in several classical anxiety paradigms, such as elevated plus maze (Haller *et al.*, 2004*b*) and light/dark box (Martin *et al.*, 2002). Nevertheless, contradictory data do also exist. The implications of the susceptibility of the ECS to environmental variables (see 2.6.3.1.1), the differential expression, basal activation and sensitivity of CB1 receptor on glutamatergic and GABAergic synapses (see 2.6.3.1.2 and 2.5) as well as the promiscuity of endocannabinoids (see 2.5) that could provide an explanation for these contradicting findings will be discussed here.

2.6.3.1.1 ECS susceptibility to environmental variables

Several parameters need to be considered when interpreting data from anxiety assays. The administration route of drugs in pharmacological approaches represents a relevant starting point in

[2] This chapter has been modified from Ruehle *et al.* (2012).

the analysis of the behavioral results, since anxiogenic and anxiolytic effects of ECS enhancement were related to different brain areas (Rubino *et al.*, 2008*a*). Thus, the same dose of Δ^9-THC is able to promote anxiolytic responses when injected in the PFC, while microinjections in the BLA lead to an anxiogenic response. Moreover, the appropriate selection of the studied species is fundamental. Haller *et al.* (2007) have proposed that contradictory anxiety-like results obtained in rats and mice can be explained by the different cannabinoid responsiveness of GABAergic and glutamatergic neurons in these two species. In addition, data from the analysis of CB1 receptor deficient animals revealed that significant differences between CB1 receptor knock-out animals and their wild-type littermates can only be found under aversive conditions (Haller *et al.*, 2004*a*; Jacob *et al.*, 2009). Therefore, the light conditions during the test, as well as the housing and the handling prior to the test, are important parameters to be kept well-defined in experiments involving anxiety and the ECS. Regarding these variables, FAAH is of particular interest. A plethora of studies involving pharmacological blockade of FAAH by the specific inhibitor URB597 demonstrated anxiolytic behaviors in a variety of species using different anxiety paradigms (Moreira *et al.*, 2008; Scherma *et al.*, 2008; Patel & Hillard, 2008; Rubino *et al.*, 2008*b*). Nevertheless, recent discrepant findings revealed that the anxiolytic effect of URB597 depends largely on the experimental conditions (Naidu *et al.*, 2007; Trezza & Vanderschuren, 2008; Haller *et al.*, 2009) and is only significant under stress conditions. In summary, dependent on the stress level, which is associated with the protocol used (inescapable *vs.* escapable stressors, aversive conditions, previous exposure), the animal model used and the administration route in pharmacologic protocols, a bimodal response will be seen as long as the experimental conditions do not exceed the buffering function of the ECS.

2.6.3.1.2 CB1 receptor-dependent regulation of biphasic responses in anxiety

Despite the difficulty to generate a physiological model that considers the vast amount of interactions associated with the ECS, two neurotransmitters have emerged as points of reference for the complexity in anxiety behavior. Evidence from pharmacological and genetic alterations of GABAergic and glutamatergic transmission indicates that these neurotransmitters appear to exert their functions on anxiety in opposite ways (Millan, 2003). Due to the expression of the CB1 receptor on axon terminals of both subpopulations, it is tempting to predict the relevance of the localization of this receptor as an explanation for the dual role of the ECS in the regulation of anxiety.

Activation of CB1 receptor by endocannabinoids was shown to inhibit GABA (Laaris *et al.*, 2010) and glutamate release (Kawamura *et al.*, 2006; Hoffman *et al.*, 2010). The enhancement of GABAergic transmission via benzodiazepines ($GABA_A$ receptor positive allosteric modulators) has been used as an effective acute treatment for patients with anxiety disorders. Consequently, it could be assumed that a prominent increase in the endocannabinoid tone, and consequently CB1 receptor

activation specifically on GABAergic neurons, would lead to an anxiogenic response via a decrease in GABAergic transmission (Roohbakhsh *et al.*, 2009). However, two important characteristics of the ECS must be considered to implement this simplified view of the anxiogenic effect of cannabinoids. Firstly, a different basal activation was demonstrated for CB1 receptor expressed on glutamatergic neurons and GABAergic neurons, being higher on the latter (see 2.5.2). The lower basal activation of CB1 receptor on glutamatergic terminals suggests that their reactivity to an increase in the endocannabinoid tone would be higher than that of CB1 receptor on GABAergic terminals (Katona & Freund, 2008). Secondly, the capacity of endocannabinoids to activate other receptors such as TRPV1 could underlie the anxiogenic effect in some cases (Rubino *et al.*, 2008*b*).

On the other hand, excitatory neurotransmission, mediated mostly by glutamate transmission, is enhanced by stress, and stress is a key component regarding the vulnerability of developing mood and anxiety disorders (Simon & Gorman, 2006). In fact, inhibition of glutamate release in the periaqueductal gray (PAG) area by CB1 receptor activation was proposed as an explanation for the anxiolytic effect of AEA injections into this area (Lisboa *et al.*, 2008). Likewise, experiments performed by Naderi *et al.* (2008) showed that ineffective doses of diazepam and the FAAH inhibitor URB597 became effective when applied in combination. These results suggest a possible synergistic action on glutamatergic inhibition (by increase in AEA) and GABAergic enhancement (by the activation of $GABA_A$ receptors).

The use of mutant mouse lines with specific deletion of the CB1 receptor from cortical and striatal GABAergic neurons (GABA-$CB1^{-/-}$) and cortical glutamatergic neurons (Glu-$CB1^{-/-}$) revealed an ambivalent role for this receptor not only in anxiety, but also in impulsivity (Lafenêtre *et al.*, 2009) and exploratory behavior (Jacob *et al.*, 2009; Häring *et al.*, 2011). Lafenêtre *et al.* (2009) showed that the lack of CB1 receptor on GABAergic neurons promoted a more impulsive response towards a novel object and palatable food, whereas Glu-$CB1^{-/-}$ mice were strongly inhibited in their approach behavior. Similarly, Häring *et al.* (2011) demonstrated that GABA-$CB1^{-/-}$ mice displayed an increased exploration of a novel object and a novel juvenile conspecific, whereas Glu-$CB1^{-/-}$ mice showed decreased exploration times. These responses can be related to anxiolytic and anxiogenic profiles, respectively. However, it is important to keep in mind that neophobia and anxiety behaviors are likely to be controlled by different neuronal mechanisms. Testing the conditional mutant mouse lines in anxiety paradigms showed recently that the anxiolytic-like effect of the low dose of cannabinoids was abrogated only in Glu-$CB1^{-/-}$ mice, while the anxiogenic-like effect of the high dose of cannabinoids was abolished specifically in GABA-$CB1^{-/-}$ mice (Aparisi Rey *et al.*, accepted). These findings corroborate the hypothesis that CB1 receptor-mediated reduction of glutamate release has anxiolytic properties, while reduction of GABA release induces anxiogenic effects.

In summary, data from pharmacological and genetic experiments concerning CB1 receptor involvement in anxiety merge to the idea that the location of the CB1 receptor on glutamatergic and GABAergic synapses is a very important factor accounting for the biphasic effect of the ECS in anxiety. In addition to the localization, also the level of basal activation (see 2.5.2) may account for the biphasic effect commonly described. In this scenario, GABAergic localization and high basal activation would confer an important role in the development of anxiogenic responses to cannabinoids to the CB1 receptor. On the other hand, glutamatergic localization and low basal activation are factors that give the CB1 receptor an essential function in the development of anxiolytic responses to cannabinoids. Furthermore, it is important to emphasize the relevance of the different sensitivities of CB1 receptor to agonists (see 2.5.3), since not every neuronal population is equally sensitive to CB1 receptor activation.

In addition to the modulation of glutamatergic and GABAergic neuronal transmission, the CB1-receptor can influence the monoaminergic regulation of anxiety. Cannabinoid-mediated enhancement of noradrenergic transmission seems to be associated with anxiogenic responses (Page *et al.*, 2007, 2008), whereas cannabinoid-mediated stimulation of serotonergic signaling seems to be associated with anxiolytic responses after mild activation (FAAH inhibition, low doses of WIN55,212-2) (Gobbi *et al.*, 2005; Bambico *et al.*, 2007; Cassano *et al.*, 2011) and to anxiogenic-like reactions after stronger activation (HU-210) (McLaughlin *et al.*, 2009).

2.6.3.1.3 Stress/Reward induction of ECS plasticity

For proper ECS-dependent regulation of anxiety, it is necessary that every constituent of the ECS functions optimally. Therefore, experiences which alter any element of the system (e.g. CB1 receptor or endocannabinoid synthesizing and degrading enzymes), would lead to an impairment of the physiological reaction to (endo)cannabinoids. Recent evidence suggests that stress alters the endocannabinoid content in limbic areas and PFC (Rademacher *et al.*, 2008). Further experiments confirmed that chronic psychoemotional stress (i.e. social defeat) blocked the normal reduction of inhibitory postsynaptic potentials (IPSPs) produced after application of the CB1 receptor agonist HU-210 to corticostriatal slices of C57BL/6 mouse brains (Rossi *et al.*, 2008). In addition, this blockade was counteracted by pretreatment with CB1 and glucocorticoid receptor antagonists, revealing the importance of HPA-axis reactivity in this process. CB1 receptor downregulation on GABAergic neurons is likely to be the cause for this absence of reduction, due to the fact that basal properties and sensitivity of these synaptic transmission processes were not affected. Interestingly, stress did not affect the CB1 receptor-mediated reduction of excitatory postsynaptic potentials (EPSPs), suggesting a more static profile of the CB1 receptor on glutamatergic terminals. In agreement with the data on IPSPs, an increase of AEA levels by genetic or pharmacological inactivation of its

degrading enzyme was able to reverse the stress-induced effect, and this response was also mediated by the CB1 receptor (Rossi *et al.*, 2010). Analyzing the implication of this stress-dependent downregulation of the CB1 receptor at the behavioral level, Campos *et al.* (2010) concluded that an anxiogenic increase of AEA signaling, via injections of the AEA reuptake inhibitor AM404 into the ventral hippocampus, turned out to be anxiolytic (tested on the elevated plus maze), when the animals were pre-exposed to restraint stress. Consequently, it can be hypothesized that the anxiogenic properties of the enhancement of AEA signaling (via AM404) rely on the activation of CB1 receptor on GABAergic terminals. In addition, the stress-mediated downregulation of CB1 receptor on GABAergic terminals results in a stronger activation of CB1 receptor on glutamatergic terminals, leading to an anxiolytic response. These findings corroborate a model of endocannabinoid adaptation, involving a stress-mediated re-orientation of endocannabinoid signaling (via CB1 receptor downregulation on GABAergic terminals) towards GABAergic disinhibition in order to prevent overexcitation and restore the excitatory-inhibitory equilibrium required for appropriate emotional reactivity.

2.6.3.2 Fear

Besides its involvement in the modulation of anxiety behaviors, the ECS also regulates acquired fear induced by specific cues. Natural stimuli that signal danger (e.g. pain, sight or smell of predators and loud tones) elicit an innate fear response. This reaction is used in the fear-conditioning paradigm, where an initially neutral stimulus (called conditioned stimulus, CS, e.g. an acoustic, visual or olfactory cue) is presented together with a fear-inducing stimulus (unconditioned stimulus, US, e.g. a mild electric shock delivered to the paws). After one or more pairings of the US with the CS, the subject associates the two stimuli and the presentation of the CS alone is able to evoke a fear response (LeDoux, 2000) (Figure 2.4). Instead of a discrete cue such as a tone and/or light, which are often used as CS, stimuli present in the environment where the US is presented may also acquire aversive properties and elicit conditioned emotional responses (called context conditioning) (Radulovic & Tronson, 2010). In rodents, freezing (Fanselow, 1980) or a startle response to a sudden strong stimulus other than the CS (e.g. Chhatwal *et al.*, 2005; Lin *et al.*, 2006) are often used as an indicator of fear.

After conditioning, the acquired short-term fear memory is consolidated in a more stable long-term memory, a process involving new gene expression and protein synthesis (Pape & Paré, 2010). Fear expression in a long-term test (re-exposure to CS-only after at least 24 hours) measures the combined effects of acquisition, consolidation and retrieval of the fear memory.

With each CS-only exposure, two opposite processes are initiated. Short exposure triggers a second round of memory consolidation, so that new information can be integrated into the original

memory. This process of reconsolidation stabilizes the original memory and requires protein synthesis. When protein synthesis is pharmacologically blocked, the fear memory can be lost (Tronson & Taylor, 2007). Prolonged or repeated exposure to the CS triggers extinction, resulting in a decline of CS-evoked fear response (Myers & Davis, 2007). Three different mechanisms have been proposed to explain extinction. Firstly, its behavioral properties indicate that a new inhibitory memory is formed that competes with the initial fear memory. Secondly, the original fear memory is weakened by changes in synaptic efficacy induced during fear conditioning. Different from these two mechanisms involving associative learning, non-associative processes play a role in the third mechanism for extinction. Here, the responsiveness to the presentation of the non-reinforced CS is decreased by a process called habituation (Herry *et al.*, 2010; Pape & Paré, 2010). The reduced response to the CS seen during and shortly after the extinction session is not stable, because the original memory reappears with the passage of time (spontaneous recovery), in a new context (renewal) and upon unpredictable US presentations (re-instatement) (Myers & Davis, 2007).

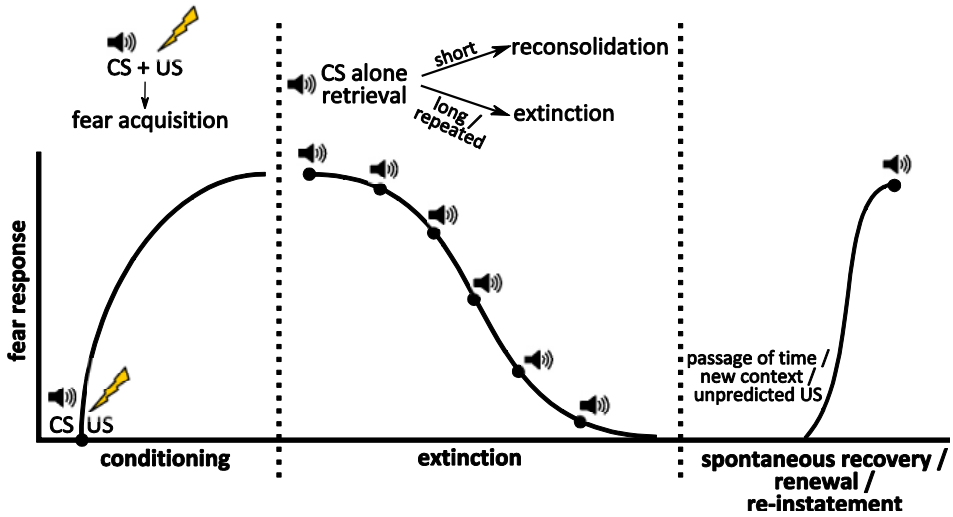

Figure 2.4: Phases of fear conditioning.
During fear conditioning, a conditioned stimulus (CS, e.g. tone) is presented together with a fear-inducing stimulus (unconditioned stimulus, US, e.g. foot shock). This triggers the transition from a baseline state to a state of fear upon CS retrieval (representation of the CS alone). Re-exposure to the CS alone can induce reconsolidation (short exposure) or extinction (long or repeated exposure). Even when extinction has been established, transitions back to the state of fear can rapidly occur after longer time, in a new context or after reminders (spontaneous recovery, renewal or re-instatement, respectively) (adapted from Myers & Davis, 2007; Quirk & Mueller, 2008; Tronson *et al.*, 2012).

Various brain regions have been implicated in the different phases of conditioned fear learning (Figure 2.5), with a major role being attributed to the amygdala (Pape & Paré, 2010). The BLA is important for acquisition and consolidation of fear memories, although the actual memory does not seem to be stored in this structure (McGaugh, 2002; Paré, 2003). For the reconsolidation and extinction of fear memories, the amygdala has also been implicated. Protein synthesis in this area is required for proper reconsolidation (Nader *et al.*, 2000). The hippocampus stores spatial components (i.e. contextual) of the fear memory (Paré, 2003). In extinction, the hippocampus and medial PFC

(mPFC), especially the infralimbic (IL) area, are involved besides the amygdala (Herry *et al.*, 2010; Pape & Paré, 2010; Sotres-Bayon & Quirk, 2010; Lin *et al.*, 2010). As spontaneous recovery is impaired in rats with a lesion in the mPFC, this area is also involved in the reappearance of fear responses after extinction (Zelinski *et al.*, 2010). Importantly, limited studies in humans hint at a considerable similarity of these processes and pathways between species (Paré, 2003; Delgado *et al.*, 2008).

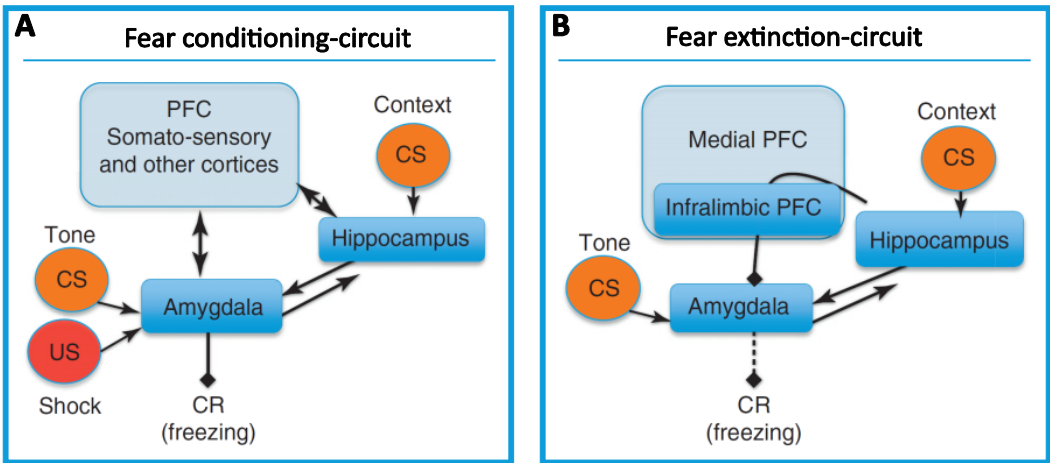

Figure 2.5: Circuits involved in fear conditioning and extinction.
(A) The amygdala plays a central role during acquisition and consolidation of fear memories. Representation of the context conditioned stimulus (CS) are formed within hippocampal–cortical networks. Cue CS (e.g. tone) and unconditioned stimulus (US) representations are thought to be processed within the basolateral amygdala, whose output is also critical for the expression of conditioned fear. After conditioning, the CS induces a fear state resulting in freezing as a conditioned response (CR). **(B)** During extinction, the infralimbic prefrontal cortex (PFC) is recruited in concert with the hippocampal–amygdala circuit and exerts a key role in fear reduction by inhibiting the amygdala. This results in loss of the CR (dashed line) (adapted from Tronson *et al.*, 2012).

Components of the ECS, including the CB1 receptor and the endocannabinoid synthesizing and degrading enzymes, are present in many circuits that were implicated in the different phases of fear conditioning (Kano *et al.*, 2009). In recent years, research efforts have focused on elucidating the role of the ECS in fear memory processing.

2.6.3.2.1 Fear responses during acquisition

The effects of endocannabinoid signaling on behavior during the initial acquisition phase of conditioned fear have not been studied extensively. Since the ECS is also implicated in pain processing (Sagar *et al.*, 2009; Guindon & Hohmann, 2009), studies have mainly attempted to choose conditions that do not change nociception, a response which was monitored by freezing behavior during the conditioning session (Tan *et al.*, 2010), shock reactivity (Lin *et al.*, 2009) or pain threshold (Marsicano *et al.*, 2002). These precautionary measures reduce the risk of confounding during the association process and improve the validity of the investigation of subsequent phases of fear memory processing. The pain threshold of the complete CB1 receptor knock-out mouse was not different from that of wild types upon first exposure (Marsicano *et al.*, 2002). However, these

animals showed a decreased reaction upon repeated shock presentations (Azad *et al.*, 2004). This emphasizes the importance of a careful choice of experimental conditions.

2.6.3.2.2 Fear expression

The fear response to the first CS/context exposure after the conditioning session, also called fear expression, is a result of acquisition, consolidation and retrieval of the fear memory. The involvement of the ECS in fear expression is not yet clear, as very mixed outcomes were reported (for review see Ruehle *et al.,* 2012).

2.6.3.2.3 Fear reconsolidation

It is proposed that upon each re-exposure to the CS or the shock context, the original fear memory is retrieved and thereby destabilized so that the memory can be strengthened and updated with new relevant information before reconsolidation (Tronson & Taylor, 2007). Some studies have reported the ECS to be involved in this process of reconsolidation. These studies have employed various strategies to distinguish reconsolidation from extinction: intensified training (Kobilo *et al.*, 2007), shorter re-exposure (Suzuki *et al.*, 2004, 2008; de Oliveira Alvares *et al.*, 2008) or post-re-exposure injection of the substance to be studied (Lin *et al.*, 2006).

Injections of the CB1 receptor antagonist SR141716 did not affect reconsolidation of the fear memory (Suzuki *et al.*, 2004, 2008; Kobilo *et al.*, 2007), but abolished the amnesia induced by injections of the protein synthesis inhibitor anisomycin (Suzuki *et al.*, 2008). In addition, hypo-activation of the ECS by hippocampal AM251 injections improved reconsolidation (de Oliveira Alvares *et al.*, 2008) and hyperactivation by AEA, WIN55,212-2 or HU-210 injections in rats all reduced reconsolidation of the fear memory. These effects were independent of the injection site (hippocampus, amygdala or insular cortex), the paradigm (cued or contextual fear conditioning, or conditioned taste aversion) and the time of measurement (at re-exposure, after re-instatement or spontaneous recovery after 7 days) (Lin *et al.*, 2006; Kobilo *et al.*, 2007; de Oliveira Alvares *et al.*, 2008). These studies all point to an amnesic role of endocannabinoid signaling. Therefore, it seems likely that the activation of the ECS reduces the reconsolidation of fear memories, whereas hypo-activation of the ECS promotes their reconsolidation, and thereby leads to enduring fear responses.

2.6.3.2.4 Fear extinction

The most prominent involvement of the ECS in fear is found in extinction in the classical fear conditioning paradigm (Marsicano *et al.*, 2002) as well as in fear-potentiated startle (Chhatwal *et al.*, 2005) and in the more hippocampus-dependent trace (Reich *et al.*, 2008) and context conditioning paradigms (Suzuki *et al.*, 2004). As several groups showed that endocannabinoid signaling is dispensable for extinction of appetitive memories (e.g. Niyuhire *et al.*, 2007; Manwell *et al.*, 2009),

the role of the endocannabinoids in extinction seems to be specific for aversive memories. In recent years, many studies focused on uncovering the mechanism of CB1 receptor signaling in fear extinction and on its function in the different brain regions involved in extinction learning. Here, only studies that reported similar initial freezing to CS presentation were selected, so that extinction behavior could be compared from a similar starting point.

CB1 receptor knock-out mice are impaired in short-term freezing reduction over a 200-second tone presentation (within-session) as well as in long-term extinction (between-session) after cued conditioning (Marsicano *et al.*, 2002). In the same study, similar results were obtained in wild-type mice treated with the CB1 receptor antagonist SR141716 before extinction training. Thus, CB1 receptor signaling did not seem to be involved in consolidation of the extinction memory, as the authors found no effect of pharmacological blockade immediately after extinction training (Marsicano *et al.*, 2002). CB1 receptor knock-out mice also showed a sustained freezing response in a sensitization paradigm in which fear response to a new, potentially harmful stimulus was measured after experiencing an inescapable foot shock (Kamprath *et al.*, 2006). This CB1 receptor-dependent lack of habituation to neutral as well as conditioned stimuli suggests that the endocannabinoid signaling is critically involved in this non-associative learning process (Kamprath *et al.*, 2006). This is consistent with the findings that endocannabinoids mediate habituation to homotypic stressors (Patel *et al.*, 2005). To dissect the role of the ECS in short- *vs*. long-term habituation in extinction of acquired fear to a cue, Plendl & Wotjak (2010) compared CB1 receptor knock-out mice and wild-type littermates in different exposure modalities. Freezing behavior was analyzed in two different protocols, one with shorter tone presentations (10x 20 s) with variable intervals and the other with constant tone presentation (over 200 s). These experiments showed that CB1 receptor signaling is dispensable for between-session extinction, whereas within-session extinction was strongly dependent on intact CB1 receptor signaling. These recent findings underline the involvement of the ECS in non-associative habituation learning. Another study suggested that endocannabinoids reduce the basal state of responsiveness during an aversive encounter (Reich *et al.*, 2008). In this study, systemic injections of the CB1 receptor antagonist AM251 prior to extinction training sessions in a trace conditioning paradigm (foot shock not directly after CS offset, but after a short delay), impaired freezing reduction. The strength of this impairment depended on the current state of the ECS, rather than on the history of AM251 *vs.* vehicle injections. Additionally, the fact that the observed levels of baseline freezing (before the CS) in the extinction context were also dependent on the current state of the ECS, was interpreted to indicate an involvement of CB1 receptor signaling in the generalization of the fear response (Reich *et al.*, 2008). An explanation for the high levels of generalized freezing in the setup used by Reich *et al.* might be the strong conditioning protocol (eight CS-US pairings), as the fear-reducing effect of the ECS highly depends on the strength of the harmful stimulus which was

encountered (Kamprath *et al.*, 2009). In the latter study, several conditional CB1 receptor knock-out mice with deletion of CB1 receptor only in specific neuronal subpopulations were tested to uncover the neurotransmitter systems that are involved in CB1 receptor-controlled fear adaptation. The fear-alleviating effect of endocannabinoids depended on endocannabinoid-driven modulation of glutamatergic transmission (Kamprath *et al.*, 2009). Furthermore, CB1 receptor on cortical glutamatergic neurons was shown to be responsible for the increased fear response observed after repeated social stress (Dubreucq *et al.*, 2012). This is consistent with the finding that stress habituation mediated by the ECS also crucially involves the modulation of glutamatergic neurotransmission (Patel & Hillard, 2008). In the conditional CB1 receptor knock-out mice used by Kamprath *et al.* (2009) and Dubreucq *et al.* (2012), the CB1 receptor is deleted on all cortical glutamatergic neurons, including some of the main brain regions involved in fear extinction, i.e. in hippocampus, PFC and BLA. The question in which of these regions the ECS-driven modulation of glutamatergic neurotransmission leads to the observed phenotype still needs to be addressed.

In cued fear conditioning, (endo)cannabinoids are thought to exert one of their main effects in the BLA, as presentation of the CS during the extinction trial increases endocannabinoid levels selectively in the BLA (Marsicano *et al.*, 2002). In several recent studies, the relevance of amygdala-specific endocannabinoid signaling was addressed. BLA-targeted infusion of CB1 receptor antagonist was found to impair extinction both in fear conditioning (unilateral SR141716) (Roche *et al.*, 2007) and in inhibitory avoidance (bilateral AM251) (Ganon-Elazar & Akirav, 2009). There is recent evidence that CB1 receptor is not only present in the BLA, but also on axon terminals of glutamatergic projection neurons from BLA to the medial part of the CeA and on GABAergic neurons projecting from the lateral to the medial CeA (Kamprath *et al.*, 2011). With local infusion of CB1 receptor antagonist into the BLA or the CeA, before the extinction training in a cued conditioning paradigm, the authors demonstrated that the CB1 receptor in the BLA is involved in long-term extinction processes whereas CB1 receptor in the CeA is more important for acute fear expression and within-session reduction of freezing.

As the hippocampus is known to process contextual information and thus transfers the contextual representation to the amygdala, where it is associated with the US (Phillips & LeDoux, 1992) (Figure 2.5), contextual fear conditioning is often used to investigate the function of hippocampal endocannabinoid signaling in fear conditioning. Bilateral infusion of the CB1 receptor antagonist AM251 into the dorsal hippocampus of rats after an extinction session blocked extinction consolidation, since there was no extinction retention detectable in the test on the following day (de Oliveira Alvares *et al.*, 2008).

The PFC is also thought to be involved in extinction, as extinction training induced synaptic plasticity in this area (Herry & Garcia, 2002) (Figure 2.5). Two recent studies addressed PFC function in extinction. Local infusion of SR141716 into the insular cortex of rats blocked extinction of conditioned taste aversion (Kobilo *et al.*, 2007). IL infusion of the CB1 receptor antagonist AM251 blocked cue-alone-induced reduction of fear-potentiated startle in rats (Lin *et al.*, 2009). Thus, cortical blockade of CB1 receptor signaling seems to decrease the inhibitory output of the amygdala, which is necessary to reduce the fear output (Quirk & Mueller, 2008).

These pharmacological studies with either systemic or brain-region specific blockade of endocannabinoid signaling in mice and rats together with the investigations that used complete or conditional CB1 receptor knock-out mice showed that the ECS is crucial for efficient extinction learning. Therefore, it is tempting to hypothesize that the activation of CB1 receptor would improve extinction, but the available data reveal a more complicated picture.

Recent studies that found a significant effect of treatment with CB1 receptor agonist on extinction were mostly performed with rats, suggesting that the agonist treatment might have species-specific effects (analogous to the data of Haller *et al.* (2007) discussed in the section on ECS susceptibility to environmental variables, 2.6.3.1.1). Several studies with rats showed that systemic treatment with AM404, an inhibitor of endocannabinoid uptake and/or metabolism as well as with URB597, an inhibitor of the AEA-degrading enzyme FAAH, enhanced extinction in several paradigms (Chhatwal *et al.*, 2005; Pamplona *et al.*, 2008; Bitencourt *et al.*, 2008; Manwell *et al.*, 2009) and that this extinction is more resistant to re-instatement (Chhatwal *et al.*, 2005). When CB1 receptor agonists were administered locally, similar facilitation of extinction was demonstrated for several brain regions that modulate and process learned fear (de Oliveira Alvares *et al.*, 2008; Lin *et al.*, 2009; Ganon-Elazar & Akirav, 2009).

Systemic treatment with CB1 receptor agonist also appears to influence extinction, but in a dose-dependent manner, resembling the biphasic effect found for anxiety-related behaviors. Low doses of WIN55,212-2 were shown to reduce within-session extinction in a context conditioning paradigm and even resulted in long-term reduction in a drug-free test one week later (Pamplona *et al.*, 2008). However, treatment with high doses of this agonist disrupted extinction in context conditioning (Pamplona *et al.*, 2006) and had no extinction-improving effect in fear-potentiated startle (Chhatwal *et al.*, 2005). Chronic treatment with a CB1 receptor agonist led to impaired extinction as shown in a study by (Ashton *et al.*, 2008), demonstrating that treatment with a high dose of Δ^9-THC over six days strongly delayed cued extinction. Seven days of chronic treatment with WIN55,212-2 made rats resistant to the reduction of fear-potentiated startle, which was induced by extinction training in non-treated rats (Lin *et al.*, 2008). Also, local infusion of WIN55,212-2 into the

IL, which was previously shown to improve extinction, did not have any effect after seven days of chronic treatment. The authors showed that the pretreated rats had significantly lower levels of CB1 receptor in synaptoneurosome preparations from the IL and that the inhibition of GABA release in the IL, which would produce the startle-reducing effect of WIN55,212-2, was attenuated by seven days of chronic WIN55,212-2 treatment (Lin *et al.*, 2008). Thus, acute treatment with CB1 receptor agonist improves extinction in rats when administered in a low dose, whereas it has no effect or even delays extinction when an acute high dose or chronic treatment is used. This effect of high dose or chronic agonist treatment might be due to internalization/desensitization of CB1 receptor upon strong or continuous activation (Wu *et al.*, 2008), leading to a resistance to exogenous as well as endogenous cannabinoids and therefore having the same effect as blocking CB1 receptor signaling.

2.7 Aims and outline of the thesis

The ECS has emerged as an important regulator of synaptic transmission, and short- and long-term plasticity in the nervous system. The underlying mechanisms at the cellular levels have been intensively investigated, but the causal role of endocannabinoids and the CB1 receptor in the context of neuronal networks has remained an unsolved question. In particular, available pharmacological and genetic approaches have allowed establishing the *necessary* role of CB1 receptor signaling in specific functions, but have not provided evidence for its *sufficient* role. To be able to investigate the sufficient role of CB1 receptor in specific circuits, the aim of this thesis was to generate a mouse line for cell-type specific rescue of CB1 receptor deficiency (**Chapter 3**). After proving that the rescued allele was fully functional, the novel genetic tool can be applied to questions regarding cell type-specific functions. The great majority of CB1 receptor is located on GABAergic neurons in the brain, but the discrete location of CB1 receptor on glutamatergic neurons is necessary for endocannabinoids to exert important functions. However, the sufficient role of cortical glutamatergic CB1 receptor has not yet been analyzed, and addressing this question was one goal of this thesis. Therefore, the newly generated Stop-CB1 mouse line was used to generate a mouse line for conditional rescue of CB1 receptor deficiency in cortical glutamatergic neurons. With this mouse line, the sufficient role of CB1 receptor on cortical glutamatergic neurons in endocannabinoid-mediated retrograde modulation of glutamatergic transmission, body weight, feeding response, chemically induced epileptiform seizures, innate anxiety and fear extinction was addressed.

The great majority of the studies investigating the role of the CB1 receptor have been carried out in mice to gain further knowledge for human pathologies. The human *CNR1* gene (coding for the CB1 receptor) was shown to produce transcript variants with different exon assemblies in the 5' untranslated region and to produce three protein variants by alternative splicing. To date, the molecular structure of the mouse *Cnr1* gene is poorly characterized, and it is not known whether its structure is similar to that of the human *CNR1* gene. Thus, the second aim of this thesis was to characterize the exon-intron-structure of the mouse *Cnr1* gene and to analyze the use of different transcript variants in different brain regions and cell-types to improve the understanding of regulatory processes and allelic variations contributing to pathological phenotypes observed in the rodent model (**Chapter 4**).

3 Generation of a mouse line for cell-type specific rescue of CB1 receptor deficiency

3.1 Introduction

Gene targeting is one of the most powerful tools to study gene function. In 2007, Mario R. Capecchi, Sir Martin J. Evans and Oliver Smithies were awarded with the Nobel Prize in Physiology or Medicine for their discoveries leading to targeted mutagenesis of embryonic stem (ES) cells by homologous recombination. By inactivation of single genes, “knock-out” mice have elucidated the role of various gene functions. To date, approximately half of all the genes of the mammalian genome have been knocked out and ongoing international efforts are aiming to create knock-out mice for all known genes (Skarnes *et al.*, 2011). Limitation of conventional knock-out strategies, such as developmental compensation processes masking the loss-of-function phenotype as well as the lack of temporal and/or spatial selectivity maybe even leading to lethality in an early developmental stage, have been overcome by a more sophisticated approach called “conditional” gene targeting. Using the Cre/loxP system, it is possible to disrupt or modify the targeted allele in a more selective way (for review see Sauer, 1998). Cre recombinase of the P1 bacteriophage efficiently catalyzes recombination between two of its consensus 34 base pair DNA recognition sites (loxP sites) (Hamilton & Abremski, 1984) (Figure 3.1A). These loxP sites consist of two 13 bp palindromic sequences flanking a core spacer sequence of 8 bp, which gives an intrinsic orientation to the loxP site. When two loxP sites are oriented "head-to-head", Cre recombinase catalyzes an inversion of the sequence between the two loxP sites (Figure 3.1B). When loxP sites are oriented "head-to-tail", Cre recombinase catalyzes an excision of the interposed sequence (Figure 3.1C). For the generation of conditional knock-out mice, "head-to-tail"-oriented loxP sites are introduced 5’ and 3’ of the gene of interest (GOI) by homologous recombination in ES cells. Subsequent delivery of Cre recombinase by mating the mice with the loxP-flanked GOI with transgenic lines harboring tissue- and/or time-specific expression of Cre recombinase produces spatially or temporally restricted gene inactivation of the GOI in the offspring (Figure 3.1D).

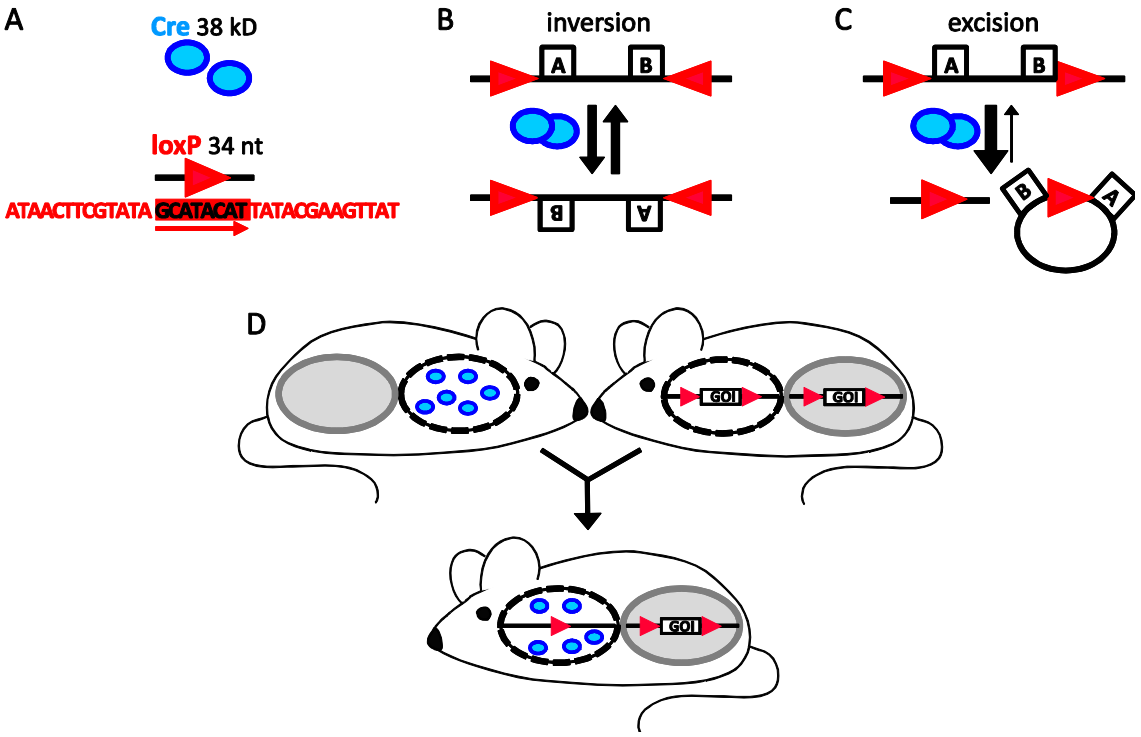

Figure 3.1: Conditional gene targeting using the Cre/loxP system.
(A) Graphical representation of Cre recombinase (blue circle) and loxP site (red triangle). Nucleotide sequence of the loxP site consists of two sequences forming a palindrome separated by a core nucleotide stretch with a distinct orientation (red arrow). **(B)** When loxP sites are oriented "head-to-head", Cre recombinase catalyzes an inversion of the sequence between the two loxP sites. **(C)** When loxP sites are oriented "head-to-tail", Cre recombinase catalyzes an excision of the flanked sequence. **(D)** To generate conditional knock-out mice, loxP sites are inserted 5' and 3' of the gene of interest (GOI) with a "head-to-tail" orientation. Mating these mutants with a mouse with selective expression of Cre recombinase results in offspring with a selective deletion of the GOI.

Using the Cre/loxP system, conditional CB1 receptor knock-out mice lacking the CB1 receptor in cortical glutamatergic neurons (Cre recombinase under the control of regulatory sequences of the *NEX* gene) or in cortical and striatal GABAergic neurons (Cre recombinase under the control of regulatory sequences of intragenic regions of the *Dlx5* and *Dlx6* genes) have previously been generated (Marsicano *et al.*, 2003; Monory *et al.*, 2006, 2007). In the phenotypical analysis of the conditional knock-out animals, opposing roles for CB1 receptor function in glutamatergic and GABAergic neurons became apparent in feeding behavior, novelty seeking and innate anxiety (see Paragraph 2.5, 2.6 and Table 3.1). Furthermore, CB1 receptor on glutamatergic neurons was shown to be necessary for protection against chemically induced epileptiform seizures and two of the "tetrad" effects induced by Δ^9-THC (hypolocomotion, hypothermia), for which CB1 receptor on GABAergic seems to be dispensable (see 2.6 and Table 3.1). CB1 receptor on glutamatergic neurons was also shown to be necessary for proper extinction of cued fear (Dubreucq *et al.*, 2012), possibly due to dysregulated habituation to aversive stimuli (Kamprath *et al.*, 2006, 2009). By virally induced Cre recombinase expression in the hippocampus of mice homozygous for the loxP-flanked CB1

receptor gene, it was shown that CB1 receptor in hippocampal neurons is necessary for protection against chemically induced epileptiform seizures (Monory *et al.*, 2006).

Table 3.1: Overview over the behavioral effects of loss of CB1 receptor in cortical glutamatergic or GABAergic neurons ([a]novel palatable food, novel objects, novel social interaction partners; [b]in a cued conditioning and a sensitization paradigm).

	Phenotype of conditional knock-out compared with wild-type mice		
	Glu-CB1$^{-/-}$	GABA-CB1$^{-/-}$	
food intake after fasting	reduced	increased	Bellocchio *et al.*, 2010
seizure susceptibility	increased	normal	Monory *et al.*, 2006
novelty seeking[a]	reduced	increased	Jacob *et al.*, 2009; Lafenêtre *et al.*, 2009; Häring *et al.*, 2011
innate anxiety	increased	reduced	Aparisi Rey *et al.*, accepted
fear extinction	reduced[b]	normal	Kamprath *et al.*, 2009; Dubreucq *et al.*, 2012
tetrad effect of THC	reduced hypolocomotion reduced hypothermia	normal	Monory *et al.*, 2007

These studies and all data present in the literature on the functions of the CB1 receptor are, from the methodological point of view, based on "loss-of-function" approaches. In other words, pharmacological or genetic blockade of the receptor and its eventual behavioral and neuronal consequences are clear indications of the *necessary* role of the ECS for these functions. However, these approaches present limitations (e.g. unspecificity of drugs and compensatory mechanisms of genetic manipulations) and do not provide definitive information concerning the possible *sufficient* role of the cell-type expression of CB1 receptor for the given function, or whether additional neuronal subtypes and circuits containing the CB1 receptor are involved in these behaviors. To establish these precise causal relationships, "rescue" strategies are needed. Generally, these strategies involve viral or transgenic re-expression of deleted genes (e.g. Self, 2005; de Luca *et al.*, 2005; Han *et al.*, 2007; Coryell *et al.*, 2008; Gerstein *et al.*, 2012). However, these approaches are strongly limited by the fact that transgenes and viruses do not exactly reproduce the wild-type expression of the natural gene in terms of levels and cell-types. Thus, a complementary strategy using the Cre/loxP system was applied to generate knock-in mice with a silenced CB1 receptor gene as a default state, but with the ability to re-activate CB1 receptor gene expression in a region- and cell type-specific manner (Figure 3.2), in order to learn to which extent this specific region or cell type contributes to the re-appearance of the wild-type phenotype. This genetic approach has been successfully used in other genetic models (Nagy *et al.*, 1998; Nagy, 2000; Dragatsis & Zeitlin, 2001; Balthasar *et al.*, 2005; Hnasko *et al.*, 2006). By rescuing the gene of interest in its endogenous genomic locus, rather than ectopic overexpression, the gene's function is restored at endogenous sites and levels (Nagy, 2000), increasing the physiological relevance of the rescue and its consequent interpretations.

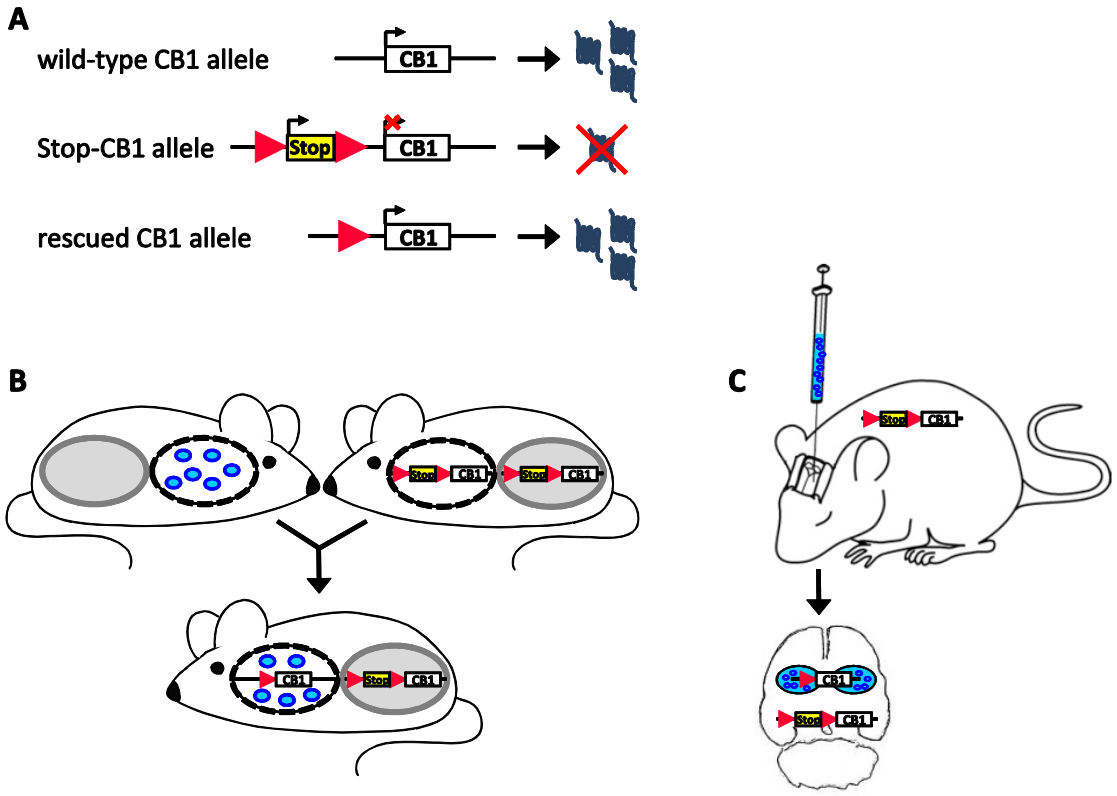

Figure 3.2: Strategy for the generation of a mouse line for conditional rescue of CB1 receptor deficiency.
(A) Insertion of a loxP-flanked stop cassette upstream of the CB1 receptor coding sequence (white box) blocks the expression of the CB1 receptor. After excision of the stop cassette, CB1 receptor expression is rescued. Transgenic **(B)** or viral **(C)** delivery of Cre recombinase selectively rescues the CB1 receptor under the control of its endogenous regulatory sequences in the subset of cells where Cre recombinase is expressed. Red triangles: loxP sites, Stop: stop cassette; CB1: CB1 receptor open reading frame; blue circles: Cre recombinase.

3.2 Material and Methods

3.2.1 The targeting construct

The targeting construct was cloned as described in Schneider (2007). Briefly, to generate the Stop-CB1 targeting construct, a loxP-flanked stop cassette from a modified pSV-Cre plasmid (gift from J. K. Elmquist, Harvard Medical School, Boston, MA, USA), consisting of an SV40 promoter driven neomycin resistance coding sequence (Neo^R), a herpes simplex virus thymidine kinase (HSV-TK) polyadenylation signal (pA) sequence and two additional AATAAA sequences from the Promega pGL3-control vector was used (Balthasar *et al.*, 2005). The stop cassette was PCR amplified with primers having 5' overhangs complementary to a part of the sequence in the 5' untranslated region (UTR) of the coding exon of the CB1 receptor gene (originally termed *Cnr1*, but for the purpose of this chapter, CB1 receptor gene is used) (fwd: 5'-CCTCCTGGCA CCTCTTTCTC AGTCAATAAC TTCGTATTAG CATACATTAT ACGAAGTTAT AAGCTTAGGT GGCACTTTTC GGGGAAAT, rev: 5'-TCTTTGATTA GGCCAGGCTC AACGATAACT TCGTATAATG TATGCTATAC GAAGTTATAC TAGTAGAGAA ATGTTCTGGC ACCT). With the reverse primer, an additional *Spe*I site (marked in grey) was inserted 5' of the second loxP site to facilitate further discrimination between wild-type and targeted allele. Fragments 5' and 3' of the target site of the stop cassette were PCR amplified using a plasmid from a lambda phage DASHII genomic library constructed from E14 embryonic stem cells (Marsicano *et al.*, 2002) as template. By overlap extension PCR, the three fragments (the two PCR products of the regions 5' and 3' of the target site of the stop cassette and the amplified stop cassette with the overhangs complementary to these two fragments) were amplified for few cycles without primers to assemble the complete template. Then, primers complementary to the outsides of the 5' and 3' fragments were added, and the whole construct was amplified. Thus, the stop cassette was inserted in the 5' UTR of the coding exon of the CB1 receptor gene 32 nucleotides upstream of the ATG without any additional changes in the 5' UTR. The PCR product was cut with NotI and EcoRV on the endogenous genomic sites and inserted in a plasmid containing the CB1 coding sequence, the 5' UTR and a part of the upstream intron (Marsicano *et al.*, 2002). For the final targeting construct, a 7.3 kb left homology arm and a 6.4 kb right homology arm (from plasmids from the phage library containing upstream and downstream sequences of the CB1 coding sequence (CDS)) were added to allow homologous recombination in ES cells.

3.2.2 Embryonic stem cell culture

Tissue culture dishes were purchased from NUNC (Langenselbold, Germany)**.** Sterile plastic tubes (50 ml and 15 ml) were purchased from Greiner (Solingen, Germany). All cell culture reagents were purchased from LIFE Technologies GIBCO (Darmstadt, Germany), if not stated otherwise. Fetal

calf serum (FCS) was purchased from PAA (Cölbe, Germany), DMSO from Carl Roth (Karlsruhe, Germany) and mitomycin C and β-mercaptoethanol from Sigma Aldrich (Munich, Germany).

3.2.2.1 Mouse embryonic fibroblast feeder cells

3.2.2.1.1 Preparation of mouse embryonic fibroblasts

In order to maintain their undifferentiated and totipotent status, ES cells need the presence of factors that inhibit differentiation. Early experiments showed that primary mouse embryonic fibroblast (MEF) cells constitute a very good source of these factors (Bradley *et al.*, 1984). Primary MEF cells were obtained from mouse embryos at embryonic day 12.5-14. The pregnant mouse was sacrificed, and embryos were isolated from the uterus. Embryos without any extra-embryonic tissue were transferred to a petri dish containing sterile phosphate buffered saline (PBS, Ca^{2+} and Mg^{2+} free) and, brains and inner organs were removed. Carcasses were washed twice in sterile PBS, and 5-7 carcasses were pooled and quickly minced on ice with a sterile scalpel. Tissue was homogenized by passing through a nylon cell strainer (40 µm, BD Falcon Cell Strainer) with a syringe plunger in a 50 ml tube filled with pre-warmed complete MEF medium (MEF medium: Dulbecco´s Modified Eagles Medium (DMEM, with glutamax (L-alanyl-L-glutamine), high glucose), supplemented with 10% FCS, 0.1 mM non-essential amino-acids (10 mM stock), 1 mM sodium pyruvate (100 mM stock), 100 U/ml penicillin and 100 U/ml streptomycin (10000 U/ml penicillin/streptomycin stock solution)). Cell clumps were allowed to sediment for 1 min, and the supernatant was centrifuged at 180 rcf for 10 min. The cell pellet was resuspended in 10 ml of complete MEF medium per embryo, and one embryo was plated per 15 cm diameter cell culture dishes. After overnight culture at 37°C, 10% CO_2 (cell culture incubator: Sanyo, Wood Dale IL, USA), the medium was replaced with fresh medium. After 2-3 days, when the cells formed a confluent monolayer, they were washed twice in PBS and trypsinized in 0.05% trypsin (with 0.481 mM EDTA and supplemented with 1% chicken serum) for 5 min at 37°C. Trypsin reaction was stopped with complete MEF medium, cells were centrifuged at 180 rcf and replated at a dilution of 1:5 and further incubated. After another 2-3 days, the cells were confluent. The cells were trypsinized as described above. Cells were resuspended in 0.5 ml MEF feeder medium per plate, put on ice and 0.5 ml ice cold 2x freezing medium (4 ml MEF medium + 4 ml FCS + 2 ml DMSO) was added drop-wise, whilst shaking the tube. 1 ml of cell suspension was transferred to each freezing vial (Nalgene, Germany) and the cells were frozen in an isopropanol cryobox pre-cooled to -20°C to -80°C. After 24 h the cells were transferred to liquid nitrogen for longer storage.

3.2.2.1.2 MEF cell culture

One aliquot of MEF passage 0 (EF0) was thawed in a 37°C water bath, transferred to a tube containing 10 ml of pre-warmed MEF medium and pelleted by centrifugation at 180 rcf for 4 min.

Cells were resuspended in a final volume of 80 ml, split onto 4 plates (15 cm diameter) and cultured at 37°C with 10% CO_2 in a humidified incubator. The cell culture medium was changed on the next day. After 3-5 days, when the cells were confluent, they were washed twice with PBS and trypsinized for 4 min with 1x Trypsin supplemented with 1% chicken serum. After stopping the reaction with 5 ml MEF medium per plate, the cell suspension was pelleted, resuspended in MEF medium and plated in a 1:4 dilution. These steps were repeated once more to obtain 64 plates out of one vial EF0.

3.2.2.1.3 Mitotic inactivation of MEF cells with Mitomycin

In order to block cell proliferation, mitosis of MEF cells was inactivated with mitomycin c. To this end, the medium on confluent MEF cells was replaced with 10 ml inactivation medium (MEF medium containing 10 µg/ml mitomycin c predissolved in DMSO) and incubated for 2-4 h at 37°C. Cells were then washed twice in PBS, trypsinized as above, counted and plated at a density of 3.5 x 10^6 cells/10 cm diameter culture dish for direct use as feeder cell plates for ES cells.

To freeze mitotically inactivated MEFs, 4 x 10^6 cells were resuspended in 0.5 ml MEF medium, and the freezing procedure was carried out as described above. One vial of frozen mitomycin-treated primary mouse embryonic fibroblasts was thawed per 10 cm diameter culture dish and plated one day prior to ES cell plating.

3.2.2.2 Embryonic stem cell culture

3.2.2.2.1 Thawing and expanding embryonic stem cells

One aliquot of v6.5 C57BL/6(F) x 129/sv(M) ES cells (Rideout 3rd *et al.*, 2000) was quickly thawed in a 37°C water bath and then transferred to a 15 ml tube containing 7 ml of pre-warmed ES cell medium (complete ES cell medium: Dulbecco´s Modified Eagles Medium (DMEM, without glutamax, high glucose), supplemented with 10% FCS, 2 mM L-glutamine (200 mM stock), 0.1 mM non-essential amino-acids (10 mM stock), 1 mM sodium pyruvate (100 mM stock), 100 U/ml penicillin and 100 U/ml streptomycin (10000 U/ml penicillin/streptomycin stock), 0.1 mM β-mercaptoethanol (100 mM stock) and leukemia inhibitory factor (LIF, medium supernatant from human embryonic kidney (HEK)-cells transfected with LIF plasmid, kind gift of Prof. Ari Waisman, University Medical Center, Mainz, Germany). The cells were centrifuged for 4 min at 180 rcf, and the pellet was resuspended in 2 ml ES cell medium with fire-polished Pasteur pipettes to single out the cells. Then, the cell suspension was plated onto a 10 cm diameter feeder cell plate. The medium was changed daily, and cells were grown in a humidified cell culture incubator at 37°C with 10% CO_2.

After 2-4 days, the ES cells grew confluent and needed to be split. Medium was changed 2 h prior to splitting. The cells were washed twice with PBS, trypsinized for 4 min at 37°C and homogenized with a fire-polished Pasteur pipette in trypsin in order to obtain a single cell

suspension. After transferring the cell suspension to a tube with pre-warmed ES cell medium and centrifugation, cells were resuspended in ES cell medium and plated at a concentration of 3 x 10^6 cells/10 cm diameter feeder plate.

3.2.2.2.2 Electroporation of embryonic stem cells and selection for neomycin resistance

ES cells from confluent dishes were trypsinized, as described above. The cells were washed once in PBS and resuspended at a concentration of 13 x 10^6 cells/ml in PBS. 800 µl of the cell suspension (containing 1 x 10^7 cells) in PBS was mixed with 25 µg of the linearized targeting plasmid (dissolved in PBS) and incubated on ice for 10 min. The suspension was then transferred to a pre-cooled electroporation cuvette (0.4 cm gap, blue cap, Bio-Rad, Hercules CA, USA) and placed into the ShockPod Shocking Cuvette Chamber of the Gene Pulser Xcell eukaryotic system (Bio-Rad, Hercules CA, USA). ES cells were electroporated with a pulse of 240 V and 500 µF and placed on ice for 10 min. The electroporated ES cells were resuspended in 50 ml pre-warmed ES cell medium, and 10 ml were plated per 10 cm diameter feeder cell dish. A plate with 1 x 10^7 non-electroporated cells was prepared as survival control.

After two days of recovery (daily medium change), the medium was changed to Geneticin-containing ES-cell medium (complete ES cell medium containing 200 µg/ml Geneticin, G418; 50 mg/ml stock solution, GIBCO, Darmstadt, Germany), to select for neomycin-resistant ES cells. After 8 days of selection (with daily change of the Geneticin-containing medium) all cells on the survival control plate were dead, and small colonies were visible on the plates with the electroporated cells.

3.2.2.2.3 Picking and expanding of neomycin-resistant ES cell colonies

Medium was changed 2 h prior to picking of the neomycin-resistant ES cell clones. Directly prior to picking, the plate was washed twice in PBS and 8 ml PBS (containing 100 U/ml penicillin and 100 U/ml streptomycin) was added. Single colonies were located under the microscope, picked with a pipette tip and resuspended in a well of a round bottomed 96-well dish containing 50 µl of a 1:1 dilution of trypsin and PBS. After picking one row, the cells were resuspended in the trypsin, incubated for 3 min, resuspended again, and trypsin reaction was stopped by addition of 100 µl complete ES cell medium (without G418) per well. The complete row was then transferred to a flat bottomed 96-well dish with feeder cells in 50 µl complete ES cell medium per well. Medium was changed on the next day.

When the cells were almost confluent, they were split 1:3 on 96-well plates either containing feeder cells or a gelatin coating (50-100 µl 0.1% gelatin solution per well, incubated for 30 min, dried for 10 min). To this end, medium was changed 2 h prior to trypsin treatment. The cells were washed

twice with PBS, trypsinized for 4 min at 37°C and homogenized by pipetting up and down with the multipipette to obtain a single-cell suspension. Trypsin reaction was stopped by adding 100 µl complete ES cell medium. 50 µl of the single cell suspension were added to a well containing 150 µl of ES cell medium. The expansion continued until two 96 well-feeder plates and 3 gelatin-pretreated 96 well-plates were obtained for each clone. Clones from gelatin-treated plates were used for genomic DNA extraction (see 3.2.5.1), while cells grown on feeder plates were frozen.

For freezing ES cell clones on 96-well plates, the splitting procedure was followed and the trypsin reaction was stopped by adding 50 µl ES cell medium. 100 µl of ice cold 2x ES cell freezing medium (1 part DMSO, 2 parts FCS, 2 parts of complete ES cell medium) were added and the plates were placed at -20°C for 1-2 h. Then they were transferred to a Styrofoam box (to slow the cooling down) and placed into the -80°C freezer.

After identification of correctly targeted ES cell clones by Southern blot analysis, the corresponding plate was thawed in a 37°C water bath, and the selected clone was immediately transferred to a 15 ml tube, containing 7 ml of pre-warmed ES cell medium. For the expansion, the ES cells were split progressively onto larger feeder plates (24-well plates, 6-well plates, 6 cm diameter plates, 10 cm diameter plates) and onto gelatin plates to confirm their identity by Southern blot analysis.

To freeze ES cells from 10 cm diameter dishes, the splitting procedure was followed, and the cells were resuspended in half the final volume of ES cell medium. Then, the cells were put on ice, and ice cold 2x freezing medium was added drop-wise whilst shaking the tube. One ml of the cell suspension was then transferred to each cryovial, and frozen in a pre-cooled isopropanol cryobox. After 24 h, the cells were transferred to liquid nitrogen for longer storage. Cells were frozen at a concentration of 2 x 10^6 cells/ vial.

3.2.2.3 Preparation of ES cells for blastocyst injection

To prepare the cells for injection into blastocysts, the splitting procedure was followed and all cells were re-plated on a fresh 10 cm diameter culture dish and incubated at 37°C for 20 min. As feeder cells sediment faster than ES cells, they will start to get adherent, while ES cells are still in the medium. Thus, the cell-suspension was transferred to a new 10 cm diameter plate. The old plate was gently washed with 2 ml fresh medium and the medium was transferred to the new plate, too. After 15 min incubation the medium was transferred to a 15 ml tube, the cells were counted while centrifuging for 3 min at 180 rcf. The cells were resuspended in cold MEF medium at a concentration of 3 x 10^6 cells/ 1 ml. After 5 min incubation on ice, when residual cell clumps have sedimented, the cell suspension was carefully transferred without any clumps to a new tube, spun down in a pre-

cooled centrifuge for 3 min at 1000 rpm and the cells were resuspended in cold HEPES buffered MEF feeder medium (20 µl HEPES/ 1 ml MEF medium). These cells were used for blastocyst injection.

3.2.3 Generation of the Stop-CB1 mouse line

All experimental protocols were carried out in accordance with the European Communities Council Directive of 24 November 1986 (86/609/EEC) and approved by the Ethical Committee on animal care and use of Rhineland-Palatinate, Germany. Animals were housed in a temperature- and humidity-controlled room (22°C±1; 50%±1) with a 12 h-12 h light-dark cycle (lights on at 7 am) and had access to food and water *ad libitum* except when stated differently for the experimental procedure.

Blastocyst injections were performed by staff of the ZVTE (Zentrale Versuchstiereinrichtung, University Medical Center, Mainz, Germany). To this end, four female C57BL/6J mice were injected with pregnant-mare serum gonadotropin to induce superovulation to provide 50-100 blastocysts. Two days later, the same females were injected with human chorionic gonadotropin, and mated with four males. On the same day, 2-4 NMRI females were mated with 2-4 vasectomized males to create pseudo-pregnant foster mothers. Two days later, blastocysts were flushed out of the uteri of the superovulated C57BL/6J females. The collected blastocysts were micro-injected with the single cell targeted ES cells (see above). The micro-injected blastocysts were implanted into the uteri of the NMRI foster mothers. 19-20 days later, the foster mothers gave birth to the implanted pups, or a C-section was performed. When the pups were a week old, coat color could be seen and chimerism was determined. Chimeric males were bred to C57BL/6J females to produce germ line transmission. Germ line transmitted animals were backcrossed to C57BL/6J background for > 8 generations. The behavioral experiments were performed on adult (3–6 months old) male mice.

3.2.4 Generation of mouse lines with cell-type specific rescue of CB1 receptor

3.2.4.1 Generation of the complete rescue line CB1-RS

By crossing Stop-CB1 mice to a mouse line expressing Cre recombinase in an early stage of preimplantation embryogenesis (EIIa-Cre) (Lakso *et al.*, 1996) the loxP flanked stop cassette was excised during this developmental stage. Presence of the Ella-Cre allele was determined using the primers G100 and G101 (see 3.2.7), and germ line transmission of the rescued allele was assessed. Mice were backcrossed to C57BL/6J to lose the Cre allele, and were then bred to homozygosity for the rescued allele carrying one residual loxP site in the CB1 receptor 5' UTR. These mice are called CB1-RS hereafter.

3.2.4.2 Generation of the Glu-CB1-RS line

To obtain selective excision of the stop cassette in cortical glutamatergic neurons, Stop-CB1 mice were crossed to NEX-Cre mice (Schwab *et al.*, 2000). These mice are called Glu-CB1-RS hereafter.

3.2.5 Isolation of genomic DNA

3.2.5.1 DNA preparation from ES cells

ES cells were grown on 96-well plates coated with 0.1% gelatin until they reached complete confluence. Cells were washed twice in PBS (139.9 mM NaCl, 2.7 mM KCl, 10.1 mM Na_2HPO_4-H_2O, 1.8 mM KH_2PO_4, pH 7.4) and 50 µl ES cell lysis buffer (20 mM NaCl, 10 mM Tris/HCl pH 7,5, 10 mM EDTA pH 8, 0,5% Sarcosyl, 1 mg/ml Proteinase K) was added. Plates were incubated overnight at 56°C in a sealed humid chamber. After cooling down and spinning down briefly, 200 µl 100% ethanol were added per well and plates were shaken at room temperature (RT) for 1-2 h until white filaments representing genomic DNA appeared. Supernatant was removed from the precipitated DNA by turning the plate around, and the DNA was washed twice in 70% ethanol. After drying, the DNA was dissolved in digest buffer for subsequent Southern blot analysis or in TE (10 mM Tris-HCl pH 8.0, 1 mM Na_2EDTA) for PCR analysis.

3.2.5.2 DNA preparation from mouse tail biopsies

A mouse tail tip (approximately 1-2 mm) was cut and incubated overnight on a thermo mixer at 56°C in 500 µl TENS- buffer (50 mM Tris-HCl pH 8, 100 mM EDTA, 100 mM NaCl, 1% SDS) with Proteinase K (25 µl of 10 mg/ml stock; freshly added). After centrifugation at RT for 10 min at 13000 rcf, 500 µl of the supernatant was transferred to a fresh reaction tube containing 500 µl isopropanol. After mixing by inversion and centrifugation as above, the supernatant was removed, precipitated, DNA washed once with 70% ethanol, air-dried, dissolved in 200 µl $T_{1/10}$E buffer (10 mM Tris-HCl pH 8.0, 0.1 mM Na_2EDTA) and stored at 4°C until further use.

3.2.6 Southern blot

Correct homologous recombination of the targeting plasmid with the endogenous CB1 receptor gene locus was confirmed by Southern blot analysis.

3.2.6.1 DNA digest

For Southern blot analysis, 20-30 µg genomic DNA, prepared from one well of a confluent ES cell 96-well plate, or prepared from mouse tail biopsies, were digested with XbaI (5' homologous recombination), SpeI (3' homologous recombination) or EcoRI (copy number analysis of Neomycin resistance cassette). DNA from 96-well plates was directly resuspended in digestion solution. Digestion

solution contained 1 µl high concentrated enzyme (40-100 Units/µl, New England Biolabs, Frankfurt, Germany), corresponding buffer, 0.4 µl 100 x BSA (A6793, Sigma Aldrich, Munich, Germany), 0.7 µl Spermidin (Sigma Aldrich) and 0.3 µl RNase A (Sigma Aldrich) in a total volume of 40 µl. DNA was digested overnight at 37°C. After 16 h of incubation, additional 25 Units of each enzyme were added and further incubated. Complete digestion of the DNA was checked by gel electrophoresis.

3.2.6.2 Electrophoresis and transfer

Digested genomic DNA was separated overnight at 25 V on a 0.7% agarose gel in 1x TAE (40mM Tris acetate, 1 mM EDTA; for 50 x TAE: 212 g (2 M) Tris-HCl were dissolved in 500 ml H_2O, 100 ml 0.5 M Na_2EDTA (pH 8.0) and 57.1 ml glacial acetic acid were added, ad 1000 ml) with Lambda-HindIII (Fermentas, St Leon-Rot, Germany) or GeneRuler 1kb Plus DNA Ladder (Fermentas) as marker. The gels were then photographed on a UV transilluminator. For depurination, the gel was shaken in 0.25 M HCl for 5-10 min, rinsed in tap water, denatured in 0.5 M NaOH, 1.5 M NaCl for 30 min, rinsed again in tap water and neutralized in 1.5 M NaCl, 1 M Tris-HCl pH 7.2 for 30 min. Capillary blot was performed as described (Sambrook *et al.*, 2001) to transfer DNA onto Hybond-N+ membranes (GE Healthcare, Freiburg, Germany). Blotting was performed overnight in 10x SSC (prepared from 20x SSC stock; 3 M NaCl, 300 mM sodium citrate; pH 7).

3.2.6.3 Probe preparation

The 3' and 5' probes binding genomic DNA outside of the homology arms and the probe binding the neomycin resistance cassette were prepared by PCR (program: 95°C/5 min, 27 x (95°C/45 s, 55°C/45 s, 72°C/45 s), 72°C/5 min) with the primers shown in Table 3.2.

Table 3.2: PCR primers for synthesis of Southern blot probes

Name	Sequence	Position
XH6-fwd	CTAAGCCACAGAGCAGAAGTAAATGG	10323 bp upstream of CB1 ATG (in wt allele)
XH6-rev	CTTCTTTGCATTATTGTCTGCTCC	9799 bp upstream of CB1 ATG (in wt allele)
SpeX4-fwd	TTCCACACATAAATGCCCAGAGG	7510 bp downstream of CB1 ATG
SpeX4-rev	CGTGTAGTGAGCAAGCAAAGGC	7965 bp downstream of CB1 ATG
Neo-fwd	TGCTCGACGTTGTCACTGAAGC	238 bp downstream of Neo ATG
Neo-rev	TACCGTAAAGCACGAGGAAGCG	714 bp downstream of Neo ATG

The probes were purified by agarose gel electrophoresis followed by gel extraction using the NucleoSpin Extract II kit (Machery-Nagel, Dueren, Germany) according to the manufacturer´s instructions. Probe labeling was performed with Amersham Rediprime II DNA Labeling System (GE Healthcare, Freiburg, Germany) according to the manufacturer´s instructions. Briefly, 25 ng of template DNA, in a volume of 45 µl TE, was boiled at 95°C for 5 min, and then placed on ice for 5 min. Afterwards, the denatured template was transferred to the reaction tube, 5 µl [α-^{32}P] dCTP (3000 Ci/mmol, 50 µCi; PerkinElmer, Rodgau, Germany) were added and mixed. The labeling reaction was carried out at 37°C for 10 min, and then stopped by adding 5 µl EDTA solution provided by the

supplier. The radioactive probe was purified using Illustra MicroSpin G-50 columns (GE Healthcare, Freiburg, Germany) according to the manufacturer´s instructions. Incorporation of the labeled nucleotide was checked with a scintillation counter.

3.2.6.4 Hybridization

The membrane was put between two sheets of hybridization-mesh, transferred to a hybridization bottle, and pre-hybridized with 30-40 ml pre-warmed hybridization buffer for 3-4 h at 65°C in a hybridization oven (rotating the bottles continuously). To prepare 500 ml of hybridization buffer, 50 ml 50x Denhardt´s solution (5 g Ficoll, 5 g Polyvinylpyrrolidine 5 g BSA, ad 500 ml H_2O, filtered, aliquoted in 50 ml tubes and stored at -20°C), 300 ml H_2O and 25 ml 10% sodium dodecyl sulfate (SDS) were pre-warmed separately to 37°C. The Denhardt´s solution was added to the water, then SDS and 125 ml 20x SSPE (175,3 g NaCl, 27,6 g NaH_2PO_4 x H_2O, 7,4 g Na_2EDTA add 800 ml H_2O, titrate to pH 7,4, ad 1000 ml, autoclaved) were added. After filtration of the solution, 5 ml denatured ss-DNA (10 mg/ml) were added, mixed well, aliquoted and stored at -20°C. To prepare the hybridization solution, the labeled probe was denatured by boiling for 5 min at 95°C and ~10^6 cpm were added per 1 ml pre-warmed hybridization buffer (total volume for hybridization: 5-10 ml). The pre-hybridization buffer in the hybridization bottles was exchanged to the hybridization solution and incubated rotating overnight at 65°C. The membranes were subjected to stringent washes with pre-heated (65°C) wash-buffers according to the following protocol: 50 ml of 2x SSC/0.1% SDS for 30 min, then 50 ml of 0.2x SSC/0.1% SDS for 30 min at 65°C. Afterwards the membrane was checked with a hand radioactive counter whether radioactivity was below ~200 cpm, otherwise the membrane was washed in 50 ml 0.1x SSC/0.1% SDS for another 30 min. For the detection of the signals, membranes were rinsed with 2x SSC, sealed in plastic bags and exposed for 1-2 days to autoradiography films (Kodak Biomax MS film, Sigma Aldrich, Munich, Germany) in Kodak cassettes with intensifying screens at -80°C.

3.2.7 PCR Genotyping

Standard genotyping of the mouse lines was carried out by PCR with the primers listed in Table 3.3 under the following conditions: 95°C/5 min, 27 x (95°C/45 s, 55°C/45 s, 72°C/45 s), 72°C/5 min.

Stop-CB1 mice were genotyped using primers S87, S88 and S89. PCR amplification results in a fragment size of 543 bp for the wild-type allele, 462 bp for the knock-in allele and 577 bp for the rescued allele (after excision of the loxP-flanked stop cassette by Cre recombinase).

EIIa-Cre mice were genotyped using primers G100 and G101 to amplify a 300 bp fragment inside the coding sequence of Cre recombinase.

For Nex-Cre mice, a promoter specific forward primer G80 was used to be able to distinguish the line from the Ella-Cre line with PCR genotyping. The reverse primer G123 is binding to the coding sequence of Cre recombinase. PCR results in a 391 bp product.

Table 3.3: PCR primers for genotyping of the CB1 rescue mouse lines

Name	Direction	Sequence	Position
S87	forward	CAAGAAATGAGAACCGTGTC	264 bp upstream of CB1 receptor ATG (in wt allele)
S88	forward	TGTGTGAATCGATAGTACTAAC	151 bp before end of loxP flanked stop cassette, in HSV-Tk pA
S89	reverse	GTTCTCCTTGAACGATGAGA	259 bp downstream of CB1 receptor ATG
G100	forward	CGGCATGGTGCAAGTTGAATA	157 bp downstream of Cre ATG
G101	reverse	GCGATCGCTATTTTCCATGAG	441 bp downstream of Cre ATG
G80	forward	TCT TTT TCA TGT GCT CTT GG	149 bp upstream of Cre ATG in Nex promoter
G123	reverse	CGCGCCTGAAGATATAGAAGA	221 bp downstream of Cre ATG

3.2.8 Virus production and injection

The production of the adeno-associated virus (AAV) expressing Cre recombinase under the ubiquitous chicken β-actin promoter was done as previously described (Monory *et al.*, 2006; Guggenhuber *et al.*, 2010). Adult male mice (10-12 weeks old) were anaesthetized (fentanyl 0.05 mg/kg, midazolam 5 mg/kg, medetomidine 0.5 mg/kg i.p.) and 1 µl of AAV-Cre was injected in the dorsal hippocampus (–2.0 mm AP, ±2.0 mm ML, –2.0 mm DV from bregma) using a stereotactic frame (David Kopf Instruments, Tujunga, CA, USA). Virus was infused at a rate of 200 nl/min, using a microprocessor-controlled mini-pump (UltraMicroPump, World Precision Instruments, Sarasota, FL, USA) with 34 gauge beveled needles (NanoFil, World Precision Instruments, Sarasota, FL, USA). Anesthesia was antagonized (naloxone 1.2 mg/kg, flumazenil 0.5 mg/kg, atipamezole 2.5 mg/kg s.c.), and post-surgery analgesia was achieved by buprenorphine (0.06 mg/kg s.c.). Histological analysis was performed 4 weeks after vector infusion, when transgene protein expression had peaked to remain at stable levels.

3.2.9 In situ hybridization

Animals were sacrificed by decapitation under deep isoflurane anesthesia. Brains were isolated, snap-frozen on dry-ice, and stored at -80°C. For sectioning, brains were mounted on Tissue Tek (Polysciences, Warrington, PA, USA), and 17 µm-thick coronal sections were cut from forebrain on a cryostat Microtome HM560 (Microm, Walldorf, Germany). Sections were mounted onto frozen SuperFrost/Plus slides (Fisher Scientific, Ingolstadt, Germany), dried on a 42°C-warming plate and stored at -20°C until used.

Slides were warmed-up for 30 min at RT, fixed in ice-cold 4% paraformaldehyde in PBS, rinsed three times in PBS, incubated for 10 min in 0.1 M triethanolamine-HCl (pH 8.0) to which 0.63 ml of

acetic anhydride were added drop-wise, rinsed twice in 2x SSC (1x SSC contains 150 mM NaCl, 15 mM Na_3 citrate, pH 7.4), dehydrated in graded series of ethanol, delipidized in chloroform for 5 min, rinsed in 100% and 95% ethanol and air-dried. Hybridization was carried out overnight at 64°C in 90 µl of hybridization buffer containing ^{35}S-labeled riboprobe (35,000 to 70,000 cpm/µl). Hybridization buffer consisted of 50% formamide, 20 mM Tris-HCl pH 8.0, 0.3 M NaCl, 5 mM EDTA pH 8.0, 10% dextran sulphate (D8906, Sigma, Germany), 0.02% Ficoll 400 (F2637, Sigma, Germany), 0.02% polyvinylpyrrolidone (MW 40,000, PVP40, Sigma, Germany), 0.02% BSA, 0.5 mg/ml tRNA (Roche Molecular Diagnostics, Germany), 0.2 mg/ml fragmented herring sperm DNA and 200 mM DTT.

After incubation in a humid chamber overnight, slides were rinsed four times for 5 min each in 4x SSC at RT, incubated 30 min at 37°C in 20 µg/ml of RNase A in 0.5 M NaCl, 10 mM Tris-HCl pH 8.0, 5 mM EDTA to remove all non-hybridized (single-stranded) RNA molecules, rinsed at RT in decreasing concentrations of SSC (1x, 0.5x and 0.1x SSC) containing 1 mM DTT, washed twice for 30 min each at high stringency in 0.1x SSC/1mM DTT at 64°C and washed twice for 10 min at RT in 0.1x SSC.

At this point, ^{35}S-labeled slides were dehydrated in graded ethanol series, air-dried and exposed to Biomax MR film (Kodak). On the next day, slides were dipped in photographic emulsion (NTB-2 from Kodak, diluted 1:1 in distilled water, pre-warmed to 42°C). After exposure for 5 to 20 days at 4°C, slides were developed for 3 min (D-19, Kodak), fixed for 6 min (Kodak fixer), rinsed for 30 min in tap water and air-dried. Slides were mounted in DPX (BDH, Poole, UK).

3.2.10 Western blot

Animals were sacrificed by decapitation in isoflurane anesthesia. Hippocampi were quickly isolated and homogenized by sonication in Tris buffered saline (TBS; 25 mM Tris, 150 mM NaCl, 2 mM KCl, pH 7.4) containing protease inhibitors (complete protease inhibitor cocktail tablets, Roche Applied Science, Mannheim, Germany). Samples were centrifuged for 10 min at 13000 rcf at 4°C to remove cell debris. The supernatant was transferred to a new reaction tube and protein concentration was determined by the method of Bradford (Bradford, 1976) using bovine serum albumin (NEB, Frankfurt, Germany) as standard. Aliquots containing 20 mg of total protein were mixed with 5x Laemmli reducing sample buffer (for 100 ml: 15.0 g SDS, 15.6 ml 2 M Tris-HCL pH 6.0, 57.5 g 87% glycerol, 16.6 ml β-mercaptoethanol, 0.4% (w/v) bromphenol blue), heated for 5 min to 60°C and separated by SDS-polyacrylamide gel electrophoresis (PAGE). 20 mg of total protein were resolved by 10% SDS-PAGE using a Bio-Rad electrophoresis system (Mini-PROTEAN 3) with Tris-glycin running-buffer (25 mM Tris-base, 190 mM glycine, 0.1 % SDS) according to the manufacturer´s instruction (Bio-Rad Laboratories GmbH, Munich, Germany). PageRuler Prestained Protein Ladder

(Thermo Scientific, St. Leon-Rot, Germany) was used as a molecular weight marker. For electroblotting, a tank transfer system (Mini Trans-Blot cell) was used according to the manufacturer´s instruction (Bio-Rad Laboratories GmbH, Munich, Germany). The proteins were transferred in transfer buffer (25 mM Tris-base, 190 mM glycine, 20% ethanol (v/v)) onto nitrocellulose membranes (Protran, Whatman; GE Healthcare, Dassel, Germany) at 300 mA for 60 min. Blocking was carried out in 5% (w/v) non-fat dry milk in TBS-T (TBS + 0.1% Tween20 (v/v) (TBS-T)) for 1 h at RT. Membrane was incubated in 1% non-fat dry milk in TBS-T with rabbit anti-CB1 primary antibody (1:500, Frontier Science, Hokkaido, Japan) at 4°C overnight. Tubulin was used as loading control (mouse anti-α-tubulin, 1: 500000, Sigma-Aldrich, St. Louis, MO, USA). Antibodies were detected by the appropriate horseradish peroxidase (HRP)-conjugated secondary antibodies (1:1000, Dianova, Hamburg, Germany) followed by ECL-detection (GE Healthcare, Freiburg, Gemany). Chemiluminescence was visualized and quantified with the Fusion SL system (Vilber Lourmat, Marne-la-Vallée, France).

3.2.11 Immunohistochemistry

Mice were deeply anesthetized with pentobarbital, and afterwards trans-cardially washed and perfused with PBS/heparin (5 U/ml) and 4% paraformaldehyde (PFA) solution, respectively. After isolation, the brains were post-fixed for 24 h in 4% PFA solution, treated with 30% sucrose/PBS solution for 48 h and stored at -80°C until use. For section preparation, 30-µm thick brain slices were prepared on a cryostat Microtome HM560 (Microm, Walldorf, Germany), and stored at -20°C in cryoprotection solution (25% glycerin, 25% ethylene glycol, 50% PBS) until use.

All incubation steps were performed in wells of a 12-well plate (100-500 µl solution per well) on a wave shaker at RT. Sections were first rinsed from cryoprotection solution in PBS (10 min) and then treated twice with a 100% methanol solution containing 1.5% H_2O_2, each time for 20 min. After two additional 10 min washing steps in PBS, the sections were pre-incubated in blocking solution (4% normal goat serum, 0.3% Triton X-100 in PBS) for 1 h. After the blocking, the sections were incubated overnight with the primary antibodies (polyclonal anti-CB1 receptor from rabbit, diluted 1:1000, CB1-Rb-Af380-1, Frontier Science, Hokkaido, Japan) and polyclonal anti vesicular glutamate transporter 1 (VGluT1) from guinea pig (diluted 1:500; AB5905, Chemicon/Millipore, Billerica, MA, USA), which were diluted in blocking solution. On the next day, the sections were washed twice in PBS and treated with biotin blocking kit, according to the manual of Molecular Probes (E21390, Invitrogen, Darmstadt, Germany). Sections were then washed twice with PBS-T (PBS/0.1%, Triton X-100) and subsequently incubated for 1.5 h with the biotin-labeled secondary antibody against rabbit from goat (Vectastain Elite ABC Kit, PK-6101, Vector Labs, Burlingame, CA, USA) diluted (1:200) in the blocking solution. The detection was done according to the manual of Molecular Probes, using streptavidin-

HRP conjugate combined with Alexa Fluor 488-labeled tyramide (TSA Kit #22, Invitrogen, Darmstadt, Germany). The treatment was followed by two 10 min washing steps in PBS and a 15 min treatment in 4% PFA solution. After another PBS step for 10 min, sections were treated twice with 100% methanol solution containing 1.5% H_2O_2, each for 10 min. The sections were then rehydrated twice for 10 min in PBS, followed by an incubation in blocking solution containing the HRP-conjugated anti-guinea pig-IgG from donkey (1:500; 706-035-148, Jackson Immuno Research, Newmarket, UK). The incubation was followed by five 10 min washing steps in PBS. The final detection step was done for 3 min according to TSA Plus Cyanine 3 System manual (diluted 1:60; NEL744001, Perkin Elmer, Waltham, MA, USA). Sections were washed twice in PBS for 10 min and then counterstained for 10 min with DRAQ5 (BioStatus Limited, Leicestershire, UK) diluted 1:500 in PBS. After the counterstaining, the sections were washed twice for 10 min in PBS, and then carefully transferred into a Petri dish filled with PBS. Sections were then mounted on glass slides to dry for 1 h at 37°C. The remaining salt was washed off by dipping the slides for 2 s into distilled water. Finally, the sections were dried overnight in a dust free environment at RT and covered with Mowiol 4-88 mounting medium (Roth, Karlsruhe, Germany).

Fluorescence labeling was visualized using the confocal laser-scanning microscope Zeiss LSM T-PMT 719 (Zeiss Microsystems, Jena, Germany), equipped with appropriate excitation and emission filters for maximum separation of Cyanine 3 and Alexa Fluor 488 signals. Applying the Zeiss Confocal Software and Adobe Photoshop (Version 7.0, Adobe Inc., San Jose, CA, USA), images were saved and processed.

3.2.12 Autoradiography

Brain sectioning (17 µm thick sections) and mounting on slides was performed as described above (see 3.2.9). ^{3}H-CP55,940 binding was carried out as described in (Herkenham *et al.*, 1991). Slides were warmed-up for 20 min at RT and pre-incubated for 30 min at 30°C in blocking buffer (50 mM Tris HCl (pH 7.4), 5% (w/v) fat-free BSA (Sigma-Aldrich, St. Louis, MO)). Sections were then incubated for 2 h at 30°C in blocking buffer containing 5 nM ^{3}H-CP55,940 (specific activity 139.6 Ci/mmol, Perkin Elmer, Waltham, MA, USA). Nonspecific binding was determined by incubating adjacent sections in blocking buffer containing 5 nM ^{3}H-CP55,940 in the presence of 10 µM CP55,940 (Tocris, Bristol, UK, dissolved in DMSO). After the incubation, sections were washed twice for 1.5 h at 4°C in washing buffer (50 mM Tris HCl (pH 7.4.), 1% (w/v) fat-free BSA). Sections were then dipped briefly in distilled water to wash off remaining salt and dried overnight. Labeled sections, together with a tritium standard (American Radiolabeled Chemicals, St. Louis, MO, USA), were exposed to uncoated, tritium-sensitive phosphor storage screens (Perkin Elmer, Waltham, MA, USA) for 60 h.

Phosphor storage screens were scanned with a Cyclone Plus Phospho Imager (Perkin Elmer, Waltham, MA, USA).

Ligand binding to the CB1 receptor was quantified using the Optiquant software (Perkin Elmer, Waltham, MA, USA). A standard curve was compiled using the tritium standard. 10 slices equally distributed over bregma positions -1.6 until -2.7 were used for quantification. Hippocampal formations were encircled and total of bound ^{3}H-CP55,940 was measured. Unspecific binding was subtracted (per area) and the sum of bound ^{3}H-CP55,940 was calculated for each hippocampus in one hemisphere. Mean values for each mouse line were computed and put into relation to the mean of bound ^{3}H-CP55,940 in hippocampi of the control group.

3.2.13 RNA isolation and qPCR

Animals were sacrificed by decapitation in isoflurane anesthesia. Hippocampi were quickly isolated and snap frozen at -80°C. Frozen hippocampi were transferred to tubes from a Precellys ceramic kit (ceramic bead diameter 1.4 mm, 2 ml tube; Peqlab, Erlangen, Germany) containing homogenization buffer from the Nucleo-Spin RNAII-Kit (Macherey-Nagel, Dueren, Germany; ß-Mercaptoethanol added, Carl Roth, Karlsruhe, Germany), and tissue was homogenized with a Precellys 24 (Peqlab, Erlangen, Germany) at 6000 rpm for 20 s. Total RNA was isolated using the Nucleo-Spin RNAII-Kit (Macherey-Nagel, Dueren, Germany). Reverse transcription of 450 ng of DNase-treated total RNA was done using the High Capacity cDNA Reverse Transcription Kit (Applied Biosystems, Carlsbad, CA). In the quantitative PCR (qPCR), the cDNA equivalent to 22.5 ng RNA was amplified using commercial TaqMan assays (Applied Biosystems, Carlsbad, CA) for mouse cannabinoid receptor 1 (Cnr1; Mm00432621_s1) and glucoronidase beta (Gusb; Mm00446953_m1) with an ABI 7300 real time PCR cycler (Applied Biosystems, Carlsbad, CA). Reactions were performed in triplicates. Data analysis was done using the Relative Expression Software Tool (REST) (Pfaffl *et al.*, 2002) using Gusb as reference gene.

3.2.14 Electrophysiology

3.2.14.1 Slice preparation

As previously described (Monory *et al.*, 2006; Lourenco *et al.*, 2010; Kamprath *et al.*, 2011), mice (P20-P30) were anesthetized with isofluorane (5%) and decapitated, their brains were rapidly removed and put into oxygenated (95% O_2, 5% CO_2) ice-cold artificial cerebrospinal fluid (ACSF) containing (in mM): 125 NaCl, 2.5 KCl, 2 $CaCl_2$, 10 $MgCl_2$, 1.25 NaH_2PO_4, 26 $NaHCO_3$, 16 glucose (pH 7.4). Parasagittal hippocampal or coronal amygdalar slices (300 µm thick) were cut on a vibratome (Leica Microsystems, Wetzlar, Germany) at 4°C. The slices were allowed to equilibrate for at least 1 h

at RT, and then transferred to a recording chamber continuously superfused with ACSF (~1.5 ml/min).

3.2.14.2 Electrophysiological recordings *in vitro*

Whole-cell voltage-clamp recordings were made at RT from CA1 or BLA pyramidal cells visualized by infrared video microscopy (S/W-camera CF8/1, Kappa, Gleichen, Germany). Patch pipettes (3-4 MΩ) were filled with an intracellular solution containing (in mM): 145 CsCl, 10 HEPES, 5 EGTA, 2 $MgCl_2$, 2 $CaCl_2$, 2 Na_2ATP, 5 phosphocreatine, 0.33 GTP (pH 7.2). Neurons were voltage-clamped at -70 mV. Cells were discarded from analysis if the access resistance changed by >20% over the course of the experiment. Recordings were made using an EPC 10.0 (HEKA Elektronik) or a Multiclamp 700B (Molecular Devices) amplifier, filtered at 0.5-1 kHz, digitized at a sampling rate of 10 kHz, and analyzed off-line using the programs IGOR PRO 5.0 (Wavemetrics) or Clampfit (Molecular Devices).

3.2.14.3 Recordings of eEPSCs/eIPSCs

After reaching stable baseline (~10 min after establishing the whole cell configuration for infusion of intracellular solution), extracellular stimuli (100 µs, 50-600 µA) were delivered through a bipolar stainless-steel electrode placed either in the stratum radiatum or in the basal amygdala (100 µm from the recorded neuron). Glutamatergic and GABAergic components of synaptic responses were isolated by addition of gabazine (10µM) or picrotoxin (100 µM) and CGP55845 (50 µM), or DNQX (10 µM) and AP-5 (50 µM), respectively. Some slices were preincubated with the CB1 antagonist AM251 (2 mM) at least 1 h before testing DSE.

3.2.14.4 Induction and calculation of DSE/DSI magnitude

DSE/DSI tests consisted of 60 evoked responses (evoked every 3 s) before the depolarization step (from −70 to 0 mV, 3 s) and 100-150 responses thereafter. At least three DSE/DSI tests were applied to each cell (Lourenco *et al.*, 2010).

The presence of CB1 receptor at synaptic terminals and/or the quality of the patch were checked before starting each experiment by one DSE/DSI test. Control experiments showed that this "initial" DSE/DSI (not recorded) had no effect on following recorded DSE/DSI (data not shown).

DSE/DSI magnitude was calculated as follows (Wilson & Nicoll, 2001):

$$\Delta \text{ of ePSCs} = \left[\frac{(X2 - X1)}{X1} \right] * 100, \text{ where}$$

x_1 = mean of last 5 evoked PSC amplitudes before the depolarization

x_2 = mean of first three evoked PSCs amplitudes after depolarization.

Statistical analyses were conducted on relative values (Δ).

3.2.15 Refeeding after fasting

The animals were single-housed starting one week before the experiment and fasted for 24 h before testing. On the day of testing, the animals were refed and food intake was measured by weighing the residual food in the tray at the indicated intervals.

3.2.16 Induction of acute excitotoxic seizures

Kainic acid (KA; Ascent scientific, Bristol, UK) was dissolved in 0.9% saline and administered (30 mg/kg; i.p.) in a volume of 10 ml/kg body weight to induce epileptiform seizures. Before injection, the animals were given a light isoflurane inhalation anesthesia to reduce injection stress. A trained observer blind to the genotype of the mice monitored the severity of seizures for 2 h and scored every 15 min according to the following scale (Racine, 1972; Monory *et al.*, 2006): 0 – no response; 1 – immobility and staring; 2 – forelimb and/or tail extension, rigid posture; 3 – repetitive movements, head bobbing; 4 – rearing and falling; 5 – continuous rearing and falling: 6 – severe clonic-tonic seizures; 7 – death.

3.2.17 Open field

The open field is a white, square-shaped plastic apparatus (40 cm x 40 cm x 40 cm). Light was adjusted to 100 lx in the center or the open-field box. The animals were placed in the center and allowed to explore freely during 5 min. Locomotion was monitored using Ethovision software (Noldus, Wageningen, the Netherlands).

3.2.18 Anxiety

3.2.18.1 Elevated plus maze

The elevated plus maze (EPM) is a cross-shaped set-up, elevated 100 cm above the floor. It consists of 4 arms, 2 opposite open arms and 2 opposite enclosed arms. The floor of the arms is made of white plastic, 35 cm long and 6 cm wide and the arms are interconnected by a central platform of 6 x 6 cm. Black plastic walls (20 cm high) surround the enclosed arms. Light intensity in the middle of the open arms was 140 lx. The animals were placed into the center of the maze, facing an enclosed arm, and were allowed to explore freely over 5 min (Walf & Frye, 2007). After each test, the plus-maze was cleaned with 70% ethanol. Animals were tracked using Ethovision software (Noldus, Wageningen, the Netherlands) with the three body-point module (nose point, center, tail base). Time in each arm was measured when all three body points (nose, center, tail base) were inside the arm. Entries to arms were assessed manually by a trained observers blind to the genotype.

Time spent in and entries to the open arms were calculated relative to time spent in or entries to all arms, respectively.

3.2.18.2 Light/dark test

The light/dark (LD) test was performed in a box (39 cm x 39 cm) divided into a lit compartment (two-thirds of the surface area, white) and a dark compartment (one-third, black box, with a 26 cm-high lid). Lit and dark compartments were directly connected by a small entrance (5 x 5 cm). Light was adjusted to 100 lx in the center of the lit compartment. The animals were placed in the dark compartment and allowed to explore the apparatus during 5 min. The latency to first enter the lit compartment with all four paws, percentage of time spent in the light, number of entries to the lit compartment and risk assessments (incomplete entries to the light) were assessed by trained observers blind to the genotype.

3.2.19 Cued fear conditioning

Procedures and setups were used as previously described (Kamprath & Wotjak, 2004). For conditioning, mice were placed in the conditioning context (square shaped, 15 cm x 20 cm, grid floor, cleaned with 1% acetic acid) and a house light (25 lx) turned on. After three minutes, a tone (80 dB, 9 kHz sine wave, 10 ms rising and falling time) was presented to the animals for 20 s which co-terminated with a 2 s scrambled electric foot shock of 0.6 mA. Mice were returned to their home cages 60 s later. On day 1 (d1), day 2 (d2), day 3 (d3) and day 10 (d10) after the conditioning day, conditioned mice were placed into a neutral, new environment (test context, cylinder shaped, 15 cm diameter, with bedding, cleaned with 70% ethanol), and the house light (5 lx) was switched on. After three minutes, a 200 s continuous tone (same settings as in conditioning) was presented. Mice were returned to their home cages 60 s after the end of the tone presentation. Animals were tracked using Ethovision software. Freezing (here defined as the complete absence of movements except those necessary for breathing) was scored with the Ethovision immobility filter set at 0.5% change of the pixels representing the mouse.

3.2.20 Data analysis

The results were analyzed using IBM SPSS Statistics Software for Windows (version 19, Armonk, NY, USA). Differences were considered significant at $p<0.05$. All data are expressed as mean +/- SEM.

One-way ANOVA with genotype as independent variable was used to investigate the distance moved in the open field, distance moved in the EPM paradigm, relative time spent in the open arms on the EPM and relative open arm entries on the EPM.

Univariate ANOVA with genotype as independent variable and bodyweight or distance moved as covariate was used to analyze food intake or anxiety measures (latency to first entry of lit compartment and time spent in lit compartment in the light/dark test), respectively. Covariates did not have significant effects and were thus not included in the model.

Repeated measures ANOVAs with genotype and time (day or interval) as independent variables were used to analyze freezing in fear extinction and seizure severity after KA injection.

Significant genotype effects were further analyzed using Bonferroni's *post-hoc* analysis for multiple comparisons.

The Kaplan-Meier method was used to evaluate survival, followed by the log rank test to identify significant differences.

Electrophysiological data were analyzed with one sample t-tests against the baseline value.

3.3 Results

3.3.1 Generation of the Stop-CB1 mouse line

3.3.1.1 The targeting strategy

To generate the Stop-CB1 mouse line for rescue of CB1 receptor deficiency, a targeting vector with a modified CB1 receptor allele was constructed for homologous recombination in ES cells. To achieve silencing of the CB1 receptor gene, a loxP-flanked stop cassette consisting of an SV40 promoter driven Neo^R and three polyadenylation signals (Figure 3.3A) (Balthasar *et al.*, 2005) was inserted in the 5' UTR of the coding exon of the CB1 receptor gene 32 nucleotides upstream of the CB1 receptor start codon with overlap extension PCR. During this cloning step, an additional XbaI restriction site was inserted in the upstream intron and a SpeI restriction site was inserted upstream of the 3' loxP site to facilitate distinction between wild-type and knock-in allele. The complete targeting construct was assembled from a genomic library by adding 7.3 kb of 5' sequences (upstream of the loxP-flanked stop cassette) and 6.4 kb of 3' sequences (containing the CB1 receptor coding sequence) for homologous recombination in ES cells. Sequencing data confirmed the identity of the construct and the lack of mutations in the loxP-flanked stop cassette, the surrounding 5' UTR and the complete CB1 receptor open reading frame.

3.3.1.2 Homologous recombination in embryonic stem cells

The linearized targeting vector was electroporated into v6.5 C57BL/6(F) x 129/sv(M) embryonic stem cells (Rideout 3rd *et al.*, 2000). After one week of selection for neomycin resistance, surviving clones were picked and expanded. For correct integration into the genome, homologous recombination should occur between the left arm of the targeting vector and the homologous genomic region and the right arm and the corresponding genomic region (Figure 3.3B). To screen for homologous recombination, the genomic DNA was digested with restriction enzymes which produce different DNA fragment sizes in the endogenous allele and the knock-in allele after homologous recombination. For the initial screening, correct recombination of the left arm was investigated. Genomic DNA was digested with XbaI, and Southern blot hybridization with the XH6 probe was performed. Presence of the endogenous allele resulted in a single band of 10 kb, whereas correct integration resulted in an additional 8 kb band (Figure 3.3C, top, double band because only one allele of the diploid ES cells obtained the modified allele). Out of the approximately 300 screened clones, six showed correct homologous recombination in the left arm. For these ES cell clones, the genomic DNA was also digested with SpeI. Southern blot hybridization with the SpeX4 probe resulted in a single band of 11 kb for the endogenous allele, whereas correct integration resulted in an additional 8 kb band (Figure 3.3C, middle). All 6 ES cell clones showed as well correct homologous

recombination in the right arm. To exclude additional random integration of the targeting vector in the ES cell genome, genomic DNA was digested with EcoRI and Southern blot hybridization was carried out with an internal probe derived from the Neo^R in the stop cassette (Figure 3.3C, bottom). One of the correctly targeted ES cells clones had an additional random integration of the targeting construct (data not shown).

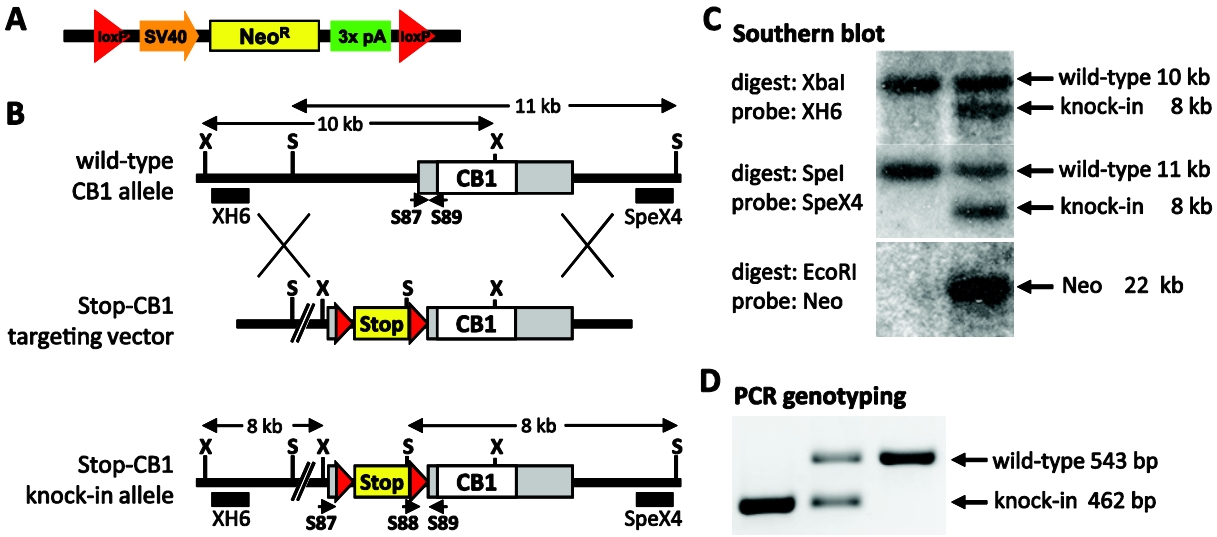

Figure 3.3: Targeted insertion of the stop cassette into the mouse CB1 receptor gene.
(A) Schematic illustration of the loxP (red triangles)-flanked stop cassette consisting of an SV40 promoter (SV 40, orange arrow), which drives transcription of a neomycin resistance coding sequence (Neo^R, yellow box). Transcription is stopped by three polyadenylation signals (pA, green box). **(B)** Schematic representation of the homologous recombination of the wild-type CB1 receptor allele (top) with the linearized Stop-CB1 targeting vector (middle) and the resulting knock-in allele after correct homologous recombination (bottom). The loxP-flanked stop cassette is inserted in the 5' UTR of the coding exon. Restriction sites for XbaI (X) and SpeI (S), binding sites of the Southern blot probes (XH6, SpeX4) and the primers for routine genotyping (S87, S88, S89) are indicated. Red triangles: loxP sites, Stop: stop cassette; grey box: UTR of the exon containing CB1 receptor CDS; CB1: CB1 receptor open reading frame. **(C)** Southern blot analysis of neomycin-resistant ES cell clones for left arm homologous recombination (top), right arm homologous recombination (middle) and test for random integration in the genome with the Neo probe recognizing the neomycin-resistance in the Stop cassette (bottom). Correct genomic targeting introduced an additional XbaI and SpeI site, and the decreased fragment size after digestion with the corresponding enzymes could be detected. **(D)** PCR genotyping: S87 (forward primer) and S89 (reverse primer) correspond to the wild-type sequence surrounding the newly introduced stop cassette and produced a PCR product of 543 bp in the wild-type allele. S88 (forward primer) recognizes the 3' end of the stop cassette in front of the loxP site and amplified a 462 bp fragment together with S89 in the knock-in allele.

3.3.1.3 Blastocyst injection, generation of chimeras and germ line transmission

Three correctly recombined ES cell clones without random integration were injected into C57BL/6J blastocysts to generate chimeric mice. Blastocysts were implanted in pseudo-pregnant NMRI foster mothers. Chimerism of the offspring was determined by the coat color of the pups, as the v6.5 stem cells lead to agouti coat color that could be easily distinguished from the black coat color resulting from the C57BL/6J blastocysts, into which the ES cells were injected. From the blastocyst injection of clone IVB5, four male chimeric mice were born. Two out of these had almost

complete agouti-colored coats and were thus mainly derived from the targeted ES cells. These chimeric founder mice were mated with C57BL/6J females, and germ-line transmission was revealed by the coat color of the offspring (black, no germ line transmission; agouti, germ line transmission of agouti ES cells). Germ line transmission was confirmed by Southern blot analysis of tail biopsy-derived genomic DNA. For routine genotyping, PCR genotyping was performed (Figure 3.3D). The heterozygous offspring was backcrossed to C57BL/6J mice for 10 generations to generate Stop-CB1 mice on a C57BL/6J background.

Heterozygous Stop-CB1 mice were intercrossed, in order to generate homozygous null mutants (stop/stop). Such breeding gave rise to 53% (279/531) heterozygous (stop/wt), 20% (106/531) homozygous mutant (stop/stop) and 27% (146/531) wild-type (wt/wt) mice. These proportions correspond roughly to the expected Mendelian transmission, thus revealing no embryonic lethality of the mutation.

3.3.2 Generation of mouse lines with cell-type specific rescue of CB1 receptor deficiency

To further dissect the role of the CB1 receptor on specific neuronal subpopulations, the Stop-CB1 mouse line was crossed to mouse lines expressing Cre recombinase in specific neuronal subpopulations.

3.3.2.1 Generation of the complete CB1 receptor rescue line

Cre recombinase-mediated excision of the stop cassette results in one remaining loxP site in the 5' UTR 32 nucleotide upstream of the internal CB1 receptor translation start codon. To analyze whether this residual loxP site in the rescued allele had any effect on the expression and functionality of the CB1 receptor and to have an appropriate control for all further experiments, a mouse line for complete CB1 receptor rescue was generated.

To this end, heterozygous animals of the Stop-CB1 line were crossed to "Cre-deleter" mice expressing Cre recombinase under the control of the adenoviral promoter EIIa (EIIa-Cre) (Lakso et al., 1996), which drives expression in the relatively undifferentiated stages of oogenesis and in pre-implantation development (Dooley *et al.*, 1989). First generation progeny showed a mosaic pattern of Cre recombinase-mediated excision of the loxP-flanked stop cassette, as Cre recombinase is mainly acting past the zygote state (Holzenberger *et al.*, 2000). These double transgenic mosaic mice were then backcrossed to C57B/6J mice to obtain germ line transmission of the Cre recombinase-mediated excision of the rescued allele. Deletion of the stop cassette throughout the whole body can be detected in the routine genotyping of tail biopsies. The additional loxP site in the 5' UTR increased

the size of the genomic region between the binding sites of the primers S87 and S89 by 34 nucleotides (Figure 3.4). In a third crossing, Cre recombinase-positive germ line-deleted animals were backcrossed to C57BL/6J mice to be able to select for Cre-negative mice heterozygous for the germ line transmission of the excised stop cassette, to circumvent further appearance of the mosaicism. The rescued CB1 receptor allele was then bred to homozygosity. This mouse line is called complete CB1 receptor rescue or in short, CB1-RS.

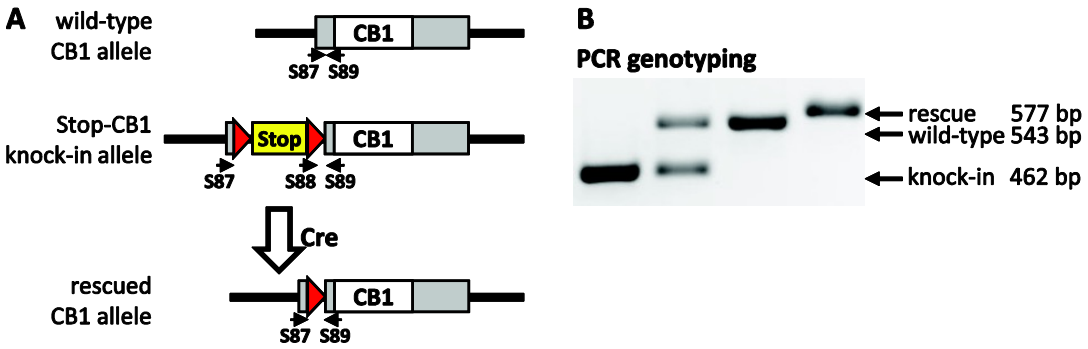

Figure 3.4: Cre recombinase mediated excision of the loxP-flanked stop cassette.
(A) After Cre recombinase mediated excision of the loxP-flanked stop cassette, only one loxP site remained in the 5' UTR of the exon containing the CB1 receptor CDS. **(B)** In the PCR genotyping, germ line transmission of the rescued CB1 receptor allele resulted in a 577 bp band, as the sequence between the binding sites of S87 and S89 contains the additional 34 nucleotides of the remaining loxP site after stop cassette excision.

3.3.2.2 Cortical glutamatergic CB1 receptor rescue

By crossing the Stop-CB1 mouse line to a mouse line that expresses Cre recombinase under the control of the NEX regulatory sequences (Schwab *et al.*, 2000; Monory *et al.*, 2006), the loxP flanked stop cassette was excised in cortical glutamatergic neurons and CB1 receptor is re-expressed in these cells. This mouse line expressing the CB1 receptor on cortical glutamatergic neurons is called Glu-CB1-RS.

3.3.3 Silencing of CB1 receptor expression

Introduction of the loxP-flanked stop cassette into the 5' UTR of the CB1 receptor CDS was performed to silence the CB1 receptor gene. The stop cassette contains three polyadenylation signals to block transcription of the CB1 receptor mRNA. In addition, at the end of the Neo^R is a stop codon to stop transcription. This dual strategy, with the polyadenlation signals to block RNA synthesis and the stop codon at the end of the Neo^R to stop transcription, aimed at inhibiting the production of CB1 receptor effectively.

3.3.3.1 CB1 receptor mRNA

To determine whether the insertion of the stop cassette blocked CB1 receptor mRNA expression, *in situ* hybridization was performed with a full length CB1 receptor probe on brain sections of homozygous Stop-CB1 mice and wild-type littermates (Figure 3.5A-D).

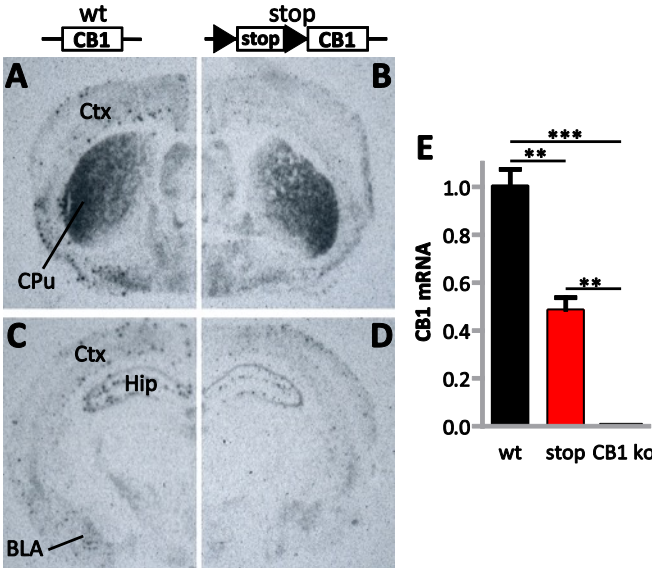

Figure 3.5: Reduction but not attenuation of CB1 receptor mRNA expression in Stop-CB1 mice.
(A-D) *In situ* hybridization in striatal (A+B) and hippocampal (C+D) brain sections of a wild-type mouse (wt; A, C) and a Stop-CB1 littermate (stop; B, D). There is only a reduction instead of a loss of mRNA in the stop animal compared with the wild-type littermate. Ctx: neocortex; CPu: caudate putamen; Hip: hippocampus; BLA: basolateral amygdala. **(E)** Hippocampal CB1 receptor mRNA was quantified in wild-type mice (n=3) and Stop-CB1 littermates (n=4). Transcription downstream of the stop cassette was not completely abolished in the Stop-CB1 mice. As a control, mRNA of hippocampi of conventional CB1 receptor knock-out mice was quantified (ko, n=2), where no mRNA was detectable. Columns represent mean + SEM; ***p<0.001; **p<0.01.

Stop-CB1 mice showed the same expression pattern of CB1 receptor mRNA, but with reduced intensity as compared with wild-type animals. Non-cortical areas, such as striatum (dorsolateral caudate putamen, CPu), showed a uniformly distributed CB1 receptor expression, whereas in the hippocampus (Hi), neocortex (Ctx) and BLA, both low CB1-expressing pyramidal cells (uniform grey stain) and high CB1-expressing interneurons (black spots) were detected. To quantify the remaining CB1 receptor mRNA, qPCR with a probe recognizing an mRNA sequence coding for the CB1 receptor transmembrane region was performed on hippocampal cDNA from Stop-CB1 mice, wild-type littermates and the conventional CB1 knock-out mice as a control (Figure 3.5E). Glucoronidase beta was used as reference gene to normalize gene expression. Homozygous Stop-CB1 mice (n=4) expressed about 45% of CB1 receptor mRNA as compared with wild-type animals (n=3). In the CB1 knock-out control (n=2), no CB1 receptor mRNA was detected. Thus, the stop cassette significantly reduced the expression of CB1 receptor mRNA by 55%, but failed to abolish the expression completely.

3.3.3.2 CB1 receptor protein

The presence of the stop cassette was not sufficient to fully block transcription of CB1 receptor gene. However, the aim of the approach was to eliminate the presence of CB1 receptor protein. Receptor autoradiography with the radiolabelled CB1 receptor agonist ^{3}H-CP55,940, Western blot and immunohistochemical analysis using specific CB1 receptor antibodies revealed that no CB1 receptor protein was detectable in Stop-CB1 mice (Figure 3.6). Thus, Stop-CB1 mice do not contain detectable levels of CB1 receptor protein and should therefore display similar phenotypes as null-mutant CB1 receptor mice.

3.3.4 Region- and cell type-specific rescue of CB1 receptor expression

3.3.4.1 Transgenic rescue of CB1 receptor in CB1-RS and Glu-CB1-RS mouse lines

To verify the complete rescue of CB1 receptor expression, histological analyses were performed with CB1-RS mice. These mice showed a very similar pattern of agonist binding and immunoreactivity as wild-type animals (Figure 3.6C, G, K). Quantification of the bands of Western blot analysis (Figure 3.6M, N) and of the bound CB1 receptor agonist ^{3}H-CP55,940 in autoradiography of the hippocampus (Figure 3.6O) confirmed that there is no difference in the receptor protein level or binding between CB1-RS and wild type, respectively.

In Glu-CB1-RS mice, agonist binding with ^{3}H-CP55,940 revealed the rescue of CB1 receptor in cortical areas (including neocortex, amygdala and hippocampus) and in the striatum (Figure 3.7A-H). Importantly, these areas are the ones where CB1 receptor-containing cortical neurons are believed to project to (Marsicano & Kuner, 2008). The very strong binding observed in the outflow nuclei of the striatum (globus pallidus, entopeduncular nucleus and substantia nigra) and in the cerebellum was not rescued in Glu-CB1-RS mice (Figure 3.7A-H). In agreement with the low levels of CB1 receptor expression in cortical glutamatergic neurons (Marsicano & Lutz, 1999; Kawamura *et al.*, 2006; Marsicano & Kuner, 2008; Bellocchio *et al.*, 2010), Glu-CB1-RS mice displayed lower binding levels as compared with CB1-RS mice. Quantification of CB1 receptor protein in extracts from hippocampus with Western blot analysis revealed 28% of CB1 receptor in Glu-CB1-RS as compared with CB1-RS animals. Quantification of hippocampal agonist binding resulted in 39% bound ^{3}H-CP55,940 in Glu-CB1-RS as compared with CB1-RS animals (Figure 3.6O). Detailed immunohistochemical analysis of CB1 receptor expression in the hippocampus of Glu-CB1-RS mice revealed the strongest signal in the inner third of the molecular layer of the dentate gyrus (Figure 3.6H), which colocalization with VGluT1, a marker for glutamatergic terminals (Figure 3.7I-L). This expression pattern was previously described for CB1 receptor on terminals of glutamatergic afferent fibers of mossy cells, projecting to the inner third of the molecular layer of the dentate gyrus (Monory *et al.*, 2006). In the amygdala of Glu-CB1-RS mice, weak immunostaining was detected in

the basal but not in the lateral part of the BLA. Also in the central part of the amygdala, a faint signal was detected (Figure 3.6L, CeA indicated by white arrow).

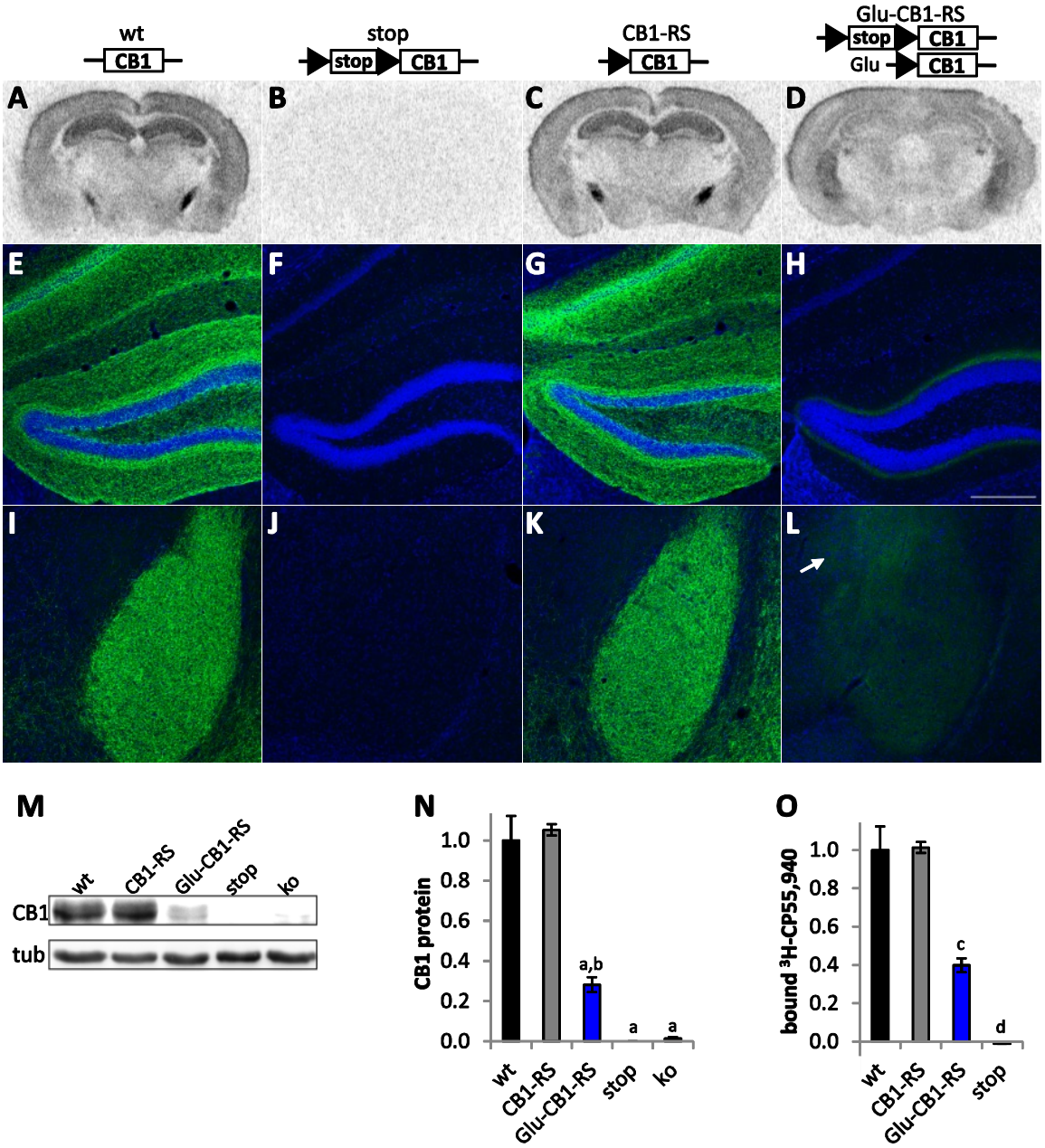

Figure 3.6: Disruption and rescue of CB1 receptor expression.
(A-D) Autoradiography with ^{3}H-CP55,940 and **(E-L)** immunostaining on brain sections of wild-type (wt), Stop-CB1 (stop), CB1-RS and Glu-CB1-RS mice (CB1: green, nuclear staining: blue; white arrow indicates CeA). Scale bar: 200 µm. **(M, N)** Western blot analysis of hippocampal protein extracts (M, representative Western blot; N, quantification of n=3 per group). **(O)** Quantification of bound ^{3}H-CP55,940 in the hippocampus (wt n=4, CB1-RS n=4, Glu-CB1-RS n=3, stop n=3). Columns represent mean +/- SEM. [a] p<0.001 *vs.* wt and CB1-RS, [b] p<0.1 *vs.* stop and ko; [c] p<0.001 *vs.* wt, CB1-RS and stop, [d] p<0.001 *vs.* wt, CB1-RS and Glu-CB1 RS.

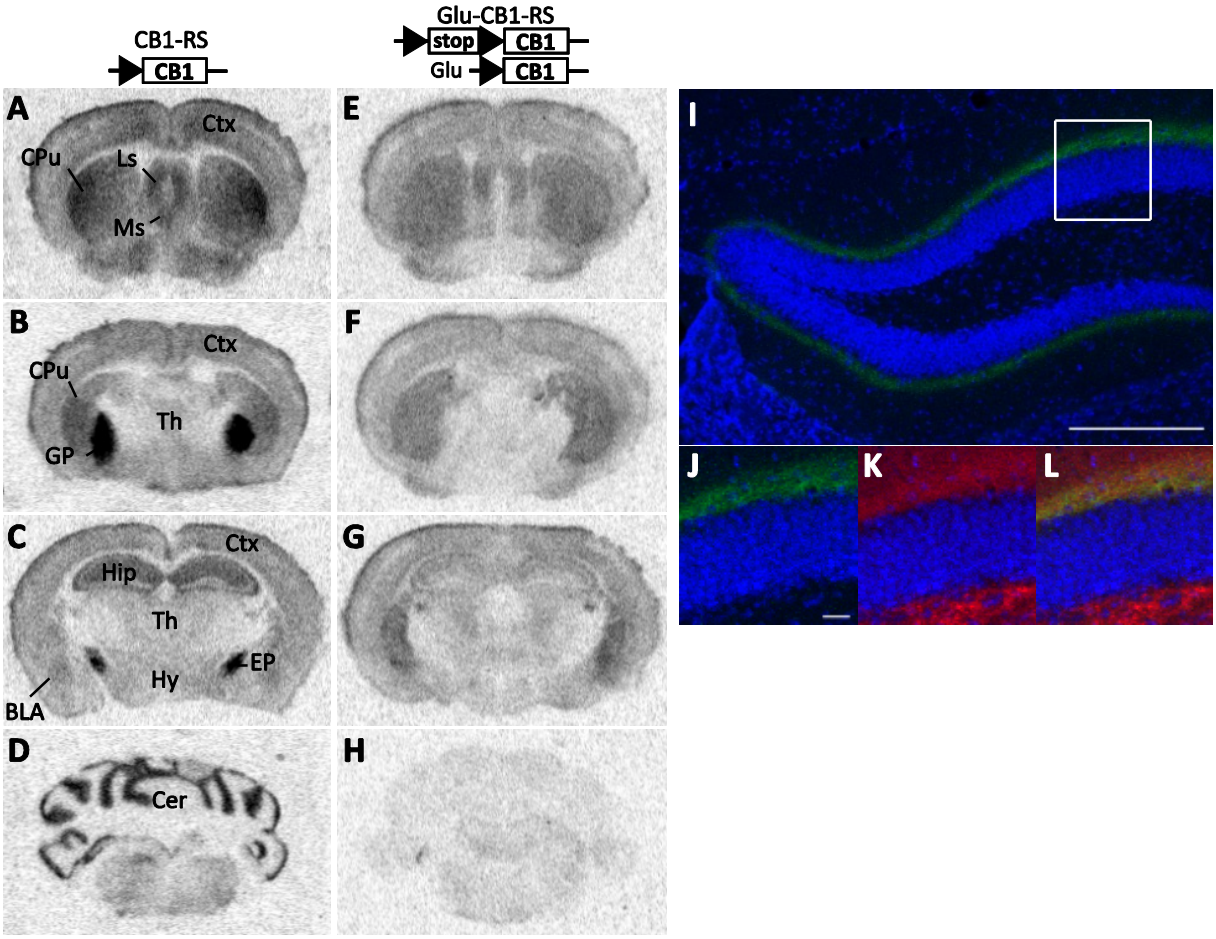

Figure 3.7: Detailed histological analysis of CB1 receptor binding and immunohistochemistry in Glu-CB1-RS mice. (A-H) Autoradiography with ^{3}H-CP55,940 on brain sections of CB1-RS (A-D) and Glu-CB1-RS mice (E-H). BLA: basolateral amygdala; Cer: cerebellum; CPu: caudate putamen; Ctx: neocortex; EP: entopeduncular nucleus; GP: globus pallidus; Hip: hippocampus; Hy: hypothalamus; Ls: lateral septum; Ms: medial septum; Th: thalamus. **(I)** Immunostaining of hippocampal sections revealed a strong CB1 positive signal in the inner third of the molecular layer of dentate gyrus. Scale bar: 200 µm, CB1 receptor: green, nuclear staining: blue. **(J-L)** High magnification of the dentate gyrus cells shown in I. Immunostaining with CB1 (J) and VGluT1, a marker for glutamatergic terminals (K, red), shows co-expression in the inner molecular layer (L). Scale bar: 25 µm.

3.3.4.2 Viral delivery of Cre recombinase rescues CB1 receptor

To test whether not only transgenic, but also viral delivery of Cre recombinase can induce CB1 receptor rescue, adeno-associated virus expressing Cre-recombinase (AAV-Cre) was infused into the hilus of dentate gyrus of Stop-CB1 mice. CB1 receptor expression was rescued locally in the dorsal hippocampus (Figure 3.8).

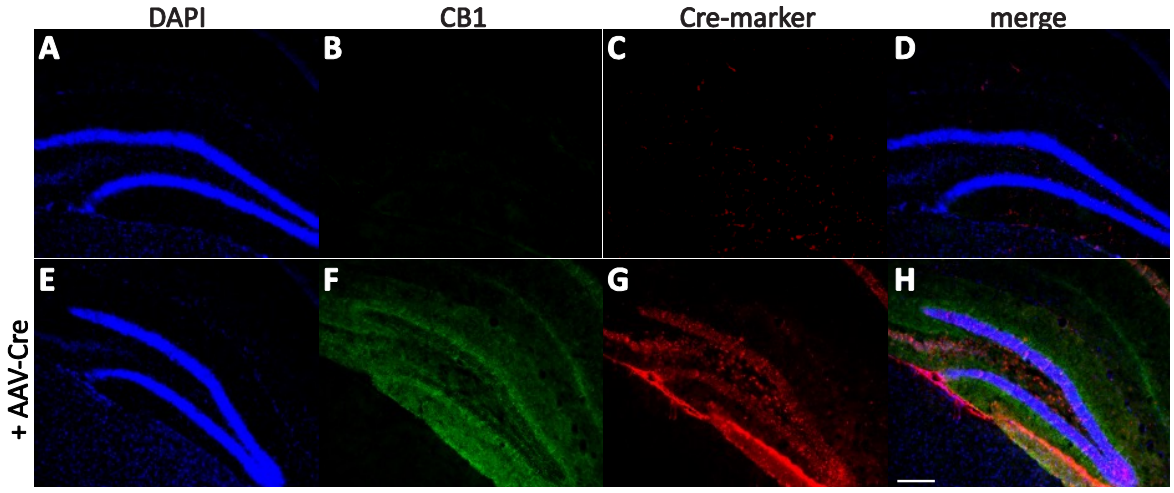

Figure 3.8: Viral delivery of Cre-recombinase rescues CB1 receptor.
Hippocampal sections of Stop-CB1 mice without virus **(A-D)** or with infusion of AAV-Cre **(E-H)**. Sections were stained with DAPI (blue, nuclear marker), CB1 receptor antibody (green) and HA antibody (red, for HA-tagged Cre recombinase). Scale bar: 150 µm.

3.3.5 Electrophysiology

When an action potential arrives at the postsynapse, endocannabinoids are released, travel retrogradely through the synaptic cleft and activate presynaptic CB1 receptor. This leads to a suppression of neurotransmitter release and thus, to a reduced activation of the postsynaptic cell (Kano *et al.*, 2009). In CB1 receptor knock-out mice, DSE and DSI are completely absent (Wilson *et al.*, 2001; Ohno-Shosaku *et al.*, 2002*b*). DSE and DSI measurements in the Stop-CB1 and rescue mouse lines were performed in collaboration with Melanie Wickert (Lutz' group) and with the laboratories of Hans-Christian Pape (Münster) and Giovanni Marsicano (Bordeaux). Experiments were performed by Hector Romo-Parra (all measurements in BLA as well as DSE and DSI of Glu-CB1-RS in hippocampus), by Federico Massa and by Melanie Wickert (DSE and DSI of wt, stop and CB1-RS in hippocampus).

In the hippocampus, DSE (Figure 3.9A, B) and DSI (Figure 3.9C, D) were measured in pyramidal neurons upon stimulation in Schaffer collateral projections. Depolarization of the patched cell produced a significant reduction of evoked glutamatergic (DSE) or GABAergic (DSI) currents in wild-type and CB1-RS mice (DSE: wt $p=0.004$, CB1-RS $p<0.001$; DSI: wt $p=0.002$, CB1-RS $p=0.001$). In Stop-CB1 mice, depolarization did not evoke any DSE or DSI, proving the absence of the CB1 receptor from the presynaptic terminals. In Glu-CB1-RS mice, depolarization evoked significant DSE ($p<0.001$), but did not evoke any DSI, corroborating the selective rescue of CB1 receptor on glutamatergic cells.

In the BLA, DSE (Figure 3.9E, F, I) and DSI tests (Figure 3.9G, H) were performed upon stimulation in the BLA. Depolarization of the patched cell produced a significant reduction of glutamatergic (DSE) and GABAergic (DSI) evoked responses in CB1-RS mice (DSE: $p<0.001$, DSI:

p=0.016). In Stop-CB1 mice, depolarization did not evoke any DSE and DSI. DSE in Glu-CB1-RS mice showed a different kinetic, with a prolonged reduction of evoked excitatory postsynaptic currents (p=0.023 for the mean of the first three responses and p=0.004 for the mean of three responses 160 s after depolarization, Figure 3.9E, F, I). The effect was mediated by the CB1 receptor, as it was blocked by the CB1 receptor antagonist AM251 (Figure 3.9I). Depolarization did not evoke any DSI in Glu-CB1-RS mice (Figure 3.9G, H).

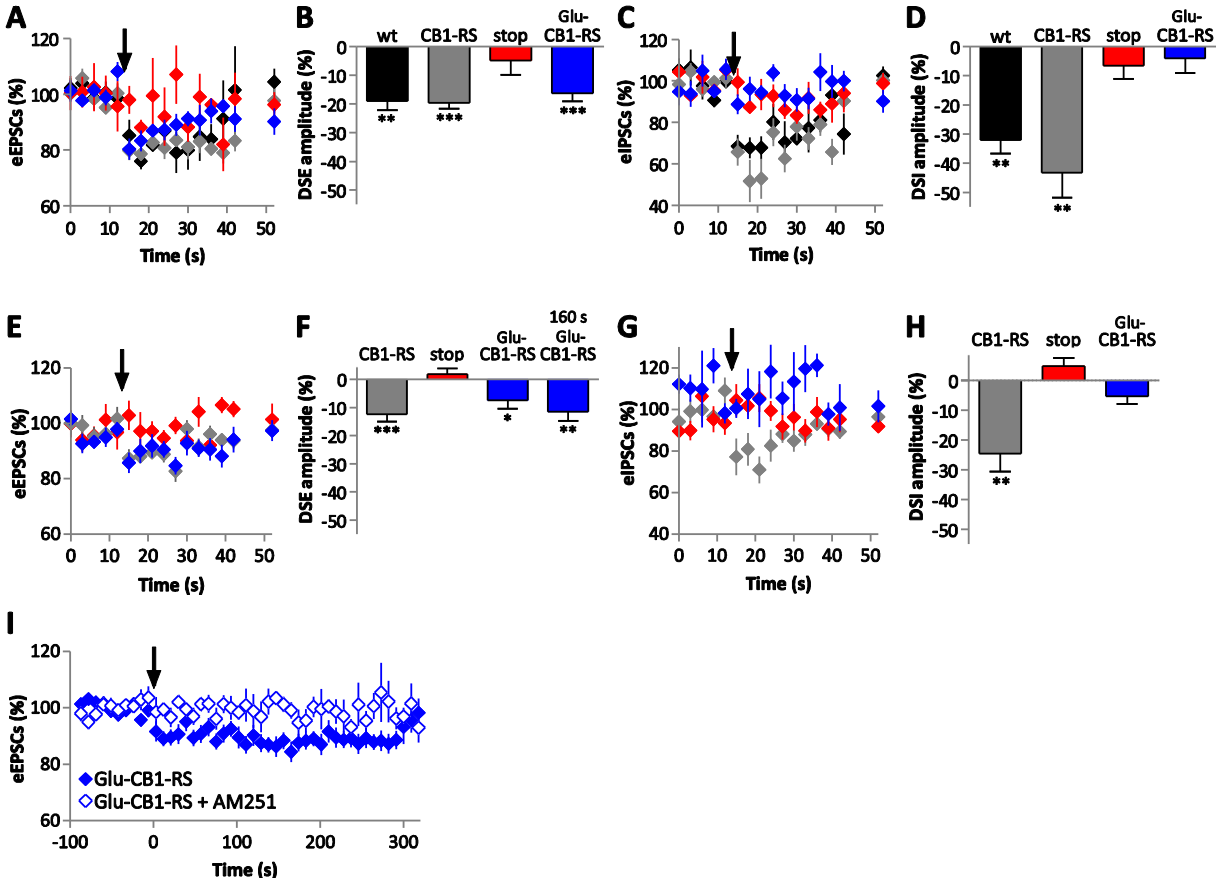

Figure 3.9: Loss and rescue of DSI and DSE.
(A-D) DSE (A, B) and DSI (C, D) in pyramidal hippocampal neurons of wild-type (wt, black, n=5 for DSE, n=5 for DSI), CB1-RS (grey, n=6 for DSE, n=8 for DSI), Stop-CB1 (red, n=3 for DSE, n=4 for DSI) and Glu-CB1-RS mice (blue, n=8 for DSE, n=9 for DSI). **(E-H)** DSE (E, F) and DSI (G, H) in BLA neurons of CB1-RS (grey, n=14 for DSE, n=5 for DSI,) Stop-CB1 (red, n=6 for DSE, n=10 for DSI) and Glu-CB1-RS mice (blue, n=18 for DSE, n=5 for DSI). Amplitudes were calculated using the mean of five evoked EPSCs (eEPSCs or eIPSCs for DSI) just before and three after depolarization. Maximal effect of DSE in Glu-CB1-RS was 160 s after depolarization (mean of three responses after 160 s compared with baseline). Data are mean +/- SEM; ***p<0.001, **p<0.01, *p<0.05 *vs.* 0. **(I)** Prolonged DSE in BLA neurons of Glu-CB1-RS mice is blocked by the CB1 receptor antagonist AM251 (each data point represents the average of 3 responses, n=12 for Glu-CB1-RS +AM251). (These experiments were performed by Hector Romo-Parra, Federico Massa and Melanie Wickert.)

3.3.6 Phenotypes of Stop-CB1 mice and global rescue of CB1 receptor functions

Reflecting the plethora of functions ascribed to the ECS, null-mutant CB1 receptor mice display well-known phenotypes. Thus, they have decreased body-weight (Cota *et al.*, 2003), are hypophagic in fasting-refeeding experiments (Di Marzo *et al.*, 2001), are more susceptible to kainic acid (KA)-induced epileptiform seizures (Marsicano *et al.*, 2003), display a decreased exploration of open arms in an elevated plus maze (Haller *et al.*, 2004*a*), and are impaired in extinction of freezing responses in cued fear conditioning tests (Marsicano *et al.*, 2002). To verify the functional disruption and reactivation of the CB1 receptor in Stop-CB1 and CB1-RS mice, respectively, the phenotypes of these mice and wild-type animals were compared in the above mentioned paradigms.

3.3.6.1 Refeeding after fasting

CB1 receptor knock-out mice have reduced bodyweight and a reduced food intake after fasting as compared with wild-type animals (Di Marzo *et al.*, 2001; Cota *et al.*, 2003). Body weight was measured in Stop-CB1 mice (n=18), their wild-type littermates (n=18) and CB1-RS mice (n=19, age range of all groups 2.5 to 4.0 month). Stop-CB1 mice had significantly reduced body weight as compared with wild-type and CB1-RS mice ($p=0.031$ for stop *vs.* wt, $p=0.017$ for stop *vs.* CB1-RS), whereas weight of wild-type and CB1-RS mice did not differ significantly (Figure 3.10A).

Food consumption of Stop-CB1 mice in the first hour after 24 h fasting was significantly different from their wild-type littermates and CB1-RS mice ($p<0.001$ for stop *vs.* wt, $p=0.005$ for stop *vs.* CB1-RS, (Figure 3.10B). The food intake of CB1-RS animals did not differ from that of wild-type animals.

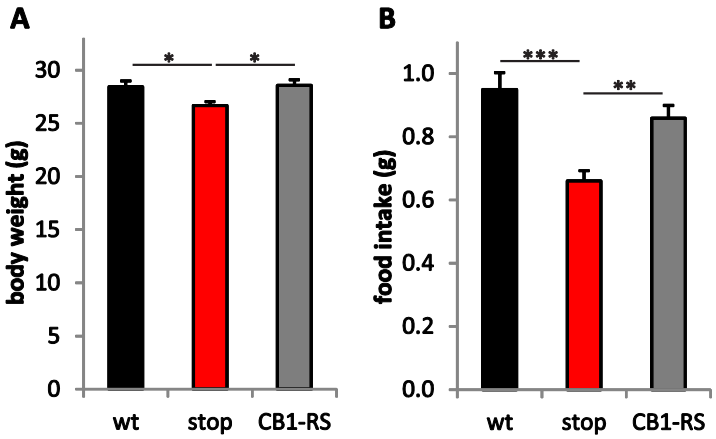

Figure 3.10: Bodyweight and food intake of Stop-CB1, CB1-RS and wild-type animals.
(A) Food intake and **(B)** body weight were significantly decreased in Stop-CB1 mice (stop, n=18) compared with their wild-type littermates (wt, n=18) and CB1-RS animals (n=19). Columns represent mean + SEM; ***p<0.001, **p<0.01, *p<0.05.

3.3.6.2 Acute excitotoxic seizures

The ECS has neuroprotective properties that can be tested with the injection of KA, which activates glutamate receptors and, thus, induces activation of excitatory pathways leading to acute epileptiform seizures (Marsicano *et al.*, 2003). After injection of 30 mg/kg KA into Stop-CB1 animals (n=15), their wild-type littermates (n=17) and CB1-RS mice (n=20), seizure behavior was monitored and quantified over 2 h (Figure 3.11A). There was a significant interaction between the effect of time (T) and of genotype (G) ($p<0.004$), indicating that the genotypes reacted differently to the KA over time. *Post-hoc* analyses revealed significantly higher seizure susceptibility in Stop-CB1 than in CB1-RS and wild-type mice for all time-points ($p<0.001$-0.014). There was no significant difference between wild-type and CB1-RS mice at any of the time-points (see detailed statistical analysis in Table 3.4). Excessive seizure activity can lead to death. With Kaplan-Meier survival analysis, a significant difference between genotypes was found ($p<0.0001$ in log rank test; Figure 3.11B). One hour after seizure induction, only 7% of the Stop-CB1 mice survived, while 94% of the wild-type and 86% of the CB1-RS animals were still alive.

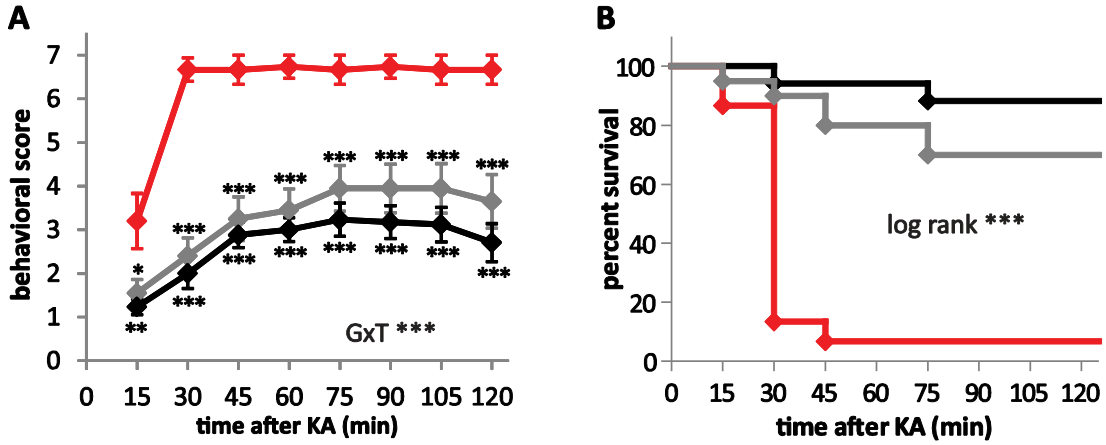

Figure 3.11: Susceptibility to kainic acid (KA)-induced epileptiform seizures of Stop-CB1, CB1-RS and wild-type animals.
(A) Behavioral scores over a period of 120 min after KA injection. Seizure severity was increased in Stop-CB1 mice (red, n=15) as compared with wild-type (black, n=17) and CB1-RS mice (grey, n=20), indicating a decreased seizure protection. Curves represent mean +/- SEM; GxT***: $p<0.001$ for interaction of genotype and time; ***$p<0.001$, **$p<0.01$, *$p<0.05$ in *post-hoc* against Stop-CB1. **(B)** Kaplan-Meier survival curves of the three genotypes after injection of KA. ***$p<0.001$ in log rank test.

Table 3.4: Detailed statistical analysis for the single time-points after KA injection in Stop-CB1 (stop), CB1-RS and wild-type (wt) animals.

Time after KA (min)		15	30	45	60	75	90	105	120
G		0.003	<0.001	<0.001	<0.001	<0.001	<0.001	<0.001	<0.001
***post-hoc* G**	**stop - wt**	0.004	<0.001	<0.001	<0.001	<0.001	<0.001	<0.001	<0.001
	stop - CB1-RS	0.014	<0.001	<0.001	<0.001	<0.001	<0.001	<0.001	<0.001
	wt - CB1-RS	1.000	1.000	1.000	1.000	0.732	0.644	0.604	0.547

3.3.6.3 Innate anxiety

If the experimental conditions are chosen appropriately, CB1 receptor knock-out mice show increased anxiogenic responses in classical anxiety paradigms, such as the elevated-plus maze (EPM) (Haller *et al.*, 2004*a*). Stop-CB1 mice (n=10), their wild-type littermates (n=10) and CB1-RS animals (n=10) were placed in the center of the EPM, and behavior was monitored for 5 min. There was no significant difference in locomotion between the genotypes (p=0.334, Figure 3.12A). Stop-CB1 mice spent less time on the open arms (p<0.001 for stop *vs.* wt, p=0.008 for stop *vs.* CB1-RS, Figure 3.12B) and had fewer entries to the open arms (p=0.01 for stop *vs.* wt, p=0.046 for stop *vs.* CB1-RS, Figure 3.12C) than their wild-type littermates or CB1-RS mice.

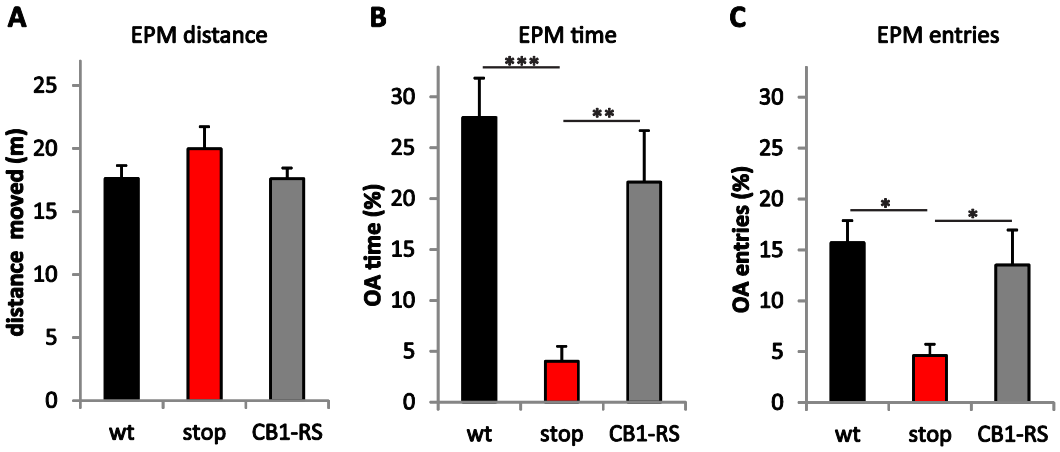

Figure 3.12: Behavior of Stop-CB1, CB1-RS and wild-type animals on the elevated-plus maze (EPM).
(A) Distance moved did not differ between the genotypes (n=10 for each genotype). **(B)** Time spent in the open arms (OA) and **(C)** entries to the OA: Stop-CB1 mice (stop) have less OA entries and spent less time in the OA than their wild-type littermates (wt) and CB1-RS animals. Columns represent mean + SEM; ***p<0.001, **p<0.01 and *p<0.05.

3.3.6.4 Extinction of conditioned fear

In auditory fear conditioning, CB1 receptor knock-out mice were shown to have impaired extinction learning (Marsicano *et al.*, 2002). Stop-CB1 mice, their wild-type littermates and CB1-RS mice were conditioned to associate a tone with a foot shock in a single tone-shock pairing. On the day after conditioning (d1), animals were exposed to a novel context (hereafter called extinction context). After 180 s exploration, when baseline behavior was monitored, the tone was presented continuously over 200 s. Tone-induced freezing, defined as freezing to the tone minus baseline freezing response of the same day, was measured. After termination of the tone, the animals stayed in the box for another 60 s, and their behavior after the tone was monitored. This extinction protocol was repeated on d2, d3 and d10 to evaluate between-session extinction of the freezing behavior. The initial fear response to the tone presentation in the extinction context, 24 h after conditioning, was similar for all genotypes (p=0.988). Within-session extinction of freezing (evaluated analyzing the

tone-induced freezing in 20 s bins) revealed a significant effect for genotype and time on all extinction days (for detailed statistical analysis, see Table 3.5). *Post-hoc* analysis revealed a significantly higher freezing response of Stop-CB1 animals than of their wild-type littermates on all extinction days. Freezing response of CB1-RS animals did not differ from wild-type animals, but was significantly lower than that of Stop-CB1 animals on d1, d2 and d10. Between-session extinction (defined as the reduction in initial freezing response between the extinction days) was present in all genotypes, but did not differ between genotypes. The total freezing response to the 200 s tone presentation of Stop-CB1 animals was significantly stronger than of their wild-type littermates and CB1-RS animals (Figure 3.13B). Baseline freezing in the extinction context did not differ between genotypes (Figure 3.13C). Notably, there was a significant difference in the freezing response after termination of the tone (p=0.005): Stop-CB1 animals showed a stronger freezing response than the wild-type animals after termination of the tone. Freezing response after the tone did not differ between wild-type and CB1-RS and between CB1-RS and Stop-CB1 animals (Figure 3.13D).

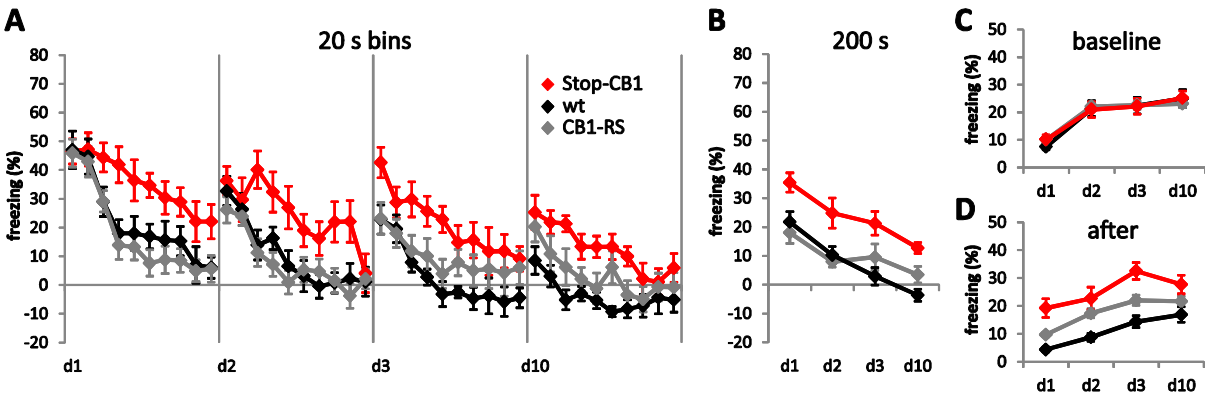

Figure 3.13: Conditioned freezing of Stop-CB1, CB1-RS and wild-type mice in response to repeated presentations of a fear-conditioned auditory stimulus at different days after training.
(A) Freezing response (after subtraction of baseline freezing of the same day) of Stop-CB1 (red, n=10), wild-type (wt, black, n=10) and CB1-RS animals (grey, n=10) over the course of tone presentations per day (d1-d10, as indicated) analyzed in 20 s bins. Within-session extinction of Stop-CB1 animals was reduced compared with wt and CB1-RS. **(B)** The total freezing response (after subtraction of baseline freezing) over the days of Stop-CB1 was stronger than of wt or CB1-RS mice. **(C)** Baseline freezing response before the tone started did not differ between genotypes. **(D)** Freezing response after the tone was terminated. Data are mean +/- SEM; detailed statistical analysis in Table 3.5.

Table 3.5: Statistical analysis of the performance of Stop-CB1, CB1-RS and wild-type mice in fear extinction.

		repeated measures ANOVA for 20 s intervals				repeated measures ANOVA for days			
		d1	d2	d3	d10	tone-baseline	initial 20s - baseline	baseline	after tone
G x T		n.s.	0.062	n.s.	n.s.	n.s.	0.055	n.s.	n.s.
T		<0.001	<0.001	<0.001	<0.001	<0.001	<0.001	<0.001	<0.001
G		<0.001	0.005	0.010	<0.001	<0.001	n.s.	n.s.	0.005
post-hoc G	stop - wt	0.033	0.025	0.008	<0.001	0.001	-	-	0.004
	stop - CB1-RS	0.005	0.008	n.s.	0.027	0.003	-	-	n.s.
	wt - CB1-RS	n.s.	n.s.	n.s.	n.s.	n.s.	-	-	n.s.

3.3.6.5 Summary

In the performed behavioral analyses, Stop-CB1 mice showed the same phenotypes as conventional knock-out mice, proving a functional disruption of the CB1 receptor allele by the stop cassette. The rescued allele with the loxP site in the 5' UTR was shown to restore full functionality for the CB1 receptor, as there were no significant differences between wild-type mice and CB1-RS mice in any of the behavioral paradigms tested.

3.3.7 Reactivation of CB1 on cortical glutamatergic neurons

In order to investigate to what extent CB1 receptor-driven modulation of glutamatergic transmission in cortical neurons is sufficient to rescue the phenotypes observed in CB1 receptor knock-out animals, we subjected the Glu-CB1-RS mice to several behavioral paradigms.

3.3.7.1 Refeeding after fasting

Body weight was measured in Glu-CB1-RS mice (n=24), their Stop-CB1 littermates (n=28) and CB1-RS mice (n=25, age range of all groups 2.5 to 4.0 month). Both Stop-CB1 mice and Glu-CB1-RS had significantly reduced body weight as compared with CB1-RS (Figure 3.14A, $p<0.001$ for Stop-CB1 *vs.* complete, $p<0.001$ for Glu-CB1-RS *vs.* CB1-RS), whereas the body weight of Glu-CB1-RS animals did not differ significantly from their Stop-CB1 littermates ($p=1$). Thus, CB1 receptor expression on cortical glutamatergic neurons is not sufficient to rescue the reduction in body weight observed upon complete inactivation of the CB1 receptor gene.

Food consumption of Stop-CB1 mice in the first hour after 24 h starvation was significantly lower than of CB1-RS mice (Figure 3.14, $p<0.001$). Food intake of Glu-CB1-RS mice was significantly higher than of Stop-CB1 mice ($p=0.037$), and it did not differ significantly from the food intake of the CB1-RS ($p=0.121$). Thus, expression of the CB1 receptor on cortical glutamatergic neurons is a sufficient condition to restore normal fasting-induced food intake.

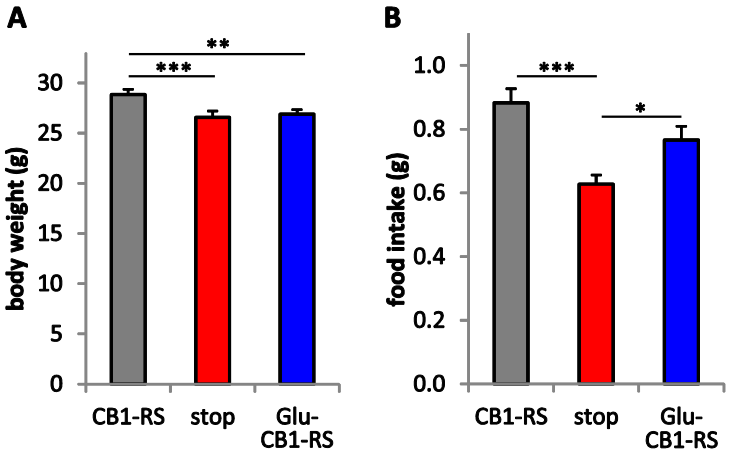

Figure 3.14: Bodyweight and food intake of Glu-CB1-RS, Stop-CB1 and CB1-RS mice.
(A) Body weight of both Stop-CB1 (stop, n=28) and Glu-CB1-RS mice (n=24) was lower than of CB1-RS mice (n=25). **(B)** Food intake of Glu-CB1-RS mice was higher than of stop animals (n=28), but did not differ significantly from the CB1-RS control. Food intake of stop animals was significantly lower than of CB1-RS controls. Columns represent mean + SEM; ***p<0.001, **p<0.01, *p<0.05.

3.3.7.2 Acute excitotoxic seizures

Neuroprotective properties of the CB1 receptor on cortical glutamatergic neurons were tested by injection of 30 mg/kg KA to CB1-RS animals (n=25), Stop-CB1 animals (n=30) and their Glu-CB1-RS littermates (n=22). Epileptiform behavior was monitored over 2 h (Figure 3.15A). There was a significant interaction between the effect of time and genotype ($p<0.001$), indicating that the genotypes reacted differently to the KA over time. *Post-hoc* analyses revealed significantly higher seizure susceptibility in Stop-CB1 than in CB1-RS mice for all time-points ($p<0.001$-0.021) and than in Glu-CB1-RS mice for the first 90 min ($p<0.001$-0.044). There was no significant difference between Glu-CB1-RS and the CB1-RS control group at any of the time-points (see detailed statistical analysis in Table 3.6). Kaplan-Meier survival analysis revealed a significant difference between survival proportions of Glu-CB1-RS animals, Stop-CB1 animals and CB1-RS mice ($p<0.0001$ in log rank test, Figure 3.15B). 60 min after seizure induction, 40% of the Glu-CB1-RS mice survived, while only 3% of the Stop-CB1 animals were still alive. 64% of the CB1-RS animals survived the first hour after KA injection. Thus, CB1 receptor expression on cortical glutamatergic neurons is to a large extent sufficient for the neuroprotective properties of CB1 receptor signaling against KA-induced epileptiform seizures.

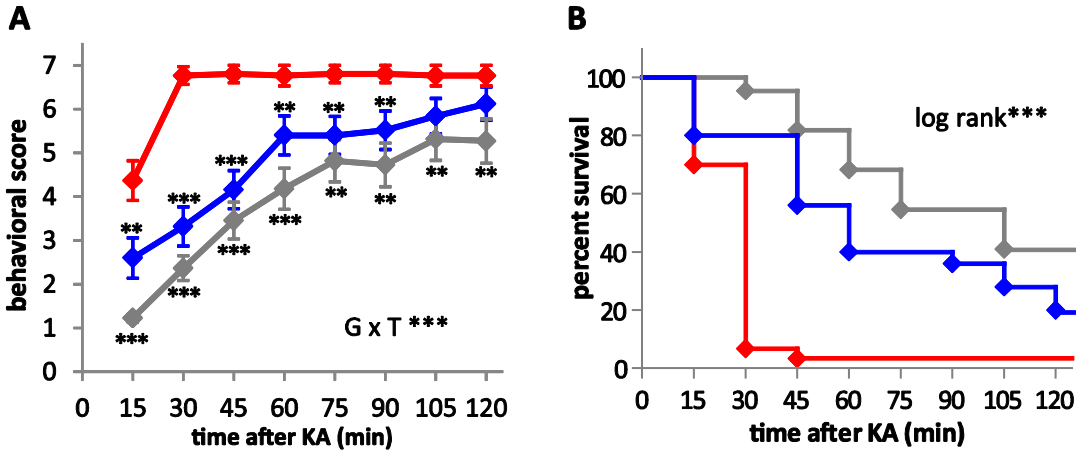

Figure 3.15: Reduced seizure severity in KA-induced epileptic seizure in Glu-CB1-RS mice.
(A) Behavioral scores over a period of 120 min after KA injection. Seizure severity was significantly increased in Stop-CB1 mice (red, n=30) compared with CB1-RS at all time-points (grey, n=25) and to Glu-CB1-RS mice (blue, n=22) for the first 90 min. Seizure severity of Glu-CB1-RS mice did not differ from that of CB1-RS mice at any time-point. Curve represent mean +/- SEM; GxT***: p<0.001 for interaction of genotype and time; ***p<0.001, **p<0.01, *p<0.05 in *post-hoc* against Stop-CB1. **(B)** Kaplan-Meier survival curves of the three genotypes after injection of KA. ***p<0.001 in log rank test.

Table 3.6: Detailed statistical analysis for the single time-points after KA injection in Glu-CB1-RS, Stop-CB1 (stop) and CB1-RS animals

Time after KA (min)		15	30	45	60	75	90	105	120
G		<0.001	<0.001	<0.001	<0.001	0.001	0.001	0.021	0.020
post-hoc G	stop - CB1-RS	<0.001	<0.001	<0.001	<0.001	0.001	0.001	0.021	0.016
	stop - Glu-CB1-RS	0.006	<0.001	<0.001	0.030	0.021	0.044	0.209	0.600
	CB1-RS - Glu-CB1-RS	0.074	0.137	0.536	0.098	0.864	0.469	1.000	0.362

3.3.7.3 Innate anxiety

3.3.7.3.1 Elevated-plus maze

Innate anxiety behavior of CB1-RS animals (n=23), Stop-CB1 animals (n=21) and their Glu-CB1-RS littermates (n=24) was tested on the EPM. Animals were placed in the center of the EPM. During the 5 min exploration of the EPM, Glu-CB1-RS animals moved a significantly bigger distance than CB1-RS animals (p=0.002), whereas there was no significant difference in the distance moved to the Stop-CB1 animals or between Stop-CB1 and CB1-RS mice (Figure 3.16A). Stop-CB1 animals spent significantly less time on the open arms and had significantly less entries to the open arms than CB1-RS animals (p=0.001 and p=0.002, respectively; Figure 3.16B+C). Time spent on the open arms of the Glu-CB1-RS animals was intermediate between the times of the other genotypes and showed a tendency to differ from Stop-CB1 animals (p=0.078). From these results it can be concluded that expression of the CB1 receptor on cortical glutamatergic neurons partially rescues the increased anxiety observed upon CB1 receptor loss.

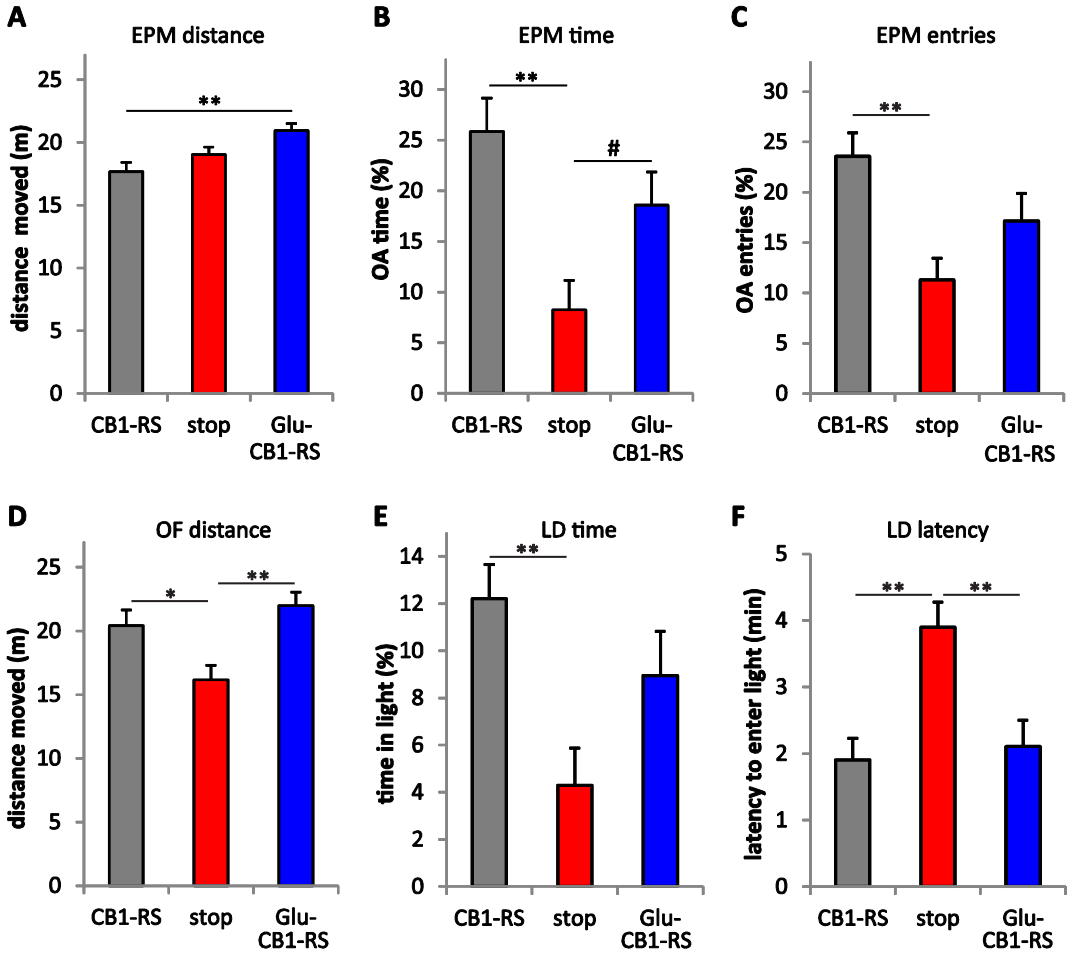

Figure 3.16: Glu-CB1-RS mice show partial rescue of the anxiety phenotype as compared with Stop-CB1 animals. (A) Glu-CB1-RS animals (n=24) moved a significantly bigger distance on the elevated-plus-maze (EPM) than CB1-RS animals (n=23), while Stop-CB1 animals (n=21) did not differ from CB1-RS mice and Glu-CB1-RS mice regarding this parameter. **(B)** Time spent on the open arms (OA) and **(C)** entries to the OA: Stop-CB1 animals spent less time on the OA and had fewer entries to the OA than CB1-RS animals. The time spent on and the entry number to the OA of Glu-CB1-RS mice was between Stop-CB1 and CB1-RS animals, but did not differ significantly from any of the two. **(D)** Locomotion in the open field (OF) of Stop-CB1 animals (n=23) was decreased compared as with CB1-RS (n=23) and Glu-CB1-RS mice (n=24). **(E)** Time spent in the lit compartment of the light/dark (LD) box of Stop-CB1 animals was decreased as compared with CB1-RS animals. The lit-compartment time of Glu-CB1-RS mice was between Stop-CB1 and CB1-RS animals, but did not differ significantly from any of the two. **(F)** Stop-CB1 animals entered the lit compartment later than CB1-RS and Glu-CB1-RS animals, but there was no difference in entry latency between Glu-CB1-RS and CB1-RS. Columns represent mean + SEM; ***p<0.001, **p<0.01, *p<0.05, #p=0.078.

3.3.7.3.2 Light/dark test

Innate anxiety behavior in the light/dark test was measured in CB1-RS animals (n=23), Stop-CB1 animals (n=23) and their Glu-CB1-RS littermates (n=24). To control for differences in locomotion, an open field test was performed with the same animals on the day before the light/dark test (Figure 3.16D). In the open field test, animals were placed in the middle of the arena and could freely explore the arena for 5 min. There were significant differences in the distance moved between CB1-RS and Stop-CB1 animals (p=0.032), and between Stop-CB1 and Glu-CB1-RS animals (p=0.002). These differences in locomotion could potentially interfere with the anxiety measures. However, in the

statistical analysis, the differences in locomotion in the open field test had no confounding influence on the parameters analyzed in the light/dark test[3] and was therefore omitted from the final analysis. For the light/dark test, the animals were placed in the dark compartment of the light/dark box, and behavior was monitored over five minutes. The time spent in the lit compartment and latency to first enter the lit compartment were measured (Figure 3.16E+F). Stop-CB1 animals spent less time in the lit compartment ($p=0.004$) and entered it significantly later ($p=0.001$) than CB1-RS animals. Glu-CB1-RS animals and CB1-RS animals did not differ significantly in the time spent in the lit compartment or entry latency. Latency of Glu-CB1-RS animals to enter the lit compartment was significantly shorter than that of their Stop-CB1 littermates ($p=0.003$), but there were no significant differences between Glu-CB1-RS animals and Stop-CB1 littermates in time spent in the lit compartment. The results of the light/dark box paradigm showed that the CB1 receptor on cortical glutamatergic neurons partially rescued the increased anxiety observed under specific conditions upon CB1 receptor loss.

3.3.7.4 Extinction of conditioned fear

After auditory fear conditioning, the initial fear response to the tone presentation in the extinction context, was similar for CB1-RS animals (n=23), Stop-CB1 animals (n=21) and their Glu-CB1-RS littermates (n=24) ($p>0.27$). Analysis of within-session extinction of freezing (tone-induced freezing in 20-s bins) revealed a significant effect for genotype and time on all extinction days and a significant interaction of genotype and time on d2, d3 and d10 (Figure 3.17A, for detailed statistical analysis, see Table 3.7). *Post-hoc* analysis of genotype for extinction on d1 revealed a significantly higher fear response of Glu-CB1-RS than of Stop-CB1 animals and CB1-RS mice. The significant interactions of genotype and time on extinction d2, d3 and d10 indicate different reductions of the freezing response over time for the genotypes. As the initial freezing response for each extinction day did not differ between the genotypes ($0.149<p<0.705$), *post-hoc* analyses for genotype gave an indication of the differences in extinction (freezing reduction). On d2, d3 and d10, there was a significantly higher freezing response in Glu-CB1-RS and Stop-CB1 animals than in CB1-RS mice (see Table 3.7 for repeated measure ANOVA for the intervals per extinction day). On d3, Glu-CB1-RS even had a tendency for higher freezing than Stop-CB1 animals ($p=0.074$). Between-session extinction (reduction in initial freezing response between the extinction days) was present in all groups ($p<0.001$) but, as mentioned above, did not differ between groups. The total freezing response to the 200 s tone presentation was significantly higher in Stop-CB1 and Glu-CB1-RS animals than in CB1-RS animals (Figure 3.17B). Glu-CB1-RS animals even had a strong tendency ($p=0.055$) towards a higher freezing response than Stop-CB1 animals. Thus, CB1 receptor on cortical glutamatergic neurons did

[3] In an ANOVA with 'distance moved' as covariate for 'time spent in the lit compartment' and 'latency to enter the lit compartment', distance did not have a significant influence on time ($p=0.112$) and latency ($p=0.162$).

not rescue the knock-out phenotype of reduced extinction, but even led to a slightly more sustained freezing response to the conditioned stimulus. Notably, there was a significant interaction between genotype and time for the baseline freezing response, and baseline freezing significantly increased over the extinction days (Figure 3.17C). On d10, Glu-CB1-RS animals had a significantly higher baseline freezing than both other groups ($p<0.001$). Furthermore, Stop-CB1 animals and Glu-CB1-RS animals showed a significantly stronger freezing response after the tone presentation than CB1-RS animals (Figure 3.17D).

As freezing responses of Glu-CB1-RS animals were similar or even more sustained than of Stop-CB1, expression of the CB1 receptor on cortical glutamatergic neurons does not rescue the delayed within-session extinction observed upon CB1 receptor loss.

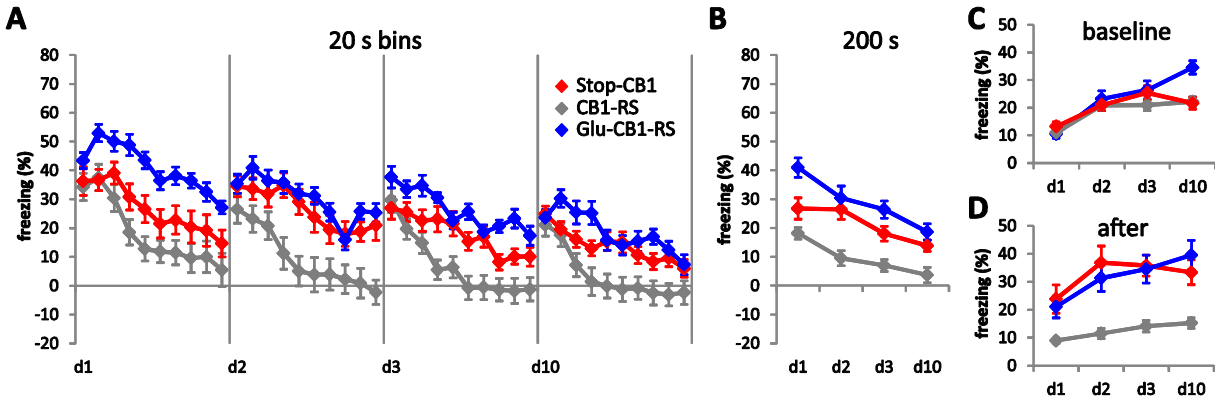

Figure 3.17: Glu-CB1-RS mice have a more sustained freezing response during extinction of conditioned fear. Conditioned freezing of Glu-CB1-RS, Stop-CB1 and CB1-RS in response to repeated presentations of a fear-conditioned auditory stimulus at different days after training. **(A)** Freezing response (after subtraction of baseline freezing of the same day) of Glu-CB1-RS (blue, n=24), Stop-CB1 (red, n=21) and CB1-RS animals (grey, n=23) over the course of tone presentations per day (d1-d10, as indicated) analyzed in 20 s bins. Within-session extinction of Stop-CB1 animals is reduced as compared with CB1-RS. Glu-CB1-RS animals showed an increased freezing response as compared with CB1-RS and Stop-CB1 on d1 and at some time intervals on d3. On d2-10, within-session of Glu-CB1-RS did not differ from that of Stop-CB1 and was reduced as compared with CB1-RS animals. **(B)** The total freezing response (after subtraction of baseline freezing) over the days of Stop-CB1 was stronger than of CB1-RS mice. Total freezing of Glu-CB1-RS was also higher than of CB1-RS and had a tendency to be higher than that of Stop-CB1 animals **(C)** Glu-CB1-RS animals had higher baseline freezing than both other groups on d10. **(D)** Freezing response of Stop-CB1 and Glu-CB1-RS was higher compared with CB1-RS animals after the tone was terminated. Data are mean +/- SEM; detailed statistical analyses in Table 3.7.

Table 3.7: Statistical analysis of the performance of Stop-CB1, CB1-RS and Glu-CB1-RS mice in fear extinction.

		Repeated measures ANOVA for 20 s intervals				Repeated measures ANOVA for days			
		d1	d2	d3	d10	tone-baseline	initial 20s-baseline	baseline	after
G x T		0.143	0.007	0.006	0.031	0.136	n.s.	<0.001	n.s.
T		<0.001	<0.001	<0,001	<0.001	<0.001	p<0,001	<0.001	<0.001
G		<0.001	<0.001	<0.001	<0.001	<0.001	0.151	<0.091	<0.001
***post-hoc* G**	**stop - CB1-RS**	0.190	0.003	0.010	0.017	0.002	-	0.623	0.001
	stop - Glu-CB1-RS	0.005	1	0.074	0.560	0.055	-	1	1
	Glu-CB1-RS - CB1-RS	<0.001	<0.001	<0.001	<0.001	<0.001	-	0.090	0.001

3.3.7.5 Summary

In the analyzed physiological measures and behavioral analyses, Stop-CB1 animals showed the phenotypic alterations as previously described for the complete loss of CB1 receptor. Re-expression of the CB1 receptor on cortical glutamatergic neurons was sufficient to restore normal phenotypes or at least to reduce the altered phenotypes in some paradigms, whereas a worsened phenotype was also found in others (summarized in Table 3.8). Expression of the CB1 receptor on cortical glutamatergic neurons was not sufficient to rescue the reduction in body weight observed upon complete knock-out of CB1 receptor, but was sufficient to restore normal fasting-induced food intake. A large extent of the neuroprotective properties of CB1 receptor signaling seems to be mediated by the CB1 receptor on cortical glutamatergic neurons, as these were sufficient to restore protection against KA-induced epileptiform seizures almost completely, concomitant with a full rescue of DSE (but not DSI) in the hippocampus. Whereas the CB1 receptor on cortical glutamatergic neurons partially rescued the increased anxiety observed under aversive conditions upon CB1 receptor loss, freezing responses upon re-exposure to a conditioned stimulus were similar or even increased as compared with the freezing responses observed upon CB1 receptor loss. In the BLA, DSE was rescued, but showed a different kinetic as compared with a prolonged reduction of eEPSCs compared with the wild type.

Table 3.8: Summary of the phenotype of Glu-CB1-RS mice in the analyzed physiological measures and behavioral paradigms

Paradigm	phenotype Stop-CB1	phenotype Glu-CB1-RS	Rescue?
bodyweight	reduced	similar to Stop-CB1	no
refeeding after fasting	reduced food intake	normal food intake	yes
epilepsy	higher seizure susceptibility	almost normal seizure susceptibility	partial rescue (almost complete)
anxiety	higher anxiety	intermediate anxiety	partial rescue
fear extinction	sustained immobility response	more sustained immobility response	worsened phenotype
DSE in the hippocampus	no DSE	normal DSE	yes
DSE in the BLA	no DSE	DSE with different kinetic	yes, with modification

3.4 Discussion

3.4.1 Generation of the Stop-CB1 mouse line

3.4.1.1 Strategic considerations

To gain further insights into the modulatory function of the CB1 receptor in neuronal circuits, a conditional rescue mouse line was generated, allowing selective reactivation of CB1 receptor in specific cell populations. To this end, a gene targeting construct for the introduction of a loxP-flanked stop cassette into the CB1 receptor gene was previously cloned in the Lutz lab (Schneider, 2007). Two sites for the insertion of the stop cassette were conceivable, either the introduction of the cassette into an intron, or the insertion between the splice acceptor site of the protein encoding exon and the translational ATG start codon. Although several studies showed that the introduction of a loxP-flanked stop cassette into an intron is functional to generate a null allele (e.g. Wakita *et al.*, 1998; Hnasko *et al.*, 2006), one study described alternatively spliced transcripts using cryptic splice donor/acceptor sites in the stop cassette (Forlino *et al.*, 1999). The strategy to insert the stop cassette into the 5' UTR has been shown to efficiently block transcription (Dragatsis & Zeitlin, 2001; Balthasar *et al.*, 2005; Begriche *et al.*, 2011). Therefore, in the gene targeting construct used to generate the Stop-CB1 mouse line, the stop cassette was introduced in the protein encoding exon, 32 nucleotides upstream of the CB1 receptor translation start.

3.4.1.2 Functional silencing of the CB1 receptor

The Stop-CB1 mouse line was generated from the targeting construct by homologous recombination in ES cells. Correctly targeted ES cell clones were injected into mouse blastocysts, and the resulting chimeric mice were bred to achieve germ line transmission of the targeted allele.

Analysis of mRNA expression in homozygous Stop-CB1 mice revealed that transcription was not completely abolished, but reduced by 55%. As a very similar stop cassette consisting of an SV40 promoter, a Neo^R and three polyadenylation signals was previously shown to fully block transcription of the target gene (Balthasar *et al.*, 2005; Begriche *et al.*, 2011), the potency to stop transcription seems to depend on the insertion site. As the three polyadenylation signals in the stop cassette do not completely stop the transcription after the Neo^R CDS, a transcript is produced containing (at least part of) the CB1 coding sequence. However, the aim of the approach was to eliminate the presence of CB1 receptor protein, which was shown to be fully achieved. As the Neo^R coding sequence ends with a stop codon, only the first transcript is translated into the corresponding protein before the ribosome disassembles. As there is no additional ribosomal entry site, the longer transcript containing the sequence of the CB1 receptor did not lead to the production of any CB1 receptor protein. Thus, similar to CB1 receptor null mutants, the Stop-CB1 animals were shown to lack CB1

receptor protein. DSI and DSE were completely absent in the hippocampus of Stop-CB1 animals, as it was previously shown for CB1 receptor knock-out mice (Wilson *et al.*, 2001; Ohno-Shosaku *et al.*, 2002*b*), thus validating the absence of the receptor on presynaptic terminals. Also, postsynaptic depolarization in the BLA of Stop-CB1 mice did not produce a suppression of glutamatergic or GABAergic transmission. This absence of DSE and DSI in the Stop-CB1 mice clearly indicates the absence of CB1 receptor. Behavioral tests with the Stop-CB1 mouse line reproduced the phenotype as described for CB1 receptor null-mutant animals, namely reduced body weight, decreased food intake after fasting, increased susceptibility to epileptiform seizures, increased anxiety and impaired extinction of learned fear (Di Marzo *et al.*, 2001; Marsicano *et al.*, 2002, 2003; Cota *et al.*, 2003; Haller *et al.*, 2004*a*). Hence, from the phenotypical point of view, Stop-CB1 mice can also be considered as CB1 receptor null mutants.

3.4.1.3 Functional reactivation of the CB1 receptor

Cre recombinase-mediated excision of the stop cassette leaves a residual loxP site in the rescued allele. To assess whether the rescued CB1 receptor allele functions similarly to the wild-type allele, the Stop-CB1 mouse line was crossed to a Cre-deleter mouse line, leading to global rescue of the CB1 receptor. In the resulting CB1-RS mice, CB1 receptor was re-expressed in a pattern identical to that of wild-type mice. DSE and DSI in hippocampal slices of CB1-RS mice were also similar to that of wild-type mice. Animals with re-expression of the CB1 receptor throughout the whole organism did not differ from wild-type animals in any of the tested paradigms. Hence, the CB1-RS mouse line showed complete rescue of the mutant phenotype.

Region- or cell type-specific delivery of Cre recombinase into Stop-CB1 mice allowed detailed analysis of the physiological functions of the CB1 receptor in different brain areas and neuronal subpopulations. Brain region-specific rescue was shown to be functional, as infusion of AAV-Cre into the dentate gyrus was able to rescue CB1 receptor expression in the dorsal hippocampus. Cell type-specific rescue was achieved by crossing the Stop-CB1 mouse line to a mouse line expressing Cre recombinase in cortical glutamatergic neurons. In the resulting Glu-CB1-RS mice, the pattern of functional CB1 receptor protein represents the projections of cortical glutamatergic neurons and the CB1 receptor immunoreactivity colocalized with a marker for glutamatergic terminals, thus corroborating the cell-type specificity of the rescue.

3.4.1.4 Choice of appropriate control groups

To be able to further dissect the sufficient role of CB1 receptor in the different neuronal networks, the phenotypes of mice with cell type-specific rescue of CB1 receptor were compared with the phenotypes of Stop-CB1 and CB1-RS mice. By comparison to the Stop-CB1 mice, it can be assessed whether the phenotype of animals with region- or cell type-specific rescue differs from the

null-mutant phenotype and thus whether CB1 receptor plays a role in this specific circuitry in the investigated process. However, to analyze whether CB1 receptor in the specific circuitry is sufficient to restore the wild-type phenotype completely, CB1-RS mice were used as the appropriate control. Comparing three groups made the experimental design more complicated as it was not possible to generate them in a way that all analyzed animals were littermates. All experiments described in this thesis were carried out with Stop-CB1 and wild-type mice or Stop-CB1 and Glu-CB1-RS mice being littermates and CB1-RS mice from a separate breeding. As the mouse lines were generated from the same Stop-CB1 founder line with only few generations in between, the genetic background was very homogeneous.

3.4.2 Role of CB1 receptor on cortical glutamatergic neurons

The Glu-CB1-RS mouse line was used to determine in which brain functions CB1 receptor signaling on cortical glutamatergic neurons plays a sufficient role.

3.4.2.1 Effects on long-term and short-term metabolic regulation

Body weight (representing long-term metabolic regulation) of Glu-CB1-RS mice was similar to that of Stop-CB1 mice. Previous studies with mouse lines with specific deletions of the CB1 receptor showed that CB1 receptor in cortical glutamatergic neurons is *not necessary* for long-term metabolic regulation as these mice had no alterations in body weight (Bellocchio *et al.*, 2010). CaMKII-CB1$^{-/-}$ mice, which lack the CB1 receptor from both forebrain principal neurons (including projections to the hypothalamus and projections to the nucleus of the solitary tract) and partly from sympathetic neurons, had a lean phenotype (Quarta *et al.*, 2010), showing the necessary role of the CB1 receptor for long-term metabolic regulation in these neurons. In agreement with these data, we found that CB1 receptor functionality on cortical glutamatergic neurons alone was *not sufficient* to rescue the reduction in body weight observed upon complete CB1 receptor loss.

Modulation of glutamatergic transmission by the CB1 receptor was previously shown to be *necessary* for the acute orexigenic effect of endocannabinoid signaling (Bellocchio *et al.*, 2010). As short-term food intake after fasting was rescued to wild-type level in Glu-CB1-RS mice, CB1 receptor-dependent acute inhibition of cortical glutamatergic transmission is also *sufficient* for the fasting-induced hyperphagic effect of cannabinoids.

This discrepancy that CB1 receptor signaling on cortical glutamatergic neurons was not sufficient for long-term energy balance regulation, but was sufficient for acute feeding regulation is in good agreement with the major role of hypothalamic circuits in the regulation of long-term energy balance and a key role of cortical influences in acute feeding challenges (Berthoud, 2007), especially as in these acute challenges, processes related to stress and reward play an important role.

3.4.2.2 Partial rescue of anxiety

Behavior of Glu-CB1-RS mice did not differ from CB1-RS mice in any of the anxiety measures in the tested paradigms (EPM, LD test) and had a tendency or was significantly different from the Stop-CB1 mice in time spent in the open arms of the EPM and entries into the lit compartment in the LD test, respectively. However, looking at open-arm entries in the EPM and at time spent in the lit compartment of the LD box, the phenotype of Glu-CB1-RS animals was intermediate between CB1-RS and Stop-CB1, but did not differ significantly from either group. Thus, rescue of the CB1 receptor on cortical glutamatergic neurons was not completely sufficient to restore the wild-type phenotype, but CB1 receptor-dependent inhibition of cortical glutamate release was proven to play a major role in the complex response to a novel anxiogenic environment.

Previous studies showed the necessary role of CB1 receptor-mediated modulation of cortical glutamatergic transmission for normal exploration, impulsivity and novelty seeking (Jacob *et al.*, 2009; Lafenêtre *et al.*, 2009; Häring *et al.*, 2011), paradigms that are related to anxiety, but for which the underlying mechanisms are likely to be different. In a recent study, Aparisi Rey *et al.* (accepted) showed the necessary role of the CB1 receptor on cortical glutamatergic terminals to mediate the anxiolytic effect of low doses of cannabinoids, as systemic injection of low dose of a CB1 receptor agonist (CP55,940) failed to induce an anxiolytic effect in Glu-CB1$^{-/-}$ animals. However, no anxiogenic phenotype for Glu-CB1$^{-/-}$ animals was observed on the EPM upon vehicle injection. Similarly, another study with Glu-CB1$^{-/-}$ mice described only a trend towards increased anxiety on the EPM (Dubreucq *et al.*, 2012). The experiments in these studies were performed under low aversive conditions to avoid well-characterized alterations of the basal state of the ECS (Haller *et al.*, 2004*a*; Kamprath *et al.*, 2009; Jacob *et al.*, 2009; Dubreucq *et al.*, 2012). For the current study, more aversive experimental conditions were chosen to induce activation of the ECS.

In the Glu-CB1-RS mice, CB1 receptor expression was rescued in glutamatergic neurons in several brain regions, which further complicated the interpretation of the partial rescue of the anxiety phenotype. A region-dependent role of a modulation of glutamatergic signaling (either by CB1 receptor activation or by direct stimulation of excitatory signaling) in the regulation of anxiety is emphasized by two recent studies (Rubino *et al.*, 2008*a*; Yizhar *et al.*, 2011). One of these studies injected the CB1 receptor agonist Δ^9-THC in low doses (Rubino *et al.*, 2008*a*), thus potentially activating CB1 receptor preferentially on glutamatergic terminals (Aparisi Rey *et al.*, accepted). In the second study, the excitatory-inhibitory (E/I) balance was elevated with an optogenetic approach (Yizhar *et al.*, 2011). In these studies, anxiogenic or anxiolytic effects on the EPM not only depended on the dose of Δ^9-THC injected (Rubino *et al.*, 2008*a*), but also arose dependent on whether manipulation was in the BLA, hippocampus, cingulate PFC, prelimbic PFC, or infralimbic PFC. Despite

their diverse approaches, these studies emphasized the different outcomes of manipulating activity of specific neuronal subpopulations and brain regions, even between different subregions within the PFC. Since in the Glu-CB1-RS, the CB1 receptor was rescued in glutamatergic neurons of regions including the BLA, hippocampus and the different subregions of the PFC, the overall phenotype of these animals probably results from a mixture of anxiogenic and anxiolytic effects in the different regions. As this CB1 receptor-mediated reduction of glutamatergic transmission in cortical regions was largely sufficient to rescue the increased anxiety observed upon complete CB1 receptor loss, the decreased E/I balance in these circuits seems to reestablish a balance closer to the wild-type situation. The Stop-CB1 mouse line in combination with stereotactic injection of AAV expressing Cre recombinase under the control of cell type-specific promoters will be a valuable tool to further dissect the role of the CB1 receptor in these neuronal subcircuits. However, CB1 receptor-mediated modulation may be needed on other components of anxiety-related neuronal circuitry to achieve a complete rescue of the anxiety phenotype. Candidates include subcortical inputs that were recently shown to also express the CB1 receptor (Häring *et al.*, in revision) and GABAergic signaling.

3.4.2.3 Seizure protection and synaptic transmission in the hippocampus

Wild-type levels of protection against KA-induced epileptiform seizures were largely reconstituted upon rescue of CB1 receptor on cortical glutamatergic neurons. Previously, loss-of-function approaches showed the *necessary* role of CB1 receptor for protection against excitotoxic seizures in glutamatergic terminals of the hippocampus (Monory *et al.*, 2006). In epileptic human patients, CB1 receptor is specifically down-regulated on glutamatergic, but not on GABAergic axon terminals in the hippocampus, underlining the importance of the preclinical data (Ludányi *et al.*, 2008). In the chronic phase of pilocarpine-induced status epilepticus, CB1 receptor was redistributed with upregulation on glutamatergic and downregulation on GABAergic neurons, maybe serving as a compensatory mechanism for the induced hyperexcitable state (Falenski *et al.*, 2009; Bhaskaran & Smith, 2010*a*). In line with these findings, viral overexpression of CB1 receptor in hippocampal glutamatergic neurons led to increased seizure protection (Guggenhuber *et al.*, 2010). Thus, our findings now complete the picture by showing that endogenous levels of CB1 receptor-mediated reduction of excitatory signaling is largely *sufficient* for protection against excitotoxic seizures.

These findings are in good agreement with the findings on synaptic transmission in the underlying brain region. In the hippocampus, CB1 receptor-mediated retrograde regulation of GABAergic transmission was completely absent, whereas retrograde regulation of glutamatergic transmission was fully rescued.

3.4.2.4 Fear extinction and synaptic transmission in the BLA

The delayed fear extinction observed upon complete CB1 receptor loss was not rescued in the Glu-CB1-RS. Instead, Glu-CB1-RS mice showed a similarly high or even further increased freezing response (dependent on the extinction day) when compared with Stop-CB1 animals. The initial freezing response to the CS presentation did not differ between the groups (CB1-RS, Stop-CB1, Glu-CB1-RS), proving that the experimental conditions were chosen in a way that the groups had similar fear acquisition and expression. Thus, extinction behavior could be compared from a similar starting point. The lack of a phenotype in fear acquisition and expression is in good agreement with previous studies using similar experimental conditions (Marsicano *et al.*, 2002; Kamprath *et al.*, 2006; Plendl & Wotjak, 2010). Like it was found in a previous study (Plendl & Wotjak, 2010), the CB1 receptor-mediated effect was selective for short-term (within-session) rather than long-term (between-session) extinction.

CB1 receptor on cortical glutamatergic neurons was shown to be necessary for the fear alleviating effect of endocannabinoids (Kamprath *et al.*, 2009; Dubreucq *et al.*, 2012). The present study revealed that rescue of CB1 receptor on glutamatergic neurons was not sufficient to restore the wild-type reduction of conditioned freezing to the CS, suggesting that additional neuronal subpopulations or regions with CB1 receptor expression are required to re-establish a functional fear (extinction) circuit. One possibility is that CB1 receptor-driven modulation of GABA release is necessary to restore normal extinction. CB1 receptor is expressed on presynaptic terminals of GABAergic, CCK-positive interneurons in the BLA (Marsicano & Lutz, 1999; McDonald & Mascagni, 2001; Katona *et al.*, 2001), and there is evidence that interactions between the ECS and CCK neurotransmitter systems play an important role in the extinction of conditioned fear (Chhatwal *et al.*, 2009). Recently, it was shown that loss of the CB1 receptor on GABAergic synapses did not change extinction of conditioned freezing (Dubreucq *et al.*, 2012), but it might be that CB1 receptor is required on both cortical glutamatergic and forebrain GABAergic neurons for wild-type fear extinction behavior. A second possibility is that a subcortical contribution of CB1 receptor function is needed to complement cortical glutamatergic CB1 receptor function. Mice lacking CB1 receptor on dopamine D1 receptor-expressing neurons, which are found mostly in the striatum, exhibited attenuated within session extinction (Terzian *et al.*, 2011). Although in this mouse line, the CB1 receptor was not only deleted from a majority of striatal neurons, but also from low CB1 receptor-expressing neurons of layer VI of the neocortex (Monory *et al.*, 2007), these results might point to an important role of subcortical CB1 receptor-driven modulation of neurotransmitter release for fear extinction. Furthermore, fine-tuned regulation of glutamatergic thalamic projections also controls fear extinction (Lee *et al.*, 2012), and it was recently shown that CB1 receptor is also expressed in subcortical areas projecting to cortical areas, including the amygdala (Häring *et al.,* 2012, in revision).

The BLA is one of the most important brain structures for conditioned fear, as it associates shock and sensory inputs and is responsible for extinction acquisition (Quirk & Mueller, 2008). In Glu-CB1-RS mice, the CB1 receptor is rescued on cortical glutamatergic terminals, including those projecting to the BLA, but also those projecting to various subregions of the PFC, a region also known to exhibit important functions for extinction of conditioned fear (Herry *et al.*, 2010; Pape & Paré, 2010; Sotres-Bayon & Quirk, 2010; Lin *et al.*, 2010). The PFC exhibits bidirectional control over conditioned fear responses, in which the PL area was shown to excite amygdala output, thus increasing freezing to the CS, and in which the IL area was shown to inhibit amygdala output, thus decreasing freezing to the CS (Vidal-Gonzalez *et al.*, 2006; Sierra-Mercado *et al.*, 2011). Elevating the E/I balance in both IL and PL PFC with an optogenetic approach reduced conditioned freezing, whereas a decreased E/I balance increased conditioned freezing (Yizhar *et al.*, 2011). Thus, the differential CB1 receptor-driven modulation of cortical inputs to the BLA might also account for the lack of freezing reduction in the Glu-CB1-RS mice.

In the BLA of mice with cortical glutamatergic rescue of CB1 receptor, DSI was completely absent, corroborating the cell-type specificity of the rescue. DSE was present, but displayed a much extended time course as compared with CB1-RS animals. This effect was shown to be BLA specific, as glutamatergic CB1 receptor rescue fully restored DSE in hippocampal CA1. Furthermore, DSE could be blocked by the CB1 receptor antagonist AM251, proving that it was mediated by CB1 receptor. This modified synaptic transmission is probably correlated with the deteriorated extinction learning. Endocannabinoid levels were recently shown to determine the time course of the endocannabinoid-mediated retrograde synaptic transmission, as pharmacological blockade (Pan *et al.*, 2009) and genetic deletion (Pan *et al.*, 2011) of MAGL, the primary enzyme degrading 2-AG, resulted in changes in endocannabinoid-mediated suppression of synaptic transmission in various types of neurons *in vitro* (decreased magnitude and extended time course). Thus, it could be hypothesized that selective rescue of CB1 receptor on glutamatergic terminals induces alterations in endocannabinoid signaling (e.g. by affecting the enzymatic machinery for endocannabinoid production and degradation) and thereby produces the observed modified synaptic transmission and the lack of extinction.

3.4.3 Conclusions and outlook

The use of the Cre/loxP system to re-express genes in specific neuronal subpopulations under the endogenous regulatory elements is a very powerful tool to investigate whether the gene product is not only *necessary*, but also *sufficient* to restore the full functionality of the GOI in a specific circuit. Employing this approach, we have shown that CB1 receptor function in cortical glutamatergic neurons is largely sufficient to regulate feeding response, anxiety and susceptibility to chemically-induced epileptiform seizures. Interestingly, long-term metabolic regulation and appropriate fear

extinction appear to require additional cell types expressing the CB1 receptor. Our experiments constitute an essential step towards the dissection of CB1 receptor function in the framework of neuronal circuits.

The Stop-CB1 mouse line was also used to generate a mouse line with rescue of the CB1 receptor on GABAergic neurons. These mice are currently tested in the paradigms analyzed in this thesis and will complement the findings on the sufficient role of CB1 receptor signaling in glutamatergic and GABAergic neuronal subpopulations. Furthermore, Glu/GABA-CB1-RS mice with CB1 receptor rescue in both cortical glutamatergic and forebrain GABAergic neurons are presently generated to analyze the sufficient role of synergistic modulation of glutamatergic and GABAergic transmission, especially in extinction of conditioned fear. These experiments will be complemented with stereotactic injection of AAV expressing Cre recombinase under the control of cell type-specific promoters, into the candidate brain regions discussed above. These AAV experiments will further address the question in which brain regions or neuronal subpopulations CB1 receptor signaling is sufficient to fully restore wild-type levels of innate anxiety or extinction of conditioned fear.

In addition to dissecting the sufficient role of CB1 receptor to modulate excitatory and inhibitory transmission, the newly generated Stop-CB1 mouse line in combination with transgenic or viral delivery of Cre recombinase form a genetic toolkit which can be used to investigate a broad range of questions. These might involve the investigation of the sufficient contribution peripheral CB1 receptor to the regulation of energy balance or the dissection of the sufficient role of CB1 receptor on astrocytes. Furthermore, this new mouse line will be very useful for biochemical work investigating cell-type specific signaling.

4 Molecular structure of the mouse *Cnr1* gene

4.1 Introduction

Although the great majority of the studies investigating the function of the CB1 receptor has been carried out in mice, the molecular structure and regulation of the mouse *Cnr1* gene (encoding the CB1 receptor) has remained poorly characterized. The structure of the human *CNR1* gene is better understood, as several studies analyzed the exon-intron structure, splice variants and promoter regions (e.g. Shire *et al.*, 1995; Rinaldi-Carmona *et al.*, 1996; Zhang *et al.*, 2004; Ryberg *et al.*, 2005; Börner *et al.*, 2008; Blázquez *et al.*, 2011; Nicoll *et al.*, 2012). Allelic variations in the human *CNR1* gene were associated with several disorders, including addiction (Zhang *et al.*, 2004; Chen *et al.*, 2008; Haughey *et al.*, 2008; Benyamina *et al.*, 2011; Okahisa *et al.*, 2011), eating and metabolic disorders (Benzinou *et al.*, 2008; Lieb *et al.*, 2009; Monteleone *et al.*, 2009; Schleinitz *et al.*, 2010; Frost *et al.*, 2010), and schizophrenia (Zammit *et al.*, 2007; Chavarría-Siles *et al.*, 2008; Ho *et al.*, 2011). Thus, further characterization of the mouse *Cnr1* gene could add to a better understanding of regulatory processes and allelic variations contributing to pathological phenotypes observed in the rodent model. This introductory section gives a short overview of the current knowledge of the *CNR1*/*Cnr1* genes of human and mouse.

4.1.1 Identification of human, rat and mouse *CNR1*/*Cnr1* genes

The CB1 receptor cDNA was first identified from a rat brain library in 1990 (Matsuda *et al.*, 1990), followed shortly after by the identification of the cDNA encoding human (Gérard *et al.*, 1991) and mouse (Chakrabarti *et al.*, 1995) CB1 receptors. The genes coding for human, rat, and mouse CB1 receptors are found on chromosomes 6, 5, and 4, respectively. The human, rat and mouse receptors are highly conserved: human and rat share 93% identity at the nucleic acid level (97% at the amino acid level); the human and mouse clones have 90% nucleic acid identity (97% amino acid identity); and the mouse and rat clones have 95% nucleic acid identity (99.5% amino acid identity) (Onaivi *et al.*, 2002; Abood, 2005). In a molecular phylogenetic analysis, the sequence diversity in 62 examined species varied from 0.41% to 27% (Murphy *et al.*, 2001).

4.1.2 Exon-intron structure and promoter regions of the human *CNR1* gene

4.1.2.1 Splice variants diverging in the N-terminus

For the human CB1 (hCB1) receptor, two splice variants that affect the amino-terminal (N-terminal) part of the protein were identified, namely hCB1a (Shire *et al.*, 1995; Rinaldi-Carmona *et al.*, 1996) and hCB1b (Ryberg *et al.*, 2005; Xiao *et al.*, 2008). The first variant, hCB1a is a truncated

version of hCB1, resulting from the excision of a 167 bp intron from the 5' extremity of the CDS. This specific splicing event generates an altered N-terminal amino acid sequence truncated by 61 amino acid residues with a substitution of the first 89 amino acids for a different 28-residue sequence due to a frame shift and the use of a different start codon (Shire *et al.*, 1995) (Figure 4.1). The second variant, hCB1b results from the excision of a 99 bp intron with an in-frame deletion of 33 amino acids of the hCB1 receptor amino terminus (Ryberg *et al.*, 2005) (Figure 4.1).

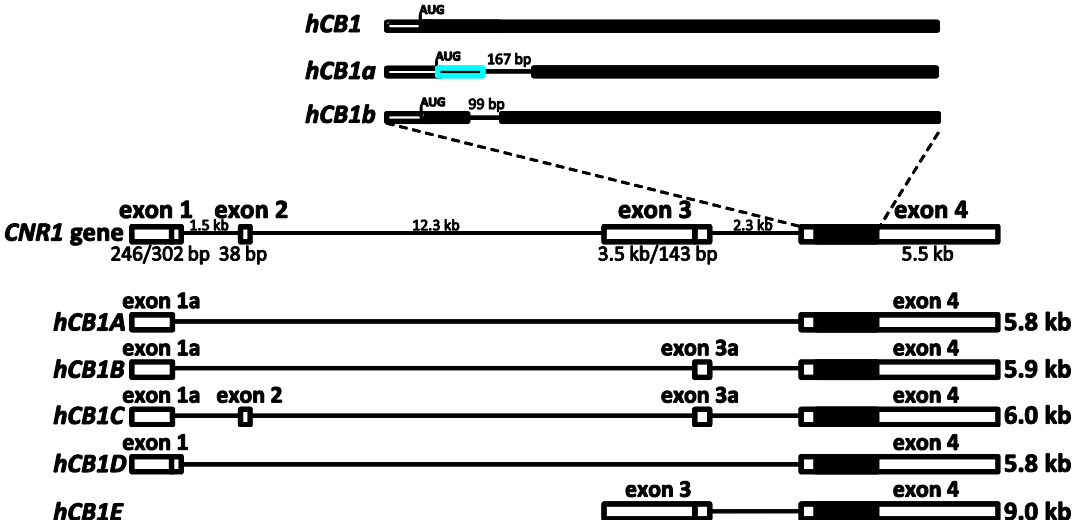

Figure 4.1: Schematic structure of the exon-intron structure of the human *CNR1* gene and characterized splice variants. The biggest exon (exon 4; exons are displayed by boxes) contains the protein coding sequence (black box). In the 5' extremity of the coding sequence, two introns were identified. The resulting transcripts have a deletion of 167 bp for hCB1a and of 99 bp for hCB1b. For hCB1a, a different start codon is used leading to a frame shift for the first 28 amino acids (indicated by blue frame). At least three more exons (exon 1, 2 and 3) are located 5' of the protein encoding exon. By alternative splicing, five different mRNA variants were identified, termed *CB1A-E* (adapted from Shire *et al.*, 1995; Zhang *et al.*, 2004; Ryberg *et al.*, 2005).

Both hCB1a and hCB1b mRNAs are expressed in several tissues including brain (Shire *et al.*, 1995; Ryberg *et al.*, 2005; Xiao *et al.*, 2008). The original reports described an abundance of 1% to 20% of the splice variant hCB1a as compared with hCB1 by reverse transcription-polymerase chain reaction (RT-PCR) analysis. However, these percentages were assessed by semi-quantitative analysis and seem to overestimate the real percentages due to overexposure of the autoradiograms (Howlett *et al.*, 2002). Like hCB1, the splice variants are located in the membrane, and they show normal trafficking (Straiker *et al.*, 2012). Pharmacological properties of the splice variants were investigated in several studies, but contradictory results were found. For example, Ryberg *et al.* (2005) described that 2-AG acts as an inverse agonist on hCB1a and hCB1b, while Xiao *et al.* (2008) and Straiker *et al.* (2012) described that 2-AG acts as an efficacious agonist. These contradictory data might be caused by the different cell types, homologous or heterologous expression systems and/or the different stimulation protocols used. Interestingly, Straiker *et al.* (2012) found that upon expression in autaptic neurons (derived from CB1 receptor-deficient mice), hCB1 rescued a typical endocannabinoid

signaling (i.e. DSE) much less efficient than the rat CB1 receptor, whereas the human splice variants hCB1a and hCB1b both fully rescued DSE. The physiological significance of these very low abundant human CB1 receptor splice variants still needs to be addressed, but the different affinity for cannabinoid ligands and the different signaling properties add yet another degree of complexity to the analysis of CB1 receptor function.

4.1.2.2 Splice variants differing in the 5' UTR

In addition to the protein encoding exon (exon 4), three additional exons were identified, which are assembled to transcript variants with different 5' UTRs (Zhang *et al.*, 2004). The sizes of the exons upstream of the protein encoding exon are 302 bp for exon 1 (or 246 bp if an alternative splice donor site is used), 38 bp for exon 2 and 3.5 kb for exon 3 (or 143 bp if an alternative splice acceptor site is used) (Figure 4.1). Each of the described splice sites contains the consensus GT-AG splice donor/acceptor motifs (Zhang *et al.*, 2004). From the genomic assembly, the authors identified five *CB1*/*Cnr1* mRNA transcript variants (*hCB1A*, *hCB1B*, *hCB1C*, *hCB1D* and *hCB1E*). Semi-quantitative analysis of fluorescent densities after RT-PCR revealed that mRNA that contains exon 3 has a much lower abundance than mRNA that contains exon 1 (Zhang *et al.*, 2004). Ace View, a database providing a non-redundant sequence representation of all available mRNA sequences (mRNAs from GenBank or RefSeq, and single pass cDNA sequences from dbEST and Trace, (Thierry-Mieg & Thierry-Mieg, 2006), http://www.ncbi.nlm.nih.gov/IEB/Research/Acembly), also identified all of the transcripts described by Zhang *et al.* (2004), and even suggests the existence of more transcript variants (release Human 2010).

4.1.2.3 Promoter and regulatory regions of the human *CNR1* gene

Promoter regions regulating the expression of a specific mRNA transcript are located upstream of the first exon used. For the human *CNR1* gene, promoter regions would thus be expected upstream of exon 1 (*hCB1A-D*) and the long variant of exon 3 (*hCB1E*).

In a neuronal cell line, promoter regions between -2 kb and -1 kb upstream of *CNR1* exon 1 reduced transcription of a reporter gene, whereas regions upstream of -2 kb and regions downstream of -1 kb enhanced basal transcription (Zhang *et al.*, 2004). This analysis was confirmed and refined in a recent study in striatal neuroblasts (Blázquez *et al.*, 2011). Here, the sequence upstream of exon 1 comprising -1.1 kb to -0.9 kb was shown to contain negative regulatory elements, while the sequence comprising -0.9 kb to -0.65 kb was shown to contain enhancer elements, as deletion of the respective region from a 3 kb sequence upstream of exon 1 increased or decreased activity in a reporter assay, respectively (Blázquez *et al.*, 2011). In immune cells, two promoter regions (-3 kb to -2.5 kb and -2 kb to -1.6 kb upstream of exon 1) were shown to reduce transcription, while a more proximal region (-0.65 kb to -0.56 kb) rather enhanced transcription (Börner *et al.*,

2008). This suggests that the distal promoter sequence upstream of approximately -2 kb had opposite effects on transcription of the *CNR1* gene in immune and neuronal cells, indicating different control mechanisms in cell types derived from different tissues (Börner *et al.*, 2008). Regulatory sequences upstream of exon 3 yield in a lower transcription than regulatory sequences upstream of exon 1, consistent with the higher abundance of mRNA transcripts containing exon 1 sequences (Zhang *et al.*, 2004).

Recently, a *cis*-regulatory region termed ECR1 was identified in the second intron of the *CNR1* gene (Nicoll *et al.*, 2012). The authors found that the region contains a polymorphic site (rs9444584-C/T). They showed that the C variant is active in hypothalamus and dorsal root ganglia-derived cells, where it is responsive to MAPK signaling, but that it is inactive in the hippocampus; whereas the T variant is a MAPK-inducible enhancer in hippocampal cells. As the single nucleotide polymorphism (SNP) is in strong linkage disequilibrium with two other SNPs that are associated with several disorders, including addiction (Haughey *et al.*, 2008), obesity (Benzinou *et al.*, 2008) and reduced fronto-temporal white matter volumes upon *Cannabis* misuse in schizophrenia patients (Ho *et al.*, 2011), these findings underline the importance also to improve the characterization of regulatory, untranslated and untranscribed regions for a better understanding of *CNR1* dysregulation in pathological conditions.

4.1.3 Exon-intron structure of the mouse *Cnr1* gene

To date, very little is known about the gene structure of the mouse *Cnr1* gene. The classical splice donor/acceptor sequences present in the CDS of the human *CNR1* gene are not present at the same positions in the mouse or rat *Cnr1* genes, which led to the conclusion that the N-terminal splice variants could be unique for the human CB1 receptor (Howlett *et al.*, 2002; Xiao *et al.*, 2008).

Regarding the 5' UTR, several studies and databases describe different findings about the *Cnr1* gene structure. In the search for ideal positions to place genetic modifications to create a conditional knock-out mouse for the CB1 receptor, Marsicano (2001) identified the existence of an approximately 2 kb intron sequence from position -2102 to -62 upstream of the ATG of the mouse CB1 (mCB1) receptor. McCaw *et al.* (2004) described that the mCB1 receptor mRNA is encoded by two exons separated by an 18.4 kb intron. By adding an RNA linker to previously uncapped mRNA transcripts (5' RNA ligase-mediated rapid amplification of cDNA ends, 5' RLM-RACE), the authors identified multiple transcription start sites within a GC-rich promoter region upstream of the first exon. The most 5' transcription start site identified in this study was about 500 bp upstream of the splice donor of the first exon. The 18393 bp intron is also described in the NCBI gene database (http://www.ncbi.nlm.nih.gov/, Gene ID: 12801) and in the Ensembl Genome Browser (Flicek *et al.*,

2011; http://www.ensembl.org/) (Cnr1-001, ENSMUST00000057188), separating a 527 bp exon and a 5280 bp exon containing the CB1 receptor CDS (Figure 4.2). In the Ensembl Genome Browser, an additional protein coding transcript is described, consisting of two exons of 493 bp and 5268 bp (the longer one containing the CDS) separated by a 16857 bp intron (Cnr1-003, ENSMUST00000084736). A third splice variant is described in Ensembl (Cnr1-002, ENSMUST00000133462) as a processed transcript that does not code for a protein. This Cnr1-002 transcript consists of 3 exons of 566 bp, 86 bp and 105 bp separated by two introns of 1450 and 8517 bp length. The 3' splice donor site of the first exon is similar to that of the first exon of Cnr1-001, but transcription starts 39 bp 5' of the transcription start described for the first exon of Cnr-001. As this processed transcript has only one reference, it might be that it is only a partial transcript.

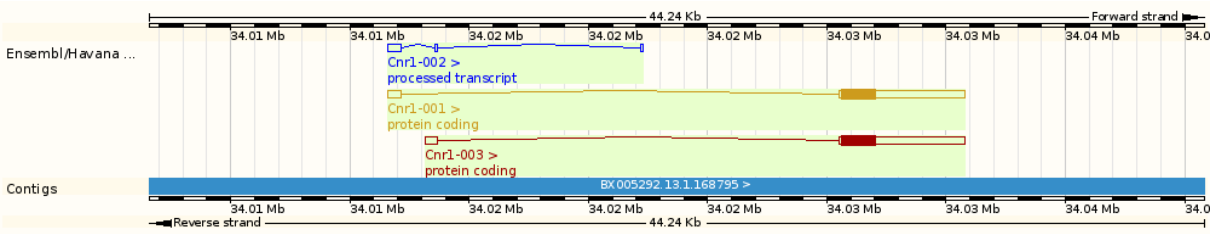

Figure 4.2: Ensembl genome browser describes three splice variants for the mouse *Cnr1* gene.
Cnr1-001 (shown in yellow) and Cnr1-003 (red) have the same protein encoding exon, but have introns of different length (18393 bp and 16857 bp, respectively) and different first exons. An additional processed transcript Cnr-002 (blue) is described to be non-protein coding. Boxes represent exons, filled boxes represent coding sequences, and lines represent introns.

To improve the understanding of the structure of the mouse *Cnr1* gene locus and its regulation, one aim of this thesis was to analyze the exon-intron structure of the mouse *Cnr1* gene.

4.2 Material and Methods

4.2.1 Animals

For characterization of the mouse *Cnr1* gene, C57BL/6N animals were used. To analyze whether the transcripts coding for the CB1 receptor protein differ between different brain regions and neuronal cell types, mutant lines with cortical glutamatergic deletion of CB1 receptor (Glu-CB1$^{-/-}$) and deletion of CB1 receptor from cortical and striatal GABAergic neurons (GABA-CB1$^{-/-}$) were used. Respective Cre-negative littermates were used as control mice. Generation, breeding and genotyping of these lines were previously described (Monory *et al.*, 2006; Massa *et al.*, 2010).

4.2.2 Tissue preparation

Animals were sacrificed by decapitation under deep isoflurane anesthesia. Brain regions of interest were quickly isolated on ice under a binocular microscope, snap-frozen on dry-ice and stored at -80°C for RNA isolation.

To obtain punches, whole brains were isolated, snap-frozen on dry-ice and stored at -80°C. After mounting on Tissue Tek (Polysciences, Warrington, PA, USA), coronal sections were cut on a cryostat Microtome HM560 (Microm, Walldorf, Germany). Brains were trimmed until the area of interest was reached. To determine the exact location (distance from bregma according to Paxinos & Franklin, 2008), 15 µm sections were stained with toluidine blue. Tissue punches with a 0.8 – 2.0 mm diameter (see Table 4.1) were taken with sample corers (Fine Science Tools, Heidelberg, Germany) from infralimbic cortex, caudate putamen, BLA, dorsal hippocampus and cerebellum and were stored at -80°C until RNA extraction.

Table 4.1: Coordinates of isolated brain punches

Brain region	Distance from bregma			Diameter (mm)	Depth (mm)
	AP	ML	DV		
Infralimbic cortex	+1.94	±0.00	+3.10	1.0	0.5
Caudate putamen	+1.10	±1.80	+3.10	1.0	1.0
BLA	-0.82	±2.80	+4.70	0.8	1.2
Dorsal hippocampus	-1.52	±1.40	+1.75	1.0	1.0
Cerebellum	-5.80	±1.20	+2.10	2.0	2.0

4.2.3 RNA isolation and cDNA synthesis

Frozen tissue samples were transferred to tubes from a Precellys ceramic kit (ceramic bead diameter 1.4 mm, 2 ml tube for bigger tissue parts, 0.5 ml tube for punches) containing homogenization buffer RLT from the RNeasy Mini-Kit (Qiagen, Hilden, Germany; ß-Mercaptoethanol

added, Carl Roth, Karlsruhe, Germany) and tissue was homogenized with a Precellys 24 (Peqlab, Erlangen, Germany) at 6000 rpm for 20 s. Total RNA was isolated using the RNeasy Mini-Kit (Qiagen, Hilden, Germany) including the on-column DNA digestion step (RNase-Free DNase kit, Qiagen, Hilden, Germany). Total RNA was reverse-transcribed using the High Capacity cDNA Reverse Transcription Kit with random primer hexamers (Applied Biosystems, Carlsbad, CA).

4.2.4 Identification of novel transcripts

4.2.4.1 PCR on cDNA transcripts

To identify novel splice junctions, primer pairs flanking putative introns were designed using Vector NTI software (Invitrogen, Darmstadt, Germany). Information from the literature and consensus splice donor and acceptor sites was used as a basis for primer design (primers are listed in Table 4.2). Putative exon junctions were PCR amplified with Phusion High-Fidelity DNA Polymerase (New England Biolabs, Frankfurt, Germany) on cDNA templates. PCR conditions were 95°C for 5 min, followed by 30 cycles of 95°C for 30 s, 56°C for 30 s, 72°C for 90 s, followed by a final extension of 72°C for 5 min.

Table 4.2: PCR primers for exon junction overlapping PCR on cDNA.
Positions are indicated relative to the coding region start calculated from the genomic sequence.

Primer	Sequence	Direction	Position (bp)
NH2term fwd	GGTTATGAAGTCGATCTTAGACGG	forward	-4 to +20
NH2term rev	TCCCCACACTGGATGTTGT	reverse	+203 to +284
Ex4CDS	AAGGTGGTATCTGCAAGGCC	reverse	+19 to +38
Endex1	CAGACCGACTGACTTACTGACC	forward	-18755 to -18734
Ex2beg	GTTGAAAGATACCTCTCTGGGTCC	forward	-17547 to -17524
Havex2	TCCACACAGGAACAGAATGC	forward	-17149 to -17130
Ex3a	TCCTGGAGTCCTTCAGACATGG	forward	-5564 to -5542
Ex3beg1	ACTGAGGGAACTAGGTCTGAGC	forward	-2210 to -2190

4.2.4.2 5' RLM-RACE

Putative 5' ends of transcripts were analyzed using the GeneRacer Kit (Invitrogen, Darmstadt, Germany) for full-length RLM-RACE according to the manufacturer's instructions. Briefly, total RNA was treated with calf intestinal phosphatase to remove the 5' phosphate from all RNA molecules that did not have a 7-methylguanosine cap. The RNA was then treated with tobacco acid pyrophosphatase to remove the cap from the 5' end of capped mRNA. This exposed the 5' phosphate to which an RNA GeneRacer Oligo (5'-CGACUGGAGC ACGAGGACAC UGACAUGGAC UGAAGGAGUA GAAA-3') was ligated using T4 RNA ligase. A cDNA template was generated from the RNA by reverse transcription using Superscript III Reverse Transcriptase and random primers. RNA was removed from the RNA-cDNA-duplex by RNaseH digestion to produce single-stranded cDNA. 5' ends were PCR-amplified with Phusion High-Fidelity DNA Polymerase (New England Biolabs, Frankfurt, Germany)

using first-strand cDNA as a template and an outer adapter forward primer and gene-specific reverse primers (Table 4.3) with a thermal cycling protocol for touchdown PCR (Table 4.4). The PCR product was purified using the NucleoSpin Extract II Kit (Macherey Nagel, Dueren, Germany). Purified PCR product was then used as a template for a second round of PCR using nested primers (Table 4.3). PCR conditions for the second round of amplification were 94°C for 5 min, followed by 19 cycles of 95°C for 30 s, 66°C for 30 s, 72°C for 90 s, followed by a final extension of 72°C for 5 min.

Table 4.3: PCR primers for 5' RLM-RACE

Primer	Sequence		Position (bp)
GeneRacer 5' Primer	CGACTGGAGCACGAGGACACTGA	fwd	1 - 23 in RNA GeneRacer Oligo
GeneRacer 5' Nested Primer	GGACACTGACATGGACTGAAGGAGTA	fwd	15 - 40 in RNA GeneRacer Oligo
RACE-Ex4 rev	GGTCTGTGGTGATGGTACGGAAGG	rev	+57 to +43
RACE-Ex4-nested rev	GAAGGTGGTATCTGCAAGGCCG	rev	+39 to +17
RACE-Ex3 rev	GCTCTGCCTCTTGCTCCCAAGC	rev	2 upstream of 3' splice donor Ex3
RACE-Ex3-nested rev	GAAAGTTCCACGAGGACCTCCC	rev	30 upstream of 3' splice donor Ex3
RACE-Ex3a rev	GGGAACCCATGTCTGAAGGACTCC	rev	60 upstream of 3' splice donor Ex 3a
RACE-Ex3a-nested rev	TCTGAAGGACTCCAGGAGCTCG	rev	71 upstream of 3' splice donor Ex3a
RACE-Ex2 rev	CCCCACAGATAATCAGTACCCGCG	rev	508 upstream of 3' splice donor Ex2
RACE-Ex2-nested rev	CTCTGAGCATGTGCATCTCCCC	rev	539 upstream of 3' splice donor Ex2
RACE-Ex1 rev	GCGATCGGTCAGTAAGTCAGTCGG	rev	273 upstream of 3' splice donor Ex1
RACE-Ex1-nested rev	GGTCAGTAAGTCAGTCGGTCTGCG	rev	279 upstream of 3' splice donor Ex1

Table 4.4: Cycling protocol for 5' RLM-RACE touchdown PCR

		4 cycles		4 cycles		24 cycles			
Temperature	95°C	95°C	72°C	95°C	70°C	95°C	68°C	72°C	72°C
Time	2 min	30 s	30 s	30 s	90 s	30 s	30 s	90 s	3 min

4.2.4.3 Subcloning and sequencing of PCR products

PCR-amplified DNA from RT-PCR or 5' RLM-RACE was separated on 1.5% (w/v) agarose gels and DNA bands were extracted using the NucleoSpin Extract II Kit (Macherey Nagel, Dueren, Germany). A-overhangs were added using a Taq-Polymerase (Promega, Madison, WI). PCR products with A-overhangs were cloned into a TOPO-TA vector according to the manufacturer's instructions (Invitrogen Darmstadt, Germany). The insert sequence of individual clones was determined by sequencing (Eurofins MWG Operon, Ebersberg, Germany). The intron and exon sequences and the 5' ends of the CB1 receptor transcripts were identified by Align Sequences Nucleotide BLAST (http://blast.ncbi.nlm.nih.gov/) comparing the sequences of cDNA clones with the genomic sequence of the *Cnr1* gene.

4.2.5 Cloning of mCB1a and mCB1b

Two separate PCRs were performed with Phusion High-Fidelity DNA Polymerase (New England Biolabs, Frankfurt, Germany) on hippocampal cDNA: one with the forward primer S21 binding upstream of the start codon and the reverse primer S18 (for mCB1a) or S20 (for mCB1b) overlapping the exon junction of mCB1a or mCB1b; and the second with the forward primer S5 (for mCB1a) or S11 (for mCB1b) overlapping the exon junction of mCB1a or mCB1b and the reverse primer S22 binding in the 3' UTR downstream of the stop codon (see Table 4.5). PCR conditions were 94°C for 5 min, followed by 32 cycles of 95°C for 30 s, 56°C for 30 s, 72°C for 90 s, followed by a final extension of 72°C for 5 min. The two PCR products each for mCB1a and mCB1b were loaded on a 1% agarose gel, DNA bands with a size of 180 bp and 1449 bp for mCB1a and of 163 bp and 1399 bp for mCB1b were excised and DNA content was extracted using the NucleoSpin Extract II Kit (Macherey Nagel, Dueren, Germany). The purified products of the first and second part were then used in a nested overlap-extension PCR with the primer pair S23-KpnI S24-NotI to amplify the complete sequences of mCB1a or mCB1b and add restriction endonuclease recognition sites for KpnI on the 5' end and NotI on the 3' end. PCR conditions were used as described above.

Table 4.5: PCR primers for cloning of mCB1a and mCB1b.
Added restriction sites are indicated in blue, non-complementary sequences are indicated in brown.

Primer	Sequence		Position / Function
S5	CGAAGATATCAAAGGAGACACA	fwd	overlaps splice junction mCB1a
S11	GCTCAAATGACATTCAGGAGAACG	fwd	overlaps splice junction mCB1b
S18	TGTTGGTTGTGTCTCCTTTGATAT	rev	overlaps splice junction mCB1a
S20	TTGTCCTCGTTCTCCTGAATGTCA	rev	overlaps splice junction mCB1b
S21	GGTTCCCTCCTGGCACCTCTTT	fwd	-62 to -40
S22	AGGATCGCCGAGCAACTGCA	rev	+1635 to +1655
S23-KpnI	ATATATGGTACCTCAGTCACGTTGAGCCTGGC	fwd	-39 to -19
S24-NotI	ATATATGCGGCCGCCCGATGAGACAACAGACTTCTA	rev	+1479 to +1501
J1-BamHI	GCGGATCCACCATGGCATACCCATATGATGTCCCCG ACTACGCGAAGTCGATCTTAGACGGCCTTG	fwd	adds Kozak sequence and HA11-tag to mCB1/mCB1a/mCB1b; +4 to +25
J2-NotI	GGCGCGGCCGCTCACAGAGCCTCGGCAGA	rev	+1405 to + 1422

PCR products were then digested with the restriction enzymes KpnI and NotI (New England Biolabs, Frankfurt, Germany) and the digested products were purified by gel extraction with the NucleoSpin Extract II Kit (Macherey Nagel, Dueren, Germany). The vector pcDNA3 was also digested with KpnI and NotI, dephosphorylated with Antarctic phosphatase (New England Biolabs, Frankfurt, Germany) according to the manufacturer's instructions. Vector backbone and insert were then ligated with T4 DNA ligase (New England Biolabs, Frankfurt, Germany) according to the manufacturer's instructions. Ligated DNA was transfected into chemically competent *DH5α E. coli,* positive clones were picked and expanded (Sambrook *et al.*, 2001). Plasmid DNA was purified with

the NucleoSpin Plasmid Kit (Macherey Nagel, Dueren, Germany). To verify correct cloning, the plasmids were sequenced (Eurofins MWG Operon, Ebersberg, Germany).

A hemagglutinin (HA)-epitope tag was added to each splice variant via PCR, and these labeled constructs were then used to generate stably expressing cell lines. Primers used for this PCR amplification were designed using ApE cDNA plasmid software (http://biologylabs.utah.edu/jorgensen/wayned/ape/). The 5' primer (J1-BamHI, see Table 4.5) consisted of a BamHI restriction site followed by a strong Kozak consensus sequence in frame with the HA11 epitope, and the common beginning of the three variants. The antisense primer (J2-NotI, see Table 4.5) contained a NotI restriction site directly after the stop codon. The PCR products for the three mCB1 variants were then digested with BamHI and NotI and subcloned into both CAG and pcDNA3 vectors. The constructs were verified by sequencing.

4.2.6 QPCR

Quantification of cDNA was performed with an ABI 7300 real time PCR cycler (Applied Biosystems, Carlsbad, CA). Reactions were performed in duplicates.

4.2.6.1 TaqMan

To quantify the splice variants mCB1a and mCB1b, fluorogenic 5' nuclease chemistry (Taqman) was used. The cDNA was amplified using commercial FAM dye-labeled TaqMan assays (Applied Biosystems, Carlsbad, CA) for mouse cannabinoid receptor 1 (Cnr1; Mm00432621_s1) and mouse glucuronidase beta (Gusb; Mm00446953_m1). For mCB1a and mCB1b, custom Taqman assays were designed using Primer Express Software (Applied Biosystems, Carlsbad, CA; see Table 4.6) and ordered from Applied Biosystems (Carlsbad, CA).

Table 4.6: Custom Taqman assays for mCB1a and mCB1b.
Different colors indicate annealing to different exons.

	Forward primer	Reverse primer	FAM-labelled reporter
mCB1a	GATACCACCTTCCGTACCATCAC	AATGTTGGTTGTGTCTCCTTTGATAT	TCCTCTACGTGGGCTC
mCB1b	GATACCACCTTCCGTACCATCAC	GTTGTCCTCGTTCTCCTGAATGT	ACAGACCTCCTCTACGTGG

PCR efficiencies were monitored to be in the expected range with standard curves of serial dilutions of whole brain cDNA. PCR was performed in a volume of 20 µl containing 10 µl TaqMan Gene Expression Mastermix (2x concentrated; Applied Biosystems, Carlsbad, CA), 1 µl TaqMan assay (20x concentrated) and 9 µl prediluted cDNA (prediluted to approximately 3 ng/µl after cDNA synthesis) according to the thermal cycling protocol indicated in Table 4.7. As a cDNA loading control, expression levels of the quantified transcripts were normalized to that of the reference gene Gusb. To compare the expression levels of the novel splice variants mCB1a and mCB1b with that of mCB1,

expression levels of mCB1a and mCB1b were normalized to the expression level of mCB1 (assay Cnr1).

Table 4.7: Thermal cycling conditions for qPCR using TaqMan assays.
([a]UDG: uracil DNA glycosylase. This step before PCR cycling destroys any contaminating dU-containing product that might have been carried over from previous qPCR reactions.)

	UDG[a] incubation	Denaturation / activation of polymerase	PCR 50 cycles	
Temperature	50°C	95°C	95°C	60°C
Time	2 min	10 min	15 s	1 min

4.2.6.2 SYBR green

To quantify the 5' exons, SYBR green chemistry was used. Transcript-specific primer pairs for Gusb, the CB1 receptor coding sequence (CB1 CDS) and the exon junction to exon 7 were designed using Vector NTI software (Invitrogen, Darmstadt, Germany; see Table 4.8). PCR efficiencies were tested with standard curves of serial dilutions of whole brain cDNA. PCR was performed in a volume of 20 µl containing 10 µl Power SYBR Green PCR Mastermix (2x concentrated; Applied Biosystems, Carlsbad, CA), 3 µl each of forward and reverse primer (2 µM) and 4 µl prediluted cDNA (prediluted to approximately 5 ng/µl after cDNA synthesis) using the thermal cycling protocol indicated in Table 4.9. Expression levels of the quantified transcripts were first normalized to that of the reference gene Gusb and then to that of control mice.

Table 4.8: PCR primers for qPCR using SYBR green chemistry.
Different colors indicate annealing to different exons.

	Forward primer	Reverse primer	Intron overlapping	Product size (bp)
Gusb	CTCTGGTGGCCTTACCTGAT	CAGTTGTTGTCACCTTCACCTC	yes	73
CB1 CDS	CTTCCACGTGTTCCACCGCA	CCCACAGATGCTGTGAAGGAGG	no	87
Exon 1-7	GATGCGAAGGGTTCCCTCCT	GCAAGGCCGTCTAAGATCGA	yes	97
Exon 2-7	CCATGGCTGAGGGTTCCCTC	CAAGGCCGTCTAAGATCGAC	yes	98
Exon 5-7	CCTTCAGACATGGGTTCCCA	AGGAGGGAACCCTGACTCCC	yes	89
Exon 6-7	CAAGAGGCAGAGCAGGGTTC	AGGCCGTCTAAGATCGACTTCA	yes	100

Table 4.9 : Thermal cycling conditions for qPCR using SYBR green

	Denaturation / activation of polymerase	PCR 40 cycles			Dissociation stage		
Temperature	95°C	95°C	60°C	72°C	95°C	60°C	95°C
Time	15 min	15 s	30 s	30 s	15 s	1 min	15 s

4.2.7 Cell culture and transfection

HEK293 cells were grown in Dulbecco's modified Eagle's medium containing 10% FCS and 100 units/ml penicillin and 100 µg/ml streptomycin (all substances from Gibco, Carlsbad, CA, USA) at 37°C in a 5% CO_2 humidified incubator and split the day before transfection. Cells were transfected with the CB1 receptor variant-containing plasmids via Lipofectamine 2000 (Invitrogen, Carlsbad, CA, USA) following the manufacturer's instructions. Stable cell lines of all constructs were generated by selection using Geneticin (G418; Invitrogen). G418-resistant colonies were evaluated for the surface expression of CB1 receptor by live cell immunostaining using an antibody directed towards the N-terminal extracellular HA epitope tag (Covance, Berkeley, CA, USA) and a fluorescein isothiocyanate (FITC) secondary antibody (Jackson ImmunoResearch Laboratories Inc., West Grove, PA, USA). Clones expressing uniform and moderate to high levels of CB1 receptor were expanded and used for subsequent experiments. The relative levels of expression of CB1 receptor between the mutant and wild-type lines were not significantly different. Three stable cell lines were generated and analyzed for each CB1 receptor variant.

4.2.8 Western blot

Stably transfected HEK293 cell lines grown to approximately 90% confluency in 6-well dishes were chilled on ice for 5 min. Following a wash with ice-cold 1x PBS (137 nM NaCl, 10 mM NaH_2PO_4, 2.7 mM KCl, pH 7.4), cells were covered with 200 µl lysis buffer (100 mM Tris (pH 7.4), 150 mM NaCl, 0.5% CHAPS, 1 mM EDTA, 6 mM $MgCl_2$ and 100 mM PMSF) and incubated on ice 5 minutes. Cells were then scraped and lysates were sonicated and spun down at 10,000 x g and 4°C. The supernatant was collected and protein concentration was determined by the method of Bradford (Bradford, 1976). The samples were normalized to total protein, and 25 µg protein of each sample was run on a 10% Tris-glycine SDS-PAGE. The separated proteins were transferred to nitrocellulose and immunoblotting was performed using a mouse monoclonal anti-HA11 antibody (Cat# MMS-101P, CRP, Berkeley, CA, USA). Primary antibody was diluted 1:1000 in Odyssey blocking buffer (LI-COR Biosciences, Lincoln, NE, USA). As secondary antibody, goat anti-mouse conjugated IR680 dye (Cat# A21057, Invitrogen, Carlsbad, CA) was used diluted 1:5000 in a 50:50 mixture of PBS and Odyssey blocking buffer. Western blots were scanned on an Odyssey near-IR scanner (LI-COR Biosciences, Lincoln, NE, USA), and images were processed using Photoshop CE.

4.2.9 Quantitative internalization assay

Agonist-induced internalization of the mCB1 receptor and its splice variants was assessed in stably transfected HEK293 cell lines as described in (Daigle *et al.*, 2008*a*). Briefly, HEK293 cells stably

expressing mCB1, mCB1a or mCB1b were seeded onto poly-D-lysine coated 96-well plates and grown until ~95% confluent. Before drug treatment, cells were washed once in HEPES-buffered saline (HBS; 130 mM NaCl, 5.4 mM KCl, 1.8 mM $MgCl_2$ and 10 mM HEPES, pH 7.5) containing 0.2 mg/ml BSA (Sigma-Aldrich) and patted dry. Cells were then incubated in HBS/BSA containing a final concentration of 1 µM WIN-55,212-2 at 37°C for the times indicated in section 4.3.1.5. At the end of the incubation, wells were emptied and the plate was placed on ice. Cells were immediately fixed in 100 µl 4% paraformaldehyde (PFA) for 20 min at RT. After fixation, cells were washed five times for 5 min in PBS and blocked for 60 min with LI-COR Odyssey Blocking Buffer (LI-COR Biosciences, Lincoln, NE, USA). Cells were then incubated overnight at 4°C in 40 µl mouse monoclonal anti-HA11 antibody (1:150, Covance Inc., Berkley, CA, USA) with gentle shaking. The following day, cells were washed five times for 5 min in Tris-buffered saline (TBS) containing 0.05% Tween-20 (TBST; Tris-Base 10 mM, 137 mM NaCl, 0.05% Tween-20, pH 7.4) and then incubated for 1 h in the dark with donkey anti-mouse IgG conjugated to IRDye 800CW (1:800; Rockland Immunochemicals, Gilbertsville, PA, USA) in Odyssey Blocking Buffer. Cells were then washed four times for 5 min in TBST in darkness. After a short rinse in TBS, the immunocomplex was visualized on a LI-COR Odyssey near-IR scanner (LI-COR Biosciences, Lincoln, NE, USA) according to the manufacturer's instructions.

4.2.10 Quantitative measurement of MAPK phosphorylation

Stably expressing HEK293 cells were seeded on poly-D-lysine coated 96-well plates and grown until ~95% confluent. The cells were serum-starved overnight in 100 µl DMEM containing penicillin/streptomycin and only 0.1% FBS prior to the experiment. Before drug treatment, media containing 0.1% FBS was replaced and an additional 100 µl media with WIN55,212-2 was added to a final concentration of 100 nM. Cells were then incubated at 37°C for the times indicated in section 4.3.1.5. After drug treatment, medium was removed and the cells were fixed by immediate addition of 100 µl ice-cold 4% PFA and incubated for 15 min on ice and for additional 30 min at RT. Cell membranes were permeabilized by addition of 100 µl ice-cold methanol and incubation at -20^{o}C for 20 min. Cells were then washed five times for 5 min with Triton wash solution (0.1% Triton X-100 in PBS or TBS) and patted dry. Cells were then blocked for 1.5 h in 100 µl Odyssey Blocking Solution with gentle shaking. Following blocking, cells were incubated overnight at 4°C with anti-phospho-p44/42 MAPK antibody (Thr202/Tyr204; 20G11, Cell Signaling Technologies, Danvers, MA, USA) diluted 1:200 in Odyssey Blocking buffer. Cells were then washed five times for 5 min in TBST. Cells were briefly rinsed in PBS and incubated for 1.5 h with donkey anti-mouse IgG conjugated to IRDye 800CW (1:800; Rockland Immunochemicals, Gilbertsville, PA, USA) in Odyssey Blocking Buffer protected from light. Cells were washed 5 times for 5 min in TBST and patted dry. Immunofluorescence was scanned with a LI-COR Odyssey near-IR scanner (LI-COR Biosciences,

Lincoln, NE, USA). Integrated intensity values were used for analysis and were averaged and normalized to basal level activity.

4.2.11 Data analysis

The results were analyzed using Prism4 Software (GraphPad, La Jolla, CA, USA) or SPSS Statistics Software version 19 (IBM, Armonk, NY, USA). Differences were considered significant at $p<0.05$. All data are expressed as mean + or +/- SEM.

Statistical analysis of the expression of the splice junctions in the CB1 receptor 5' UTR and of the splice variants with shortened N-terminal were performed with one-way ANOVA.

Assays for quantitative measurement of internalization and p44/p42 MAPK phosphorylation were analyzed using two-way ANOVA.

Significant genotype effects were further analyzed using Bonferroni's *post-hoc* analysis for multiple comparisons.

4.3 Results

4.3.1 Discovery and characterization of two novel CB1 receptor splice variants with modified N-termini in mouse

4.3.1.1 Discovery

To analyze whether splice variants for the mCB1 receptor do exist, primers designed to amplify the sequence coding for the N-terminal extracellular domain of the mCB1 receptor were used in a PCR on cDNA templates from several brain tissues (forward primer "NH2term fwd" binding to -4 to +20 and reverse primer "NH2term rev" binding to +203 to +284, counting the CDS start as +1, Figure 4.3A). Gel electrophoresis of the PCR products showed a major band of approximately 300 bp corresponding to the unspliced mCB1 receptor sequence and two much weaker, smaller products for some of the template cDNAs (e.g. from hippocampus, basolateral amygdala; Figure 4.3B). The 300 bp band (corresponding to mCB1), and the gel areas between 150 and 250 bp and between 100 bp and 150 bp were excised and DNA was extracted. A second PCR on the extracted DNA resulted in strong, distinct bands of approximately 300 bp (corresponding to mCB1, 306 bp), 190 bp and 120 bp separated on an agarose gel. The PCR products were purified and subcloned, and insert DNA was sequenced. Alignment of the resulting sequence from the 190 bp PCR product with the sequence of the mCB1 receptor showed 100% sequence identity up to +103, then a gap corresponding to an intron of 117 bp and again 100% sequence identity from +220 (Figure 4.3C). The 120 bp PCR product had 100% sequence identity up to +87, then a gap corresponding to an intron of 186 bp and again 100% sequence identity from +274. As the intron sizes of 117 bp and 186 bp are dividable by three and there is no alternative ATG upstream of the exon junction, it is highly likely that the same start codon as for mCB1 is used for mCB1a and mCB1b.

Comparison of the splice donor and acceptor sites with the conserved sequences (Lim & Burge, 2001) showed that at the donor site, at the 3' end/5' start of the intron, instead of the canonical AG/GT, AG/GA or AG/TA is present for mCB1a or mCB1b, respectively. Investigation of the splice acceptor sites of mCB1a and mCB1b revealed the presence of the canonical AG at the 3' splice site with an upstream region with enrichment of pyrimidine and the presence of the conserved G at the 5' site of the acceptor exon for both variants.

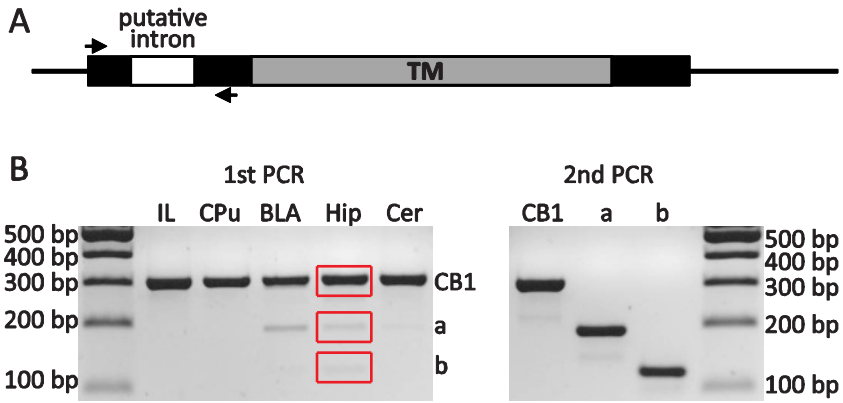

C

```
                                                    -60
.....intron.....  gg ttccctcctg  mCB1
.....intron.....  gg ttccctcctg  mCB1a
.....intron.....  gg ttccctcctg  mCB1b

-50          -40          -30          -20          -10
gcacctcttt ctcagtcacg ttgagcctgg cctaatcaaa gactgaggtt  mCB1
gcacctcttt ctcagtcacg ttgagcctgg cctaatcaaa gactgaggtt  mCB1a
gcacctcttt ctcagtcacg ttgagcctgg cctaatcaaa gactgaggtt  mCB1b

1            10           20           30           40
     NH2term fwd
ATGAAGTCGA TCTTAGACGG CCTTGCAGAT ACCACCTTCC GTACCATCAC  mCB1
ATGAAGTCGA TCTTAGACGG CCTTGCAGAT ACCACCTTCC GTACCATCAC  mCB1a
ATGAAGTCGA TCTTAGACGG CCTTGCAGAT ACCACCTTCC GTACCATCAC  mCB1b

50           60           70           80           90
CACAGACCTC CTCTACGTGG GCTCAAATGA CATTCAGTAC GAAGATATCA  mCB1
CACAGACCTC CTCTACGTGG GCTCAAATGA CATTCAGTAC GAAGATATCA  mCB1a
CACAGACCTC CTCTACGTGG GCTCAAATGA CATTCAG--- ----------  mCB1b

100          110          120          130          140
AAGGAGACAT GGCATCCAAA TTAGGATACT TCCCACAGAA ATTCCCTCTA  mCB1
AAG------- ---------- ---------- ---------- ----------  mCB1a
---------- ---------- ---------- ---------- ----------  mCB1b

150          160          170          180          190
ACTTCCTTCA GGGGTAGTCC CTTCCAAGAA AAGATGACGG CAGGAGACAA  mCB1
---------- ---------- ---------- ---------- ----------  mCB1a
---------- ---------- ---------- ---------- ----------  mCB1b

200          210          220          230          240
CTCCCCGTTG GTTCCAGCAG GAGACACAAC CAACATTACA GAGTTCTATA  mCB1
---------- ---------- GAGACACAAC CAACATTACA GAGTTCTATA  mCB1a
---------- ---------- ---------- ---------- ----------  mCB1b

250          260          270          280          290
                                          NH2term rev
ACAAGTCTCT CTCATCGTTC AAGGAGAACG AGGACAACAT CCAGTGTGGG  mCB1
ACAAGTCTCT CTCATCGTTC AAGGAGAACG AGGACAACAT CCAGTGTGGG  mCB1a
---------- ---------- ---GAGAACG AGGACAACAT CCAGTGTGGG  mCB1b

300          310          320          330
GAGAATTTTA TGGACATGGA GTGCTTCATG ATTCTGAAT  ...TM domain...  mCB1
GAGAATTTTA TGGACATGGA GTGCTTCATG ATTCTGAAT  ...TM domain...  mCB1a
GAGAATTTTA TGGACATGGA GTGCTTCATG ATTCTGAAT  ...TM domain...  mCB1b
```

Figure 4.3: Detection of two novel splice variants, mCB1a and mCB1b, in cDNA derived from tissue punches of mouse brain.
(A) Schematic representation of the protein coding sequence (CDS) of the CB1 receptor. Black box: CDS, uniform grey box: transmembrane domain (TM), arrows: primer binding sites in the sequence coding for the N-terminus, white box: location of the putative intron. **(B)** Detection of novel splice variants by PCR. Products from the first PCR on cDNA prepared from infralimbic cortex (IL), caudate putamen (CPu), basolateral amygdala (BLA), dorsal hippocampus (Hi) and cerebellum (Cer) were separated on a gel. The strong band at about 300 bp (CB1), and the two weaker bands at 200 bp (a) and 130 bp (b, marked by red boxes) were excised and DNA was extracted. The bands detected in a second PCR represent mCB1, mCB1a and mCB1b. **(C)** Sequence alignments of mCB1 and the two novel variants mCB1a and mCB1b show the introns in the sequence coding for the N-terminal extracellular domain. Splicing of an intron of 117 bp or 186 bp at position +103 or +87 leads to different N-termini for mCB1a and mCB1b, respectively. The binding sites of the primers NH2term fwd and NH2term rev, which were used to identify the novel variants, are indicated in the sequence. Non-coding sequences are in lower-case letter, coding sequences are in upper-case letters, +1 indicates the translation start.

4.3.1.2 Quantification

To compare the expression levels of the novel splice variants mCB1a and mCB1b with that of mCB1, Taqman qPCR assays (primer-probe pairs) were designed to selectively detect mCB1a or mCB1b. The reverse primers were designed to overlap the exon junctions in the coding sequences of mCB1a or mCB1b (Figure 4.4A). The primer pairs were pretested to yield only the specific product in a non-quantitative PCR with the same conditions as the quantitative PCR. To detect the overall amount of all three splice variants of the mCB1 receptor, an assay amplifying a sequence in the transmembrane domain was used. Expression levels of mCB1a and mCB1b were normalized to the expression level of mCB1.

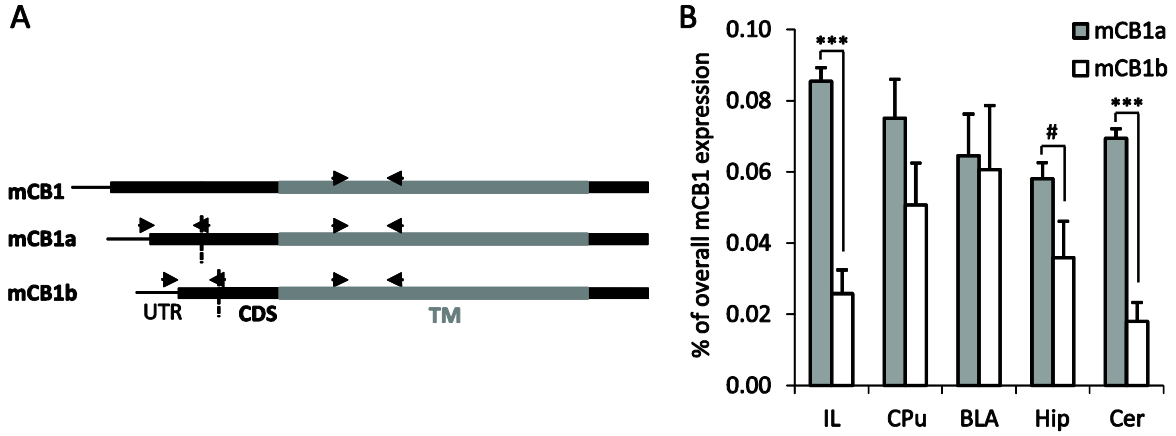

Figure 4.4: Quantification of mCB1a and mCB1b.
(A) Schematic illustration of the amplicons of the Taqman qPCR assays used to detect mCB1a, mCB1b and mCB1. For selective amplification of mCB1a and mCB1b, the assays have exon junction-spanning reverse primers. The assay detecting all three splice variants recognizes an amplicon in the transmembrane domain. **(B)** Quantification of the ratio of the novel splice variants to the complete amount of mCB1 receptor in infralimbic cortex (IL), caudate putamen (CPu), basolateral amygdala (BLA), dorsal hippocampus (Hip) and cerebellum (Cer) of C57Bl/6N mice (n=5). Data are mean + SEM; ***p<0.001; #p<0.1.

Quantification revealed that both mCB1a and mCB1b have very low expression levels between 0.02% and 0.1% relative to the overall mCB1 receptor level in all the analyzed brain tissues of

C57Bl/6N mice (Figure 4.4B; n=5). The expression level of mCB1b is significantly lower than of mCB1a in the infralimbic cortex ($p<0.001$) and in the cerebellum ($p<0.001$), and has a tendancy to be lower in the hippocampus ($p=0.098$).

4.3.1.3 Cloning and generation of stably transfected cell lines

As a next step, the full-length transcripts of mCB1a and mCB1b were cloned. To this end, a two-step PCR was used to be able to select for the low abundant splice variants instead of the non-spliced mCB1 transcript. In the first step, two separate PCRs were performed, one with a forward primer binding upstream of the start codon and a reverse primer overlapping the exon junction of mCB1a or mCB1b; and the second with a forward primer overlapping the exon junction of mCB1a or mCB1b and a reverse primer binding to the 3' UTR downstream of the stop codon (Figure 4.5). The two PCR products for mCB1a and mCB1b were purified and used together as templates for the second PCR. In this overlap extension nested PCR, primers binding upstream of the start codon and downstream of the stop codon (but binding inside of the primers used in the first reaction) were used to amplify the whole transcript. The primers had 5' overhangs with restriction sites for KpnI and NotI for subsequent cloning of the amplified sequences in the vector pcDNA3.

Figure 4.5: Cloning of the full-length transcripts of mCB1a and mCB1b.
Schematic illustration of the cloning strategy: In the first step, two separate PCRs were carried out with the primer pairs S21/S18 and S5/S22 for mCB1a and with the primer pairs S21/S20 and S11/S22 for mCB1b. The purified products of the first and second part were then used in a nested overlap-extension PCR with the primer pair S23-KpnI/S24-NotI to amplify the complete sequences of mCB1a or mCB1b and add restriction endonuclease recognition sites for KpnI on the 5' end and NotI on the 3' end.

In collaboration with the laboratory of Ken Mackie (Jim Miller-Wagner and Jill Farnsworth, Indiana University, Bloomington, IN, USA), HEK cell lines stably expressing mCB1, mCB1a or mCB1b were generated. A strong Kozak-sequence for efficient translation and an HA11-tag were added upstream of the open reading frame. For each receptor variant, three stable cell lines were generated.

4.3.1.4 Protein variants and potential differences in N-linked glycosylation

To analyze the molecular weight of mCB1a and mCB1b and compare it with the molecular weight of mCB1, Western blots with whole protein extracts from the stably transfected cells were performed (Figure 4.6A) in collaboration with the laboratory of Ken Mackie (experiments were performed by Jim Miller-Wagner and Jill Farnsworth, Indiana University, Bloomington, IN, USA).

The calculated molecular weights are 53.9 kDa for HA-mCB1, 49.7 kDa for HA-mCB1a and 47.0 kDa for HA-mCB1b. In the N-terminal extracellular tail, mCB1 has three putative N-linked glycosylation sites with the consensus sequence Asn(N)-X-Ser(S)/Thr(T) at amino acid positions 77, 83 and 112 (Figure 4.6B). Glycosylated mCB1 is running approximately 11 kDa higher than the unglycosylated protein, resulting in the observed band of around 64 kDa. The splice variant mCB1a is running a little lower that mCB1, but still seems to be fully glycosylated as it is running approximately 11 kDa higher than the calculated molecular weight of 49.7 kDa. In variant mCB1b, two of the three glycosylation sites are removed by splicing. The band representing mCB1b is running below 50 kDa, which indicates a strong reduction of post-translational glycosylation.

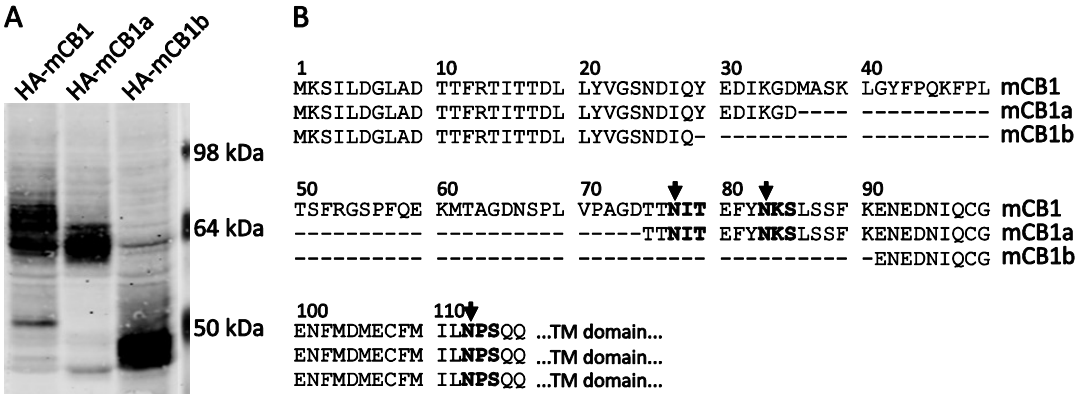

Figure 4.6: Molecular weight and glycosylation of mCB1, mCB1a and mCB1b.
(A) Representative Western blot shows bands for HA-staining of mCB1 and the splice variants mCB1a and mCB1b stably expressed in HEK293 cells. (Western blot was done by Jim Miller-Wagner and Jill Farnsworth.) **(B)** Amino acid sequence of the N-terminal tails of mCB1, mCB1a and mCB1b. Putative N-linked glycosylation consensus sequences are indicated in bold letters, and putatively glycosylated asparagines are marked with arrows.

4.3.1.5 Signaling efficiencies of mCB1 and the two novel splice variants mCB1a and mCB1b

In collaboration with the laboratory of Ken Mackie (experiments were performed by Jim Miller-Wagner and Jill Farnsworth, Indiana University, Bloomington, IN, USA), signaling efficiencies of mCB1, mCB1a and mCB1b were investigated by quantification of agonist-induced internalization and quantification of MAPK activation.

The CB1 receptor is known to rapidly internalize following agonist binding and receptor activation (Hsieh *et al.*, 1999). To investigate whether the modified N-termini of mCB1a and mCB1b

influence trafficking of the receptors upon activation, agonist-induced internalization was analyzed by confocal imaging (Figure 4.7A). After 1 h treatment with the synthetic CB1 receptor agonist WIN55,212-2 at a concentration of 1 µM, surface receptor loss was stronger for mCB1a (v) and mCB1b (vi) than for unspliced mCB1 (iv). Internalization was quantified using on-cell Western analysis. Cells expressing mCB1, mCB1a or mCB1b were stimulated with different concentrations of WIN55,212-2 and after 1 h, the amount of receptors on the surface was quantified. Starting from a concentration of 5 nM or 10 nM, respectively, mCB1a and mCB1b showed stronger internalization than the unspliced mCB1 receptor upon treatment with increasing agonist concentrations (Figure 4.7B). Analysis of the time course of surface receptor loss after stimulation with 1 µM WIN55,212-2 showed that shortly after stimulation (5 min) mCB1a internalized stronger than mCB1b (Figure 4.7C). At later time points, mCB1a and mCB1b showed similar internalization, which was significantly stronger than of the unspliced mCB1 receptor starting from 15 min or 30 min after stimulation for mCB1a or mCB1b, respectively.

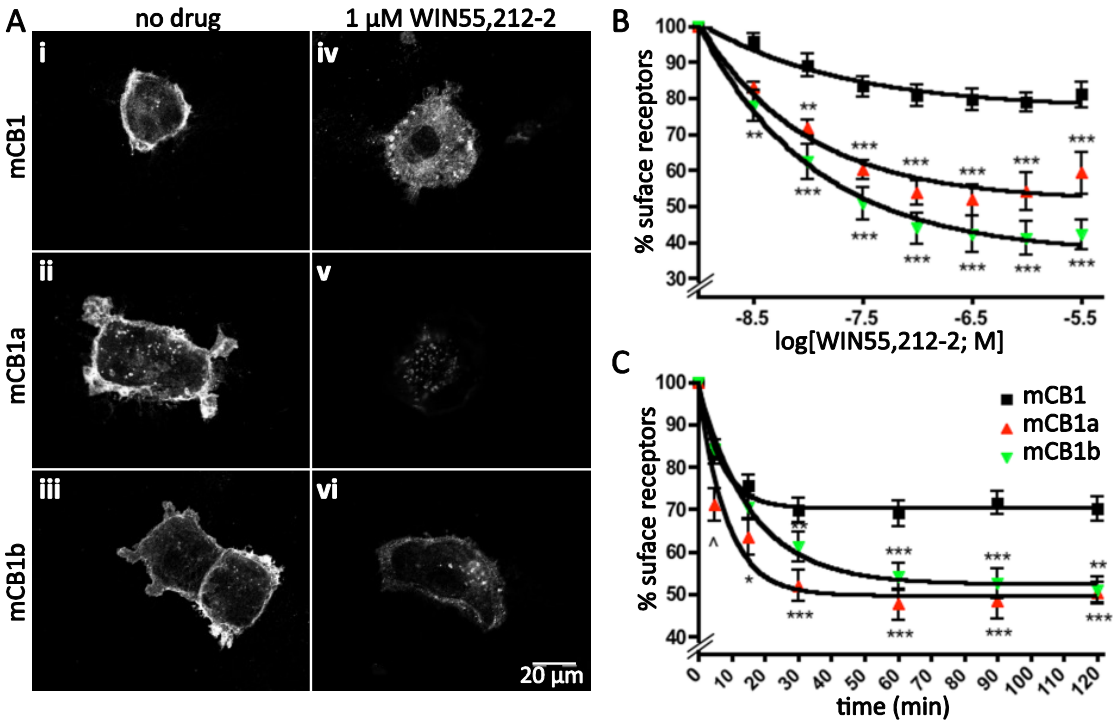

Figure 4.7: Different trafficking of mCB1a and mCB1b as compared with mCB1.
(A) Immunostaining of HEK293 cells stably expressing mCB1 (i, iv), mCB1a (ii, v) or mCB1b (iii, vi). Cells were treated with vehicle (i, ii, iii) or stimulated with 100 nM WIN55,212-2 (iv, v, vi) for 1 h. Both mCB1 and the splice variants mCB1a and mCB1b were internalized following agonist treatment. Surface receptor loss was stronger for mCB1a and mCB1b. **(B)** Dose-response curve: Following 1 h exposure to increasing concentrations of WIN55,212-2, mCB1 (black squares) and the novel splice variants mCB1a (red triangles) and mCB1b (green triangles) internalized in a concentration-dependent manner, with the internalization of the variants mCB1a and mCB1b being stronger at any agonist concentration than of the unspliced mCB1 receptor. **(C)** Time course: Cells expressing mCB1, mCB1a or mCB1b were stimulated with 1 µM WIN55,212-2 and the loss of surface receptors with time was quantified. After 5 min, surface mCB1a was reduced compared with mCB1 and mCB1b. At later time points, mCB1a and mCB1b were reduced on the cell surface compared with mCB1. Data are mean +/- SEM; n=12 from 4 independent experiments; ***p<0.001, **p<0.01, *p<0.5 in *post-hoc* test *vs.* mCB1; ^p<0.05 in *post-hoc* test of mCB1a *vs.* mCB1b. (These experiments were performed by Jim Miller-Wagner and Jill Farnsworth.)

Activation of the CB1 receptor leads to phosphorylation of p42/p44 MAPK (Bouaboula *et al.*, 1995). To analyze whether the splice variants differentially influence downstream signaling pathways, activation of the MAPK pathway was investigated. Stimulation of cells expressing the mCB1 receptor with 100 nM WIN55,212-2 resulted in a transient elevation of p44/42 MAPK phosphorylation with a peak activation of 150% over basal level at 5 min (Figure 4.8). Cells expressing mCB1a showed a similar response to cells expressing mCB1. Stimulation of cells expressing mCB1b led to a significantly decreased MAPK phosphorylation at 5 min with a slightly shifted peak response of 50% over basal activation after 7.5 min.

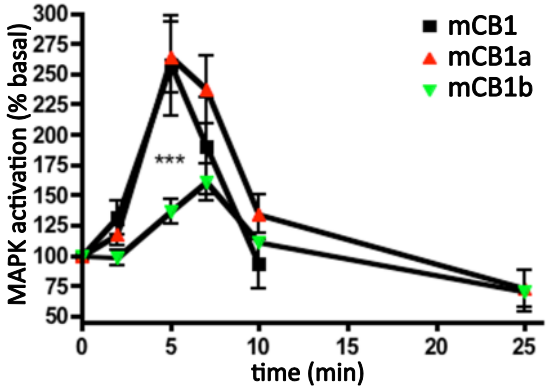

Figure 4.8: Agonist stimulation of mCB1b transfected cells leads to reduced p44/42 MAPK activation.
The time course of p44/p42 phosphorylation was quantified in HEK293 cells stably expressing mCB1, mCB1a or mCB1b after stimulation with 100 nM WIN55,212-2. Cells expressing mCB1b showed a strongly reduced response compared with cells expressing mCB1 or mCB1a. Data are mean +/- SEM; n=9 from 3 independent experiments; ***p<0.001 in *post-hoc* test *vs.* mCB1 or mCB1a. (These experiments were performed by Jim Miller-Wagner and Jill Farnsworth.)

4.3.2 Exon-intron structure of the mouse *Cnr1* 5' UTR

4.3.2.1 Characterization of the *Cnr1* 5' UTR

Integrating all the available information from genomic assemblies described in databases and publications (see 4.1.3), a scaffold of the mouse *Cnr1* gene composed of 4 exons was used as a starting point for the further analysis (Figure 4.9A). For easier understanding, a nomenclature based on all the exons identified in this thesis is already used for the scaffold. Thus, the exons are termed 1, 2, 6 and 7 starting with 1 for the most 5' exon and ending with 7 for the most 3' exon (containing the coding sequence), as later more exons were identified. In order to detect whether the putative exons are part of processed mRNA transcripts and which of the putative exons are spliced together, primers complementary to sequences in the putative exons were designed. By combining primers flanking putative intron splice sites, relatively small PCR- products should be detected, if the adjoining exons are spliced together. No or large products should be detected, if no splicing occurs or if genomic DNA is amplified, respectively. For example, the forward primer binding to the putative end of exon 1 and

the reverse primer binding to the putative beginning of exon 7 amplified a PCR product with a size of approximately 400 bp on brain cDNA templates (Figure 4.9B). On genomic DNA, these sites are more than 18.4 kb apart from each other. Amplification of the small product on cDNA suggested that exon 1 and exon 7 were spliced together. Similar PCRs were performed on cDNA prepared from several brain tissues with all possible combinations of the primers shown in Figure 4.9A (primer binding sites are indicated by black arrows). The PCR products were subcloned in TOPO-TA vector and the inserts were sequenced. Aligning the sequences of the clones with the genomic sequence of the mouse *Cnr1* gene, the putative splice junctions for exons 1-7, 2-7 and 6-7 could be confirmed and the corresponding donor and acceptor sites were identified. During the sequence analyses of the products amplified by a forward primer binding to the end of exon 2 and a reverse primer binding to the donor site of exon 7, a novel exon (exon 5) was identified (Figure 4.9A, B) with a size of 108 bp.

To determine the 5' ends of mature CB1 receptor mRNA transcripts, 5' RLM-RACE was performed. To this end, RNA-adapters were ligated to hippocampal CB1 receptor mRNA transcripts from which the 7-methylguanosine-caps were previously removed and the RNA was reverse transcribed into cDNA. PCR amplifications were performed on the cDNA template using a forward primer complementary to the RNA-adapter sequence and an exon-specific reverse primer. As PCR might preferentially amplify higher abundant and shorter products, several reverse primers complementary to sequences within the different exons were used (Figure 4.9A). PCR products were purified and a second round of PCR with nested primers was performed to reduce the amount of unspecific products. Figure 4.9C shows RACE PCR products from hippocampal cDNA, separated on a gel. The experiment was repeated with hippocampal and cerebellar RNA and electrophoretic separation of the PCR amplified products showed a plethora of bands (data not shown). The PCR products of both experiments were subcloned in TOPO-TA vector and the inserts were sequenced. Aligning the sequences of the cDNA clones with the genomic sequence of the mouse *Cnr1* gene revealed that many of the PCR products derived from unspecific amplifications, but some PCR products corresponded to the adapter-ligated sequence of the mouse *Cnr1* gene (results are illustrated in Figure 4.9D).

Sequence alignments of subcloned PCR products amplified with the reverse primer binding to exon 7 identified cDNA transcripts where exon 1 and 7 or exon 2 and 7 are spliced together. Exon sizes were 192 bp for exon 1 and 229 bp for exon 2. As these exons were shorter than the exon sizes described in the NCBI and Ensembl databases, exon lengths of exon 1 and 2 were compared with the sequences obtained after PCRs with reverse primers complementary to exon 1, 2 and 5. Intriguingly, several transcription starting points for exon 1 and exon 2 were identified. The most often sequenced starting point represented a size of 192 bp for exon 1, but also shorter transcripts and one longer

transcript with an exon size of 246 bp were found. For exon 2, even more different starting points were found in the sequence alignments, with the longest transcript representing a size of 315 bp for exon 2. All identified transcription starting points for exon 1 and 2 were downstream of the starting points described in the NCBI and Ensembl databases.

With the reverse primer binding to exon 6, four different transcripts were identified. One transcript had the transcription start in exon 6, 1016 bp upstream of the splice donor of exon 6. The other three contained a smaller part of exon 6 (termed exon 6a) using a consensus splice acceptor sequence 113 bp upstream of the splice donor of exon 6. In one of the identified transcripts, a shorter version of exon 2 was identified as well (termed exon 2a), using a consensus splice acceptor site 86 bp upstream of the splice donor site. Two of the transcripts had the transcription start in exon 1 and the third one in exon 2. In these sequences, another novel exon (exon 3) with a size of 118 bp was identified, containing GT-AG consensus splice donor and acceptor sequences.

With the reverse primer binding to exon 5, three different transcripts were identified. Two of them had the transcription start in exon 1 and the third one in exon 2. A novel exon (exon 4) with a size of 68 bp was found also containing GT-AG consensus splice donor and acceptor sites.

It is not clear whether the processed transcripts identified with the RACE reverse primer binding to exons upstream of exon 7 include exon 7 (and thus are protein-coding), but combining the results from RT-PCR and RLM-RACE, this is very likely. For example with RT-PCR, cDNA containing exon 2a, 5 and 7 was sequenced; and with RLM-RACE with reverse primer in exon 5, cDNA containing exon 1, 2a and 5 was found. Thus, the existence of a transcript variant 1-2a-5-7 is very likely, but would need to be proven in further analyses.

From the results described above, an updated structure for the *Cnr1* gene was assembled (Figure 4.9E), containing 7 exons and putative 5' transcript start sites in exon 1, 2 and 6.

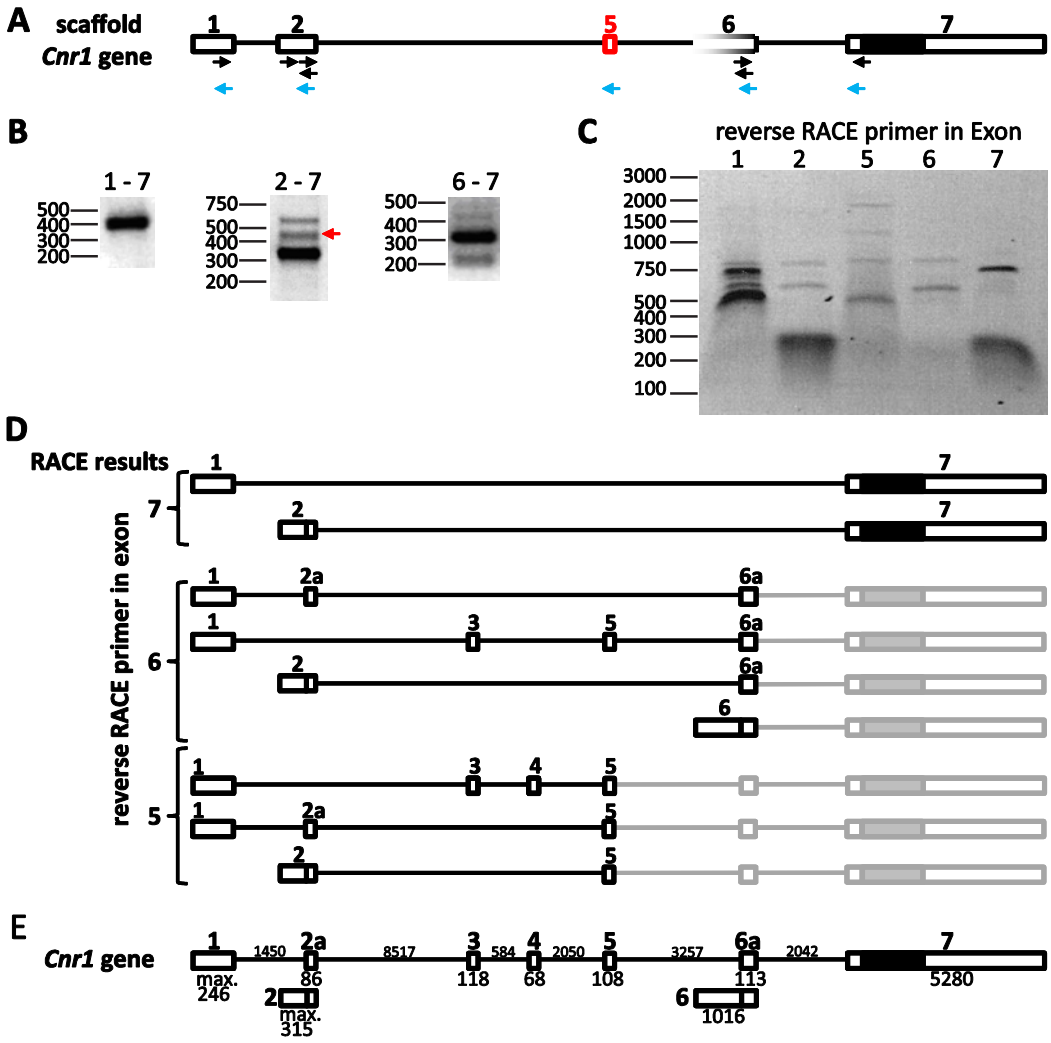

Figure 4.9: Exon-intron structure of the mouse *Cnr1* gene.
(A) Scaffold of the mouse *Cnr1* gene assembled as a starting point for further analyses. Putative exons are displayed as boxes, the CDS is displayed as a filled box and putative introns are indicated as lines. Black arrows indicate primer binding sites for RT-PCR, blue arrows indicate primer binding sites for 5' RLM-RACE. **(B)** Gel pictures displaying RT-PCR products amplified with primers binding to exons indicated above the picture. The red arrow indicates amplification of the novel exon 5. **(C)** Gel picture displaying 5' RLM-RACE PCR products amplified with the forward primer in the adapter sequence (ligated to the 5' transcript start) and with the reverse primer in the exon indicated above the gel picture. **(D)** Graphic illustration of the transcripts identified during 5' RLM-RACE PCR. Exons downstream of the reverse primer binding site are indicated in grey, as they are not necessarily part of the transcript (for details, see text). Sizes of the identified introns and exons are summarized in E. **(E)** Updated structure of the mouse *Cnr1* gene consisting of 7 exons. Intron and exon sizes are indicated above (intron) or below (exon) the structure. Sizes are indicated in bp.

4.3.2.2 Abundance of the transcript variants

4.3.2.2.1 Quantification of the transcript variants in different brain regions

To analyze how abundant the different transcripts are in specific brain regions, qPCR was performed on cDNA prepared from caudate putamen, hippocampus and cerebellum of control mice. To ensure that only transcripts with a specific splice junction were amplified in the qPCR, primer pairs were designed of which either the forward or the reverse primer overlapped the splice junction. Only the splice junctions to exon 7 were quantified (junctions 1-7, 2-7, 5-7 and 6-7), as only the transcripts including the protein encoding exon are definitely protein coding. Gusb was used as a housekeeping gene. The CB1 receptor CDS was used for normalization. The results are summarized in Table 4.10.

Table 4.10: Quantitative analysis of the transcripts containing specific exon junctions normalized to the CB1 receptor CDS.
Data are indicated in mean percentage ± SEM. Statistical analysis was performed for each exon junction (per row) and for each brain region (per column). [a] labeled values are not significantly different within row, [b] labeled values are not significantly different within column, otherwise $p<0.001$ in *post-hoc* analysis.

	Caudate putamen	Hippocampus	Cerebellum
exon junction 1-7	99.82 ± 13.96[a]	90.20 ± 9.07[a]	85.98 ± 5.73[a]
exon junction 2-7	10.99 ± 0.78[a,b]	9.65 ± 0.63[a,b]	21.22 ± 1.28
exon junction 5-7	2.07 ± 0.29[a,b]	0.51 ± 0.02[b]	1.93 ± 0.18[a,b]
exon junction 6-7	2.17 ± 0.28[b]	0.43 ± 0.03[a,b]	0.62 ± 0.06[a,b]

Quantification showed that the main transcript variant in all tested brain regions contains exon junction 1-7. The transcript variants containing exon junction 2-7 represent between 10% and 20% of the CB1 receptor-coding transcripts in the analyzed brain regions. They are significantly lower expressed relative to CB1 than the transcript variants containing exon junction 1-7 in all analyzed brain regions. All the other variants, containing either the splice junction 5-7 or 6-7 with various compositions of the upstream exons, represent a minority of 2% or less of the transcripts coding for the CB1 receptor. The sum of all the measured transcript variants in one tissue does not differ from the amount of CB1 receptor CDS transcript[4], indicating that the major transcript variants were identified in this thesis.

Comparison of the expression levels of the different transcript variants (relative to the expression of the CB1 receptor CDS) between brain regions showed that exon junction 2-7 is significantly higher expressed in cerebellum than in caudate putamen and hippocampus. Furthermore, exon junction 5-7 containing transcripts are significantly lower expressed in hippocampus than in caudate putamen and cerebellum; and exon junction 6-7 containing transcripts

[4] The sum of all transcripts is not exactly 100%, but it is also not significantly different from 100%.

are significantly higher expressed in caudate putamen. Thus, the transcript composition is brain region specific.

4.3.2.2.2 Quantification of the transcript variants in Glu-CB1$^{-/-}$ and GABA-CB1$^{-/-}$ mice

To analyze whether the transcripts coding for the CB1 receptor protein differ between different neuronal cell types, conditional CB1 receptor knock-out animals with deletion of the receptor specifically from cortical glutamatergic (Glu-CB1$^{-/-}$) or from cortical and striatal GABAergic neurons (GABA-CB1$^{-/-}$) were used (Monory *et al.*, 2006). For the generation of the conditional knock-out mice, loxP sites had been inserted in the intron upstream of the coding exon and in the coding exon (exon 7) downstream of the CB1 receptor coding sequence (Marsicano *et al.*, 2002). Thus, if Cre recombinase is present, the complete beginning of exon 7 including the CB1 receptor coding sequence is removed by excision of the DNA between the two loxP sites.

QPCRs with primers specific for the CB1 receptor CDS, the splice junctions 1-7, 2-7, 5-7, 6-7 and for Gusb as reference gene were performed on cDNA prepared form caudate putamen, hippocampus and cerebellum of Glu-CB1$^{-/-}$ and GABA-CB1$^{-/-}$ mice. For normalization, Cre-negative littermates of the conditional knock-out animals were used as calibrator (as the data scattered more within the Cre-negative littermate groups of Glu and GABA mouse lines than between the mouse lines (data not shown), the Cre-negative animals were pooled in one control group termed wild type).

Expression of mRNA containing the CB1 receptor CDS in the caudate putamen did not differ significantly between Glu-CB1$^{-/-}$ and wild type. In the GABA-CB1$^{-/-}$, less than 1% of wild-type levels of CB1 receptor CDS mRNA was detected. In the hippocampus, CB1 receptor-CDS expression in Glu-CB1$^{-/-}$ was significantly reduced to 66%, whereas in GABA-CB1$^{-/-}$, expression was significantly reduced to 28% of the wild-type level. In both caudate putamen and hippocampus, expression levels differed also significantly between Glu-CB1$^{-/-}$ and GABA-CB1$^{-/-}$. In the cerebellum, there were no differences in CB1 receptor-CDS expression between the groups. In the caudate putamen, the majority of neurons are GABAergic medium spiny neurons. If CB1 receptor expression is knocked out in GABAergic neurons, this accounts for the observed strong reduction of CB1 CDS in mRNA derived from this brain region. In the hippocampus, CB1 receptor is expressed at high levels in GABAergic interneurons and at low to moderate levels in glutamatergic neurons. Thus, the reduction of CB1 receptor CDS amounts in hippocampal mRNA of about 1/3 in Glu-CB1$^{-/-}$ and of about 2/3 in GABA-CB1$^{-/-}$ is in good agreement with the expression level data. In the cerebellum of Glu-CB1$^{-/-}$ and GABA-CB1$^{-/-}$, no recombination takes place (Monory *et al.*, 2006), explaining the unchanged expression levels of CB1 CDS in this region.

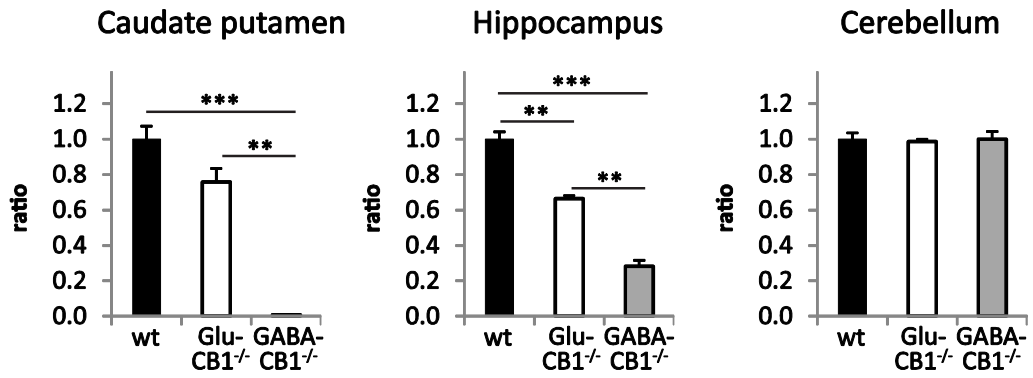

Figure 4.10: CB1 receptor-CDS mRNA expression in Glu-CB1$^{-/-}$ (white) and GABA-CB1$^{-/-}$ (grey) mice relative to that of wild-type controls (black) in different brain regions. Data are expressed as mean + SEM. For each group n=3, except for the caudate putamen samples in GABA-CB1$^{-/-}$, n=2. ***p<0.001, **p<0.01.

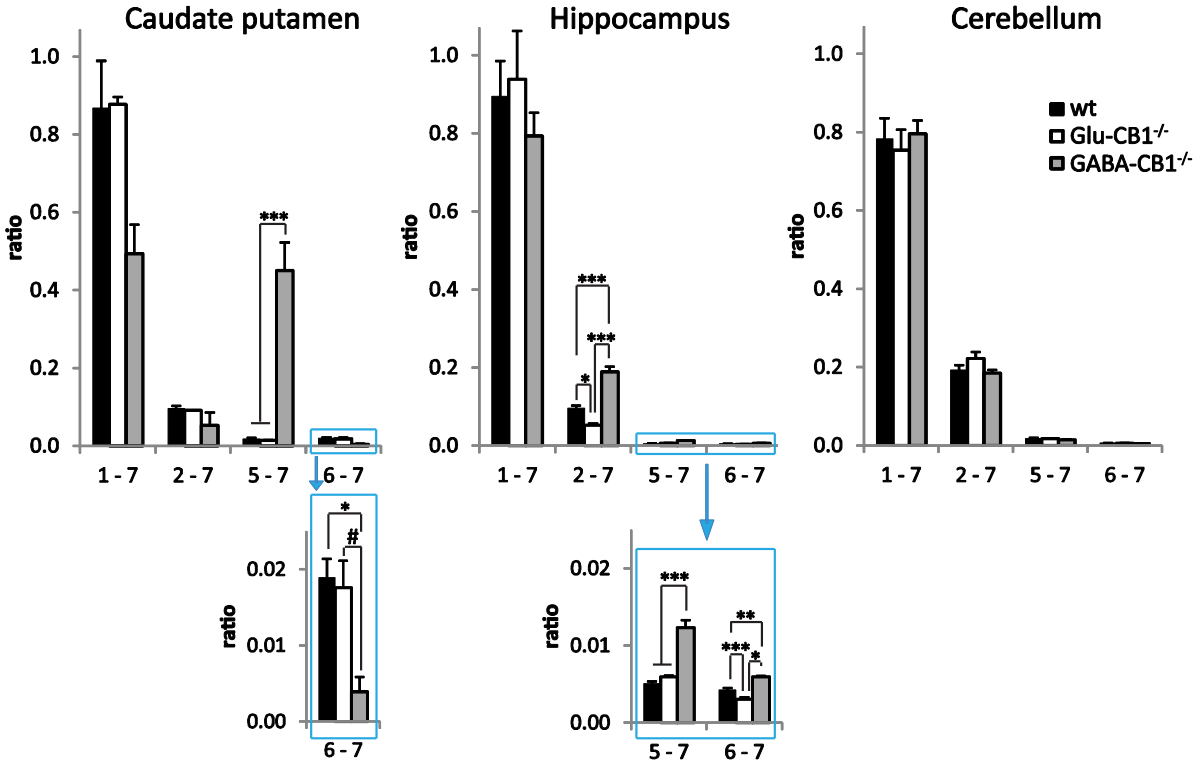

Figure 4.11: mRNA expression levels of specific exon-junctions containing transcripts.
mRNA was prepared from different brain regions of wild-type (black), Glu-CB1$^{-/-}$ (white) and GABA-CB1$^{-/-}$ (grey) mice. Expression levels were normalized to CB1 receptor-CDS mRNA levels. Data are expressed as mean + SEM. Data with low ratios (blue boxes) are magnified below. For each group n=3, except for the caudate putamen samples in GABA-CB1$^{-/-}$, n=2. ***p<0.001; **p<0.01, *p<0.05, #p<0.1.

To analyze to which extent the different transcript variants contribute to the CB1 receptor protein coding transcripts, the expression levels of the exon junctions 1-7, 2-7, 5-7 and 6-7 were normalized to their sum[5]. It is important to keep in mind that similar ratios in this analysis do not indicate similar expression levels, but specify to which percentage the transcripts containing a specific splice junction contribute to the whole amount of CB1 receptor transcripts, without considering the absolute amount.

In the caudate putamen of GABA-CB1$^{-/-}$ animals, the percentage of transcripts containing exon junction 5-7 is significantly higher than in wild-type of Glu-CB1$^{-/-}$ animals, representing about half of the total of all exon junctions compared with only 1-2% in wild-type and Glu-CB1$^{-/-}$ animals. Furthermore, the percentage of transcripts containing exon junction 6-7 is significantly reduced in GABA-CB1$^{-/-}$ to 0.4% compared with 1.9% in the wild type. Thus, since the CB1 receptor is deleted from GABAergic neurons, it might be that the remaining CB1 receptor expression arises from another cell type with a much higher percentage of transcripts containing exon junction 5-7.

In the hippocampus, the contributions of the transcripts containing exon junction 2-7 to the total of all exon junctions differ significantly between wild type, Glu-CB1$^{-/-}$ and GABA-CB1$^{-/-}$. *Post-hoc* analysis showed that the percentage of transcripts containing exon junction 2-7 is significantly reduced in Glu-CB1$^{-/-}$ and significantly elevated in GABA-CB$^{-/-}$ compared with the wild type. The percentage of transcripts containing exon junction 5-7 and 6-7 is significantly higher in GABA-CB1$^{-/-}$ than in the wild type as well, but these still only represent a small part of the total of all exon junctions (1.2% and 0.6%, respectively). In Glu-CB1$^{-/-}$, the percentage of transcripts containing exon junction 6-7 is significantly reduced, but expression levels in the wild type are below 1%.

In the cerebellum, no changes of transcript composition were detected.

[5] If the analyzed variants represent the whole CB1 receptor transcripts, the sum of the transcripts containing exon junctions 1-7, 2-7, 5-7 and 6-7 should equal the amount of CB1 receptor CDS mRNA. This was true for all analyzed groups except for caudate putamen of GABA-CB1$^{-/-}$, where the CB1 receptor CDS expression is lower than the sum. This means that the exon junctions 1-7, 2-7, 5-7 and 6-7 together are expressed at higher levels than exon 7. This is probably caused by the low n-number of caudate putamen samples in GABA-CB1$^{-/-}$ (n=2). For easier understanding, the data were normalized to the sum of all exon junctions.

4.4 Discussion

4.4.1 Two novel splice variants of the mouse CB1 receptor have shortened N-termini

Previously, it was described that the N-terminal splice variants are unique for the human CB1 receptor (Howlett *et al.*, 2002; Xiao *et al.*, 2008), as the consensus splice donor and acceptor sequences present in the CDS of the human *CNR1* gene are not present at the same positions in the mouse *Cnr1* gene. In this thesis, two novel CB1 receptor splice variants with shorter N-termini were identified in mouse (properties are summarized in Table 4.11). The first variant, mCB1a, results from the excision of a 167 bp intron resulting in an in-frame deletion of 39 amino acids following amino acid residue 35. The second variant, mCB1b, results from the excision of a 186 bp intron resulting in an in-frame deletion of 62 amino acids following amino acid residue 28.

Table 4.11: Summary of the properties of the mouse CB1 receptor splice variants.

	mCB1	mCB1a	mCB1b
size of intron in the CDS	-	117 bp	186 bp
number of amino acids lost in N-terminal tail	-	39	62
splice donor and acceptor sites of retained intron	-	donor: AG/GA acceptor: AG/G	donor: AG/TA acceptor: AG/G
N-linked glycosylation in N-terminal tail	yes	yes	no (N77 and N83 lost)
agonist-induced surface receptor loss	about 30% surface receptor loss after 30 min of 1 µM WIN55,212-2	increased surface receptor loss as compared with mCB1	increased surface receptor loss as compared with mCB1
agonist-induced p44/p42 phosphorylation	peak activation of 150% over basal level at 5 min	similar to mCB1	decreased peak response of 50% over basal activation at 7.5 min

As for the human CB1 receptor splice variants, both variants of the mouse CB1 receptor are generated by alternative splicing events in which a specific sequence may either be spliced out as an intron or be retained (Matlin *et al.*, 2005). Intron retention is the rarest mode of alternative splicing in mammals (Sammeth *et al.*, 2008). The introns in the mouse *Cnr1* gene are at different positions from the variants generated by alternative splicing described for humans. The mouse splice variants are generated by the use of splice donor sites in which only the 3' end of the exons match the consensus splice sequence (AG), whereas the 5' starts of the introns differ from the consensus sequence (consensus: GT, mCB1a: GA, mCB1b: TA). The splice acceptor sites correspond to the consensus sequence (AG/G). The transcript variants of the mouse CB1 receptor that are generated by alternative splicing have very low expression levels as compared with the unspliced CB1 receptor mRNA. This might be explained by less efficient assembly of the splice machinery at splice sites

differing from the consensus sequences because of lower affinity interactions with the splicosome components. But whether alternative splicing occurs at a specific site is not only determined by splice-site consensus sequences. Additionally, exon and intron splice enhancers or silencers define the balance of alternative splicing (Matlin *et al.*, 2005). However, a low abundance on the mRNA level does not necessarily lead to low abundance of the protein. The large N-terminus of the human CB1 receptor is thought to inhibit efficient receptor translocation across the membrane of the endoplasmatic reticulum (ER), leading to large amounts of misfolded CB1 receptor that are rerouted towards proteasome degradation (Andersson *et al.*, 2003). Furthermore, the authors demonstrated that shortening the N-terminus of the CB1 receptor or the inclusion of a signal peptide for ER export greatly increases receptor stability, and both result in increased targeting to the cell surface. Partial truncation of the N-terminal tail of the CB1 receptor was detected in various cell lineages *in vitro*, and is due to the fast proteolytic processing of *de novo* synthesized receptors in the cytoplasm prior to their translocation over the ER via a mechanism independent of the proteasome (Nordström & Andersson, 2006). One may speculate that, with the shorter N-terminal tails, the two novel splice variants would be more stable during their synthesis and would be expressed at the cell surface more readily than unspliced CB1 receptor. This hypothesis could not be tested, since it is not yet possible to distinguish the mCB1a and mCB1b proteins from the unspliced receptor protein because no splice variant-specific antibodies exist until now. Thus, the relative amount of mCB1a and mCB1b and their cellular distribution *in vivo* remain to be determined.

To investigate the novel splice variants in a cellular system, cell lines with stable expression of mCB1a and mCB1b were generated. Thus, the variants could be analyzed on protein level and the signaling efficiencies could be compared with unspliced CB1 receptor. As no specific antibodies for the splice variants exist, an HA-tag was added to the N-terminus. HA was chosen, as this tag is very short (9 amino acid residues), and was shown to leave surface expression and trafficking of rat and human CB1 receptor unchanged (Ken Mackie, personal communication). In contrast, the addition of the enhanced green fluorescent protein (eGFP) was shown to inhibit surface expression after addition to the N-terminus (McDonald *et al.*, 2007) and to influence receptor trafficking after addition to the carboxy-terminus (C-terminus) (Ken Mackie, personal communication).

In Western blots with whole protein extracts from the stably transfected cells, mCB1 and the splice variant mCB1a were shown to have a higher molecular weight than calculated from the amino acid sequences, but variant mCB1b was running at the height of its calculated molecular weight. An elevated molecular weight was previously described for the mature, glycosylated CB1 receptor in several species (Song & Howlett, 1995; Onaivi *et al.*, 1996; Andersson *et al.*, 2003). In the N-terminal extracellular tail, CB1 has three putative N-linked glycosylation sites with the consensus sequence

Asn(N)-X-Ser(S)/Thr(T) at amino acid positions 77, 83 and 112 conserved in human, rat and mouse. In the rat, it was shown that only two of the three potential N-linked glycosylation sites are glycosylated, as treatment with endoglycosidase shifted the 64 kDa band to two 59 kDa and 53 kDa bands (Song & Howlett, 1995). In the splice variant mCB1a, these putative glycosylation sites are still present, whereas in mCB1b, two of the three glycosylation sites are removed by splicing, thus explaining the lower molecular weight. The functional significance of the N-glycosylation in the N-terminal domain of the CB1 receptor is not yet clear (Vizi & Lajtha, 2008). N-terminal tail deletion mutants with deletion of the first 89 amino acids of the human CB1 receptor (and thus, the first two putative N-glycosylation sites), remained stably expressed at the cell surface, suggesting that N-linked glycosylation may not be required for transport of CB1 receptor to the plasma membrane (Andersson *et al.*, 2003). However, in this study, receptor trafficking upon stimulation was not analyzed. In other GPCRs (e.g. β-adrenergic receptors and muscarinic receptors), mutations of N-glycosylation sites abolished glycosylation, but had no obvious effect on receptor expression and function (Dohlman *et al.*, 1991).

The mCB1a and mCB1b splice variants demonstrated significant differences from mCB1 in agonist-induced internalization analyzed in stably expressing cell lines. Both novel splice variants had increased surface receptor loss in response to increasing concentrations of the agonist WIN55,212-2. Furthermore, the time course of internalization in response to 1 µM WIN55,212-2 was different, as mCB1a and mCB1b showed significantly faster internalization together with a stronger reduction of surface receptors compared with the unspliced mCB1 receptor. As the two splice variants with shortened N-termini showed very similar trafficking to each other, it is unlikely that the differences in N-linked glycosylation induced the increased surface receptor loss. Thus, either shortening of the N-terminal tail or the loss of a specific functional domain formed by amino acids missing in the splice variants leads to the observed stronger internalization. It was previously shown that phosphorylation of residues in the distal C-terminus play a role in endocytosis of the CB1 receptor (Daigle *et al.*, 2008*b*), but until now it has not been studied whether the N-terminal tail is involved in the regulation of receptor trafficking.

Agonist-induced stimulation of cells expressing the mCB1 receptor resulted in a transient activation of p44/42 MAPK phosphorylation with the classical response (Dalton & Howlett, 2012): a maximal response in the first 5 min followed by a rapid decline after 5-10 min. Cells expressing mCB1a showed a similar response to cells expressing mCB1. Stimulation of cells expressing mCB1b led to significantly decreased p44/42 MAPK activation at 5 min with a lower and slightly delayed peak after 7.5 min. The rapid decline after agonist-induced p44/42 MAPK activation was similar for mCB1b as compared with mCB1 and mCB1a. Previously, it was shown that the duration of p44/42 MAPK

activation by the CB1 receptor is regulated by receptor desensitization (uncoupling of receptor signal transduction) and not by internalization of the receptor (Daigle *et al.*, 2008*a*). The rapid decline in ERK phosphorylation after 5-10 minutes involves PKA inhibition and serine/threonine phosphatase activation (Dalton & Howlett, 2012). As the rapid decline of p44/p42 MAPK phosphorylation was similar for mCB1, mCB1a and mCB1b, receptor desensitization seems to be unchanged in the splice variants. However, the peak p44/42 MAPK activation is significantly lower in cells with stable expression of mCB1b. It was shown that the maximal response of p44/p42 MAPK activation depends on receptor-stimulated ligand-independent transactivation of multiple receptor tyrosine kinases, requires $G_{i/o}$ βγ subunit-stimulated phosphatidylinositol 3-kinase activation and Src kinase activation, and is modulated by inhibition of cAMP/PKA (Dalton & Howlett, 2012). Thus, it is possible that in cells expressing the mCB1b variant, one or several of these kinases were less potently recruited. One might speculate that differences in N-linked glycosylation of the N-termini could account for the different maximal responses, as it was also shown that the human splice variant hCB1a, which also lacks two of the three putative glycosylation motifs, also displayed a reduced MAPK activity after agonist-induced stimulation (Rinaldi-Carmona *et al.*, 1996). However, in this study dose-dependent MAPK activation was measured after 10 min. At this time point, MAPK activity would be expected to decline from the maximal response. The possibility that loss of N-linked glycosylation of the N-terminus leads to reduced peak MAPK activation needs to be carefully tested by comparing the maximal p44/p42 MAPK activation in CB1 receptors with mutations in one or several of the glycosylated Asn residues in the N-terminus. Furthermore, it would be interesting to analyze the maximal response in these mutants upon inhibition of the kinases that were shown to be involved in the strength of p44/p42 MAPK activation (Dalton & Howlett, 2012).

Differences in ligand binding might be another possible explanation for the different p44/p42 MAPK activation in mCB1b. Ligand binding properties of the novel splice variants have not yet been investigated *per se*. The hydrophobic nature of cannabinoid ligands suggests that their binding site is localized within the 7-TM bundle of the receptor (McAllister *et al.*, 2002). Andersson *et al.* (2003) showed that up to 89 amino acids of the N-terminal tail of the CB1 receptor can be deleted without affecting binding to the ligand CP55,940. Two binding regions were described: TM helices 3-4-5 for aminoylkylindoles (like WIN55,212-2) and TM helices 3-6-7 for other agonist classes like CP55,940 and the endogenous cannabinoids (Abood, 2005). Until now there is no definite implication of the N-terminal tail in agonist binding, as several studies described similar agonist binding properties for the human CB1 receptor and both its splice variants (Rinaldi-Carmona *et al.*, 1996; Xiao *et al.*, 2008), although one study found differences in agonist binding between the three variants (Ryberg *et al.*, 2005). The opposing data are probably caused by differences between the cell types, expression systems and stimulation protocols used (Xiao *et al.*, 2008).

Recently, Straiker *et al.* (2012) compared signaling properties of the rat CB1 receptor, the human CB1 receptor and the splice variants of the human CB1 receptor in autaptic hippocampal neurons, an expression system that is much closer to the actual brain physiology than expression systems using immortalized cell lines. The authors found that the human CB1 receptor rescued DSE less efficient than the rat CB1 receptor, whereas the human splice variants hCB1a and hCB1b both fully rescued DSE. With this study, the authors pointed out the necessity to better characterize the differences between the human situation and the rodent model systems often used to study pathological phenotypes. The physiological relevance of the novel splice variants of the mouse CB1 receptor is not yet clear, and might be expected to be modest due to their low expression on mRNA level. However, the splice variants can be a valuable tool to improve our understanding of CB1 receptor signaling and trafficking, in particular the role of the N-terminal domain and conformational alterations brought upon by posttranslational modifications.

4.4.2 Exon-intron structure of the mouse *Cnr1* 5' UTR

The mouse *Cnr1* gene is more complex than it was previously described. The updated *Cnr1* gene structure presented in this thesis contains 7 exons separated by 6 introns and has two retained introns in exon 7 (see 4.4.1). The *Cnr1* gene produces several transcript variants in hippocampus, caudate putamen and cerebellum with different 5' UTR exon assemblies. By combining the results from RT-PCR and 5' RLM-RACE, it could be shown that the transcripts in which exon 1-7 and exon 2-7 are spliced together represent mature CB1 receptor transcripts. These transcript variants are both described in the Ensembl database (Cnr-001 and Cnr-003, see 4.1.3). Furthermore, it was also demonstrated that transcripts with different combinations of the non-coding exons and either exon junction 5-7 or 6-7 are generated. In an analysis of expressed sequence tags of mouse genes (Strausberg *et al.*, 2002), a cDNA clone representing several of the exons identified in this thesis was described (exon 1-2a-3-4-5-7, BC075644.1 in the NCBI nucleotide database). Furthermore, a processed transcript containing exons 1-2a-5 is described in the Ensembl database (Cnr-002, see 4.1.3). Northern blot analysis with probes against the different exons could help to confirm which 5' UTR exon combinations are spliced together in mature mRNA transcripts.

In this thesis, three different exons were identified to have 5' transcription start sites. In exon 1 and 2, several putative transcription initiation sites were identified. It is unlikely that premature termination of the reverse transcriptase reaction could have generated the 5' ends of these cDNAs, as the adapter sequence was present in each cloned insert and the adapter RNA was added before the reverse transcriptase reaction. Of course it cannot be excluded that immature or degraded transcripts were ligated to the adapter sequence before the reverse transcriptase reaction, but in another study, multiple CB1 transcription start sites for exon 1 were identified as well (McCaw *et al.*,

2004), suggesting that transcription initiation can occur at several positions. All identified transcription starting points for exon 1 and 2 were downstream of the starting points described in the NCBI and Ensembl databases. A search for CpG islands (short stretches of CpG dinucleotides which are predominantly hypo-methylated and tend to be associated with genes that are frequently switched on) in the mouse *Cnr1* gene with the EMBOSS CpGplot tool (http://www.ebi.ac.uk/Tools/emboss/cpgplot/) identified a putative CpG island stretching 600 bp upstream of exon 1 and containing exon 1, suggesting that this is a frequent transcription initiation point. The possibility that the transcript variant with the transcription start in exon 6 was identified from an immature transcript cannot be excluded, as this variant was only identified once during the RACE experiment. However, in the human *CNR1* gene, a similar exon containing a transcription start site was identified in a RACE experiment (Zhang *et al.*, 2004). This exon (corresponding to exon 6 described in this thesis) was described to be located upstream of a 2.3 kb intron upstream of the coding exon. The authors confirmed the existence of this transcript with Northern blot analysis, but found that that the expression of mRNA transcripts containing this exon was very low (Zhang *et al.*, 2004). Thus, the existence and physiological relevance of this transcript variant still needs to be determined for the mouse.

Analysis of the contribution of transcripts with different 5' UTRs to the overall amount of CB1 receptor mRNA revealed that the transcript variant with exon junction 1-7 is the major transcript in caudate putamen, hippocampus and cerebellum. The transcript variant with exon junction 2-7 represents around 10-20% and the transcripts variants with exon junctions 5-7 and 6-7 represent less than 2% of the whole CB1 receptor CDS transcript. As the sum of all analyzed transcripts did not differ from the amount of CB1 receptor CDS transcript, it can be concluded that the principal transcripts were identified in this work. The contribution of the splice variants containing exon junctions 1-7, 2-7, 5-6 and 6-7 is different between caudate putamen, hippocampus and cerebellum. This indicates brain region-specific regulation of the transcription of the *Cnr1* gene.

The possible cell-type specificity of the transcript variants was analyzed in several brain regions of cortical glutamatergic and forebrain GABAergic CB1 receptor knock-out mice. As a starting point for this analysis, the expression levels of CB1 receptor mRNA in caudate putamen, hippocampus and cerebellum were assessed. In the caudate putamen, the majority of neurons are GABAergic medium spiny neurons with a strong CB1 receptor expression (Marsicano & Lutz, 1999). In the Glu-CB1$^{-/-}$, CB1 receptor expression was unchanged as compared with the wild type, whereas less than 1% CB1 receptor expression was found in the GABA-CB1$^{-/-}$. In the hippocampus, GABAergic interneurons express high levels of CB1 receptor, whereas glutamatergic neurons express the CB1 receptor in lower levels (Marsicano & Lutz, 1999). A reduction of CB1 receptor expression of 34% was found in

Glu-CB1$^{-/-}$ and a reduction of 72% in GABA-CB1$^{-/-}$. In the cerebellum, expression levels were unchanged. These quantifications confirm the findings with mRNA *in situ* analyses of Monory *et al.* (2006) and, for the first time, contribute quantitative data.

In the caudate putamen, comparison of the contribution of the different transcripts to the very strongly decreased overall amount of CB1 receptor mRNA revealed that the percentage of transcripts containing exon junction 5-7 is significantly higher in GABA-CB1$^{-/-}$ animals than in wild-type or Glu-CB1$^{-/-}$ animals, representing about half of the total of all exon junctions as compared with 1 to 2% in wild type and Glu-CB1$^{-/-}$. As the CB1 receptor is deleted from GABAergic medium spiny neurons, the remaining CB1 receptor might be located in another cell type with a different CB1 receptor transcript composition. One possibility is that the detected CB1 receptor mRNA originates from astrocytes, as it was previously shown that astrocytes in the caudate putamen express CB1 receptor (Rodríguez *et al.*, 2001; Stella, 2010). To test this hypothesis, it would be very interesting to analyze the transcript composition in the caudate putamen of the recently generated astroglial-specific CB1 receptor knock-out mouse (GFAP-CB1$^{-/-}$, Han *et al.*, 2012) and a double knock-out generated by crossing GABA-CB1$^{-/-}$ with GFAP-CB1$^{-/-}$. In the hippocampus, a decreased percentage of transcripts containing exon junction 2-7 was observed in Glu-CB1$^{-/-}$ animals, whereas this percentage was increased in GABA-CB1$^{-/-}$ animals. The changes in transcript composition were in the range of 5-10%, thus excluding the use of completely different transcript variants for expression of CB1 receptor in glutamatergic and GABAergic neurons. However, this suggests that CB1 receptor expression in glutamatergic and GABAergic neurons is fine-tuned by the use of different transcript variants. Recently, CB1 receptor expression was shown to be differentially affected in GABAergic and glutamatergic neurons in a mouse model of Huntington's disease (Chiodi *et al.*, 2012), thus emphasizing the importance of the mechanisms underlying the differential regulation of CB1 receptor expression in different cell types or brain regions.

4.4.3 Conclusions

Until now, the gene structure of the mouse *Cnr1* gene was poorly characterized, although the mouse is the most frequently used model system used to investigate the role of CB1 receptor signaling for a better understanding of human pathologies and treatment options. In this thesis, two novel CB1 receptor splice variants with shorter N-termini were identified in the mouse. In addition, analysis of the exon-intron structure of the mouse *Cnr1* gene revealed that the gene contains a much more complex 5' UTR than it was previously assumed. These findings on the exon-intron structure of the mouse *Cnr1* gene add to a better understanding of regulatory processes and allelic variations contributing to pathological phenotypes observed in the rodent model.

References

Abood ME (2005). Molecular biology of cannabinoid receptors. In *Cannabinoids – Handbook of Experimental Pharmacology Volume 168,* ed. Pertwee R, pp. 81–115. Springer, Germany.

Alger BE (2002). Retrograde signaling in the regulation of synaptic transmission: focus on endocannabinoids. *Prog Neurobiol* **68,** 247–286.

Alger BE & Kim J (2011). Supply and demand for endocannabinoids. *Trends Neurosci* **34,** 304–315.

Andersson H, D'Antona AM, Kendall DA, Von Heijne G & Chin C-N (2003). Membrane assembly of the cannabinoid receptor 1: impact of a long N-terminal tail. *Mol Pharmacol* **64,** 570–577.

Aparisi Rey A, Viveros M-P & Lutz B (2012). Biphasic effects of cannabinoids in anxiety responses: CB1 cannabinoid receptor in the balance of GABAergic and glutamatergic neurotransmission. *Neuropsychopharmacology*, manuscript accepted.

Ashton JC, Smith PF & Darlington CL (2008). The effect of delta 9-tetrahydrocannabinol on the extinction of an adverse associative memory. *Pharmacology* **81,** 18–20.

Azad SC, Monory K, Marsicano G, Cravatt BF, Lutz B, Zieglgänsberger W & Rammes G (2004). Circuitry for associative plasticity in the amygdala involves endocannabinoid signaling. *J Neurosci* **24,** 9953–9961.

Balthasar N *et al.* (2005). Divergence of melanocortin pathways in the control of food intake and energy expenditure. *Cell* **123,** 493–505.

Bambico FR, Katz N, Debonnel G & Gobbi G (2007). Cannabinoids elicit antidepressant-like behavior and activate serotonergic neurons through the medial prefrontal cortex. *J Neurosci* **27,** 11700–11711.

Begriche K, Levasseur PR, Zhang J, Rossi J, Skorupa D, Solt LA, Young B, Burris TP, Marks DL, Mynatt RL & Butler AA (2011). Genetic dissection of the functions of the melanocortin-3 receptor, a seven-transmembrane G-protein-coupled receptor, suggests roles for central and peripheral receptors in energy homeostasis. *J Biol Chem* **286,** 40771–40781.

Beinfeld MC & Connolly K (2001). Activation of CB1 cannabinoid receptors in rat hippocampal slices inhibits potassium-evoked cholecystokinin release, a possible mechanism contributing to the spatial memory defects produced by cannabinoids. *Neurosci Lett* **301,** 69–71.

Bellocchio L, Lafenetre P, Cannich A, Cota D, Puente N, Grandes P, Chaouloff F, Piazza PV & Marsicano G (2010). Bimodal control of stimulated food intake by the endocannabinoid system. *Nat Neurosci* **13,** 281–283.

Bénard G *et al.* (2012). Mitochondrial CB(1) receptors regulate neuronal energy metabolism. *Nat Neurosci* **15,** 558–564.

Ben-Ari Y & Cossart R (2000). Kainate, a double agent that generates seizures: two decades of progress. *Trends Neurosci* **23,** 580–587.

Benyamina A, Kebir O, Blecha L, Reynaud M & Krebs M-O (2011). CNR1 gene polymorphisms in addictive disorders: a systematic review and a meta-analysis. *Addict Biol* **16,** 1–6.

Benzinou M, Chèvre J-C, Ward KJ, Lecoeur C, Dina C, Lobbens S, Durand E, Delplanque J, Horber FF, Heude B, Balkau B, Borch-Johnsen K, Jørgensen T, Hansen T, Pedersen O, Meyre D & Froguel P (2008). Endocannabinoid receptor 1 gene variations increase risk for obesity and modulate body mass index in European populations. *Hum Mol Genet* **17,** 1916–1921.

Bermudez-Silva FJ, Cardinal P & Cota D (2012). The role of the endocannabinoid system in the neuroendocrine regulation of energy balance. *J Psychopharmacol (Oxford)* **26,** 114–124.

Berthoud H-R (2007). Interactions between the "cognitive" and "metabolic" brain in the control of food intake. *Physiol Behav* **91,** 486–498.

Bhaskaran MD & Smith BN (2010*a*). Cannabinoid-mediated inhibition of recurrent excitatory circuitry in the dentate gyrus in a mouse model of temporal lobe epilepsy. *PLoS ONE* **5,** e10683.

Bhaskaran MD & Smith BN (2010*b*). Effects of TRPV1 activation on synaptic excitation in the dentate gyrus of a mouse model of temporal lobe epilepsy. *Exp Neurol* **223,** 529–536.

Bitencourt RM, Pamplona FA & Takahashi RN (2008). Facilitation of contextual fear memory extinction and anti-anxiogenic effects of AM404 and cannabidiol in conditioned rats. *Eur Neuropsychopharmacol* **18,** 849–859.

Blankman JL, Simon GM & Cravatt BF (2007). A comprehensive profile of brain enzymes that hydrolyze the endocannabinoid 2-arachidonoylglycerol. *Chem Biol* **14,** 1347–1356.

Blázquez C *et al.* (2011). Loss of striatal type 1 cannabinoid receptors is a key pathogenic factor in Huntington's disease. *Brain* **134,** 119 –136.

Börner C, Bedini A, Höllt V & Kraus J (2008). Analysis of promoter regions regulating basal and interleukin-4-inducible expression of the human CB1 receptor gene in T lymphocytes. *Mol Pharmacol* **73,** 1013–1019.

Bouaboula M, Poinot-Chazel C, Bourrié B, Canat X, Calandra B, Rinaldi-Carmona M, Le Fur G & Casellas P (1995). Activation of mitogen-activated protein kinases by stimulation of the central cannabinoid receptor CB1. *Biochem J* **312,** 637–641.

Bradford MM (1976). A rapid and sensitive method for the quantitation of microgram quantities of protein utilizing the principle of protein-dye binding. *Anal Biochem* **72,** 248–254.

Bradley A, Evans M, Kaufman MH & Robertson E (1984). Formation of germ-line chimaeras from embryo-derived teratocarcinoma cell lines. *Nature* **309,** 255–256.

Cadogan AK, Alexander SP, Boyd EA & Kendall DA (1997). Influence of cannabinoids on electrically evoked dopamine release and cyclic AMP generation in the rat striatum. *J Neurochem* **69,** 1131–1137.

Calignano A, La Rana G, Giuffrida A & Piomelli D (1998). Control of pain initiation by endogenous cannabinoids. *Nature* **394,** 277–281.

Campos AC, Ferreira FR, Guimarães FS & Lemos JI (2010). Facilitation of endocannabinoid effects in the ventral hippocampus modulates anxiety-like behaviors depending on previous stress experience. *Neuroscience* **167,** 238–246.

Cannich A, Wotjak CT, Kamprath K, Hermann H, Lutz B & Marsicano G (2004). CB1 cannabinoid receptors modulate kinase and phosphatase activity during extinction of conditioned fear in mice. *Learn Mem* **11,** 625–632.

Carlson G, Wang Y & Alger BE (2002). Endocannabinoids facilitate the induction of LTP in the hippocampus. *Nat Neurosci* **5,** 723–724.

Cassano T, Gaetani S, Macheda T, Laconca L, Romano A, Morgese MG, Cimmino CS, Chiarotti F, Bambico FR, Gobbi G, Cuomo V & Piomelli D (2011). Evaluation of the emotional phenotype and serotonergic neurotransmission of fatty acid amide hydrolase-deficient mice. *Psychopharmacology (Berl)* **214,** 465–476.

Chakrabarti A, Onaivi ES & Chaudhuri G (1995). Cloning and sequencing of a cDNA encoding the mouse brain-type cannabinoid receptor protein. *DNA Seq* **5,** 385–388.

Chavarría-Siles I, Contreras-Rojas J, Hare E, Walss-Bass C, Quezada P, Dassori A, Contreras S, Medina R, Ramírez M, Salazar R, Raventos H & Escamilla MA (2008). Cannabinoid receptor 1 gene

(CNR1) and susceptibility to a quantitative phenotype for hebephrenic schizophrenia. *Am J Med Genet B Neuropsychiatr Genet* **147,** 279–284.

Chavez AE, Chiu CQ & Castillo PE (2010). TRPV1 activation by endogenous anandamide triggers postsynaptic long-term depression in dentate gyrus. *Nat Neurosci* **13,** 1511–1518.

Chen X, Williamson VS, An S-S, Hettema JM, Aggen SH, Neale MC & Kendler KS (2008). Cannabinoid receptor 1 gene association with nicotine dependence. *Arch Gen Psychiatry* **65,** 816–824.

Chevaleyre V & Castillo PE (2003). Heterosynaptic LTD of hippocampal GABAergic synapses: a novel role of endocannabinoids in regulating excitability. *Neuron* **38,** 461–472.

Chhatwal JP, Davis M, Maguschak KA & Ressler KJ (2005). Enhancing cannabinoid neurotransmission augments the extinction of conditioned fear. *Neuropsychopharmacology* **30,** 516–524.

Chhatwal JP, Gutman AR, Maguschak KA, Bowser ME, Yang Y, Davis M & Ressler KJ (2009). Functional interactions between endocannabinoid and CCK neurotransmitter systems may be critical for extinction learning. *Neuropsychopharmacology* **34,** 509–521.

Childers SR & Deadwyler SA (1996). Role of cyclic AMP in the actions of cannabinoid receptors. *Biochem Pharmacol* **52,** 819–827.

Chiodi V, Uchigashima M, Beggiato S, Ferrante A, Armida M, Martire A, Potenza RL, Ferraro L, Tanganelli S, Watanabe M, Domenici MR & Popoli P (2012). Unbalance of CB1 receptors expressed in GABAergic and glutamatergic neurons in a transgenic mouse model of Huntington's disease. *Neurobiol Dis* **45,** 983–991.

Coryell MW, Wunsch AM, Haenfler JM, Allen JE, McBride JL, Davidson BL & Wemmie JA (2008). Restoring acid-sensing ion channel-1a in the amygdala of knock-out mice rescues fear memory but not unconditioned fear responses. *J Neurosci* **28,** 13738–13741.

Cota D, Marsicano G, Tschöp M, Grübler Y, Flachskamm C, Schubert M, Auer D, Yassouridis A, Thöne-Reineke C, Ortmann S, Tomassoni F, Cervino C, Nisoli E, Linthorst ACE, Pasquali R, Lutz B, Stalla GK & Pagotto U (2003). The endogenous cannabinoid system affects energy balance via central orexigenic drive and peripheral lipogenesis. *J Clin Invest* **112,** 423–431.

Cravatt BF, Giang DK, Mayfield SP, Boger DL, Lerner RA & Gilula NB (1996). Molecular characterization of an enzyme that degrades neuromodulatory fatty-acid amides. *Nature* **384,** 83–87.

Curia G, Longo D, Biagini G, Jones RSG & Avoli M (2008). The pilocarpine model of temporal lobe epilepsy. *J Neurosci Methods* **172,** 143–157.

Daigle TL, Kearn CS & Mackie K (2008*a*). Rapid CB1 cannabinoid receptor desensitization defines the time course of ERK1/2 MAP kinase signaling. *Neuropharmacology* **54,** 36–44.

Daigle TL, Kwok ML & Mackie K (2008*b*). Regulation of CB1 cannabinoid receptor internalization by a promiscuous phosphorylation-dependent mechanism. *J Neurochem* **106,** 70–82.

Dalton GD & Howlett AC (2012). Cannabinoid CB(1) receptors transactivate multiple receptor tyrosine kinases and regulate serine/threonine kinases to activate ERK in neuronal cells. *Br J Pharmacol* **165,** 2497–2511.

Deadwyler SA, Hampson RE, Mu J, Whyte A & Childers S (1995). Cannabinoids modulate voltage sensitive potassium A-current in hippocampal neurons via a cAMP-dependent process. *J Pharmacol Exp Ther* **273,** 734–743.

Delgado MR, Nearing KI, Ledoux JE & Phelps EA (2008). Neural circuitry underlying the regulation of conditioned fear and its relation to extinction. *Neuron* **59,** 829–838.

Derkinderen P, Ledent C, Parmentier M & Girault JA (2001). Cannabinoids activate p38 mitogen-activated protein kinases through CB1 receptors in hippocampus. *J Neurochem* **77,** 957–960.

Derkinderen P, Toutant M, Burgaya F, Le Bert M, Siciliano JC, de Franciscis V, Gelman M & Girault JA (1996). Regulation of a neuronal form of focal adhesion kinase by anandamide. *Science* **273,** 1719–1722.

Derkinderen P, Valjent E, Toutant M, Corvol J-C, Enslen H, Ledent C, Trzaskos J, Caboche J & Girault J-A (2003). Regulation of extracellular signal-regulated kinase by cannabinoids in hippocampus. *J Neurosci* **23,** 2371–2382.

Devane WA, Hanus L, Breuer A, Pertwee RG, Stevenson LA, Griffin G, Gibson D, Mandelbaum A, Etinger A & Mechoulam R (1992). Isolation and structure of a brain constituent that binds to the cannabinoid receptor. *Science* **258,** 1946–1949.

Dinh TP, Carpenter D, Leslie FM, Freund TF, Katona I, Sensi SL, Kathuria S & Piomelli D (2002). Brain monoglyceride lipase participating in endocannabinoid inactivation. *Proc Natl Acad Sci USA* **99,** 10819–10824.

Dohlman HG, Thorner J, Caron MG & Lefkowitz RJ (1991). Model systems for the study of seven-transmembrane-segment receptors. *Annu Rev Biochem* **60,** 653–688.

Domenici MR, Azad SC, Marsicano G, Schierloh A, Wotjak CT, Dodt H-U, Zieglgänsberger W, Lutz B & Rammes G (2006). Cannabinoid receptor type 1 located on presynaptic terminals of principal neurons in the forebrain controls glutamatergic synaptic transmission. *J Neurosci* **26,** 5794–5799.

Dooley TP, Miranda M, Jones NC & DePamphilis ML (1989). Transactivation of the adenovirus EIIa promoter in the absence of adenovirus E1A protein is restricted to mouse oocytes and preimplantation embryos. *Development* **107,** 945–956.

Dragatsis I & Zeitlin S (2001). A method for the generation of conditional gene repair mutations in mice. *Nucleic Acids Res* **29,** E10.

Dubreucq S, Matias I, Cardinal P, Häring, Martin M, Lutz B, Marsicano G & Chaouloff F (2012). Genetic dissection of the role of cannabinoid type-1 receptors in the emotional consequences of repeated social stress in mice. *Neuropsychopharmacology*; DOI: 10.1038/npp.2012.36.

Falenski KW, Carter DS, Harrison AJ, Martin BR, Blair RE & DeLorenzo RJ (2009). Temporal characterization of changes in hippocampal cannabinoid CB1 receptor expression following pilocarpine-induced status epilepticus. *Brain Res* **1262,** 64–72.

Fanselow MS (1980). Conditioned and unconditional components of post-shock freezing. *Pavlov J Biol Sci* **15,** 177–182.

Flicek P *et al.* (2011). Ensembl 2011. *Nucleic Acids Res* **39,** D800–806.

Foldy C, Lee SY, Szabadics J, Neu A & Soltesz I (2007). Cell type-specific gating of perisomatic inhibition by cholecystokinin. *Nat Neurosci* **10,** 1128–1130.

Forlino A, Porter FD, Lee EJ, Westphal H & Marini JC (1999). Use of the Cre/lox recombination system to develop a non-lethal knock-in murine model for osteogenesis imperfecta with an alpha1(I) G349C substitution. Variability in phenotype in BrtlIV mice. *J Biol Chem* **274,** 37923–37931.

Fowler CJ & Jacobsson SOP (2002). Cellular transport of anandamide, 2-arachidonoylglycerol and palmitoylethanolamide-targets for drug development? *Prostaglandins Leukot Essent Fatty Acids* **66,** 193–200.

Freund TF, Katona I & Piomelli D (2003). Role of endogenous cannabinoids in synaptic signaling. *Physiol Rev* **83,** 1017–1066.

Frost M, Nielsen TL, Wraae K, Hagen C, Piters E, Beckers S, De Freitas F, Brixen K, Van Hul W & Andersen M (2010). Polymorphisms in the endocannabinoid receptor 1 in relation to fat mass distribution. *Eur J Endocrinol* **163,** 407–412.

Fu J, Bottegoni G, Sasso O, Bertorelli R, Rocchia W, Masetti M, Guijarro A, Lodola A, Armirotti A, Garau G, Bandiera T, Reggiani A, Mor M, Cavalli A & Piomelli D (2012). A catalytically silent FAAH-1 variant drives anandamide transport in neurons. *Nat Neurosci* **15,** 64–69.

Galve-Roperh I, Rueda D, Gómez del Pulgar T, Velasco G & Guzmán M (2002). Mechanism of extracellular signal-regulated kinase activation by the CB(1) cannabinoid receptor. *Mol Pharmacol* **62,** 1385–1392.

Ganon-Elazar E & Akirav I (2009). Cannabinoid receptor activation in the basolateral amygdala blocks the effects of stress on the conditioning and extinction of inhibitory avoidance. *J Neurosci* **29,** 11078–11088.

Gaoni Y & Mechoulam R (1964). Isolation, structure, and partial synthesis of an active constituent of hashish. *J Am Chem Soc* **86,** 1646–1647.

Gérard CM, Mollereau C, Vassart G & Parmentier M (1991). Molecular cloning of a human cannabinoid receptor which is also expressed in testis. *Biochem J* **279,** 129–134.

Gerdeman GL, Ronesi J & Lovinger DM (2002). Postsynaptic endocannabinoid release is critical to long-term depression in the striatum. *Nat Neurosci* **5,** 446–451.

Gerstein H, O'Riordan K, Osting S, Schwarz M & Burger C (2012). Rescue of synaptic plasticity and spatial learning deficits in the hippocampus of Homer1 knockout mice by recombinant Adeno-associated viral gene delivery of Homer1c. *Neurobiol Learn Mem* **97,** 17–29.

Gifford AN & Ashby CR Jr (1996). Electrically evoked acetylcholine release from hippocampal slices is inhibited by the cannabinoid receptor agonist, WIN 55212-2, and is potentiated by the cannabinoid antagonist, SR 141716A. *J Pharmacol Exp Ther* **277,** 1431–1436.

Gobbi G, Bambico FR, Mangieri R, Bortolato M, Campolongo P, Solinas M, Cassano T, Morgese MG, Debonnel G, Duranti A, Tontini A, Tarzia G, Mor M, Trezza V, Goldberg SR, Cuomo V & Piomelli D (2005). Antidepressant-like activity and modulation of brain monoaminergic transmission by blockade of anandamide hydrolysis. *Proc Natl Acad Sci USA* **102,** 18620–18625.

Gómez del Pulgar T, Velasco G & Guzmán M (2000). The CB1 cannabinoid receptor is coupled to the activation of protein kinase B/Akt. *Biochem J* **347,** 369–373.

Graham BM, Langton JM & Richardson R (2011). Pharmacological enhancement of fear reduction: preclinical models. *Br J Pharmacol* **164,** 1230–1247.

Guggenhuber S, Monory K, Lutz B & Klugmann M (2010). AAV vector-mediated overexpression of CB1 cannabinoid receptor in pyramidal neurons of the hippocampus protects against seizure-induced excitoxicity. *PLoS ONE* **5,** e15707.

Guindon J & Hohmann AG (2009). The endocannabinoid system and pain. *CNS Neurol Disord Drug Targets* **8,** 403–421.

Gulyas AI, Cravatt BF, Bracey MH, Dinh TP, Piomelli D, Boscia F & Freund TF (2004). Segregation of two endocannabinoid-hydrolyzing enzymes into pre- and postsynaptic compartments in the rat hippocampus, cerebellum and amygdala. *Eur J Neurosci* **20,** 441–458.

Haj-Dahmane S & Shen R-Y (2005). The wake-promoting peptide orexin-B inhibits glutamatergic transmission to dorsal raphe nucleus serotonin neurons through retrograde endocannabinoid signaling. *J Neurosci* **25,** 896–905.

Haller J, Barna I, Barsvari B, Gyimesi Pelczer K, Yasar S, Panlilio LV & Goldberg S (2009). Interactions between environmental aversiveness and the anxiolytic effects of enhanced cannabinoid signaling by FAAH inhibition in rats. *Psychopharmacology (Berl)* **204,** 607–616.

Haller J, Mátyás F, Soproni K, Varga B, Barsy B, Németh B, Mikics E, Freund TF & Hájos N (2007). Correlated species differences in the effects of cannabinoid ligands on anxiety and on GABAergic and glutamatergic synaptic transmission. *Eur J Neurosci* **25,** 2445–2456.

Haller J, Varga B, Ledent C, Barna I & Freund TF (2004*a*). Context-dependent effects of CB1 cannabinoid gene disruption on anxiety-like and social behaviour in mice. *Eur J Neurosci* **19,** 1906–1912.

Haller J, Varga B, Ledent C & Freund TF (2004*b*). CB1 cannabinoid receptors mediate anxiolytic effects: convergent genetic and pharmacological evidence with CB1-specific agents. *Behav Pharmacol* **15,** 299–304.

Hamilton DL & Abremski K (1984). Site-specific recombination by the bacteriophage P1 lox-Cre system. Cre-mediated synapsis of two lox sites. *J Mol Biol* **178,** 481–486.

Han J, Kesner P, Metna-Laurent M, Duan T, Xu L, Georges F, Koehl M, Abrous DN, Mendizabal-Zubiaga J, Grandes P, Liu Q, Bai G, Wang W, Xiong L, Ren W, Marsicano G & Zhang X (2012). Acute cannabinoids impair working memory through astroglial CB1 receptor modulation of hippocampal LTD. *Cell* **148,** 1039–1050.

Han J-H, Kushner SA, Yiu AP, Cole CJ, Matynia A, Brown RA, Neve RL, Guzowski JF, Silva AJ & Josselyn SA (2007). Neuronal competition and selection during memory formation. *Science* **316,** 457–460.

Häring M, Cannich A, Monory K, Marsicano G & Lutz B (2012). Identification of the cannabinoid CB1 receptor in subcortical vGluT2-positive glutamatergic neurons. *J Comp Neurol.*, manuscript in revision.

Häring M, Kaiser N, Monory K & Lutz B (2011). Circuit specific functions of cannabinoid CB1 receptor in the balance of investigatory drive and exploration. *PLoS ONE* **6,** e26617.

Hashimotodani Y, Ohno-Shosaku T & Kano M (2007). Endocannabinoids and synaptic function in the CNS. *Neuroscientist* **13,** 127–137.

Hashimotodani Y, Ohno-Shosaku T, Tsubokawa H, Ogata H, Emoto K, Maejima T, Araishi K, Shin H-S & Kano M (2005). Phospholipase Cbeta serves as a coincidence detector through its Ca2+ dependency for triggering retrograde endocannabinoid signal. *Neuron* **45,** 257–268.

Haughey HM, Marshall E, Schacht JP, Louis A & Hutchison KE (2008). Marijuana withdrawal and craving: influence of the cannabinoid receptor 1 (CNR1) and fatty acid amide hydrolase (FAAH) genes. *Addiction* **103,** 1678–1686.

Herkenham M, Lynn AB, de Costa BR & Richfield EK (1991). Neuronal localization of cannabinoid receptors in the basal ganglia of the rat. *Brain Res* **547,** 267–274.

Hermann H & Lutz B (2005). Coexpression of the cannabinoid receptor type 1 with the corticotropin-releasing hormone receptor type 1 in distinct regions of the adult mouse forebrain. *Neurosci Lett* **375,** 13–18.

Herry C, Ferraguti F, Singewald N, Letzkus JJ, Ehrlich I & Lüthi A (2010). Neuronal circuits of fear extinction. *Eur J Neurosci* **31,** 599–612.

Herry C & Garcia R (2002). Prefrontal cortex long-term potentiation, but not long-term depression, is associated with the maintenance of extinction of learned fear in mice. *J Neurosci* **22,** 577–583.

Hill MN, McLaughlin RJ, Bingham B, Shrestha L, Lee TTY, Gray JM, Hillard CJ, Gorzalka BB & Viau V (2010). Endogenous cannabinoid signaling is essential for stress adaptation. *Proc Natl Acad Sci USA* **107,** 9406–9411.

Hnasko TS, Perez FA, Scouras AD, Stoll EA, Gale SD, Luquet S, Phillips PEM, Kremer EJ & Palmiter RD (2006). Cre recombinase-mediated restoration of nigrostriatal dopamine in dopamine-deficient mice reverses hypophagia and bradykinesia. *Proc Natl Acad Sci U S A* **103,** 8858–8863.

Ho B-C, Wassink TH, Ziebell S & Andreasen NC (2011). Cannabinoid receptor 1 gene polymorphisms and marijuana misuse interactions on white matter and cognitive deficits in schizophrenia. *Schizophr Res* **128,** 66–75.

Hoffman AF, Laaris N, Kawamura M, Masino SA & Lupica CR (2010). Control of cannabinoid CB1 receptor function on glutamate axon terminals by endogenous adenosine acting at A1 receptors. *J Neurosci* **30,** 545–555.

Holzenberger M, Lenzner C, Leneuve P, Zaoui R, Hamard G, Vaulont S & Le Bouc Y (2000). Cre-mediated germline mosaicism: a method allowing rapid generation of several alleles of a target gene. *Nucleic Acids Res* **28,** e92–e92.

Howlett AC, Barth F, Bonner TI, Cabral G, Casellas P, Devane WA, Felder CC, Herkenham M, Mackie K, Martin BR, Mechoulam R & Pertwee RG (2002). International Union of Pharmacology. XXVII. Classification of cannabinoid receptors. *Pharmacol Rev* **54,** 161–202.

Hsieh C, Brown S, Derleth C & Mackie K (1999). Internalization and recycling of the CB1 cannabinoid receptor. *J Neurochem* **73,** 493–501.

Ishac EJ, Jiang L, Lake KD, Varga K, Abood ME & Kunos G (1996). Inhibition of exocytotic noradrenaline release by presynaptic cannabinoid CB1 receptors on peripheral sympathetic nerves. *Br J Pharmacol* **118,** 2023–2028.

Jacob W, Yassouridis A, Marsicano G, Monory K, Lutz B & Wotjak CT (2009). Endocannabinoids render exploratory behaviour largely independent of the test aversiveness: role of glutamatergic transmission. *Genes Brain Behav* **8,** 685–698.

Jennings EA, Vaughan CW & Christie MJ (2001). Cannabinoid actions on rat superficial medullary dorsal horn neurons in vitro. *J Physiol (Lond)* **534,** 805–812.

Kamprath K, Marsicano G, Tang J, Monory K, Bisogno T, Di Marzo V, Lutz B & Wotjak CT (2006). Cannabinoid CB1 receptor mediates fear extinction via habituation-like processes. *J Neurosci* **26,** 6677–6686.

Kamprath K, Plendl W, Marsicano G, Deussing JM, Wurst W, Lutz B & Wotjak CT (2009). Endocannabinoids mediate acute fear adaptation via glutamatergic neurons independently of corticotropin-releasing hormone signaling. *Genes Brain Behav* **8,** 203–211.

Kamprath K, Romo-Parra H, Häring M, Gaburro S, Doengi M, Lutz B & Pape H-C (2011). Short-term adaptation of conditioned fear responses through endocannabinoid signaling in the central amygdala. *Neuropsychopharmacology* **36,** 652–663.

Kamprath K & Wotjak CT (2004). Nonassociative learning processes determine expression and extinction of conditioned fear in mice. *Learn Mem* **11,** 770–786.

Kano M, Ohno-Shosaku T, Hashimotodani Y, Uchigashima M & Watanabe M (2009). Endocannabinoid-mediated control of synaptic transmission. *Physiol Rev* **89,** 309–380.

Karlócai MR, Tóth K, Watanabe M, Ledent C, Juhász G, Freund TF & Maglóczky Z (2011). Redistribution of CB1 cannabinoid receptors in the acute and chronic phases of pilocarpine-induced epilepsy. *PLoS ONE* **6,** e27196.

Kathuria S, Gaetani S, Fegley D, Valiño F, Duranti A, Tontini A, Mor M, Tarzia G, La Rana G, Calignano A, Giustino A, Tattoli M, Palmery M, Cuomo V & Piomelli D (2003). Modulation of anxiety through blockade of anandamide hydrolysis. *Nat Med* **9,** 76–81.

Katona I & Freund TF (2008). Endocannabinoid signaling as a synaptic circuit breaker in neurological disease. *Nat Med* **14,** 923–930.

Katona I, Rancz EA, Acsady L, Ledent C, Mackie K, Hajos N & Freund TF (2001). Distribution of CB1 cannabinoid receptors in the amygdala and their role in the control of GABAergic transmission. *J Neurosci* **21,** 9506–9518.

Katona I, Sperlágh B, Sík A, Köfalvi A, Vizi ES, Mackie K & Freund TF (1999). Presynaptically located CB1 cannabinoid receptors regulate GABA release from axon terminals of specific hippocampal interneurons. *J Neurosci* **19,** 4544–4558.

Katona I, Urbán GM, Wallace M, Ledent C, Jung K-M, Piomelli D, Mackie K & Freund TF (2006). Molecular composition of the endocannabinoid system at glutamatergic synapses. *J Neurosci* **26,** 5628–5637.

Kawamura Y, Fukaya M, Maejima T, Yoshida T, Miura E, Watanabe M, Ohno-Shosaku T & Kano M (2006). The CB1 cannabinoid receptor is the major cannabinoid receptor at excitatory presynaptic sites in the hippocampus and cerebellum. *J Neurosci* **26,** 2991–3001.

Kim J, Isokawa M, Ledent C & Alger BE (2002). Activation of muscarinic acetylcholine receptors enhances the release of endogenous cannabinoids in the hippocampus. *J Neurosci* **22,** 10182–10191.

Kirkham TC, Williams CM, Fezza F & Di Marzo V (2002). Endocannabinoid levels in rat limbic forebrain and hypothalamus in relation to fasting, feeding and satiation: stimulation of eating by 2-arachidonoyl glycerol. *Br J Pharmacol* **136,** 550–557.

Kobilo T, Hazvi S & Dudai Y (2007). Role of cortical cannabinoid CB1 receptor in conditioned taste aversion memory. *Eur J Neurosci* **25,** 3417–3421.

Kozak KR, Prusakiewicz JJ & Marnett LJ (2004). Oxidative metabolism of endocannabinoids by COX-2. *Curr Pharm Des* **10,** 659–667.

Kreitzer AC & Regehr WG (2001). Retrograde inhibition of presynaptic calcium influx by endogenous cannabinoids at excitatory synapses onto Purkinje cells. *Neuron* **29,** 717–727.

Kreitzer AC & Regehr WG (2002). Retrograde signaling by endocannabinoids. *Curr Opin Neurobiol* **12,** 324–330.

Laaris N, Good CH & Lupica CR (2010). Delta9-tetrahydrocannabinol is a full agonist at CB1 receptors on GABA neuron axon terminals in the hippocampus. *Neuropharmacology* **59,** 121–127.

Lafenêtre P, Chaouloff F & Marsicano G (2007). The endocannabinoid system in the processing of anxiety and fear and how CB1 receptors may modulate fear extinction. *Pharmacol Res* **56,** 367–381.

Lafenêtre P, Chaouloff F & Marsicano G (2009). Bidirectional regulation of novelty-induced behavioral inhibition by the endocannabinoid system. *Neuropharmacology* **57,** 715–721.

Lakso M, Pichel JG, Gorman JR, Sauer B, Okamoto Y, Lee E, Alt FW & Westphal H (1996). Efficient in vivo manipulation of mouse genomic sequences at the zygote stage. *Proc Natl Acad Sci U S A* **93,** 5860–5865.

LeDoux JE (2000). Emotion circuits in the brain. *Annu Rev Neurosci* **23,** 155–184.

Lee S, Ahmed T, Lee S, Kim H, Choi S, Kim D-S, Kim SJ, Cho J & Shin H-S (2012). Bidirectional modulation of fear extinction by mediodorsal thalamic firing in mice. *Nat Neurosci* **15,** 308–314.

Lee S-H, Földy C & Soltesz I (2010). Distinct endocannabinoid control of GABA release at perisomatic and dendritic synapses in the hippocampus. *J Neurosci* **30,** 7993–8000.

Lévénés C, Daniel H, Soubrié P & Crépel F (1998). Cannabinoids decrease excitatory synaptic transmission and impair long-term depression in rat cerebellar Purkinje cells. *J Physiol (Lond)* **510 (Pt 3),** 867–879.

Lieb W, Manning AK, Florez JC, Dupuis J, Cupples LA, McAteer JB, Vasan RS, Hoffmann U, O'Donnell CJ, Meigs JB & Fox CS (2009). Variants in the CNR1 and the FAAH genes and adiposity traits in the community. *Obesity (Silver Spring)* **17,** 755–760.

Lim LP & Burge CB (2001). A computational analysis of sequence features involved in recognition of short introns. *Proc Natl Acad Sci USA* **98,** 11193–11198.

Lin H-C, Mao S-C, Chen P-S & Gean P-W (2008). Chronic cannabinoid administration in vivo compromises extinction of fear memory. *Learn Mem* **15,** 876–884.

Lin H-C, Mao S-C & Gean P-W (2006). Effects of intra-amygdala infusion of CB1 receptor agonists on the reconsolidation of fear-potentiated startle. *Learn Mem* **13,** 316–321.

Lin H-C, Mao S-C, Su C-L & Gean P-W (2009). The role of prefrontal cortex CB1 receptors in the modulation of fear memory. *Cereb Cortex* **19,** 165–175.

Lin P-Y, Wang S-P, Tai M-Y & Tsai Y-F (2010). Differential involvement of medial prefrontal cortex and basolateral amygdala extracellular signal-regulated kinase in extinction of conditioned taste aversion is dependent on different intervals of extinction following conditioning. *Neuroscience* **171,** 125–133.

Lisboa SF, Resstel LBM, Aguiar DC & Guimarães FS (2008). Activation of cannabinoid CB1 receptors in the dorsolateral periaqueductal gray induces anxiolytic effects in rats submitted to the Vogel conflict test. *Eur J Pharmacol* **593,** 73–78.

Long JZ, Nomura DK, Vann RE, Walentiny DM, Booker L, Jin X, Burston JJ, Sim-Selley LJ, Lichtman AH, Wiley JL & Cravatt BF (2009). Dual blockade of FAAH and MAGL identifies behavioral processes regulated by endocannabinoid crosstalk in vivo. *Proc Natl Acad Sci USA* **106,** 20270–20275.

Lourenco J, Cannich A, Carta M, Coussen F, Mulle C & Marsicano G (2010). Synaptic activation of kainate receptors gates presynaptic CB1 signaling at GABAergic synapses. *Nat Neurosci* **13,** 197–204.

de Luca C, Kowalski TJ, Zhang Y, Elmquist JK, Lee C, Kilimann MW, Ludwig T, Liu S-M & Chua SC Jr (2005). Complete rescue of obesity, diabetes, and infertility in db/db mice by neuron-specific LEPR-B transgenes. *J Clin Invest* **115,** 3484–3493.

Ludányi A, Eross L, Czirják S, Vajda J, Halász P, Watanabe M, Palkovits M, Maglóczky Z, Freund TF & Katona I (2008). Downregulation of the CB1 cannabinoid receptor and related molecular elements of the endocannabinoid system in epileptic human hippocampus. *J Neurosci* **28,** 2976–2990.

Mackie K, Lai Y, Westenbroek R & Mitchell R (1995). Cannabinoids activate an inwardly rectifying potassium conductance and inhibit Q-type calcium currents in AtT20 cells transfected with rat brain cannabinoid receptor. *J Neurosci* **15,** 6552–6561.

Maejima T, Hashimoto K, Yoshida T, Aiba A & Kano M (2001). Presynaptic inhibition caused by retrograde signal from metabotropic glutamate to cannabinoid receptors. *Neuron* **31,** 463–475.

Maejima T, Oka S, Hashimotodani Y, Ohno-Shosaku T, Aiba A, Wu D, Waku K, Sugiura T & Kano M (2005). Synaptically driven endocannabinoid release requires Ca2+-assisted metabotropic glutamate receptor subtype 1 to phospholipase Cbeta4 signaling cascade in the cerebellum. *J Neurosci* **25,** 6826–6835.

Maglóczky Z, Tóth K, Karlócai R, Nagy S, Erőss L, Czirják S, Vajda J, Rásonyi G, Kelemen A, Juhos V, Halász P, Mackie K & Freund TF (2010). Dynamic changes of CB1 receptor expression in hippocampi of epileptic mice and humans. *Epilepsia* **51,** 115–120.

Mailleux P & Vanderhaeghen J-J (1992). Distribution of neuronal cannabinoid receptor in the adult rat brain: A comparative receptor binding radioautography and in situ hybridization histochemistry. *Neuroscience* **48,** 655–668.

Manwell LA, Satvat E, Lang ST, Allen CP, Leri F & Parker LA (2009). FAAH inhibitor, URB-597, promotes extinction and CB(1) antagonist, SR141716, inhibits extinction of conditioned aversion produced by naloxone-precipitated morphine withdrawal, but not extinction of conditioned preference produced by morphine in rats. *Pharmacol Biochem Behav* **94,** 154–162.

Marrs WR *et al.* (2010). The serine hydrolase ABHD6 controls the accumulation and efficacy of 2-AG at cannabinoid receptors. *Nat Neurosci* **13,** 951–957.

Marsicano G (2001). Physiological role of the cannabinoid receptor 1 (CB1) in the murine central nervous system. *PhD thesis*.

Marsicano G, Goodenough S, Monory K, Hermann H, Eder M, Cannich A, Azad SC, Cascio MG, Gutiérrez SO, van der Stelt M, López-Rodriguez ML, Casanova E, Schütz G, Zieglgänsberger W, Di Marzo V, Behl C & Lutz B (2003). CB1 cannabinoid receptors and on-demand defense against excitotoxicity. *Science* **302,** 84–88.

Marsicano G & Kuner R (2008). Anatomical distribution of receptors, ligands and enzymes in the brain and in the spinal cord: circuitries and neurochemistry. In *Cannabinoids and the Brain*, ed. Köfalvi A, pp. 161–201. Springer US, Boston, MA.

Marsicano G & Lutz B (1999). Expression of the cannabinoid receptor CB1 in distinct neuronal subpopulations in the adult mouse forebrain. *Eur J Neurosci* **11,** 4213–4225.

Marsicano G, Wotjak CT, Azad SC, Bisogno T, Rammes G, Cascio MG, Hermann H, Tang J, Hofmann C, Zieglgansberger W, Di Marzo V & Lutz B (2002). The endogenous cannabinoid system controls extinction of aversive memories. *Nature* **418,** 530–534.

Martin M, Ledent C, Parmentier M, Maldonado R & Valverde O (2002). Involvement of CB1 cannabinoid receptors in emotional behaviour. *Psychopharmacology (Berl)* **159,** 379–387.

Di Marzo V, Goparaju SK, Wang L, Liu J, Bátkai S, Járai Z, Fezza F, Miura GI, Palmiter RD, Sugiura T & Kunos G (2001). Leptin-regulated endocannabinoids are involved in maintaining food intake. *Nature* **410,** 822–825.

Di Marzo V & Maccarrone M (2008). FAAH and anandamide: is 2-AG really the odd one out? *Trends Pharmacol Sci* **29,** 229–233.

Di Marzo V & Matias I (2005). Endocannabinoid control of food intake and energy balance. *Nat Neurosci* **8,** 585–589.

Massa F, Mancini G, Schmidt H, Steindel F, Mackie K, Angioni C, Oliet SHR, Geisslinger G & Lutz B (2010). Alterations in the hippocampal endocannabinoid system in diet-induced obese mice. *J Neurosci* **30,** 6273–6281.

Matias I & Di Marzo V (2007). Endocannabinoids and the control of energy balance. *Trends Endocrinol Metab* **18,** 27–37.

Matlin AJ, Clark F & Smith CWJ (2005). Understanding alternative splicing: towards a cellular code. *Nat Rev Mol Cell Biol* **6,** 386–398.

Matsuda LA, Lolait SJ, Brownstein MJ, Young AC & Bonner TI (1990). Structure of a cannabinoid receptor and functional expression of the cloned cDNA. *Nature* **346,** 561–564.

Mátyás F, Yanovsky Y, Mackie K, Kelsch W, Misgeld U & Freund TF (2006). Subcellular localization of type 1 cannabinoid receptors in the rat basal ganglia. *Neuroscience* **137,** 337–361.

McAllister SD, Tao Q, Barnett-Norris J, Buehner K, Hurst DP, Guarnieri F, Reggio PH, Nowell Harmon KW, Cabral GA & Abood ME (2002). A critical role for a tyrosine residue in the cannabinoid receptors for ligand recognition. *Biochem Pharmacol* **63,** 2121–2136.

McCaw EA, Hu H, Gomez GT, Hebb ALO, Kelly MEM & Denovan-Wright EM (2004). Structure, expression and regulation of the cannabinoid receptor gene (CB1) in Huntington's disease transgenic mice. *Eur J Biochem* **271,** 4909–4920.

McCormick DA & Contreras D (2001). On the cellular and network bases of epileptic seizures. *Annu Rev Physiol* **63,** 815–846.

McDonald AJ & Mascagni F (2001). Localization of the CB1 type cannabinoid receptor in the rat basolateral amygdala: high concentrations in a subpopulation of cholecystokinin-containing interneurons. *Neuroscience* **107,** 641–652.

McDonald NA, Henstridge CM, Connolly CN & Irving AJ (2007). Generation and functional characterization of fluorescent, N-terminally tagged CB1 receptor chimeras for live-cell imaging. *Mol Cell Neurosci* **35,** 237–248.

McGaugh JL (2002). Memory consolidation and the amygdala: a systems perspective. *Trends Neurosci* **25,** 456.

McLaughlin RJ, Hill MN & Gorzalka BB (2009). Monoaminergic neurotransmission contributes to cannabinoid-induced activation of the hypothalamic-pituitary-adrenal axis. *Eur J Pharmacol* **624,** 71–76.

Mechoulam R, Ben-Shabat S, Hanus L, Ligumsky M, Kaminski NE, Schatz AR, Gopher A, Almog S, Martin BR & Compton DR (1995). Identification of an endogenous 2-monoglyceride, present in canine gut, that binds to cannabinoid receptors. *Biochem Pharmacol* **50,** 83–90.

Millan MJ (2003). The neurobiology and control of anxious states. *Prog Neurobiol* **70,** 83–244.

Monory K *et al.* (2006). The endocannabinoid system controls key epileptogenic circuits in the hippocampus. *Neuron* **51,** 455–466.

Monory K, Blaudzun H, Massa F, Kaiser N, Lemberger T, Schütz G, Wotjak CT, Lutz B & Marsicano G (2007). Genetic dissection of behavioural and autonomic effects of Delta(9)-tetrahydrocannabinol in mice. *PLoS Biol* **5,** e269.

Monory K & Lutz B (2008). The endocannabinoid system as a therapeutic target in epilepsy. In *Cannabinoids and the Brain*, ed. Köfalvi A, pp. 407–422. Springer US, Boston, MA.

Monteleone P, Bifulco M, Di Filippo C, Gazzerro P, Canestrelli B, Monteleone F, Proto MC, Di Genio M, Grimaldi C & Maj M (2009). Association of CNR1 and FAAH endocannabinoid gene polymorphisms with anorexia nervosa and bulimia nervosa: evidence for synergistic effects. *Genes Brain Behav* **8,** 728–732.

Moreira FA, Kaiser N, Monory K & Lutz B (2008). Reduced anxiety-like behaviour induced by genetic and pharmacological inhibition of the endocannabinoid-degrading enzyme fatty acid amide hydrolase (FAAH) is mediated by CB1 receptors. *Neuropharmacology* **54,** 141–150.

Morgan NH, Stanford IM & Woodhall GL (2009). Functional CB2 type cannabinoid receptors at CNS synapses. *Neuropharmacology* **57,** 356–368.

Morton GJ, Cummings DE, Baskin DG, Barsh GS & Schwartz MW (2006). Central nervous system control of food intake and body weight. *Nature* **443,** 289–295.

Mu J, Zhuang SY, Kirby MT, Hampson RE & Deadwyler SA (1999). Cannabinoid receptors differentially modulate potassium A and D currents in hippocampal neurons in culture. *J Pharmacol Exp Ther* **291,** 893–902.

Munro S, Thomas KL & Abu-Shaar M (1993). Molecular characterization of a peripheral receptor for cannabinoids. *Nature* **365,** 61–65.

Murphy WJ, Eizirik E, Johnson WE, Zhang YP, Ryder OA & O'Brien SJ (2001). Molecular phylogenetics and the origins of placental mammals. *Nature* **409,** 614–618.

Myers KM & Davis M (2007). Mechanisms of fear extinction. *Mol Psychiatry* **12,** 120–150.

Nader K, Schafe GE & Le Doux JE (2000). Fear memories require protein synthesis in the amygdala for reconsolidation after retrieval. *Nature* **406,** 722–726.

Naderi N, Haghparast A, Saber-Tehrani A, Rezaii N, Alizadeh A-M, Khani A & Motamedi F (2008). Interaction between cannabinoid compounds and diazepam on anxiety-like behaviour of mice. *Pharmacol Biochem Behav* **89,** 64–75.

Nagy A (2000). Cre recombinase: the universal reagent for genome tailoring. *Genesis* **26,** 99–109.

Nagy A, Moens C, Ivanyi E, Pawling J, Gertsenstein M, Hadjantonakis AK, Pirity M & Rossant J (1998). Dissecting the role of N-myc in development using a single targeting vector to generate a series of alleles. *Curr Biol* **8,** 661–664.

Naidu PS, Varvel SA, Ahn K, Cravatt BF, Martin BR & Lichtman AH (2007). Evaluation of fatty acid amide hydrolase inhibition in murine models of emotionality. *Psychopharmacology (Berl)* **192,** 61–70.

Nakazi M, Bauer U, Nickel T, Kathmann M & Schlicker E (2000). Inhibition of serotonin release in the mouse brain via presynaptic cannabinoid CB1 receptors. *Naunyn Schmiedebergs Arch Pharmacol* **361,** 19–24.

Nicoll G, Davidson S, Shanley L, Hing B, Lear M, McGuffin P, Ross R & Mackenzie A (2012). Allele-specific differences in activity of a novel cannabinoid receptor 1 (CNR1) gene intronic enhancer in hypothalamus, dorsal root ganglia, and hippocampus. *J Biol Chem* **287,** 12828–12834.

Niyuhire F, Varvel SA, Thorpe AJ, Stokes RJ, Wiley JL & Lichtman AH (2007). The disruptive effects of the CB1 receptor antagonist rimonabant on extinction learning in mice are task-specific. *Psychopharmacology* **191,** 223–231.

Nordström R & Andersson H (2006). Amino-terminal processing of the human cannabinoid receptor 1. *J Recept Signal Transduct Res* **26,** 259–267.

Ohno-Shosaku T, Maejima T & Kano M (2001). Endogenous cannabinoids mediate retrograde signals from depolarized postsynaptic neurons to presynaptic terminals. *Neuron* **29,** 729–738.

Ohno-Shosaku T, Shosaku J, Tsubokawa H & Kano M (2002*a*). Cooperative endocannabinoid production by neuronal depolarization and group I metabotropic glutamate receptor activation. *Eur J Neurosci* **15,** 953–961.

Ohno-Shosaku T, Tsubokawa H, Mizushima I, Yoneda N, Zimmer A & Kano M (2002*b*). Presynaptic cannabinoid sensitivity is a major determinant of depolarization-induced retrograde suppression at hippocampal synapses. *J Neurosci* **22,** 3864–3872.

Okahisa Y, Kodama M, Takaki M, Inada T, Uchimura N, Yamada M, Iwata N, Iyo M, Sora I, Ozaki N & Ujike H (2011). Association study of two cannabinoid receptor genes, CNR1 and CNR2, with methamphetamine dependence. *Curr Neuropharmacol* **9,** 183–189.

de Oliveira Alvares L, Pasqualini Genro B, Diehl F, Molina VA & Quillfeldt JA (2008). Opposite action of hippocampal CB1 receptors in memory reconsolidation and extinction. *Neuroscience* **154,** 1648–1655.

Onaivi ES, Chakrabarti A & Chaudhuri G (1996). Cannabinoid receptor genes. *Prog Neurobiol* **48,** 275–305.

Onaivi ES, Leonard CM, Ishiguro H, Zhang PW, Lin Z, Akinshola BE & Uhl GR (2002). Endocannabinoids and cannabinoid receptor genetics. *Prog Neurobiol* **66,** 307–344.

Page ME, Oropeza VC & Van Bockstaele EJ (2008). Local administration of a cannabinoid agonist alters norepinephrine efflux in the rat frontal cortex. *Neurosci Lett* **431,** 1–5.

Page ME, Oropeza VC, Sparks SE, Qian Y, Menko AS & Van Bockstaele EJ (2007). Repeated cannabinoid administration increases indices of noradrenergic activity in rats. *Pharmacol Biochem Behav* **86,** 162–168.

Pamplona FA, Bitencourt RM & Takahashi RN (2008). Short- and long-term effects of cannabinoids on the extinction of contextual fear memory in rats. *Neurobiol Learn Mem* **90,** 290–293.

Pamplona FA, Prediger RDS, Pandolfo P & Takahashi RN (2006). The cannabinoid receptor agonist WIN 55,212-2 facilitates the extinction of contextual fear memory and spatial memory in rats. *Psychopharmacology* **188,** 641–649.

Pan B, Wang W, Long JZ, Sun D, Hillard CJ, Cravatt BF & Liu Q (2009). Blockade of 2-arachidonoylglycerol hydrolysis by selective monoacylglycerol lipase inhibitor 4-nitrophenyl 4-(dibenzo[d][1,3]dioxol-5-yl(hydroxy)methyl)piperidine-1-carboxylate (JZL184) Enhances retrograde endocannabinoid signaling. *J Pharmacol Exp Ther* **331,** 591–597.

Pan B, Wang W, Zhong P, Blankman JL, Cravatt BF & Liu Q (2011). Alterations of endocannabinoid signaling, synaptic plasticity, learning, and memory in monoacylglycerol lipase knock-out mice. *J Neurosci* **31,** 13420–13430.

Pape H-C & Paré D (2010). Plastic synaptic networks of the amygdala for the acquisition, expression, and extinction of conditioned fear. *Physiol Rev* **90,** 419–463.

Paré D (2003). Role of the basolateral amygdala in memory consolidation. *Prog Neurobiol* **70,** 409–420.

Patel S & Hillard CJ (2008). Adaptations in endocannabinoid signaling in response to repeated homotypic stress: a novel mechanism for stress habituation. *Eur J Neurosci* **27,** 2821–2829.

Patel S, Roelke CT, Rademacher DJ & Hillard CJ (2005). Inhibition of restraint stress-induced neural and behavioural activation by endogenous cannabinoid signalling. *Eur J Neurosci* **21,** 1057–1069.

Paxinos G & Franklin KBJ (2008). *The mouse brain in stereotaxic coordinates, third edition: the coronal plates and diagrams*, 3rd edn. Academic Press.

Pfaffl MW, Horgan GW & Dempfle L (2002). Relative expression software tool (REST©) for group-wise comparison and statistical analysis of relative expression results in real-time PCR. *Nucleic Acids Res* **30,** e36–e36.

Phillips RG & LeDoux JE (1992). Differential contribution of amygdala and hippocampus to cued and contextual fear conditioning. *Behav Neurosci* **106,** 274–285.

Piomelli D (2003). The molecular logic of endocannabinoid signalling. *Nat Rev Neurosci* **4,** 873–884.

Plendl W & Wotjak CT (2010). Dissociation of within- and between-session extinction of conditioned fear. *J Neurosci* **30,** 4990–4998.

Puente N, Cui Y, Lassalle O, Lafourcade M, Georges F, Venance L, Grandes P & Manzoni OJ (2011). Polymodal activation of the endocannabinoid system in the extended amygdala. *Nat Neurosci* **14,** 1542–1547.

Quarta C *et al.* (2010). CB(1) signaling in forebrain and sympathetic neurons is a key determinant of endocannabinoid actions on energy balance. *Cell Metab* **11,** 273–285.

Quarta C, Mazza R, Obici S, Pasquali R & Pagotto U (2011). Energy balance regulation by endocannabinoids at central and peripheral levels. *Trends Mol Med* **17,** 518–526.

Quirk GJ & Mueller D (2008). Neural mechanisms of extinction learning and retrieval. *Neuropsychopharmacology* **33,** 56–72.

Racine RJ (1972). Modification of seizure activity by electrical stimulation. II. Motor seizure. *Electroencephalogr Clin Neurophysiol* **32,** 281–294.

Rademacher DJ, Meier SE, Shi L, Ho W-SV, Jarrahian A & Hillard CJ (2008). Effects of acute and repeated restraint stress on endocannabinoid content in the amygdala, ventral striatum, and medial prefrontal cortex in mice. *Neuropharmacology* **54,** 108–116.

Radulovic J & Tronson NC (2010). Molecular specificity of multiple hippocampal processes governing fear extinction. *Rev Neurosci* **21,** 1–17.

Reich CG, Mohammadi MH & Alger BE (2008). Endocannabinoid modulation of fear responses: learning and state-dependent performance effects. *J Psychopharmacol (Oxford)* **22,** 769–777.

Rideout 3rd WM, Wakayama T, Wutz A, Eggan K, Jackson-Grusby L, Dausman J, Yanagimachi R & Jaenisch R (2000). Generation of mice from wild-type and targeted ES cells by nuclear cloning. *Nat Genet* **24,** 109–110.

Rinaldi-Carmona M, Calandra B, Shire D, Bouaboula M, Oustric D, Barth F, Casellas P, Ferrara P & Le Fur G (1996). Characterization of two cloned human CB1 cannabinoid receptor isoforms. *J Pharmacol Exp Ther* **278,** 871–878.

Robbe D, Kopf M, Remaury A, Bockaert J & Manzoni OJ (2002). Endogenous cannabinoids mediate long-term synaptic depression in the nucleus accumbens. *Proc Natl Acad Sci USA* **99,** 8384–8388.

Roberto M, Cruz M, Bajo M, Siggins GR, Parsons LH & Schweitzer P (2010). The endocannabinoid system tonically regulates inhibitory transmission and depresses the effect of ethanol in central amygdala. *Neuropsychopharmacology* **35,** 1962–1972.

Roche M, O'Connor E, Diskin C & Finn DP (2007). The effect of CB(1) receptor antagonism in the right basolateral amygdala on conditioned fear and associated analgesia in rats. *Eur J Neurosci* **26,** 2643–2653.

Rodríguez JJ, Mackie K & Pickel VM (2001). Ultrastructural Localization of the CB1 Cannabinoid Receptor in M-Opioid Receptor Patches of the Rat Caudate Putamen Nucleus. *J Neurosci* **21,** 823–833.

Roohbakhsh A, Keshavarz S, Hasanein P, Rezvani ME & Moghaddam AH (2009). Role of endocannabinoid system in the ventral hippocampus of rats in the modulation of anxiety-like behaviours. *Basic Clin Pharmacol Toxicol* **105,** 333–338.

Rossi S, De Chiara V, Musella A, Kusayanagi H, Mataluni G, Bernardi G, Usiello A & Centonze D (2008). Chronic psychoemotional stress impairs cannabinoid-receptor-mediated control of GABA transmission in the striatum. *J Neurosci* **28,** 7284–7292.

Rossi S, De Chiara V, Musella A, Sacchetti L, Cantarella C, Castelli M, Cavasinni F, Motta C, Studer V, Bernardi G, Cravatt BF, Maccarrone M, Usiello A & Centonze D (2010). Preservation of striatal cannabinoid CB1 receptor function correlates with the antianxiety effects of fatty acid amide hydrolase inhibition. *Mol Pharmacol* **78,** 260–268.

Rubino T, Guidali C, Vigano D, Realini N, Valenti M, Massi P & Parolaro D (2008*a*). CB1 receptor stimulation in specific brain areas differently modulate anxiety-related behaviour. *Neuropharmacology* **54,** 151–160.

Rubino T, Realini N, Castiglioni C, Guidali C, Viganó D, Marras E, Petrosino S, Perletti G, Maccarrone M, Di Marzo V & Parolaro D (2008*b*). Role in anxiety behavior of the endocannabinoid system in the prefrontal cortex. *Cereb Cortex* **18,** 1292–1301.

Rueda D, Galve-Roperh I, Haro A & Guzmán M (2000). The CB(1) cannabinoid receptor is coupled to the activation of c-Jun N-terminal kinase. *Mol Pharmacol* **58,** 814–820.

Ruehle S, Aparisi Rey A, Remmers F & Lutz B (2012). The endocannabinoid system in anxiety, fear memory and habituation. *J Psychopharmacol (Oxford)* **26,** 23–39.

Ryberg E, Vu HK, Larsson N, Groblewski T, Hjorth S, Elebring T, Sjögren S & Greasley PJ (2005). Identification and characterisation of a novel splice variant of the human CB1 receptor. *FEBS Lett* **579,** 259–264.

Sagar DR, Gaw AG, Okine BN, Woodhams SG, Wong A, Kendall DA & Chapman V (2009). Dynamic regulation of the endocannabinoid system: implications for analgesia. *Mol Pain* **5,** 59.

Sambrook J, Russell DW & Sambrook DRJ (2001). *Molecular cloning: a laboratory manual*, 3rd edn. Cold Spring Harbor Laboratory.

Sammeth M, Foissac S & Guigó R (2008). A general definition and nomenclature for alternative splicing events. *PLoS Comput Biol* **4,** e1000147.

Sauer B (1998). Inducible gene targeting in mice using the Cre/lox system. *Methods* **14,** 381–392.

Scherma M, Medalie J, Fratta W, Vadivel SK, Makriyannis A, Piomelli D, Mikics E, Haller J, Yasar S, Tanda G & Goldberg SR (2008). The endogenous cannabinoid anandamide has effects on motivation and anxiety that are revealed by fatty acid amide hydrolase (FAAH) inhibition. *Neuropharmacology* **54,** 129–140.

Schleinitz D, Carmienke S, Böttcher Y, Tönjes A, Berndt J, Klöting N, Enigk B, Müller I, Dietrich K, Breitfeld J, Scholz GH, Engeli S, Stumvoll M, Blüher M & Kovacs P (2010). Role of genetic variation in the cannabinoid type 1 receptor gene (CNR1) in the pathophysiology of human obesity. *Pharmacogenomics* **11,** 693–702.

Schneider C (2007). Cell-type specific "rescue" of CB1 receptor-deficiency – generating a construct for homologous recombination. *Diploma thesis*.

Schwab MH, Bartholomae A, Heimrich B, Feldmeyer D, Druffel-Augustin S, Goebbels S, Naya FJ, Zhao S, Frotscher M, Tsai MJ & Nave KA (2000). Neuronal basic helix-loop-helix proteins (NEX and BETA2/Neuro D) regulate terminal granule cell differentiation in the hippocampus. *J Neurosci* **20,** 3714–3724.

Self DW (2005). Molecular and genetic approaches for behavioral analysis of protein function. *Biol Psychiatry* **57,** 1479–1484.

Shire D, Carillon C, Kaghad M, Calandra B, Rinaldi-Carmona M, Le Fur G, Caput D & Ferrara P (1995). An amino-terminal variant of the central cannabinoid receptor resulting from alternative splicing. *J Biol Chem* **270,** 3726–3731.

Sierra-Mercado D, Padilla-Coreano N & Quirk GJ (2011). Dissociable roles of prelimbic and infralimbic cortices, ventral hippocampus, and basolateral amygdala in the expression and extinction of conditioned fear. *Neuropsychopharmacology* **36,** 529–538.

Sigel E, Baur R, Rácz I, Marazzi J, Smart TG, Zimmer A & Gertsch J (2011). The major central endocannabinoid directly acts at GABA(A) receptors. *Proc Natl Acad Sci USA* **108,** 18150–18155.

Simon AB & Gorman JM (2006). Advances in the treatment of anxiety: targeting glutamate. *NeuroRx* **3,** 57–68.

Skarnes WC, Rosen B, West AP, Koutsourakis M, Bushell W, Iyer V, Mujica AO, Thomas M, Harrow J, Cox T, Jackson D, Severin J, Biggs P, Fu J, Nefedov M, de Jong PJ, Stewart AF & Bradley A (2011). A conditional knockout resource for the genome-wide study of mouse gene function. *Nature* **474,** 337–342.

Slanina KA & Schweitzer P (2005). Inhibition of cyclooxygenase-2 elicits a CB1-mediated decrease of excitatory transmission in rat CA1 hippocampus. *Neuropharmacology* **49,** 653–659.

Song C & Howlett AC (1995). Rat brain cannabinoid receptors are N-linked glycosylated proteins. *Life Sci* **56,** 1983–1989.

Sotres-Bayon F & Quirk GJ (2010). Prefrontal control of fear: more than just extinction. *Curr Opin Neurobiol* **20,** 231–235.

Steindel F, Häring M, Marsicano G, Lutz B & Monory K (2008). Differential coupling of G proteins to CB1 receptors in hippocampal glutamatergic and GABAergic neurons. In *18th Annual Symposium on the Cannabinoids*, p. 119. International Cannabinoid Research Society, Burlington, VT, USA.

Stella N (2010). Cannabinoid and cannabinoid-like receptors in microglia, astrocytes, and astrocytomas. *Glia* **58,** 1017–1030.

Stella N, Schweitzer P & Piomelli D (1997). A second endogenous cannabinoid that modulates long-term potentiation. *Nature* **388,** 773–778.

Straiker A, Wager-Miller J, Hutchens J & Mackie K (2012). Differential signalling in human cannabinoid CB(1) receptors and their splice variants in autaptic hippocampal neurones. *Br J Pharmacol* **165,** 2660–2671.

Strausberg RL *et al.* (2002). Generation and initial analysis of more than 15,000 full-length human and mouse cDNA sequences. *Proc Natl Acad Sci USA* **99,** 16899–16903.

Suzuki A, Josselyn SA, Frankland PW, Masushige S, Silva AJ & Kida S (2004). Memory reconsolidation and extinction have distinct temporal and biochemical signatures. *J Neurosci* **24,** 4787–4795.

Suzuki A, Mukawa T, Tsukagoshi A, Frankland PW & Kida S (2008). Activation of LVGCCs and CB1 receptors required for destabilization of reactivated contextual fear memories. *Learn Mem* **15,** 426–433.

Swanson LW & Petrovich GD (1998). What is the amygdala? *Trends Neurosci* **21,** 323–331.

Szabo B, Dörner L, Pfreundtner C, Nörenberg W & Starke K (1998). Inhibition of GABAergic inhibitory postsynaptic currents by cannabinoids in rat corpus striatum. *Neuroscience* **85,** 395–403.

Tan H, Lauzon NM, Bishop SF, Bechard MA & Laviolette SR (2010). Integrated cannabinoid CB1 receptor transmission within the amygdala-prefrontal cortical pathway modulates neuronal plasticity and emotional memory encoding. *Cereb Cortex* **20,** 1486–1496.

Terzian AL, Drago F, Wotjak CT & Micale V (2011). The dopamine and cannabinoid interaction in the modulation of emotions and cognition: assessing the role of cannabinoid CB1 receptor in neurons expressing dopamine D1 receptors. *Front Behav Neurosci* **5,** 49.

Thierry-Mieg D & Thierry-Mieg J (2006). AceView: a comprehensive cDNA-supported gene and transcripts annotation. *Genome Biol* **7 Suppl 1,** S12.1–14.

Trezza V & Vanderschuren LJMJ (2008). Cannabinoid and opioid modulation of social play behavior in adolescent rats: differential behavioral mechanisms. *Eur Neuropsychopharmacol* **18,** 519–530.

Tronson NC, Corcoran KA, Jovasevic V & Radulovic J (2012). Fear conditioning and extinction: emotional states encoded by distinct signaling pathways. *Trends in Neurosciences* **35,** 145–155.

Tronson NC & Taylor JR (2007). Molecular mechanisms of memory reconsolidation. *Nat Rev Neurosci* **8,** 262–275.

Twitchell W, Brown S & Mackie K (1997). Cannabinoids inhibit N- and P/Q-type calcium channels in cultured rat hippocampal neurons. *J Neurophysiol* **78,** 43–50.

Vidal-Gonzalez I, Vidal-Gonzalez B, Rauch SL & Quirk GJ (2006). Microstimulation reveals opposing influences of prelimbic and infralimbic cortex on the expression of conditioned fear. *Learn Mem* **13,** 728–733.

Viveros MP, Marco EM & File SE (2005). Endocannabinoid system and stress and anxiety responses. *Pharmacol Biochem Behav* **81,** 331–342.

Vizi ES & Lajtha A (2008). *Handbook of neurochemistry and molecular neurobiology: neurotransmitter systems*. Springer US, Boston, MA.

Wakita T, Taya C, Katsume A, Kato J, Yonekawa H, Kanegae Y, Saito I, Hayashi Y, Koike M & Kohara M (1998). Efficient conditional transgene expression in hepatitis C virus cDNA transgenic mice mediated by the Cre/loxP system. *J Biol Chem* **273,** 9001–9006.

Walf AA & Frye CA (2007). The use of the elevated plus maze as an assay of anxiety-related behavior in rodents. *Nat Protocols* **2,** 322–328.

Wallace MJ, Blair RE, Falenski KW, Martin BR & DeLorenzo RJ (2003). The endogenous cannabinoid system regulates seizure frequency and duration in a model of temporal lobe epilepsy. *J Pharmacol Exp Ther* **307,** 129–137.

Wettschureck N, van der Stelt M, Tsubokawa H, Krestel H, Moers A, Petrosino S, Schütz G, Di Marzo V & Offermanns S (2006). Forebrain-specific inactivation of Gq/G11 family G proteins results in age-dependent epilepsy and impaired endocannabinoid formation. *Mol Cell Biol* **26,** 5888–5894.

Wilson RI, Kunos G & Nicoll RA (2001). Presynaptic specificity of endocannabinoid signaling in the hippocampus. *Neuron* **31,** 453–462.

Wilson RI & Nicoll RA (2001). Endogenous cannabinoids mediate retrograde signalling at hippocampal synapses. *Nature* **410,** 588–592.

Wilson RI & Nicoll RA (2002). Endocannabinoid signaling in the brain. *Science* **296,** 678–682.

Wu D-F, Yang L-Q, Goschke A, Stumm R, Brandenburg L-O, Liang Y-J, Höllt V & Koch T (2008). Role of receptor internalization in the agonist-induced desensitization of cannabinoid type 1 receptors. *J Neurochem* **104,** 1132–1143.

Xiao JC, Jewell JP, Lin LS, Hagmann WK, Fong TM & Shen C-P (2008). Similar in vitro pharmacology of human cannabinoid CB1 receptor variants expressed in CHO cells. *Brain Res* **1238,** 36–43.

Yizhar O, Fenno LE, Prigge M, Schneider F, Davidson TJ, O/'Shea DJ, Sohal VS, Goshen I, Finkelstein J, Paz JT, Stehfest K, Fudim R, Ramakrishnan C, Huguenard JR, Hegemann P & Deisseroth K (2011). Neocortical excitation/inhibition balance in information processing and social dysfunction. *Nature* **477,** 171–178.

Zammit S, Spurlock G, Williams H, Norton N, Williams N, O'Donovan MC & Owen MJ (2007). Genotype effects of CHRNA7, CNR1 and COMT in schizophrenia: interactions with tobacco and cannabis use. *Br J Psychiatry* **191,** 402–407.

Zelinski EL, Hong NS, Tyndall AV, Halsall B & McDonald RJ (2010). Prefrontal cortical contributions during discriminative fear conditioning, extinction, and spontaneous recovery in rats. *Exp Brain Res* **203,** 285–297.

Zhang P-W, Ishiguro H, Ohtsuki T, Hess J, Carillo F, Walther D, Onaivi ES, Arinami T & Uhl GR (2004). Human cannabinoid receptor 1: 5′ exons, candidate regulatory regions, polymorphisms, haplotypes and association with polysubstance abuse. *Mol Psychiatry* **9,** 916–931.

Abbreviations

°C	degree Celsius
2-AG	2-arachidonoyl glycerol
5' RLM-RACE	5' RNA ligase-mediated rapid amplification of cDNA ends
AAV	adeno-associated virus
A	adenosine
ABHD6/12	α-β-hydrolase domain 6/12
ACSF	artificial cerebrospinal fluid
ad	adjust
AEA	anandamide
AM251	N-(piperidin-1-yl)-5-(4-iodophenyl)-1-(2,4-dichlorophenyl)-4-methyl-1H-pyrazole-3-carboxamide, a CB1 antagonist
AM404	n-(4-hydroxyphenyl)-arachidonoylamide, inhibitor of endocannabinoid uptake and/or metabolism
AM630	6-Iodo-2-methyl-1-[2-(4-morpholinyl)ethyl]-1H-indol-3-yl](4-methoxyphenyl) methanone, a CB2 receptor antagonist
ANOVA	analysis of variance
AP	anterior-posterior
BC	basket cells
BDNF	brain-derived neurotrophic factor
BLA	basolateral amygdala
bp	base pair
BSA	bovine serum albumine
C	cytidine
CA1/3	cornu ammonis 1/3
cAMP	cyclic adenosine monophosphate
CB1	cannabinoid type 1
CB1-RS	CB1 receptor complete rescue
CB2	cannabinoid type 2
CCK	cholecystokinin
cDNA	complementary DNA
CDS	coding sequence
CeA	central nucleus of the amygdala
Cer	cerebellum
CHAPS	3-[(3-Cholamidopropyl)dimethylammonio]-1-propanesulfonate
CNS	central nervous system
Cnr1	mouse gene encoding the CB1 receptor
CNR1	human gene encoding the CB1 receptor
COX-2	cyclooxygenase 2
CP55,940	(-)-cis-3-[2-hydroxy-4-(1,1-dimethylheptyl)phenyl]-trans-4-(3-hydroxypropyl) cyclohexanol, a CB1agonist
CPu	caudate putamen
cpm	counts per minute
Cre	recombinase from bacteriophage P1, induces recombination between loxP sites
CRHR1	corticotrophin releasing hormone receptor type 1
CS	conditioned stimulus
C-terminus	carboxy-terminus
Ctx	neocortex
Δ^9-THC	Δ^9-Tetrahydrocannabinol, a CB1 agonist
DAG	diacylglycerol

DAGL	DAG lipase
DAPI	4´,6-Diamidino-2-phenylindole
DMEM	Dulbecco´s modified Eagle´s medium
DMSO	dimethylsulfoxid
DNA	deoxyribonucleic acid
DNAse	deoxyribonuclease
DSE	depolarization-induced suppression of excitation
DSI	depolarization-induced suppression of inhibition
DV	dorso-ventral
eCB-STD	endocannabinoid-mediated short-term depression
ECS	endocannabinoid system
EDTA	ethylenediamine tetraacetic acid
EGTA	ethyleneglycol tetraacetic acid
eGFP	enhanced green fluorescent protein
E/I balance	excitatory-inhibitory balance
EP	entopeduncular nucleus
EPM	elevated plus maze
EPSC	excitatory postsynaptic current
EPSP	excitatory postsynaptic potentials
ER	endoplasmatic reticulum
ES cell	embryonic stem cell
FAAH	fatty acid amide hydrolase
FAK	focal adhesion kinase
FCS	fetal calf serum
Fig.	Figure
FITC	fluorescein isothiocyanate
FLAT	FAAH1 like AEA transporter
fwd	forward
g	gravitational force
G	genotype
G	guanosine
G418	Geneticin
GABA	gamma-aminobutyric acid
GABA-CB1$^{-/-}$	mouse line with specific deletion of the CB1 receptor from cortical and striatal GABAergic neurons
GAD65	glutamic acid decarboxylase 65k
Glu-CB1$^{-/-}$	mouse line with specific deletion of the CB1 receptor from cortical glutamatergic neurons
Glu-CB1-RS	cortical glutatamtergic rescue of CB1 receptor deficiency
GOI	gene of interest
GP	globus pallidus
GPCR	G-protein coupled receptor
Gusb	glucuronidase beta
HA tag	hemagglutinin tag
hCB1	human CB1
HEK	human ebryonic kidney
HEPES	(4-(2-hydroxyethyl)-1-piperazineethanesulfonic acid
Hip	hippocampus
HRP	horseradish peroxidase
HSV	herpes simplex virus
HU-210	(6aR)-trans-3-(1,1-dimethylhepthyl)-6a, 7, 10, 10atetrahydro-1-hydroxy-6,6-dimethyl-6Hdibenzo[b,d]pyran-9-methanol, a CB1 agonist

Hy	hypothalamus
IL	infralimbic cortex
i.p.	intraperitoneal
IPSC	inhibitory postsynaptic current
IPSP	inhibitory postsynaptic potential
JNK	c-Jun N-terminal kinase
KA	kainic acid
kb	kilobase
ko	knock-out
LD	light/dark
loxP	consensus 34 base pair DNA recognition sites for Cre recombinase
Ls	lateral septum
LTP	long-term potentiation
LY320135	4-[[6-Methoxy-2-(4-methoxyphenyl)-3-benzofuranyl]carbonyl]benzonitrile, a CB1 receptor antagonist
MAGL	monoglyceride lipase
MAPK	mitogen-activated protein kinase
MEF	mouse embryonic fibroblast
mCB1	mouse CB1
ML	medio-lateral
mPFC	medial prefrontal cortex
mRNA	messenger ribonucleic acid
Ms	medial septum
NAPE	N-arachidonoyl phosphatidylethanolamine
NAPE-PLD	NAPE-specific phospholipase D
NAT	N-acyltransferase
NCBI	National Center for Biotechnology Information
Neo^R	neomycin-resistance coding sequence
N-terminal	amino-terminal
pA	polyadenylation signal
PAG	periaqueductal gray
PAGE	polyacrylamide gel electrophoresis
PBS	phosphate buffered saline
PCR	polymerase chain reaction
PEA	phosphatidyl ethanolamine
PFA	paraformldehyde
PI	phosphatidyl inositol
PI3-K	phosphatidyl inositol-3-kinase
PKA	protein kinase A
PKB	protein kinase B/Akt
PLC	phospholipase C
PMSF	phenylmethanesulfonyl fluoride
qPCR	quantitative PCR
RACE	rapid amplification of cDNA ends
rcf	relative centrifugation force
rev	reverse
RNA	ribonucleic acid
RNase	ribonuclease
rmp	revolutions per minute
RT	room temperature
RT-PCR	reverse transcription-polymerase chain reaction
s.c.	subcutaneous
SCA	Schaffer-collateral associated cells

SDS	sodium dodecyl sulfate
SEM	standard error of the mean
SNP	single nucleotide polymorphism
SR141716	N-(piperidin-1-yl)-5-(4-chlorophenyl)-1-(2,4-dichlorophenyl)-4-methyl-1H-pyrazole-3-carboxamide HCl, also called rimonabant, a CB1 antagonist
stop	Stop-CB1
T	time
T	thymidine
Th	thalamus
TK	thymidine kinase
TM	transmembrane
Tris	Tris(hydroxymethyl)aminomethane
TRPV1	transient receptor potential vanilloid type 1
U	uracil
UDG	uracil DNA glycosylase
US	unconditioned stimulus
URB597	cyclohexylcarbamic acid 3'-carbamoylbiphenyl-3-yl ester, a FAAH inhibitor
UTR	untranslated region
VGluT1	vesicular glutamate transporter 1
vs.	*versus*
v/v	volume per volume
WIN55,212-2	R-(+)-[2,3-dihydro-5-methyl-3-(4-morpholinyl)methyl]pyrolo[1,2,3-de]-1,4-benzoxazin-6-yl]-1-naphthalenylmethanonemesylate, a CB1 agonist
wt	wild type
w/v	weight per volume

Further abbeviations were used according the international system of units (SI). The one letter code of amino acids was used for protein sequences.

List of figures

List of tables